Lakehead University

Petrology of Ijolites from the Prairie Lake Carbonatite Complex

A thesis submitted to Lakehead University in partial fulfillment of the requirements of the degree of Master of Science

Johnathan Savard

16-9-2019

ABSTRACT

This study investigates the major and trace element composition of minerals of the ijolite series rocks occurring at the Prairie Lake carbonatite complex, northern Ontario, together with comparative data for ijolites from the Fen complex, Norway. Trace element data (Sr, Zr, REE) were collected by LA-ICP-MS for clinopyroxene, garnet, and apatite. and in conjunction with the major element data are used to develop a petrogenetic model for Prairie Lake.

The ijolites and calcite ijolites (hollaites) of Prairie Lake carbonatite complex have been formed by magma mixing, crystal settling, solid-state deformation, and deuteric alteration. The complex represents at least three stages of intrusion by melts of differing composition. The initial stage is predominantly biotite pyroxenites and associated coarse carbonatite veins. The second stage is primarily members of the ijolite series together with solid state deformation creating meta-ijolites, with differentiation forming malignites (potassic nepheline syenites). The third major stage is the intrusion of the CII carbonatites derived from different batches of magmas. These latter rocks contain xenoliths of ijolite suite rocks, wollastonite apatitite and phoscorite.

Pyroxene compositions show an evolutionary trend from diopside in biotite pyroxenites to Fe-enriched diopside-augite in ijolites to aegirine in malignites. Clinopyroxene major and trace element data shows that clinopyroxene cores from the biotite pyroxenites formed at depth and were emplaced as part of a later event. These data are used to show that a continuously filled fractionating magma chamber was not present at Prairie Lake and that the complex formed as result of small intrusions of nephelinite magma into pre-existing ijolites. A similar style of petrogenesis is suggested for the Fen complex.

Table of Contents

List of Figures

List of Tables

Acknowledgements

This project has been an excellent learning opportunity, and wonderful challenge. While I have many people I would like, my deepest gratitude is extended to Dr. Roger Mitchell for providing the research project and serving as an excellent source of guidance and wisdom. I also thank the professors of the Lakehead Geology department, especially Dr. Shannon Zurevinski.

This project would not have been possible without the financial assistance of the Natural Sciences and Engineering Research Council of Canada, the faculty of Science and Environmental Studies at Lakehead University, and Almaz Petrology.

I am also greatly indebted to my family and friends for their support. I must especially thank my dear wife, Adriane Matheson-Smith, who moved to Thunder Bay and supported this endeavor every step of the way, and my friends Ryan Shannon and Rob Bogle.

1 – INTRODUCTION

Alkaline rocks make up less than 1 vol. % of igneous rocks found on the surface of the planet Earth, and yet they comprise ~50% of igneous rock names. While rocks may be considered alkaline in several ways, the broader definition is that of a rock with "more alkalis than can be accommodated by feldspar alone," while in a narrower sense they are deficient in SiO_2 in respect to the alkalis (Na_2O, K_2O, and CaO). The process of studying and cataloguing them may best be described as "similar to opening Pandora's Box. They are petrologically fascinating but exhaustively diverse" (Winter, 2010). Because of this, they have fascinated geologists for decades. One type of alkaline magma that has garnered much attention and debate surrounds carbonatites, that is igneous carbonate rocks, and their associated silicate rocks such as those of the ijolite series.

The purpose of this project is to investigate the mineralogy and petrology of ijolite series rocks from the Prairie Lake alkaline complex to determine whether the ijolites were formed in multiple pulses, with comparisons to similar ijolite series rocks occurring at the Fen Complex of Norway. This will be done primarily using pyroxene and garnet compositions, plus trace element data for apatite, clinopyroxenes and garnets.

1.1 - Petrological Definitions

The nomenclature of alkaline igneous rocks is a topic of great debate in the petrological world (e.g. Mitchell, 1996; Gittins and Harmer, 2003). The definitions of rock types recognized in this study are summarized in Table 1. Whereas this study does not focus on the carbonatites of Prairie Lake or Fen, it is important to discuss them because of their close genetic relationship to the associated silicate rocks (Wu et al., 2017). The IUGS defines carbonatites as igneous rocks composed of >50 modal % carbonate minerals containing less than 20 wt. % SiO_2 (Le Maitre, 2002). This definition is not without criticism however, as Mitchell (2005) notes that the IUGS scheme fails to take genetic origins into account. Mitchell (2005) proposes an alternative genetic classification scheme relating carbonatites to their associated magma types using an arbitrary 30 modal % carbonate cut-off regardless of silica content. This scheme divides carbonatites into "*bona fide*" primary igneous rocks, commonly tracing their origins to the mantle, whereas other carbonatites associated with potassic and sodic peralkaline magmas are classified as "*carbothermal residua*". This latter scheme allows for a more nuanced look at carbonatite origins and will be used here. The term 'carbonatite' within this paper refers to the *bona fide* igneous carbonatites, in particular those of the nephelinite-clan (Mitchell, 2005).

Table 1: Alkaline Rock Definitions

Rock Name	**Defining features**
Urtite	Nepheline > 70%, Clinopyroxene < 30%
Ijolite	Nepheline 30-70%, Clinopyroxene 30-70%
Melteigite	Clinopyroxene > 70%, Nepheline < 30%
Biotite Pyroxenite	Clinopyroxene + Biotite > 60%, Minor-absent nepheline
Hollaite	Calcite > 10%; Clinopyroxene + Nepheline
Malignite	K-Feldspar > 10%; Clinopyroxene + Nepheline
Apatitite	>50 modal % apatite
Carbonatite	>30 modal % carbonate minerals

Whereas there are a wide variety of carbonatites found across the world, several names used in the literature are important with regards to a discussion of the geology of Prairie Lake and Fen. Søvite is an old term used for calcite carbonatite; and rødberg (literally "red rock") is hematite-bearing calcite/dolomite carbonatite (Andersen, 1984; Mitchell, 2005). An additional term commonly used in the discussion of Fen is rauhaugite, commonly used by Saether (1957), however this term has never been properly defined, and can refer to either dolomite carbonatite or ankeritic ferrocarbonatite (Andersen, 1986a) and is thus not used in the present work.

One rock type that has a wide variety of names in the literature is that of pyroxene-bearing calcite carbonatite. Terms used to describe this variety of rock include silicocarbonatite, søvitic melteigite-pyroxene søvite, pyroxene søvite/silicosøvite, hollaite (for melanocratic varieties), ringite and kåsenite (for leucocratic varieties) (Brogger, 1921; Saether, 1957; Andersen, 1988). Hollaite is the preferred term used in this work.

The rocks most commonly associated with carbonatites are those of the ijolite series. The widely accepted belief is that this relationship is genetic (Mitchell, 2005), although this idea does have some detractors (e.g. Gittins and Harmer, 2003). The ijolite series are undersaturated alkaline rocks composed of nepheline and pyroxene in varying proportions. There is some debate as to the precise modal percentage divisions of the series, but it is generally accepted that the nepheline-rich member, urtite, contains less than 30 modal % pyroxene, ijolite contains between 30 to 70 modal % pyroxene, and melteigite has pyroxene in excess of 70 modal % (LeBas, 1977; Mitchell, 1996; Platt, 1996). The extrusive equivalent to the ijolite series is found as nephelinites lacking olivine (Platt, 1996).

Pyroxenite is an important rock type for the discussion of Prairie Lake as biotite pyroxenites are an important petrographic unit at Prairie Lake (Wu et al., 2017). Pyroxenite is an intrusive igneous rock composed of >60 vol.% pyroxene (Le Maitre, 2002).

Malignites were originally defined by Lawson (1896) for a suite of orthoclase-rich rocks found at Poohbah Lake, Ontario. Brögger (1921) used the term in a sense modified from Lawson's (1896) original compositional definition to refer to a undersaturated, one-feldspar assemblage of nepheline-plus pyroxene. Subsequently, the term became poorly constrained and arguably misused, leading Mitchell and Platt (1979) to re-investigate samples from the type locality at Poohbah Lake. In this work, it is recommended following Mitchell and Platt (1978) that the term malignite be applied to magmatic potassic nepheline syenite containing nepheline plus a single phase of potassium feldspar devoid of exsolution perthite, together with clinopyroxene and/or garnet.

Additional alkaline silicate rocks important for the discussion of Fen are damtjernite and vipetoite. Damtjernite is a phlogopite-bearing ultramafic lamprophyre named for Damtjern, a lake just south of the Fen complex (Saether, 1957; Barth and Ramberg, 1966). Vipetoite is a pyroxenite from Vipeto farm in the Fen complex containing titanian augite, biotite, and calcite with possible nepheline and albite (Le Maitre, 2002). In the literature these rocks are also referred to as damtjernite and vibetoite respectively after Brögger (1921) who had mistranslated the locality names, as noted by Saether (1957). As such the corrected names are used in this work.

1.1.1 - Mineralogy

The most important minerals associated with carbonatites and the ijolite suite include: carbonates (most commonly calcite or dolomite): nepheline, pyroxene, biotite, garnet, titanite, magnetite, apatite, potassium feldspar, and wollastonite together with many other rarer Zr and Nb minerals (Andersen, 1986b; Platt, 1996; Mitchell, 1996; Chakhmouradian et al., 2008)

1.1.1.1 - Clinopyroxene

Clinopyroxenes are the monoclinic members of the pyroxene group of minerals which have a general formula of "$M2M1T_2O_6$, where M2 refers to cations in a generally distorted octahedral coordination, M1 to cations in regular octahedral coordination, and T to tetrahedrally coordinated cations" (Morimoto et al., 1988).

The end-member formulae for diopside, hedenbergite, and aegirine are $CaMgSi_2O_6$, $CaFe^{2+}Si_2O_6$, and $NaFe^{3+}Si_2O_6$ respectively (Fig. 1.; Morimoto et al., 1988). The pyroxene in ijolites usually shows a limited compositional trend from diopside to aegirine-augite, though it has been suggested that this may mask processes that are more complex than simple fractionation (Platt, 1996; Mitchell, 1980; Dawson et al., 1995).

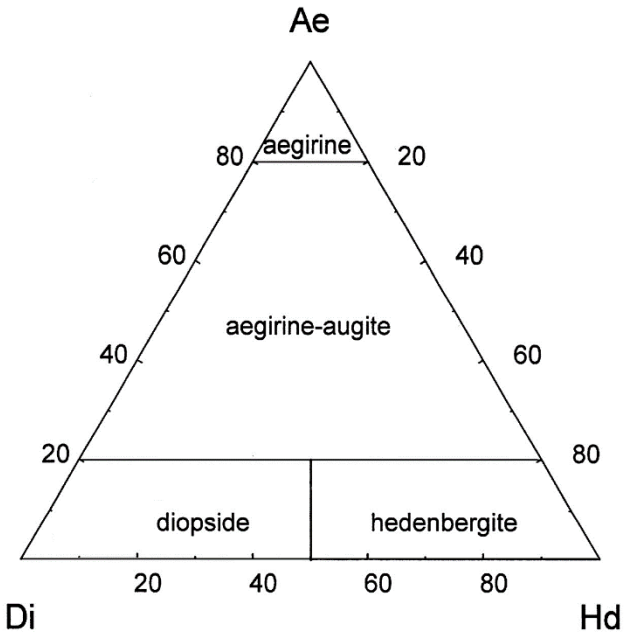

Figure 1: Aegirine, Hedenbergite, Diopside ternary based upon recommendations from Morimoto et al. (1988)

In carbonatitic systems, clinopyroxene forms in association with early carbonatite facies associated with calcites. Both Ca and Na pyroxenes crystalize early in the system and commonly

evolve through increasing Na and Fe contents (aegirine components) over the course of magmatic evolution (Reguir et al., 2012).

In alkaline and carbonatitic magmas, rare earth elements partition into two sites when clinopyroxene crystalizes, with the light rare earth elements going to the M2 site and the heavy rare earth elements going to the M1 site. Partition coefficients calculated for three complexes by Reguir et al. (2012) were unable to fit to a single REE distribution curve as a result of this bimodal distribution (Fig. 2).

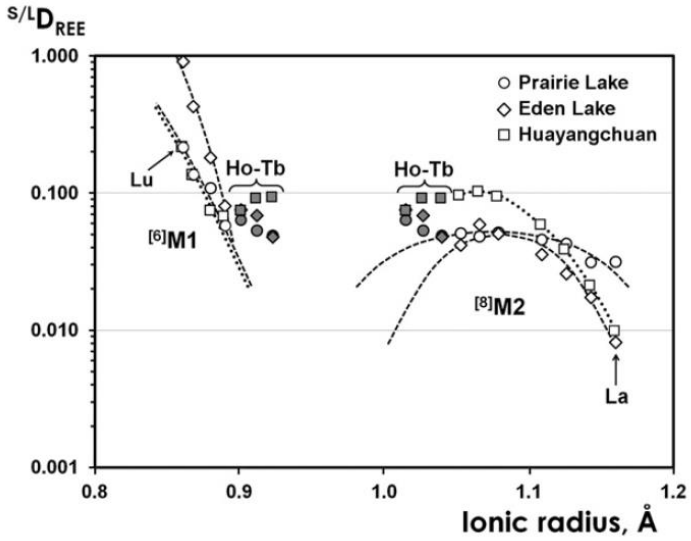

Figure 2: Clinopyroxene and amphibole partition coeefficients plotted against ionic radii (from Reguir et al., 2012)

1.1.1.2 – Garnet

Garnets are an orthosilicate mineral group with a general formula of $X_3Y_2(SiO_4)_3$ allowing for many different substitutions (Grew et al., 2013). Garnets in the ijolites are typically dark brown in colour and can contain appreciable Ti. Most commonly they are schorlomite, morimototite or Ti-rich andradite solid solutions (formerly melanite) (Platt, 1996).

1.1.1.3 – Apatite

Apatite is the name of a group of hexagonal phosphate minerals with a general formula of $M1_2M2_3(TO_4)_3X$ where the M1 and M2 sites are usually filled by calcium, the T site is filled by phosphorus, and the X site is the dominant anion resulting in an ideal formula of $Ca_5(PO_4)_3X$ where X = (F, Cl, OH) (Pasero et al., 2010).

Apatite is the most common non-carbonate phase associated with carbonatites. While extensively researched, much of the data published are either incomplete or containing notable statistical anomalies, and as a result understanding of apatite genesis in carbonatitic systems is lacking (Chakmouradian et al., 2017).

1.1.1.4 – Other Major Minerals

Nepheline is a feldspathoid with the generalized formula $Na_3K(Al_4Si_4O_{16})$; it is a characteristic mineral of alkali-rich, silica undersaturated plutonic rocks, such as ijolites (Vulić et al., 2011). An important aspect of nepheline is that most compositions lie within the Morozewicz - Buerger convergence field, which represents the ideal compositions of nephelines which crystallize in a plutonic environment (Hamilton, 1961). If samples plot outside this field, they are probably the result of cooling at higher temperatures (Hamilton, 1961).

1.2 – Alkaline Complexes

Experimental petrology has long played an important role in the debate surrounding the origins of carbonatites and their associated silicate rocks. Initial opponents to the idea of carbonatite magmas cited the experimental petrology available at the time indicating that abnormally high temperatures (~1339°C) and pressures would be required for a calcite melt (Smyth and Adams, 1923), while the rocks indicated emplacement at lower temperatures seeming to preclude an igneous origin (Bowen, 1924; Bowen, 1926; Wyllie and Tuttle, 1960). It was not until 1960 that Wyllie and Tuttle were able to show conclusively that an igneous calcite rock could form over a range of low temperatures because of the presence of H_2O into the system CaO-CO_2-H_2O, reducing the temperature required to melt calcite to 740°C.

Since that time, many advances have been made in the understanding of carbonatite origins, the most important of which has been the development of three major models of carbonatitic magma genesis:

1) Primary carbonatite magma is created by partial melting of a carbonated peridotite (Wyllie and Huang, 1976; Harmer and Gittins, 1998)
2) Liquid immiscibility results in the separation of carbonatitic magma from a silicate magma (Kjarsgaard and Hamilton 1988; Church and Jones, 1995)
3) Fractional crystallization of a carbonated silicate melt (Gittins, 1989; Cooper and Reid, 1998, Mitchell, 2005)

It is commonly thought that the origin of carbonatites may be a combination of any of the three processes.

1.3 – Prairie Lake Complex

1.3.1 - Introduction

Prairie Lake is an intrusive sub-volcanic complex consisting of carbonatite and associated silicate rocks (predominantly members of the ijolite series). It is located to the northwest of Marathon, Ontario (49º02'N; 86º43'W, Fig. 3). The complex has an area of 2.8 km^2 and shows a very strong aeromagnetic anomaly. There is poor outcrop exposure resulting from weathering and overlying glacial deposits. The complex was emplaced into Archean granites with accompanying fenitization (alkali metasomatism) at the contacts (Woolley, 1987). The carbonatite and silicate rocks were determined by U-Pb geochronology to have been emplaced at approximately the same time at around 1160 Ma (Wu et al., 2017).

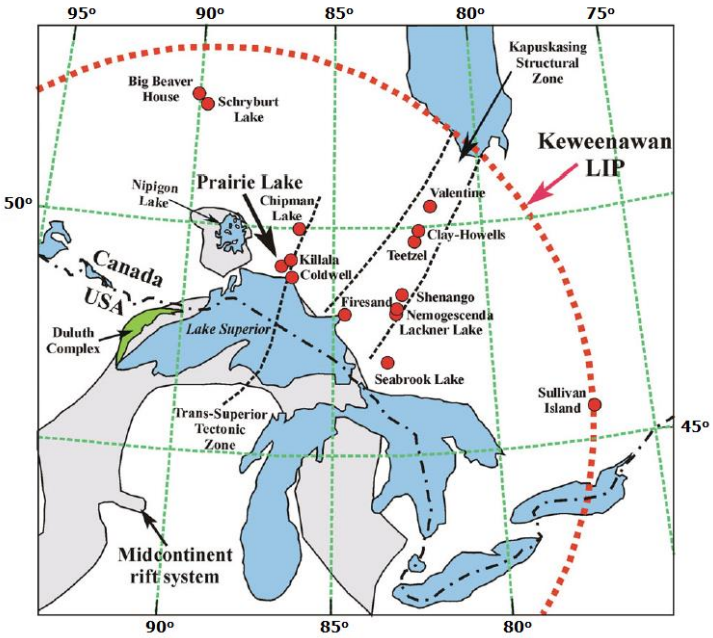

Figure 3: Location of Prairie Lake relative to other alkaline rock and carbonatite complexes. From Wu et al. (2017) after Ernst and Bell (2010), and Rukhov and Bell (2010)

Prior research on the complex has been associated with mineral exploration and potential for niobium and uranium (e.g. Sage, 1983). More recent work has investigated the timing and mechanisms of emplacement (Zurevinski and Mitchell, 2015; Wu et al., 2017).

1.3.2 - Regional Geology

The Prairie Lake complex is emplaced into Archean granites in the Wawa subprovince of the Superior province (Zurevinski and Mitchell, 2015). The Superior province consists of alternating units of metasedimentary and granite – greenstone rocks. Most of the rocks in the province are older than 2 Ga with the volcanics representing island arcs and the metasediments representing the basins between them. The Wawa terrane was formed in the late Archean and is composed of volcanic and plutonic rocks (Card, 1990).

The Prairie Lake complex has been long thought to be related to the many other alkaline intrusive suites occurring in the Midcontinent Rift (Heaman et al., 2007; Wu et al., 2017; Zurevinski and Mitchell, 2015), this being one of the best-preserved examples of an intracratonic rift from the Precambrian (Heaman et al., 2007). The development of the rift has been divided into four stages by Heaman et al. (2007).

The first stage, expressed by lamprophyre dykes and minor felsic magmatism, was from 1150 Ma to 1130 Ma, contemporaneous with the Abitibi dyke swarm. Stage 2 occurred from 1115 to 1105 Ma and is represented by alkaline rocks, rhyolites, ultramafic intrusions, together with basaltic sills and flows. This is the stage during which most alkaline and carbonatitic rocks were emplaced. Stage 3 is the main rifting event from 1100 to 1094 Ma, and is expressed by basalt flows, and mafic rocks such as the Duluth Complex as well as minor alkaline intrusions. The fourth and final stage represents the end of the rifting as recorded by porphyry and basaltic dykes (Heaman et al., 2007).

1.3.3 - Prior Research and Exploration History

The Prairie Lake carbonatite was initially investigated in 1968 by a prospector, J. Gareu, in the employ of the Newmont Mining Corporation of Canada whose discovery of radioactive showings resulted in the company performing trenching, geological, and geophysical surveys. The same year, J. Satterly of the Ontario Department of Mines published a map displaying carbonatite and alkaline rocks, making note of Prairie Lake as a possible carbonatite complex (Satterly, 1968).

Watkinson prepared an unpublished manuscript (1976) regarding the U-Nb mineralization in the complex, based on an abstract published in 1971. By 1974, Newmont had allowed all but two of its claims covering Prairie Lake to lapse; this allowed for the International Minerals and Chemical Corporation (IMC) to stake these claims to assess the phosphate potential of the apatite. This was done through mapping in 1974 and drilling in early 1976 (Putrich et al., 2014).

In 1975, Newmont optioned off its remaining two claims to New Insco Mines Limited (known as Nuinsco since 1979 and is referred to as such from here on), which also purchased the remaining claims from IMC in 1976 after finding the volume of apatite inadequate to support further research. The following few years saw Nuinsco conducting extensive exploration at the property including diamond drilling, mapping, trenching, soil sampling, and prospecting as well as conducting radiometric and magnetic surveys (Putrich et al., 2014). These data provided the information for a resource estimate of 181,000 t at 0.09% U_3O_8 and 0.25% Nb_2O_5 (Archibald, 1978).

By 1978, a logging access road, the Deadhorse Creek Road, reached near Prairie Lake and allowed for an ease of access not previously available, providing access to the interior of the

complex. Interestingly, the next several years saw relatively little activity at Prairie Lake until Nuinsco returned to the property in 1983 to investigate the potential for niobium, phosphorus and wollastonite with three drill holes (Putrich et al., 2014).

The first investigation of Prairie Lake by the Ontario Geological Survey was in 1987 conducted by R.P. Sage. This basic overview of the economic potential of the carbonatite provided a cursory glance at the geology of the complex, providing sample descriptions and characterizing the minerals present. Melnik, (1984) a student at Queen's University studied the Prairie Lake complex for an undergraduate thesis, "Textural Evidence for the Origin of the Prairie Lake Carbonatite-Alkali Rock Complex, 1984". Melnik, (1984) concluded that the textures present did not prove simple liquid immiscibility; however, the thin section scale of the study was too small to make conclusions for the complex as a whole.

The mineral marianoite [$Na_2Ca_4(Nb,Zr)_2(Si_2O_7)_2(O,F)_4$] was discovered at Prairie Lake by Chakhmouradian et al. (2008) The mineral has the same structure as wöhlerite [$Na_2Ca_4(Zr,Nb)_2(Si_2O_7)_2(O,F)$], with marianoite showing a preference for niobium in the smallest cation site. It occurs as flat, prismatic crystals forming early in the crystallization sequence prior to calcite, phlogopite and the bulk of the pyrochlore.

Zurevinski and Mitchell (2015) described the unique orbicular texture found in one ijolite at Prairie Lake. Using the mineralogy, textural analysis, and BSE imaging, the authors found the orbicules to be the result of magma mixing between two pulses of ijolitic magma.

Recently, Wu et al. (2017) determined isotopic compositions for the rocks of the Prairie Lake complex. It was concluded that there was isotopic homogeneity with the Sr-Nd isotopes being identical for the carbonatites, ijolites and syenite, with the respective $^{87}Sr/^{86}Sr$ ratios being

~0.70252, ~0.70254, and ~0.70257, and the respective $\varepsilon_{Nd}(t)_{.1160}$ values being +3.4, +3.5, and +3.6. The Sr-Nd isotope data are interesting because Prairie Lake shows the "most homogeneous isotopic composition of any carbonatitic complex". These data were further supported by baddeleyite in both the ijolite and carbonatite having identical Hf isotopic compositions. They propose that these data show that the complex has been formed from a weakly- depleted mantle producing a single magma type, which then cooled with simple crystal fractionation with no country rock assimilation.

In 2010, a prospector named Rudy Wahl discovered the Good Hope carbonatite on the northern outer rim of the complex. In 2011, Canadian International Minerals conducted trenching (making twelve trenches), channel sampling, rock sampling, soil sampling, radiometric surveys and prospecting. From September to December 2014, some minor geological mapping and sampling was conducted by Rudy Wahl. MDN Inc. conducted prospect mapping and trenching during June and July of 2015. In 2016, they drilled two holes PL-01 and PL-02 guided by aerial magnetic and radiometric surveys conducted by Prospectair earlier that year (Selway, 2017).

Plato Gold Inc optioned the property as a potential niobium prospect and began a mapping and sampling program in the summer of 2017 with drilling of 5000 m of core in 2018. The Good Hope carbonatite was the focus of an undergraduate thesis by A. Cleaver (2017) at Lakehead University who classified the carbonatite and investigated the niobium mineralization of the pyrochlores. Cleaver found that there were two paragenetic carbonatite varieties, one pyrochlore-rich and one pyrochlore-poor, representing the earlier and later stages of crystallization, respectively, though she was unable to determine the relationship between Good Hope and Prairie Lake. The pyrochlores were noted as a potential source of niobium; however,

further exploration is required to determine the size and grade of the deposit.

1.3.3.1 - Timing of Emplacement of Prairie Lake

The timing of emplacement at Prairie Lake has been a frequent area of research with a consensus arriving at an age within a few million years of 1160Ma. Initially, Prairie Lake was investigated as part of a larger study of the ages of Eastern Canadian carbonatites by Gittins et al. (1967). In their study, they used the K-Ar method on two biotite samples from the complex which resulted in two ages of 1164 Ma and 1059 Ma; they took the average age of 1112 Ma as the timing of emplacement. The complex was next investigated as part of a BSc thesis by K. J. Bottriel at Carleton University who used Rb-Sr methods on samples from Prairie Lake and Nemegosenda and placed the emplacement of Prairie Lake at 1030 ± 60 Ma (Bottriel, 1975).

Much of the early work was conducted by Bell and Blenkinsop as part of their research into alkaline complexes in the Superior Province of Ontario. In 1980, Bell and Blenkinsop published their research into ages and initial $^{87}Sr/^{86}Sr$ ratios from alkaline complexes in the Superior Province presented at GAC-MAC the previous year. The method used was whole rock Rb-Sr for the alkaline complexes including seven samples from Prairie Lake with a resulting timing of emplacement at 1023 ± 74 Ma. Bell et al. (1982) again used Prairie Lake material for Rb-Sr whole rock analysis with a resulting age of 1030 ± 70 Ma.

Bell and Blenkinsop returned to the complex in 1989 as part of their investigation of neodymium and strontium isotope geochemistry of carbonatites as a chapter in Carbonatites: Genesis and Evolution (Bell, 1989). In that publication a carbonatite sample yielded a whole-rock Rb– Sr age of 1023±74 Ma. Another chapter in Bell (1989) by Kwon et al. investigated the

Pb isotope characteristics of carbonatites, using calcite from the carbonatites at Prairie Lake, a Pb–Pb age of 1155 ± 36 Ma was reported (Kwon et al., 1989).

Sano et al. (1999) collected the first information on the timing of the emplacement for the ijolite series at Prairie Lake. Using the SIMS technique on an apatite from an ijolite, a U–Pb age with a large error of 1156 ± 45 Ma was obtained.

Rukhlov and Bell (2010) determined Lu–Hf ages on the phoscorite and silicocarbonate with TIMS using baddeleyite and zircon which has yielded an age of 1164 ± 4 Ma. Wu et al. (2010) published a similar age of 1159 ± 5 Ma, determined using Pb-Pb techniques on calzirite from carbonatite. The most recent work utilized the U-Pb method on baddeleyite from the complex by Wu et al. (2017). This placed timing of the carbonatites at 1157.2 ± 2.3 Ma, and 1158.2 ± 3.8 Ma, synchronous with the emplacement age of the ijolites at 1163.6 ± 3.6 Ma. This timing is earlier than the rest of Midcontinent Rift related events with which the Prairie Lake is thought to be related (Wu et al., 2017).

1.3.4 - Prairie Lake Geology

The rocks present in the Prairie Lake complex can be subdivided into several major types of carbonatite and silicate rocks (Fig. 4, after Zurevinski and Mitchell, 2015). The ijolite series comprises the core of the complex and is heterogenous on a meter scale. The members of the series found at Prairie Lake include ijolite (pyroxene + nepheline); melteigite (pyroxene > 70%); hollaite (calcite melteigite); and wollastonite ijolite. The former two members of the suite are the more common. There is an exposure in the southern part of the complex of a large wollastonite ijolite megaxenolith. Other minerals found within the ijolites include the marianoite–wöhlerite solid solution series, Zr bearing titanite, and zirconolite in accessory amounts (Wu et al., 2017). The rocks from the ijolite series are the principal focus of this thesis.

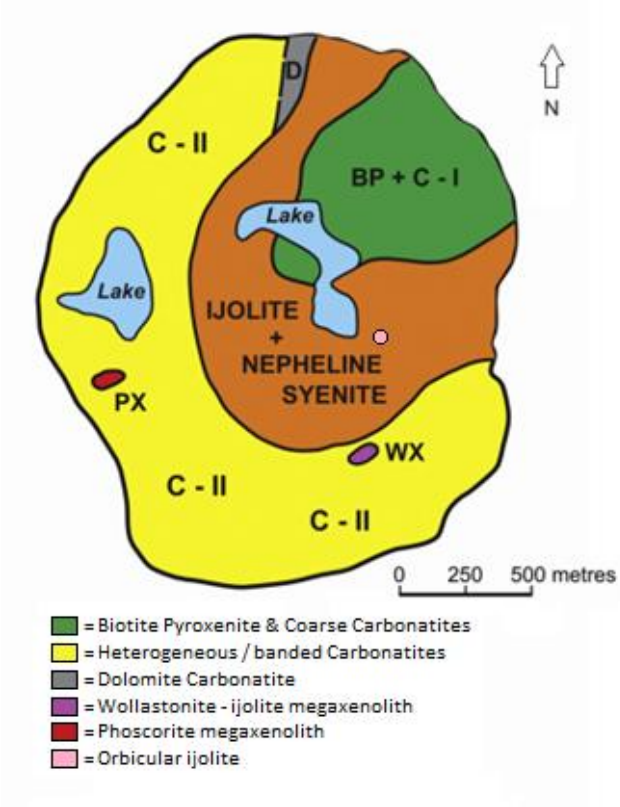

Figure 4: Map of the geology of the Prairie Lake complex. Anomaly Lake is to the left and Centre Lake is to the right. Modified from Zurevinski and Mitchell (2015).

Also present are the K-feldspar-rich rocks genetically related to the ijolite series; these are termed malignite (following Mitchell and Platt, 1979 and also called melocratic nepheline syenite *sensu lato* by Sage, 1983). The minerals present in malignite include Na-poor potassium feldspar, pyroxene and nepheline. In common with the ijolite series, they also contain accessory marianoite– wöhlerite solid solutions and Zr-bearing titanite (Wu et al., 2017).

The calcite carbonatites are categorized as C-I and C-II carbonatites. The C-I carbonatites are very coarse-grained veins and intrude biotite pyroxenite in the northeast of the complex. C-I carbonatites are composed of large interlocking grains of calcite; the associated biotite pyroxenites are very coarse grained and predominantly contain biotite and pyroxene. Neither of those rocks contain large volumes of apatite or magnetite (Wu et al., 2017).

The C-II carbonatites occur in the west and southern regions of the complex. The rocks are heterogenous with great differences of textures and modal mineralogy, showing banding/layering on a very fine scale (from cm to mm). This layering appears, in part, to be parallel to the margins of the complex and is exhibited by differences in the modes of the major minerals, including calcite (with 1-2 wt. % SrO), olivine (Fo_{88-74}), mica (tetraferri-phlogopite, and phlogopite-barian phlogopite), fluorapatite and magnetite. The C-II carbonatites contain higher amounts of apatite and magnetite in relation to the C-I carbonatites. Found "interbedded" between these layers is finer-grained carbonatite, which commonly contains ~10 cm large clasts of coarser carbonatites poor in apatite and mica. The C-II carbonatites also contain clasts of ijolite, together with 'phoscorite' and 'disaggregated phoscorite,' which are "cumulate rocks consisting of magnetite + apatite + olivine and/or diopside with perovskite and/or pyrochlore" (Wu et al., 2017).

At the north end of the complex is a small outcrop of dolomitic carbonatite. This unit occurs between carbonatite-II and biotite pyroxenite to the west and east respectively. So far the age of this unit has not been determined but is undoubtedly related to complex as a late stage unit (Wu et al., 2017).

Recently, two satellite intrusions have been discovered. To the northwest of Prairie Lake is the Good Hope carbonatite. The Good Hope carbonatite consists of pyrochlore-rich and

pyrochlore-poor calcite and dolomite carbonatites representing earlier and later crystallization respectively (Cleaver, 2017). The pyrochlore-rich portions of the Good Hope carbonatite are notable for the presence of disaggregated cumulate clasts of apatite-pyrochlore. Due north of the complex is the Ruffle Lake ferrocarbonatite. This is a sideritic carbonatite that contains elevated concentrations of rare earth elements due to the presence of REE-fluorocarbonates. The rocks have been subjected to extensive deuteric metasomatism and have similarities with the ferrocarbonatite (rødberg) occurring at the Fen Complex (Mitchell, personal communication, 2018).

2 – METHODS

2.1 - Optical and BSE-petrography

Samples from the Prairie Lake complex collected by Professor Roger H. Mitchell and Professor R.G Platt of Lakehead University over many years have been prepared for study as either polished or covered thin (30μm) sections. Samples were initially categorized into samples with carbonate minerals ~>40 vol. % and those with ~<40 vol. % arbitrarily to discard most carbonatites not directly related to the ijolites or biotite pyroxenites.

The remaining samples were investigated by optical methods utilizing a Carl Zeiss optical microscope with cross polarizing plates. The microscope was used to categorize the samples by rock type and mineralogy. Back Scattered Electron (BSE) images were collected from selected carbon coated samples using the Hitachi SU-70 FE together with quantitative X-ray Energy Dispersive Spectrometry (EDS).

2.2 – Quantitative X-ray Energy Dispersive Spectrometry

Quantitative compositional data for the minerals of the Prairie Lake and Fen complex was collected using carbon coated polished thin sections at Lakehead University using two scanning electron microscopes, predominantly the Hitachi SU-70 FE Scanning Electron Microscope with some previous work using a JEOL-JSM 5900 LV. Analyses used an accelerating voltage of 20kV with a beam current of 300 pA. X-ray spectra were analysed with an Oxford AZtec 80 mm/124 eV electron dispersive X-ray (EDX) spectrometer using a process time of 60 seconds. Standards used were: Jadeite (LU-JAD) for Na, Al ; Pyroxene (GL-DJ35) for Si, Ca; Wollastonite (LU-WOLL) for Ca, Si; Mn-Hortonolite (GL-Mnh) for Mn, Fe; Ilmenite (GL-Ilmen) for Ti; Zircon (LU-Zr) for Zr.

Pyroxene data were analyzed using an APL-Mineralogical Program with calculation of structural formulae compositions on the basis of 6 atoms of oxygen with all Na expressed as aegirine (acmite). Garnet data were analyzed using the Excel program designed by Locock (2008) to determine end-member components. Other minerals were identified on the basis of their composition aided by Nesse (2012), mindat.com and webmineral.com.

2.3 - Laser Ablation – Inductively Coupled Plasma – Mass Spectroscopy

Representative samples from several localities were selected for Laser Ablation – Inductively Coupled Plasma – Mass Spectroscopy (LA-ICP-MS). These included twenty-one samples from Prairie Lake, two samples from the associated Good Hope carbonatite, seven samples from Fen, and two samples from Mosonik.

Samples were sent to University of Manitoba for analysis using the Thermo-Finnigan Element2 High Resolution -Inductively Coupled Plasma - Mass Spectrometer with Merchantek LUV213 laser. The laser settings involved a beam size of 30µm, repetition rate of 5Hz and fluence of ~5J/cm^2. There was an oxide forming rate of 0.08%ThO/Th. Element concentrations were calculated assuming 55.6 wt. % CaO in apatite, 50 wt. % SiO_2 in clinopyroxene, and 36 wt. % SiO_2 in garnet. The standards BCR2G and NIST SRM 612 were used. Data were processed using the GLITTER program and analyzed using a combination of Excel and ioGas, data analysis software for geology and geochemistry.

3 – RESULTS

3.1 – Petrography

3.1.1 – Prairie Lake

Sixty-eight samples were selected for petrographic study which are representative of the four major rock types present: (1) biotite pyroxenite; (2) the ijolite series; (3) malignite; (4) other rocks, including apatitite, and xenocryst-bearing calcite carbonatite dykes.

Biotite pyroxenites are composed of clinopyroxene, commonly zoned, together with interlocking clusters of biotite. The ijolite series rocks consist of nepheline + clinopyroxene + garnet ± calcite, and can be divided into ijolites, micro-ijolites, urtites and hollaites. Malignites are characterized by the presence of K-feldspar, Na-zeolites and the absence of fresh nepheline. Carbonatite dike rocks contain xenocrysts derived from deeper levels of the complex set in a groundmass of calcite laths. Apatitite is composed of apatite as the dominant mineral (>50 vol. %) commonly together with wollastonite, clinopyroxene and garnet.

3.1.1.1 – Biotite Pyroxenites

Biotite pyroxenites are coarse- to medium-grained rocks composed primarily of biotite and clinopyroxene together with minor calcite and apatite (Fig. 5). Ten samples of biotite pyroxenite were investigated and divided into two groups: those with clinopyroxene displaying well-defined zonation with colourless cores and green rims enriched in Na and Fe and those that contain clinopyroxene lacking zonation. Samples PL35, PL38, PL48, and PL51 belong to the former group. The crystals are medium- to coarse-grained. Other samples display gradational zoning from a pale green core to a darker green rim with no discontinuity, as seen in samples PL47, PL52, PL54, PL55, and PL131. These are usually medium- to fine-grained and show a

predominantly subhedral clinopyroxene texture. Some samples, such as PL54, contain fractures with marginal increased green colour. PL49 contains pyroxene with less obvious zonation, than in other samples in addition to containing lighter coloured biotite.

Biotite in all samples shows a clustered, interlocking texture of varying grain sizes (<0.1 mm - ~1 mm). Most of the biotite displays deep red and orange pleochroic colours. Many samples also exhibit yellow-green colouration resulting from chloritic alteration, together with pleochroic halos characteristic of radiation damage.

Calcite is present in all samples as an interstitial phase, with amounts present varying from trace (i.e. 2-3 modal % in PL54) to a major component in samples which contain veins of calcite (C-I), ~25 modal % in PL39, and ~ 15 modal % in PL55. Garnet is absent in many samples, and if present is in minor quantities, usually as an interstitial phase (such as in PL47). Nepheline has not been observed in the biotite pyroxenites. Additional trace minerals include zircon, marianoite-wöhlerite, and pyrochlore. Sample PL49 also contains fersmite ($CaNb_2O_6$).

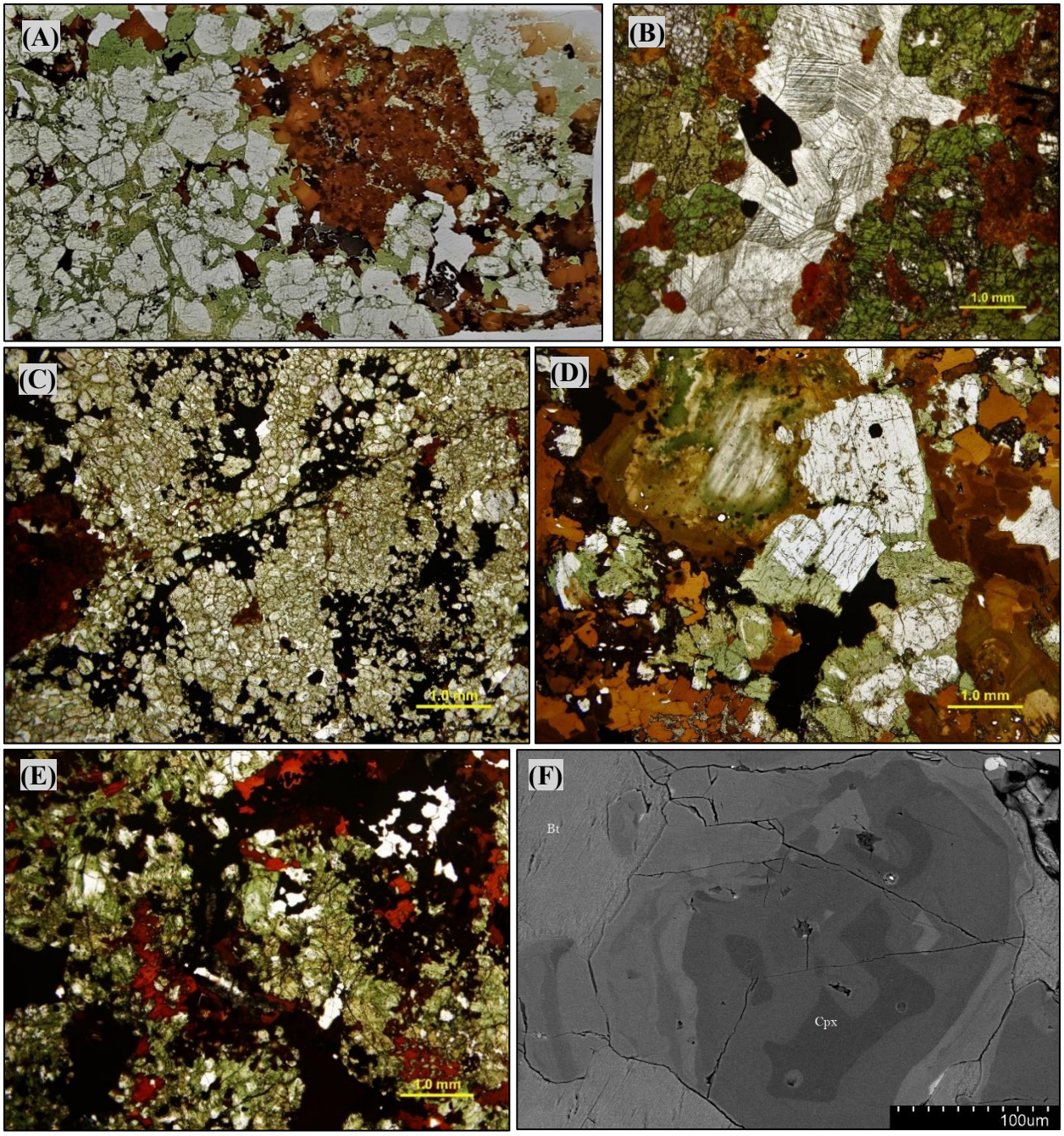

Figure 5: (A) Thin section of sample PL48, a Biotite Pyroxenite with coarse diopside cores (image is ~4cm across); (B) Carbonatite (C-I) vein in biotite pyroxenite, PL39; (C) pyroxene displaying continuous zoning from core to rim, red biotite, and interstitial garnet, PL47; (D) discoloured biotite crystal with zoned clinopyroxene, PL51; (E) Deep red biotite with clinopyroxene, PL52; (F) BSE image of zoned clinopyroxene in biotite, PL49

3.1.1.2 – Ijolite Series

Members of the ijolite series are composed of nepheline, clinopyroxene, and Ti-rich garnet in diverse proportions with some samples containing interstitial calcite, biotite, and apatite. Increases in calcite content leads to a transition to hollaite. The samples examined represent three categories: (1) ijolites; (2) urtites; and (3) hollaites.

Categorization can be difficult, as the modal proportions can vary continuously within one sample. Sample ETR7 (A, B, and C) illustrates how heterogeneous rocks in the complex can be at a small scale, this rock could be classified as three distinct rock types within a very limited area.) The left part (A) of Figure 6 is a coarse-grained garnet urtite with euhedral nepheline and interstitial garnet. In the bottom-mid-left (B) is an ijolite with fibrous clinopyroxene crystals and subhedral nepheline. The top right (C) is dominated by a micro-ijolite with poikilitic garnet in a groundmass of clinopyroxene + nepheline + accessory minerals.

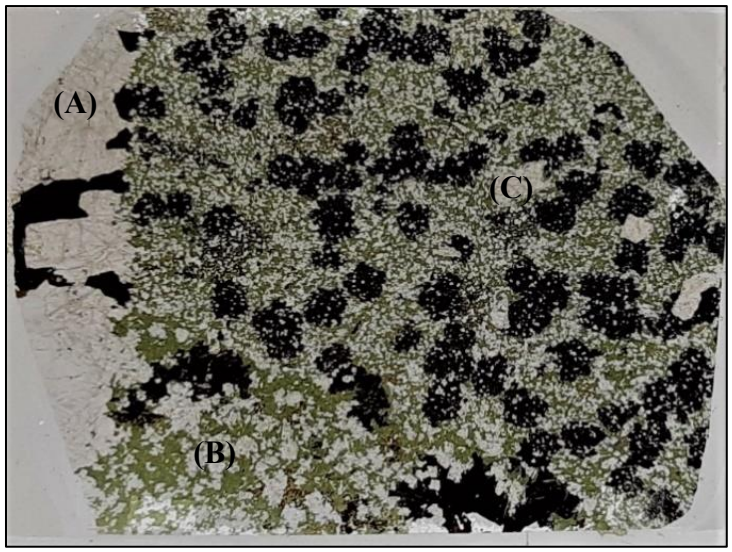

Figure 6: Sample ETR7A displaying zoning on the thin section scale (image ~4cm across)

3.1.1.2.1 – Ijolites

Ijolites from Prairie Lake are medium-to-coarse-grained, and composed of nepheline, clinopyroxene, and garnet in varying proportions with accessory calcite, apatite and mica. The

ijolites may be separated into two categories based on texture: [1] ijolites with coarse, euhedral to subhedral crystals (Fig. 7); [2] ijolites with anhedral, annealed textures (Fig. 8).

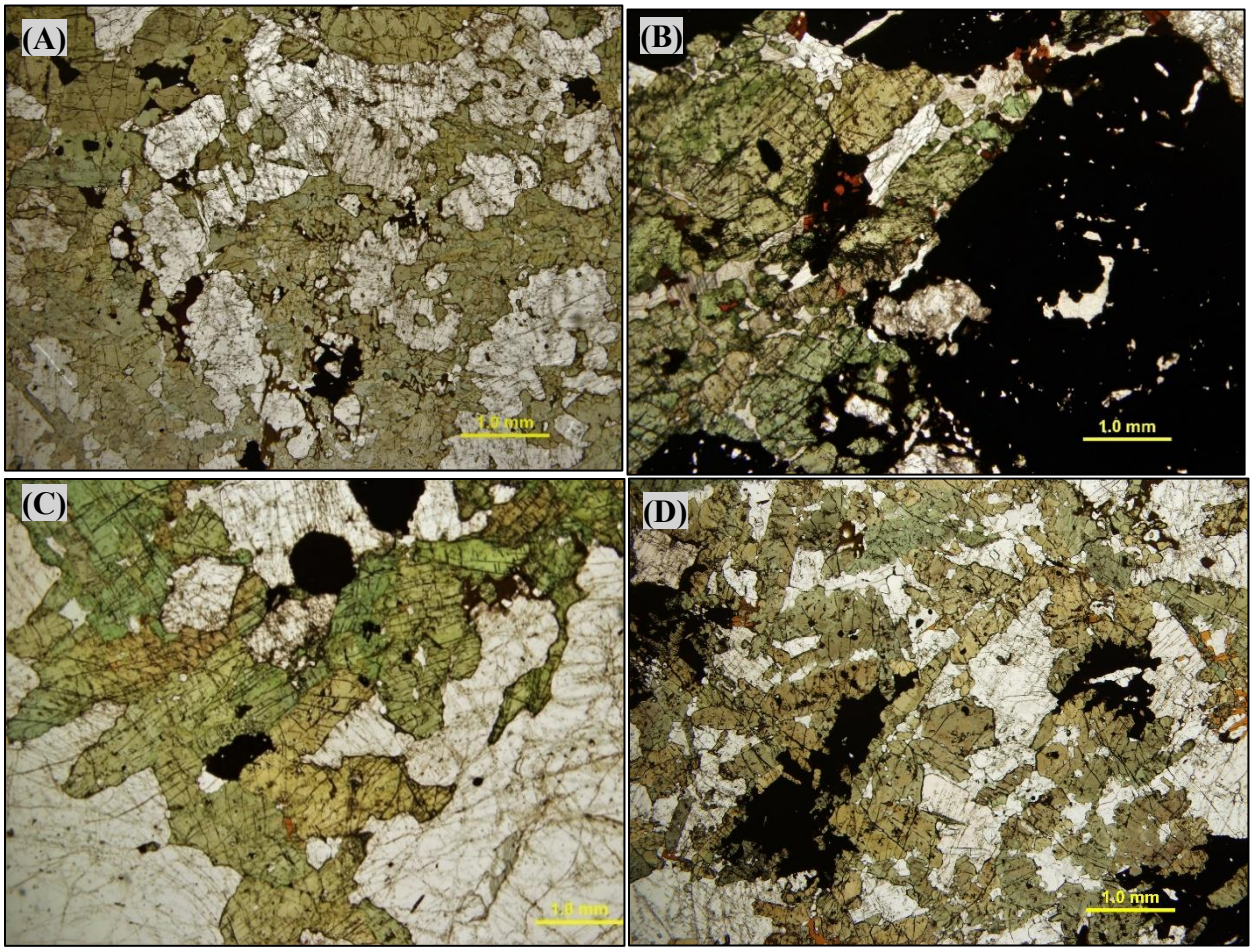

Figure 7: Examples of textures present in ijolites (A) PL64; (B) PL34; (C) PL76 (Garnet Ijolite); (D) ETR3

Only five of the samples investigated belong to the former category, ETR3, PL34, PL64, PL76, and PL81. Modal percentages of minerals, crystal size, and texture vary among samples. Clinopyroxene is an essential component in all ijolites, most abundant in PL64 (60 modal %) and least abundant in PL76 (30 modal %). Clinopyroxene crystals are green to yellow-green, vary in habit from euhedral to subhedral and can show a range in size in each sample with the coarsest crystals ~0.5 mm in maximum dimension. Crystals are usually intergrown, commonly displaying a bladed shape. Nepheline in the ijolites typically exhibits a coarse, predominantly subhedral to

euhedral texture. Nepheline is commonly altered to cancrinite where crystals are in contact with later-crystallizing calcite.

Garnet is present in all samples varying between approximately 10-45 modal percent, most abundant in PL34 and least abundant in PL81. The textures in different samples vary with garnet in PL34 displaying coarse, rounded subhedral-to-anhedral grains up to ~7.5 mm^2 in size. Garnet in PL64 and PL81 is an interstitial phase between clinopyroxene and nepheline. Garnet usually contains inclusions of clinopyroxene, nepheline calcite, biotite and apatite. Interstitial calcite with associated biotite is present in PL34, and PL81.

Samples ETR3 and PL64 display similar textures with fine-medium grained euhedral clinopyroxene crystals intergrown into euhedral nepheline. Garnet is subhedral, commonly include subhedral terminated clinopyroxene. Calcite and associated minerals are absent in these samples. Unlike most of the samples investigated, ETR3 does not display clear evidence of post-crystallization alteration, with nearly all crystals being euhedral, and little-no evidence of cancrinite or calcite veining.

Sample PL34 is garnet dominant, making up nearly 50 modal % of the rock. The garnet ranges in habit from subhedral-to-anhedral and contains many inclusions. Clinopyroxene is the next most abundant major mineral, occurring as subhedral interlocking crystals. Nepheline is predominantly subhedral with several euhedral crystals with cancrinite rims. One feature not present in other ijolites is that of an apatite vein amongst disaggregated crystals of clinopyroxene, nepheline and garnet.

PL76 is nepheline dominant (around 50 modal percent), with clinopyroxene and garnet present in about equal quantities of ~20 modal % each. The nepheline is euhedral-to-subhedral

and coarse, reaching a maximum width just over 1cm. Clinopyroxene occurs as green, subhedral-to-anhedral medium grained crystals. Garnet is subhedral with inclusions of nepheline and clinopyroxene. Calcite occurs as a prominent late-stage interstitial phase.

PL81 is predominantly composed of clinopyroxene crystals between 0.1 and 0.5mm with inclusions of nepheline. Clinopyroxene in contact with interstitial calcite displays zoning with deeper green colour. The largest crystals are several coarse, euhedral nepheline crystals, whereas subhedral nepheline of various sizes is also present. Garnet is an interstitial phase between clinopyroxene crystals. This sample contains the highest contents of biotite of any of the ijolites, occurring as deep brown interstitial crystals. Calcite appears to be the last phase to crystalize and is interstitial between other mineral phases.

A relatively common feature is that of cloudy nepheline, displaying some alteration to Na-K zeolites and K-feldspar, yet not enough feldspar is present for the rock to be classified as malignite. Zeolite alteration is present among many samples, though is perhaps best seen in PL34. Samples PL34 and PL64 contains veins cutting through crystals; with calcite veins in PL34 and cancrinite veins in both samples.

Some ijolite samples display unique textures and are clearly not “simple” ijolites. Porphyritic textures are present in two of the samples, PL65 and WT5. Interestingly the phenocrysts are different minerals, nepheline in PL65, and clinopyroxene in WT5. Both of these samples contain an ijolitic groundmass of fine-grained anhedral nepheline and clinopyroxene with minor calcite.

3.1.1.2.1.1 – Annealed Ijolites

The majority of the ijolite samples in this study display anhedral, annealed textures (Fig. 8) differentiating them from other members of the ijolite series. These allotriomorphic ijolites are mineralogically identical to other ijolites, containing nepheline, clinopyroxene, and garnet together with accessory minerals including calcite and mica. Thirteen samples display this texture with crystal size ranging from fine- to very fine-grained (typically classified as micro-ijolites), between 0.01 mm and about 0.1 mm; at coarsest, the annealed ijolites are medium grained up to 0.25cm (such as PL63, PL77 and ETR6A).

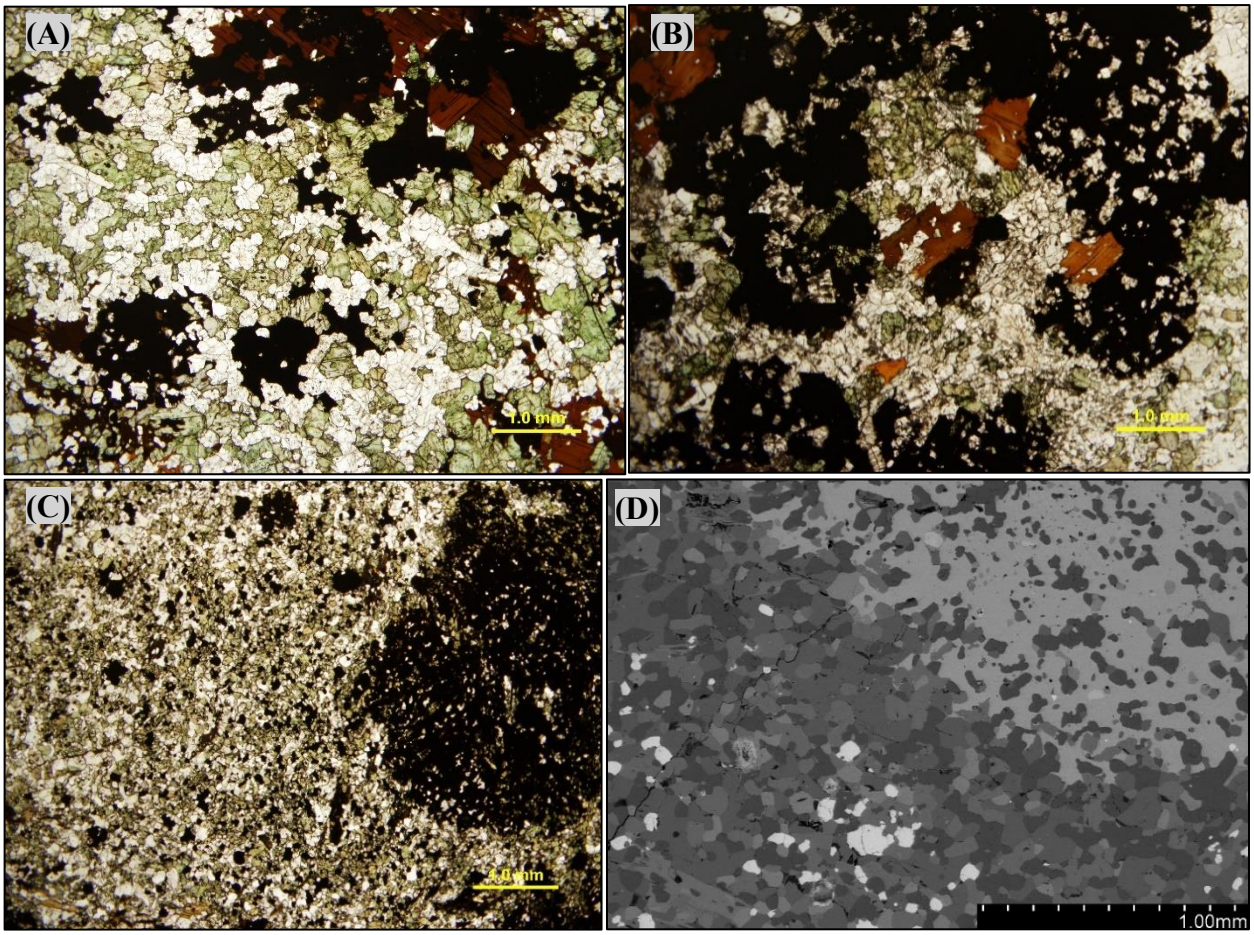

Figure 8: Annealed ijolitic textures (A) PL43 (B) PL77 (C) Photomicrograph (plane polarized light) of a micro-ijolite, PL85 (D) BSE image of the anhedral, annealed texture present in the micro-ijolites, with a poikilitic garnet in the top right corner, PL85

A relatively common feature of these annealed ijolites is the presence of poikilitic garnet (Fig. 8B) of varying size, usually between 0.1 and 0.7 mm. Five samples display rounded

poikilitic garnet ETR7C, ETR7A, PL43, PL77, and PL85. Some samples (including ETR6A and PL63) display elongated, poikilitic tabular garnets with many inclusions of clinopyroxene in the rims.

Mica is relatively rare in the allotriomorphic ijolites, only occurring in significant quantitates in medium-grained samples ETR7B, PL43, and WT3. Calcite and apatite are only as fine-grained trace minerals. Several samples contain crystals of pyrite.

3.1.1.2.3 - Urtites

Three urtite samples were investigated in this study, ETR2, PL91, and PL96A; they are garnet urtites with significant amounts of nepheline and garnet, together with minor amounts of clinopyroxene, calcite and trace amounts of apatite and biotite (Fig. 9). Cancrinite is also present, commonly when nepheline is in contact with calcite.

PL96A and ETR2 are quite similar, both are composed of euhedral crystals of nepheline chadacrysts (~1-5mm) encased in poikilitic garnets with minor interstitial clinopyroxene and calcite and trace biotite. The crystallization relationships between clinopyroxene and garnet are difficult to determine as both are interlocking crystals with euhedral faces (this is especially clear in ETR2), suggesting simultaneous growth. Clinopyroxene always exhibits euhedral crystal faces when in contact with calcite suggesting early growth. Biotite and apatite are rare and commonly occur interstitially between calcite and other minerals suggesting relatively late formation.

PL91 is richer in clinopyroxene (~15 vol. %) from other samples of urtite. Nepheline crystals in PL91 are larger (>5 mm) than those in the other urtites and primarily subhedral. Cancrinitization is common where nepheline is in contact with calcite. Veins of cancrinite cross-

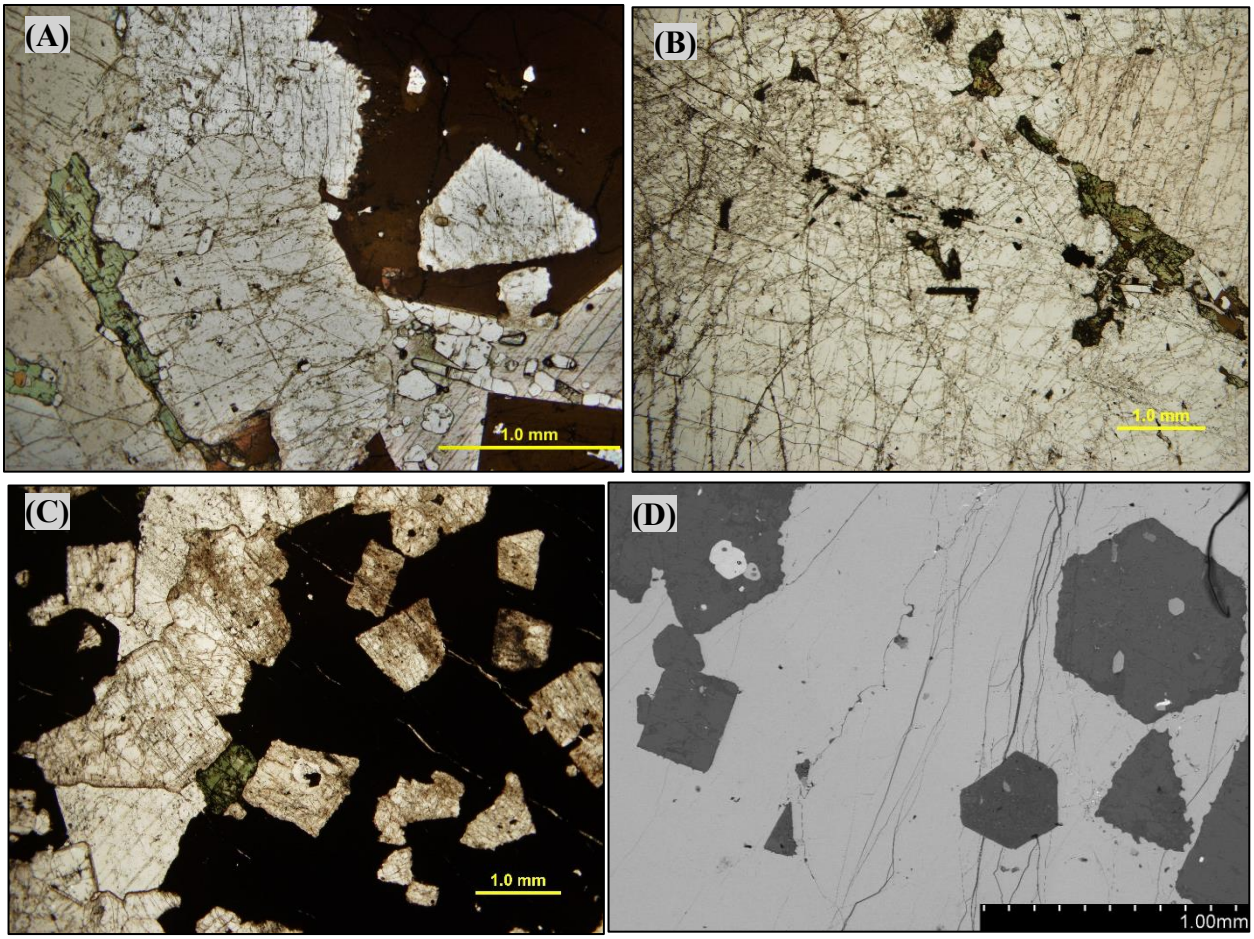

Figure 9: (A) Photomicrograph (plane polarized light) of ETR2 displaying a common garnet urtite texture; (B) PL 91 (C) PL96A (D) BSE photograph of PL96A displaying euhedral nepheline in garnet

cut the nepheline crystals. Clinopyroxene and garnet again appear as an interstitial phase between nepheline crystals. Biotite is also a phase between clinopyroxene and interstitial calcite.

3.1.1.2.4 – Hollaites (Calcite Ijolites)

Only three samples of hollaite (ijolite series with calcite >10 vol. %) were included in the study, PL86, PL90 and PL96B. They contain the same minerals as found in the ijolites, i.e. clinopyroxene, nepheline and garnet but with increased amounts of interstitial calcite (Fig. 10).

PL96B contains clinopyroxene, nepheline and garnet in approximately equal amounts (~27 vol.% each) with calcite (~5 vol. %) being the only other major mineral phase. Clinopyroxene occurs as green- to- yellow-green bladed interlocking crystals (Fig. 10). Typically, the crystals are subhedral, however euhedral faces occur when in contact with calcite. Garnet is subhedral with inclusions of nepheline and clinopyroxene. Trace amounts of wollastonite, apatite and biotite are present.

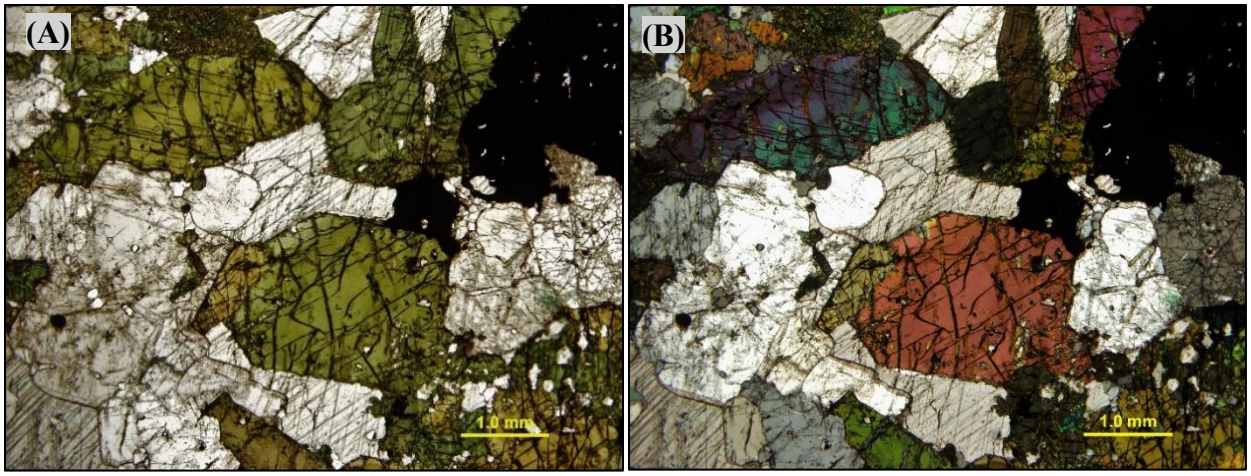

Figure 10: (A) Photomicrograph (plane polarized light), and (B) cross polarized light image of a hollaite, PL96B, displaying euhedral clinopyroxene with interstitial calcite.

PL86 is a wollastonite hollaite, with clinopyroxene, nepheline, and garnet together with minor cancrinite and zeolites. Wollastonite is present (~30 vol.%) as anhedral crystals from ~1 mm up to ~5 mm. Clinopyroxene comprises ~30 vol. % of the rock, predominantly as subhedral interlocking crystals, 1-3 mm in size, with euhedral crystal faces in contact with calcite. Clinopyroxene displays zonation, with deep green rims encasing green cores. Nepheline occurs as subhedral crystals 0.5-3 mm in size as ~20 vol. % of the sample. The nepheline is moderately zeolitized with some cancrinite. Garnet in the sample is reddish-brown, and both garnet and calcite occur as interstitial phases, with calcite occurring as a later phase. Calcite is present in ~10 vol.% of the sample. Trace apatite is also present.

PL90 (Fig. 11) contains anhedral clinopyroxene set-in coarse-grained calcite comprising ~35 vol. % of the sample. Minerals present include clinopyroxene, nepheline, biotite and garnet, with minor apatite and cancrinite. Clinopyroxene occurs as subhedral, anhedral green crystals commonly intergrown with biotite and garnet, both of which are also anhedral. Nepheline is subhedral and colourless, with cancrinitization commonly present when in contact with calcite.

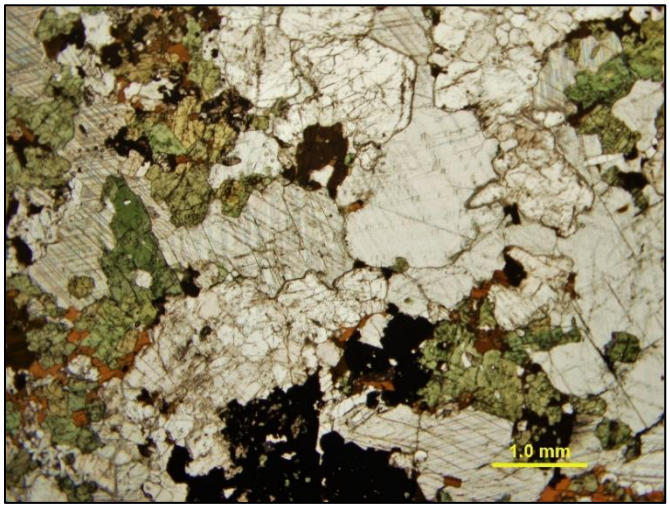

Figure 11: Photomicrograph (plane polarized light) of PL90

3.1.1.3 – Malignites

Twenty-one samples were classified as malignites, which are distinguished by the presence of interlocking plates of Na-poor K-feldspar with Na-zeolites commonly replacing primary nepheline.

Malignites from Prairie Lake contain perhaps the most complicated and diverse textures found in the complex. They display evidence of both primary igneous textures together with varying degrees of hydrothermal alteration. While the textures are diverse, they can be separated into two categories: (1) Malignites, and (2) Pegmatitic Malignites.

Malignite samples exhibit diverse textures and complex mineralogy (Fig. 12). Most malignites are primarily composed of anhedral crystals, although subhedral and euhedral crystals while uncommon, are present in some samples. Crystal sizes vary from very-fine grained crystals in malignite (on the order of a few μm in the K-feldspar-zeolites intergrowths) to a few mm in

size (such as clinopyroxene in ETR6B). The dominant minerals in malignite are clinopyroxene and K-feldspar with associated zeolites, and commonly garnet. Minor phases include calcite, biotite, cancrinite, and apatite, together with many Nb- and Zr-bearing trace minerals.

K-feldspar is found intergrown with zeolites in complex fine-grained poikilitic intergrowths. Commonly, these intergrowths replace nepheline, occurring as a pseudomorph (perhaps seen most clearly in sample P-10-G1, Fig.12C). Clinopyroxene in malignites is pale green and deep green/olive, with anhedral-to-subhedral crystals ranging in size from <0.5mm to ~5mm at largest. Biotite is usually subhedral, and brown-green in colour. Titanite is rarely present as an anhedral phase.

Many trace and accessory minerals not commonly seen in the ijolite series rocks, include marianoite–wöhlerite, zircon, and Zr- and Nb-bearing titanite. Commonly, these trace minerals are fine grained, intergrown with the K-feldspar and zeolites and are difficult to identify by optical methods and best identified by BSE-imagery and X-ray spectrometry.

Some samples of ijolite display minor amounts of zeolitization replacement of nepheline (such as PL34) and introduction of K-felspars. In some instances, ijolitic-textures are preserved where the nephelines have been entirely replaced (such as in ETR 6B) and culminates in the complete destruction of primary ijolitic textures (as in PL38). The last mineral phase to be preserved in the overprinting appears to be garnet (best seen in P-10-G1). These features are related to the last stages of differentiation of the ijolite-forming magma towards malignite.

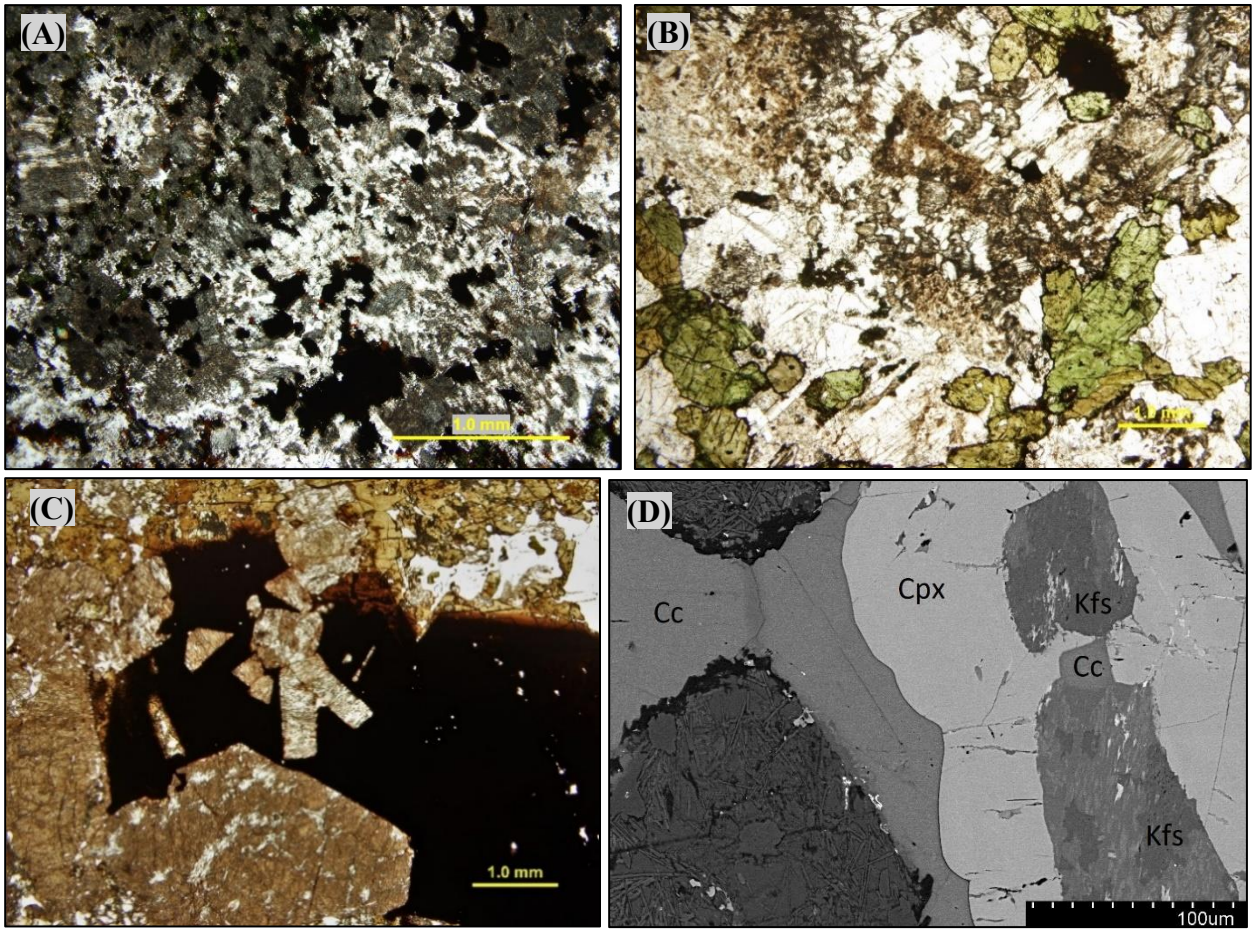

Figure 12: Photomicrograph (plane polarized light) of malignites from Prairie Lake displaying some of the diverse textures seen in these rocks. (A) PL38 (B) PL36 (C) Pseudomorphic K-feldspar and zeolites after nepheline, P10G1 (D) BSE image of K-feldspar and zeolites replacing nepheline PL-P4-36

3.1.1.3.1 – Pegmatitic Malignites

Two samples of malignite are pegmatitic, PL42 and PL46 (Fig. 13). With coarse grained crystals of clinopyroxene, and K-feldspar (intergrown with Na-zeolites and associated trace minerals) and minor interstitial calcite and garnet. Euhedral clinopyroxene (~50 vol.%) crystals range in size from ~0.5 to 1 cm^2, and display twinning and complex zoning plus mineral inclusions. Coarse grained, euhedral crystals of K- feldspar up to ~1cm can occur as seen in PL42. Interstitial calcite is present in both samples and comprises about 5-10 modal % of the

samples. Other minerals present are complex intergrowths of K-feldspar and zeolite with zirconolite, and dalyite.

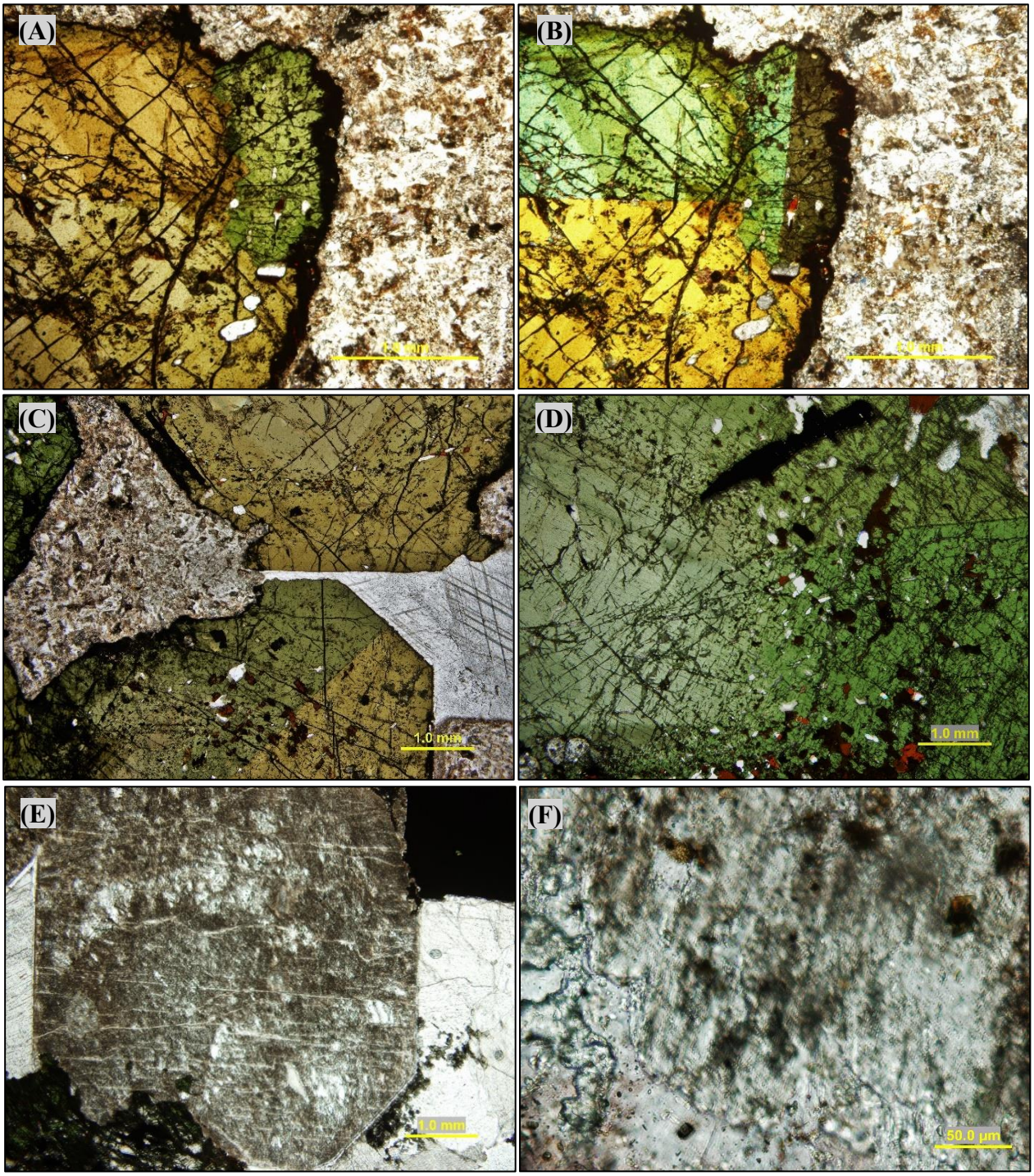

Figure 13: (A) Photomicrograph (plane polarized light), and (B) cross polarized light image of clinopyroxene twinning and zonation from PL46; (C) Zoned clinopyroxene, K-feldspar and zeolites, with interlocking calcite, PL42; (D) Included, zoned clinopyroxene crystal from PL46; (E) Euhedral crystal with K-feldspar and zeolite, PL46; (F) Photomicrograph (plane polarized

3.1.1.4 – Other rock types

3.1.1.4.1 – Apatitite

Apatitites from Prairie Lake contain > 50 vol.% apatite. Three apatitites were included in this study; WS01, WS2D and NP68 (Fig. 14). Commonly, wollastonite, garnet, and clinopyroxene are also present.

WS01 is a wollastonite-clinopyroxene apatitite with a very diverse mineral assemblage. Major minerals include apatite, clinopyroxene, wollastonite, garnet and calcite. Apatite is most commonly anhedral, with triple points occurring along the contacts some bladed crystals occurring in contact with clinopyroxene. Clinopyroxene is green-brown with no well-defined habit. Garnet occurs as opaque, tabular crystals with poorly-defined crystal faces.

WS2D is a wollastonite apatitite occurring as a mega-xenolith in the ijolites. It is primarily composed of anhedral apatite and wollastonite. Also present are minor garnet, trace clinopyroxene and biotite. Apatite makes up about >45 vol. % of the rock and occurs as fine- to medium-grained crystals meeting at triple points. Wollastonite comprises ~40 vol. % and occurs as anhedral colourless crystals with characteristic cleavage and high birefringence. Garnet is present as about 10 vol. % of the sample as dark brown – opaque crystals with minor inclusions of apatite and wollastonite.

Sample NP68 is a clinopyroxene garnet apatitite. The sample is primarily composed of ~60 vol. % anhedral apatite (visibly zoned in BSE imaging), together with clinopyroxene, garnet, pyrochlore and minor calcite. Clinopyroxene is usually 1 to 2 mm in size and commonly extensively fractured. Many euhedral-to-subhedral clinopyroxenes display clear zonation with colourless cores and green rims. Garnet appears as anhedral opaque red crystals varying in size from 0.5 to 2 mm. Calcite is present as a minor interstitial phase.

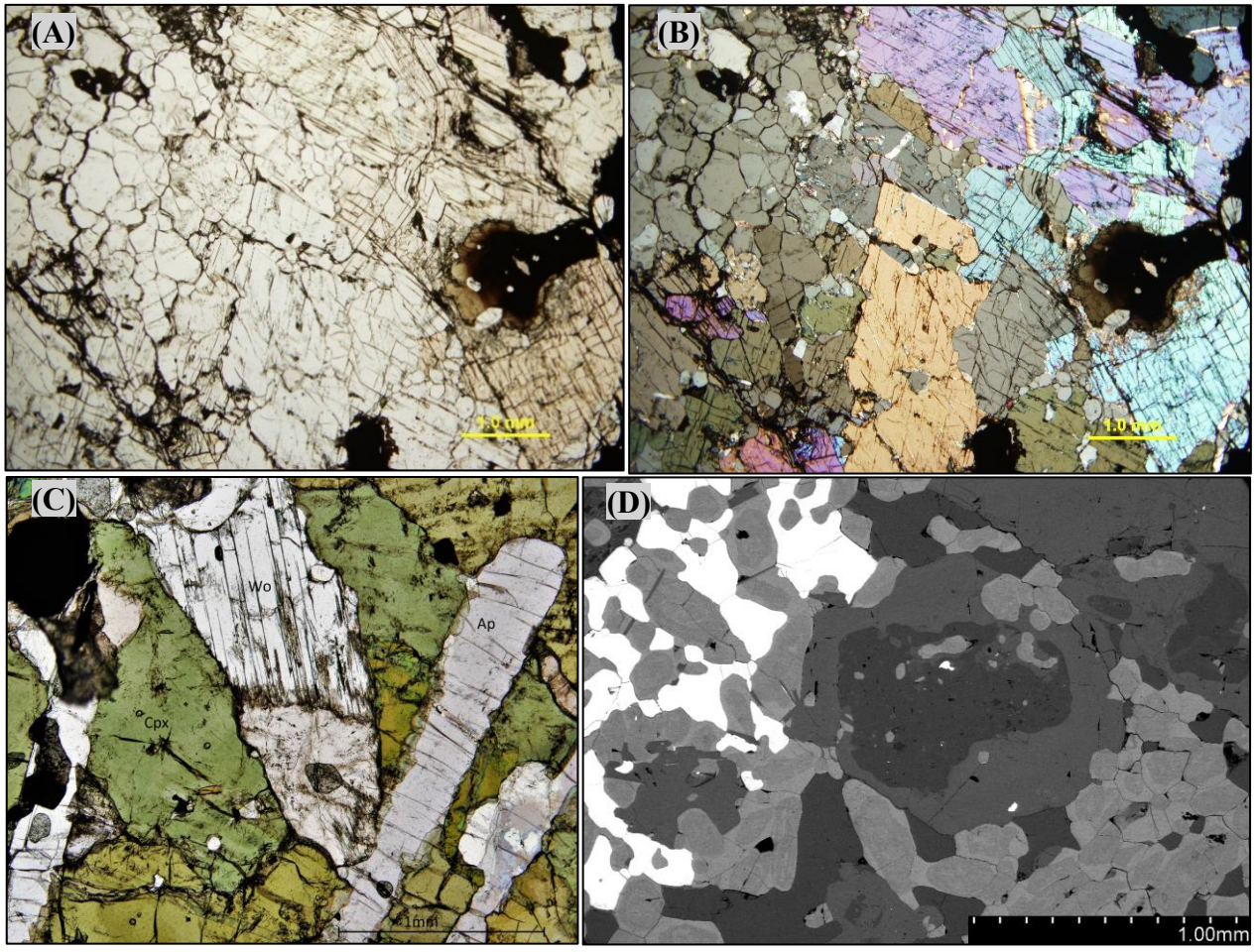

Figure 14: (A) Photomicrograph (plane polarized light), and (B) cross polarized light image of wollastonite apatitite, WS2D; (C) Clinopyroxene wollastonite apatitite, WS01 (D) BSE image of NP68 displaying zoned CPX amd apatites

3.1.1.4.2 – Hypabyssal xenolith/xenocryst-bearing carbonatite

Clasts of a micro-xenolith/ xenocryst-bearing carbonatite are found in the CII carbonatite. These clasts are of importance as they carry a suite of material not represented at the current level of exposure or as clasts in ijolite-suite rocks and malignite. These hypabyssal rocks (Fig. 15) consist of micro-xenoliths of diverse mafic silicate rocks and carbonatites set in a fine-grained matrix of serpentinized euhedral olivine, flow aligned Sr-bearing calcite laths together with fine grained apatite. Rounded-irregular (up to 0 5 mm) micro-xenoliths include: diopside-apatite-magnetite; diopside-apatite-zircon; diopside-apatite-phlogopite-calcite; apatite-diopside; dolomitic carbonatite; and apatite calcite carbonatite. Round-to-anhedral xenocrysts include: large anhedral apatite (up to 400 um); red pleochroic resorbed phlogopite laths and plates; rounded brown magnesio-hastingsite amphibole crystals; subhedral-to-anhedral Ti-magnetite; rounded pale brown clinopyroxenes with thin reaction rims; single anhedral crystals of dolomite and calcite. Calcites contain micro-inclusions (<10um) of Na-Sr-Ba-REE carbonates.

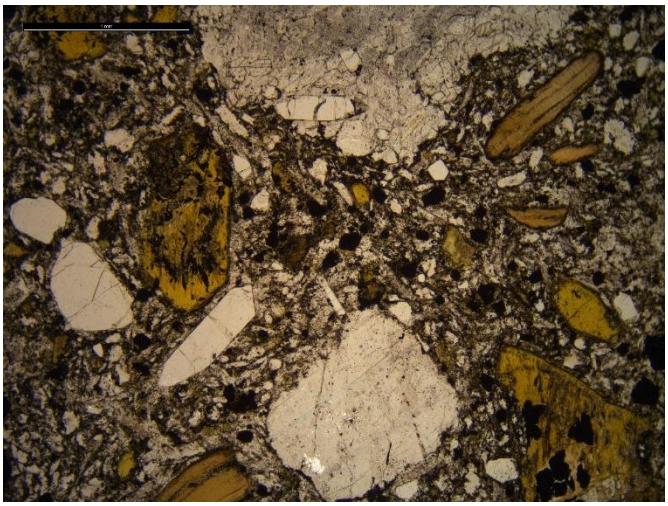

Figure 15: Photomicrograph (plane polarized light) of carbonatite dike, PLL-01 with clasts of mica, calcite and, dolomite, and altered olivines in a matrix of calcite laths

Detailed investigations of these rocks were not a part of this study but are described here as they provide some further information regarding members of silicate suite of rocks which have crystallized at depth. Preliminary data for the compositions of pyroxene and mica present in the microxenoliths and as xenocrysts show these to be Al-poor diopside ($Ae_{3.3}Hd_{10.9}Di_{85.8}$ to

$Ae_{9.0}Hd_{17.6}Di_{73.4}$), Al-rich diopside (9 mol.% $CaTiAl_2O_6$; $Ae_{3.9}Hd_{19.3}Di_{72.8}$) and phlogopite of similar composition to these minerals in the biotite pyroxenite suite. The late-stage magmas forming these rocks have sampled material which formed, as minimum, at similar depths to the biotite pyroxenites. The micro-xenolith suite demonstrates the complexity of the Prairie Complex at depth.

3.1.2 – Fen Complex

Ten representative samples were selected from the Fen complex for petrographic analysis: four samples of ijolite, two micro-ijolites, and one sample each of melteigite, urtite, hollaite and vipetoite. Photomicrographs of these are presented in Fig. 16.

The ijolites from Fen (Fen35, Fen37, Fen 48 and Fen49) are composed primarily of nepheline and clinopyroxene together with minor titanite and garnet and trace cancrinite and calcite.

Fen35 contains approximately equal quantities of subhedral clinopyroxene and subhedral-to-anhedral nepheline (~45 vol. %). Clinopyroxene is green and occurs as elongated crystals ~5 mm in length with inclusions of nepheline, calcite and titanite. Nepheline contains inclusions of clinopyroxene and apatite and alteration to cancrinite. Opaque, anhedral garnet occurs as a minor interstitial mineral. Trace biotite and titanite are present.

Fen37 contains subhedral-to-euhedral, green, bladed clinopyroxene crystals up to ~3 mm in length (~40 vol. %) in subhedral interlocking nepheline altering to cancrinite (~50 vol. %). Trace apatite is present as small (~0.5 mm) euhedral crystals and anhedral opaque garnet and brown biotite are present.

Fen48 contains euhedral, interlocking crystals of green clinopyroxene (~40 vol. %) together with titanite (~5 vol. %) and subhedral, opaque garnet (~20 vol. %) in a groundmass of interstitial nepheline (~30 vol. %).

Fen49 contains coarse (2-7 mm) euhedral crystals of green clinopyroxene (~35 vol. %) and subhedral nepheline (~55 vol. %) with minor cancrinite occurring at crystal boundaries.

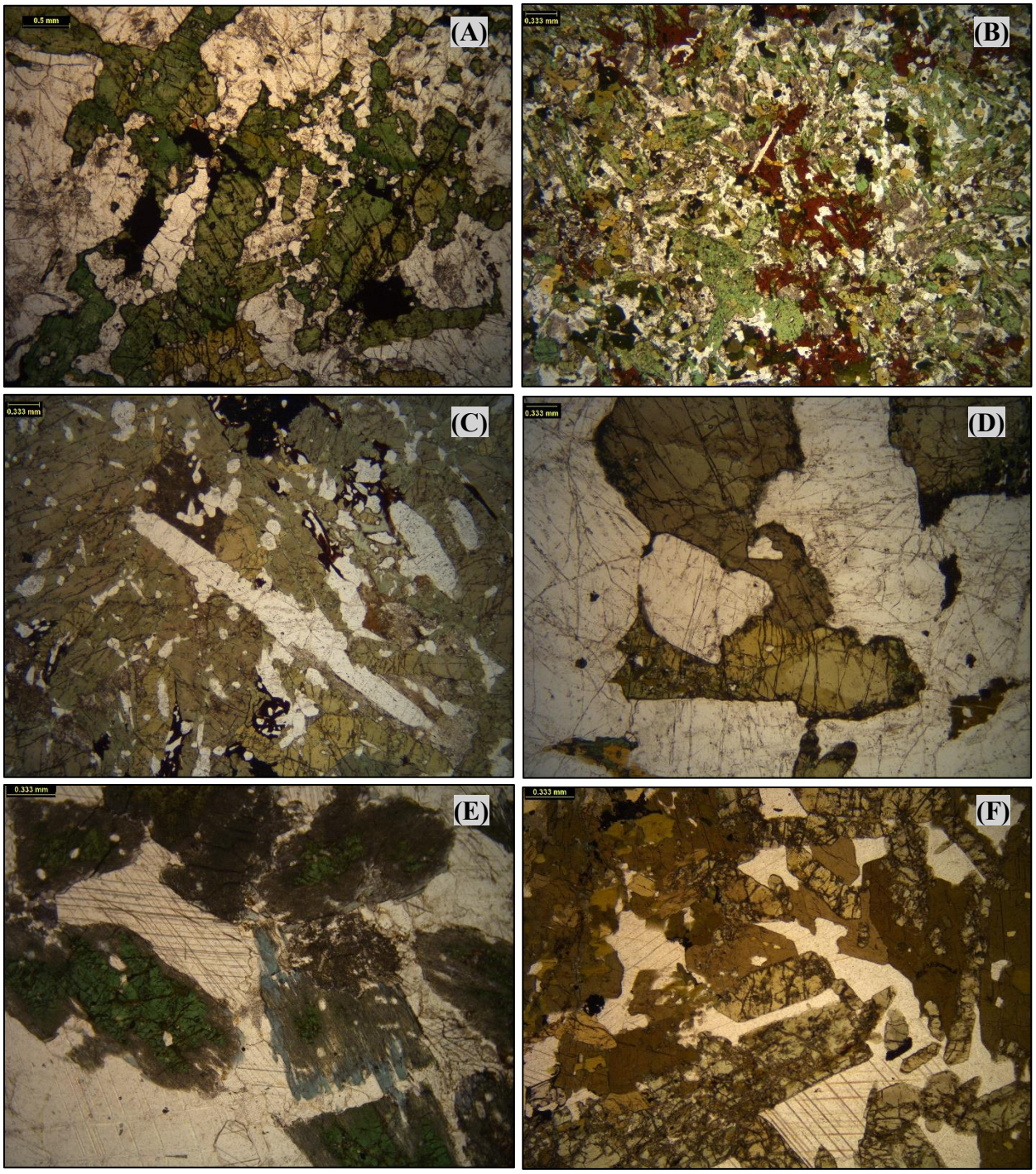

Figure 16: Photomicrographs (plane polarized light) of representative rocks from the Fen complex, Norway. (A) Ijolite (Fen35) clinopyroxene and nepheline with minor opaque garnet; (B) Micro-ijolite (Fen 200) containing clinopyroxene, nepheline and red garnet; (C) Melteigite, Fen43 clinopyroxene, nepheline and minor interstitial opaque garnet; (D) Urtite (Fen 94) euhedral nepheline with trace clinopyroxene; (E) Hollaite (Fen421) displaying clinopyroxene altering to amphibole in a calcite matrix; (F) Vipetoite, Fen70

Clinopyroxene displays complex zonation and varies in colour between brown and dark-green. Minor deep-red, anhedral garnet is present together with trace titanite and interstitial calcite.

Both samples of micro-ijolite (Fen200 and Fen201) display essentially identical mineralogy and textures, with fine grained, subhedral crystals up to a maximum of ~0.4 mm. Approximately 30 vol. % of the rocks contain subhedral, bladed green clinopyroxene up to 3 mm in length. Anhedral nepheline is replaced by K-zeolites and cancrinite. Minor brown biotite occurs as an interstitial mineral. Garnet occurs as red, anhedral crystals comprising ~15 vol. %. Calcite and apatite are present as a late stage mineral together with trace stronalsite. Sample Fen201 contains a vein of calcite ~2 mm wide containing fine grained (<0.1 mm) euhedral inclusions of clinopyroxene and mica.

Urtite (Fen94) is composed of large (5-7 mm) subhedral-to-anhedral nepheline crystals with rims of cancrinite accounting for about 90 - 95 vol. % of the sample. Minor interstitial brown-green clinopyroxene and calcite are present.

Melteigite (Fen43) has a very complicated texture, mostly consisting of large subhedral, inclusion-rich clinopyroxene, together with apatite, and late-stage, interstitial calcite and garnet. Clinopyroxene is brownish-green and makes up ~60 vol. % of the rock and contains euhedral apatite crystals 1-4 mm in size. Garnet is anhedral and opaque. Chlorite replaces mica as a minor phase. Trace Mn-ilmenite, titanite and perovskite are present.

Fen421 is a hollaite composed predominantly of subhedral-to-euhedral clinopyroxene (~30 vol. %) encased in interstitial calcite matrix (~60 vol. %). The green clinopyroxene is moderately included and fractured, with rims altering to blue amphibole. Minor K-feldspar and trace phlogopite are found in the calcite matrix. The sample lacks nepheline, garnet or titanite.

Vipetoite (Fen70) consists mainly of coarse, anhedral brown amphibole, with subhedral-to-euhedral prismatic clinopyroxene and interstitial calcite. Minor anhedral biotite is present as inclusions in amphibole. Trace ilmenite, magnetite and pyrite are present.

3.2 – Mineralogy and Compositional Variations

In alkaline rocks, one of the best methods to understand the evolution of an igneous complex is to investigate the compositions of major, minor and trace minerals which reflect melt compositional variations. Particular attention has been given in this study to clinopyroxene as it is a well-known indicator of melt fractionation and evolution (e.g. Mitchell, 1980; Hode Vuorinen et al., 2005; Reguir et al., 2012).

3.2.1 – Prairie Lake

3.2.1.1 – Clinopyroxene

The compositions of pyroxenes from Prairie Lake belong to the diopside (Di) – hedenbergite (He) – aegirine (Ae) ternary system. Three hundred and fifty-three pyroxene compositions from twenty-eight samples were analyzed and their compositions recalculated into this system are presented in Fig. 17. Crystals vary in colour and morphology, from clear euhedral diopside present as cores of pyroxenes in biotite pyroxenite and apatitite to deep-green anhedral zoned euhedral aegirine-augite in pegmatitic malignite. Commonly, ijolite pyroxenes exhibit pleochroism in shades of green, with crystals displaying anhedral- to- subhedral habit. The compositions show an evolutionary trend from unevolved (diopside-rich) compositions in biotite pyroxenite to evolved (aegirine rich) compositions in malignite.

Clinopyroxene compositions from the biotite pyroxenites all plot within the diopside field (Fig. 17). The biotite pyroxenites contain the purest diopside as colourless, euhedral crystals (up to 97 mol % Di in PL49). The compositions of clinopyroxenes in biotite pyroxenite follow a linear evolutionary trend from Di-rich compositions towards increasing Hd and Ae content to ~52 mol. % Di, 30 mol. % Hd, and 18 mol. % Ae. Representative compositions from biotite pyroxenite are presented in Table 2.

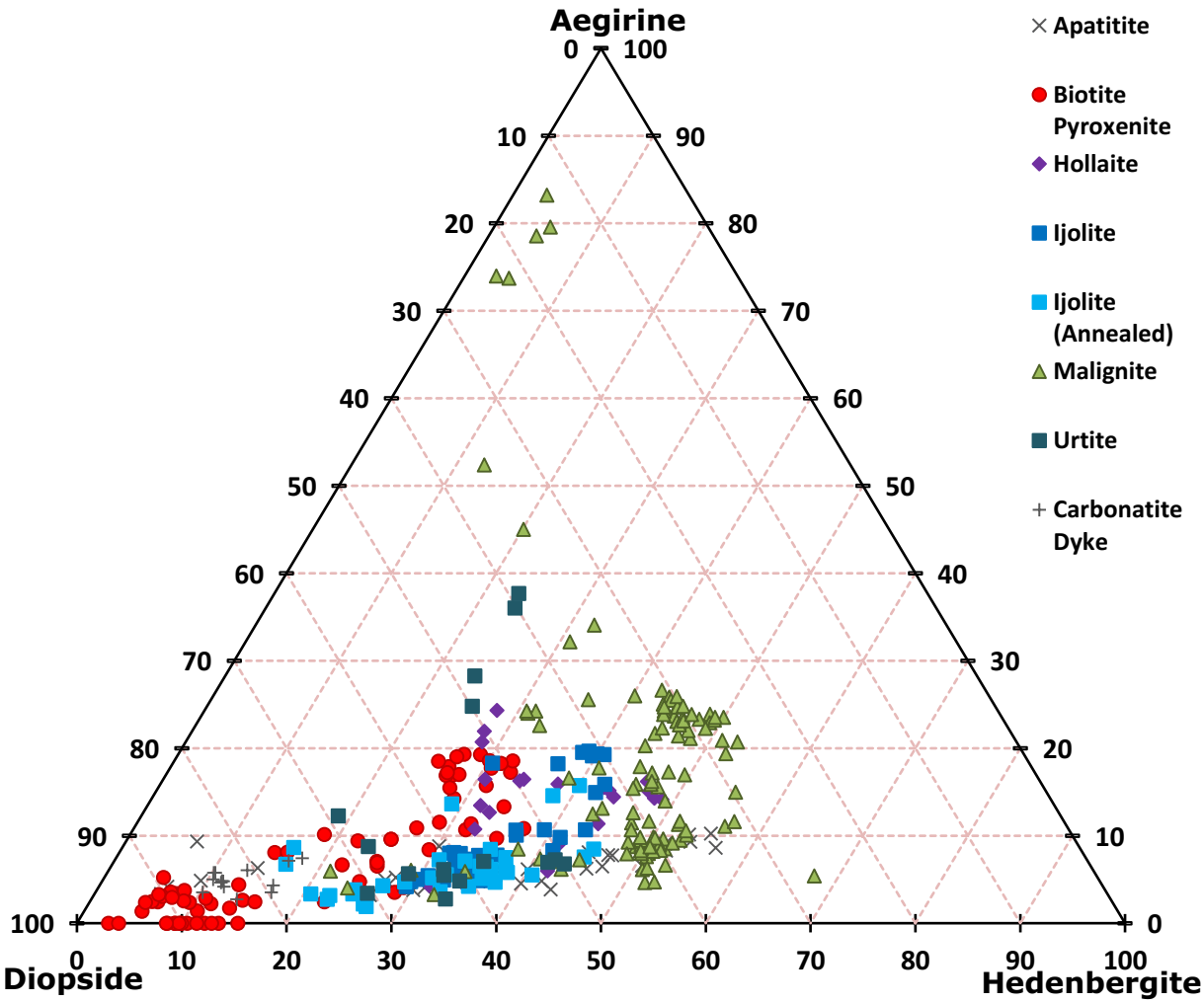

Figure 17: Clinopyroxene compositions (mol. %) from the Prairie Lake complex plotted in the aegirine-diopside-hedenbergite ternary system.

Clinopyroxene compositional data for xenolith-bearing carbonatite dykes occur in a tight cluster of Di_{75-85} coinciding with compositions of the Di-cores from the biotite pyroxenite. Clinopyroxene from apatitite NP68B exhibits two distinct compositions for cores and the rims. The cores compositions overlap with those of the diopside cores in the biotite pyroxenites, with Di contents in excess of 80-90 mol. %. Relative to the cores, the rims show a 10-20 mol. % enrichment in Hd and no marked difference in Ae content; these compositions overlap with some of those of the ijolite series rocks. Representative compositions are presented in Table 3.

Most of the pyroxenes from the ijolite series rocks (including micro-ijolites and urtites) fall along a linear trend within the diopside field, with between 20-55 mol. % Hd and less than 10 mol. % Ae. These compositions grade directly into those of the hollaites and malignites with increasing hedenbergite (>45 mol.%) and aegirine (>10 mol.%). A clear outlier of the ijolite series rocks occurs with one of the urtites (PL96A). Representative clinopyroxene compositions from ijolite-series rocks are presented in Table 4.

Clinopyroxene compositions in the malignites are either hedenbergite or aegirine-augite, with most in a well-constrained region between 50-63mol.% Hd, and 5-25mol.% Ae. Pegmatitic malignite (PL46) contains the most Ae-rich compositions with >70mol.% Ae. Representative compositions are presented in Table 5.

Four distinct trends are evident from the compositional data: (1) the biotite pyroxenite trend with the unevolved cores enriched in Di (>Di_{90}), evolving along a linear trend with increased Ae and Hd components to the enriched rims/matrix; (2) the ijolite-series rocks, which follow a parallel evolution trend to that of the biotite pyroxenites, however the ijolites have lower Ae contents. The ijolite trend is from approximately $Di_{75}Ae_5Hd_{20}$ to $Di_{40}Ae_{20}Hd_{40}$; (3) malignite, which mostly appears to be the cumulation of the ijolite trend; (4) the Apatitite trend which follows a fairly linear trend from unevolved Di-rich cores to Di-rich Hedenbergite (~$Di_{25}Ae_{10}Hd_{65}$). These trends are displayed in Fig. 18.

Table 2: Representative compositions of clinopyroxenes from biotite pyroxenites at Prairie Lake.

Sample	**PL-48**		**PL-51**		**PL-55**	
Rock Type	Biotite Pyroxenite		Biotite Pyroxenite		Biotite Pyroxenite	
SiO_2	55.39	52.05	55.18	52.71	51.88	54.46
TiO_2	b.d.	b.d.	b.d.	b.d.	0.26	b.d.
Al_2O_3	b.d.	b.d.	b.d.	0.39	0.65	b.d.
FeO	2.87	13.43	3.48	14.54	14.2	4.07
MnO	0.31	0.74	0.56	0.9	0.89	0.92
MgO	17.04	9.72	16.55	8.79	8.84	15.48
CaO	25.35	20.56	25.43	20.66	21.97	25.51
Na_2O	-	2.24	0.36	2.51	1.72	-
Total	100.96	98.74	101.56	100.5	100.41	100.44
Fe^{3+}	0	5.77	2.01	6.47	4.43	4.07
Fe^{2+}	2.87	8.25	0.56	8.72	10.21	0.92
Structural formula based on 6 atoms of oxygen						
Si	2.002	1.991	1.992	1.987	1.971	1.999
Ti	-	-	-	-	0.007	-
$Al^{(IV)}$	-	-	-	0.013	0.028	-
$Al^{(VI)}$	-	-	-	0.005	0.001	-
$FE3^{(IV)}$	-	0.157	0.024	0.184	0.126	-
FE2	0.087	0.264	0.061	0.275	0.324	0.125
Mn	0.010	0.024	0.017	0.029	0.029	0.029
Mg	0.918	0.555	0.891	0.494	0.501	0.847
Ca	0.982	0.843	0.987	0.835	0.894	1.003
Na	0	0.166	0.032	0.184	0.127	-
Mol. % end members						
$CaTiAl_2O_6$	0	0	0	0	0.75	0
$CaAl_2SiO_6$	0	0	0	0.48	0	0
$NaFeSi_2O_6$	0	16.67	3.22	18.58	12.8	0
$Ca_2Si_2O_6$	49.49	42.29	49.19	42.01	44.78	50.79
$Fe_2Si_2O_6$	4.37	13.22	3.04	13.92	16.38	6.32
$Mg_2Si_2O_6$	46.24	27.82	44.55	25.01	25.29	42.89
Recalculated into aegirine-hedenbergite-diopside						
Ae	0	16.88	3.27	19.26	13.31	0
Hd	8.63	26.78	6.18	28.87	34.09	12.85
Di	91.37	56.34	90.55	51.87	52.6	87.15

Table 3: Representative compositions of clinopyroxenes from carbonatite dykes and apatitites at Prairie Lake.

Sample	PLL-01B	PLL-01L	WS-2D	WS-2E	NP-68	
Rock Type	Carbonatite Dike	Carbonatite Dike	Apatitite	Apatitite	Apatitite	
SiO_2	52.02	53.19	50.62	51.07	53.51	51.66
TiO_2	0.82	0.64	0.78	0.20	0.24	0.26
Al_2O_3	1.79	0.84	1.36	0.81	0.05	1.55
FeO	7.91	4.64	13.89	12.39	5.38	11.06
MnO	b.d.	b.d.	0.83	0.61	0.20	0.7
MgO	13.75	16.73	8.87	9.58	16.43	11.54
CaO	22.83	24.33	23.36	24.47	22.87	22.69
Na_2O	0.93	0.48	0.62	0.86	1.3	0.52
Total	100.05	100.85	100.33	99.99	99.98	99.98
Fe^{3+}	2.4	1.24	1.6	2.22	3.35	1.34
Fe^{2+}	5.35	3.54	12.45	10.4	2.37	9.88
Structural Formula based on 6 atoms of oxygen						
Si	1.933	1.938	1.946	1.945	1.966	1.945
Ti	0.023	0.018	0.008	0.018	-	0.007
$Al^{(IV)}$	0.067	0.036	0.054	0.036	0.002	0.055
$Al^{(VI)}$	0.011	0.026	0.008	0.019	0.032	0.014
$FE3^{(IV)}$	0.067	0.008	0.046	0.045	0.06	0.038
FE2	0.166	0.108	0.400	0.331	0.073	0.0314
Mn	-	-	0.027	0.020	0.006	0.023
Mg	0.762	0.909	0.509	0.544	0.900	0.654
Ca	0.909	0.950	0.971	0.999	0.900	0.924
Na	0.067	0.034	0.046	0.064	0.093	0.038
Mol. % end members						
$CaTiAl_2O_6$	2.29	1.71	0.81	1.73	0	0.75
$CaAl_2SiO_6$	1.13	0	0.81	0	0	1.43
$NaFeSi_2O_6$	6.68	3.31	4.65	6.29	9	3.85
$Ca_2Si_2O_6$	43.62	45.44	48.01	48.61	43.74	45.33
$Fe_2Si_2O_6$	8.3	5.25	20.14	16.41	3.53	15.78
$Mg_2Si_2O_6$	37.99	44.3	25.58	26.96	43.73	32.85
Recalculated into aegirine-hedenbergite-diopside						
Ae	7.12	3.51	4.84	6.77	9.33	4.07
Hd	16.65	10.23	41.92	35.28	6.78	31.13
Di	76.23	86.26	53.24	57.96	83.9	64.8

Table 4: Representative compositions of clinopyroxenes from ijolite series rocks at Prairie Lake.

Sample	NE4-2	PL-76	PL-96A	PL-96A	PL-90	PL-95
Rock Type	Annealed Ijolite	Ijolite	Urtite	Urtite	Hollaite	Hollaite
SiO_2	52.31	50.24	52.04	52.1	53.33	52.46
TiO_2	0.9	0.37	b.d.	b.d.	b.d.	0.2
Al_2O_3	1.97	1.82	0.57	0.64	0.81	0.54
FeO	7.64	12.6	17.86	12.67	11.6	14.69
MnO	0.41	0.72	1.13	0.98	0.87	0.87
MgO	12.85	10.16	6.41	9.69	10.15	8.29
CaO	23.76	23.33	16.68	23.19	23.96	19.54
Na_2O	1.14	0.69	4.76	1.33	0.76	2.79
Total	100.98	99.93	99.45	100.6	101.48	99.38
Fe^{3+}	2.94	1.78	12.26	2.34	1.96	7.19
Fe^{2+}	5.00	11.00	6.82	10.56	9.84	8.22
Structural formula based on 6 atoms of oxygen						
Si	1.925	1.914	1.981	1.981	1.990	1.995
Ti	0.249	0.011	-	-	-	0.006
$Al^{(IV)}$	0.075	0.082	0.019	0.019	0.010	0.006
$Al^{(VI)}$	0.011	0.005	0.006	0.010	0.026	0.019
$FE3^{(IV)}$	0.081	0.046	0.351	0.067	0.055	0.206
FE2	0.154	0.350	0.217	0.336	0.307	0.261
Mn	0.013	0.023	0.036	0.032	0.028	0.025
Mg	0.705	0.602	0.364	0.549	0.565	0.470
Ca	0.937	0.952	0.680	0.945	0.958	0.796
Na	0.081	0.051	0.351	0.061	0.055	0.206
Mol. % end members						
$CaTiAl_2O_6$	2.5	1.05	0	0	0	0.28
$CaAl_2SiO_6$	1.09	0	0.65	0.97	1.03	0
$NaFeSi_2O_6$	8.16	5.05	35.66	6.8	5.64	21.19
$Ca_2Si_2O_6$	45.19	46.68	34.2	47.38	48.62	40.86
$Fe_2Si_2O_6$	7.71	17.37	11.03	17.01	15.75	13.47
$Mg_2Si_2O_6$	35.36	29.84	18.46	27.83	28.96	24.21
Recalculated into aegirine-hedenbergite-diopside						
Ae	8.65	5.13	37.68	7.05	5.93	21.95
Hd	16.36	34.9	23.3	35.27	33.13	27.9
Di	74.99	59.69	39.02	57.69	60.94	50.15

Table 5: Representative compositions of clinopyroxenes from malignites at Prairie Lake.

Sample	ETR-3	PL-38	PL-46		PL-42	
Rock Type	Malignite	Malignite	Pegmatitic Malignite		Pegmatitic Malignite	
SiO_2	48.88	51.15	49.65	51.18	50.18	49.84
TiO_2	1	b.d.	b.d.	b.d.	b.d.	0.58
Al_2O_3	3.08	0.48	0.52	0.1	0.64	1.86
FeO	12.29	19.2	19.63	24.57	22.03	16.98
MnO	0.47	1.71	1.22	1.04	1.36	1.01
CaO	23.3	17.82	19.14	6.94	18.14	22.52
MgO	10.36	5.49	5.42	2.56	4.72	6.98
Na_2O	0.78	3.85	2.82	10.2	3.14	1.11
Total	100.16	99.7	98.4	96.59	100.21	100.88
Fe^{3+}	2.01	8.37	7.27	26.28	8.09	2.86
Fe^{2+}	10.48	11.67	13.09	0.92	14.75	14.41
Structural formula based on 6 atoms of oxygen						
Si	1.865	1.990	1.964	1.989	1.960	1.922
Ti	0.029	-	-	-	-	0.017
$Al^{(IV)}$	0.136	0.010	0.024	0.005	0.030	0.078
$Al^{(VI)}$	0.003	0.012	0.012	0.007	0.011	0.007
$FE3^{(IV)}$	0.058	0.245	0.204	0.762	0.227	0.083
FE2	0.334	0.380	0.433	0.030	0.482	0.465
Mn	0.015	0.056	0.041	0.034	0.045	0.033
Mg	0.589	0.318	0.320	0.125	0.275	0.401
Ca	0.952	0.743	0.811	0.289	0.759	0.931
Na	0.058	0.245	0.216	0.769	0.238	0.083
Mol. % end members						
$CaTiAl_2O_6$	2.84	0	0	0	0	1.69
$CaAl_2SiO_6$	0.29	1.04	0	0	0	0.67
$NaFeSi_2O_6$	5.7	25.26	21.67	77.59	23.88	8.36
$Ca_2Si_2O_6$	45.51	37.75	40.63	14.59	38.12	45.67
$Fe_2Si_2O_6$	16.53	19.55	21.69	1.51	24.19	23.4
$Mg_2Si_2O_6$	29.13	16.4	16.01	6.32	13.8	20.21
Recalated into aegirine-hedenbergite-diopside:						
Ae	5.9	25.99	22.32	83.21	23.91	8.75
Hd	34.07	40.24	44.69	3.24	48.45	48.96
Di	60.03	33.76	32.99	13.55	27.65	42.29

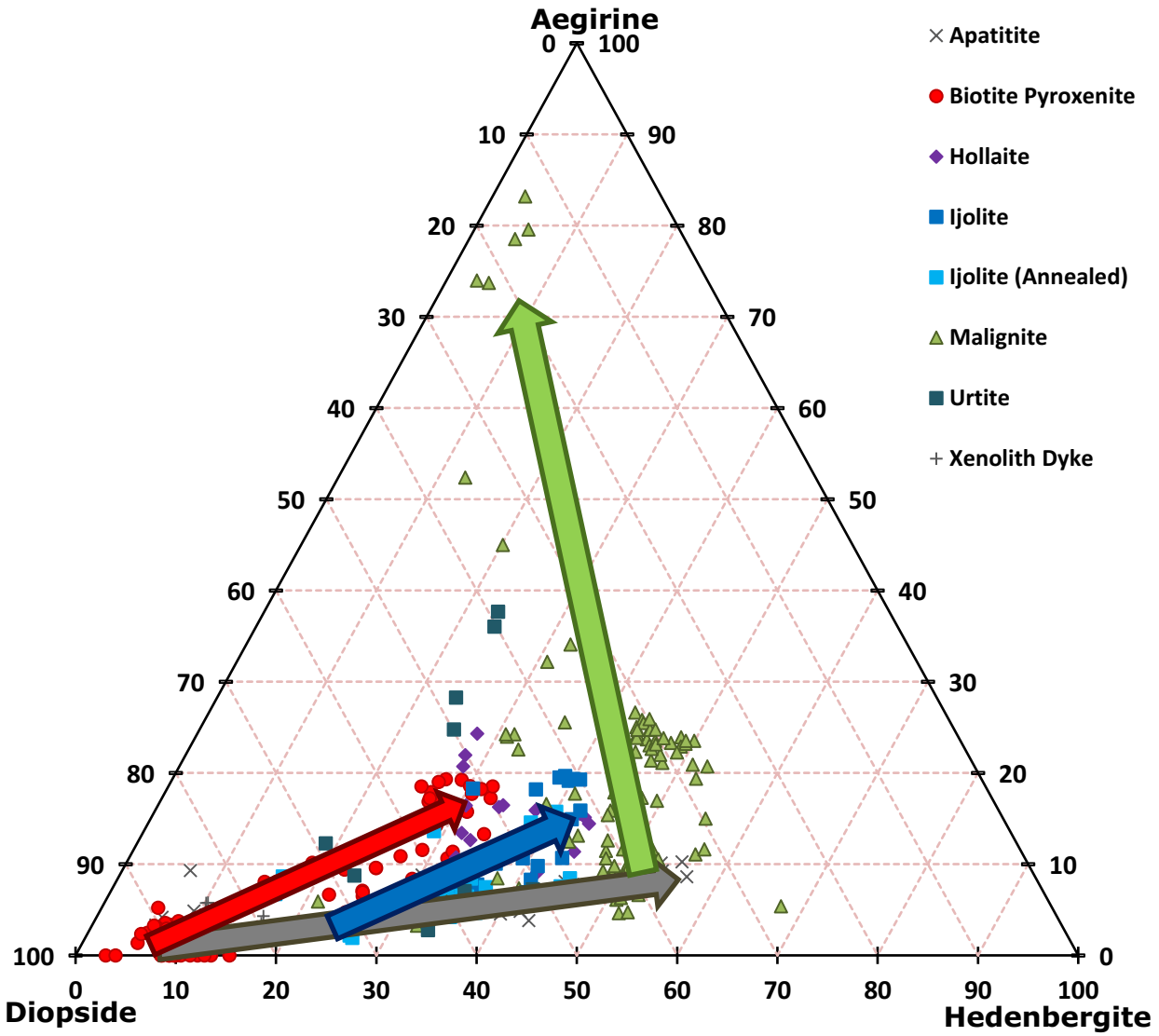

Figure 18: Clinopyroxene compositions from the Prairie Lake complex with trends from unevolved to evolved compositions displayed as arrows. The biotite pyroxenite trend (1) is red; the ijolite series trend (2) is blue; the malignite trend (3) is green; and the apatitite trend (4) is grey.

3.2.1.2 – Garnet

Garnet compositions belong to the andradite ($Ca_3Fe^{3+}{}_2Si_3O_{12}$) – schorlomite ($Ca_3Ti_2SiFe^{3+}{}_2O_{12}$) – morimotoite ($Ca_3TiFe^{2+}Si_3O_{12}$) solid solution series (Grew et al., 2013) and can be represented in the And-Sch-Mor ternary system (Fig. 19). The garnets are a late-forming mineral, with andradite grading in composition into And-rich morimotoite.

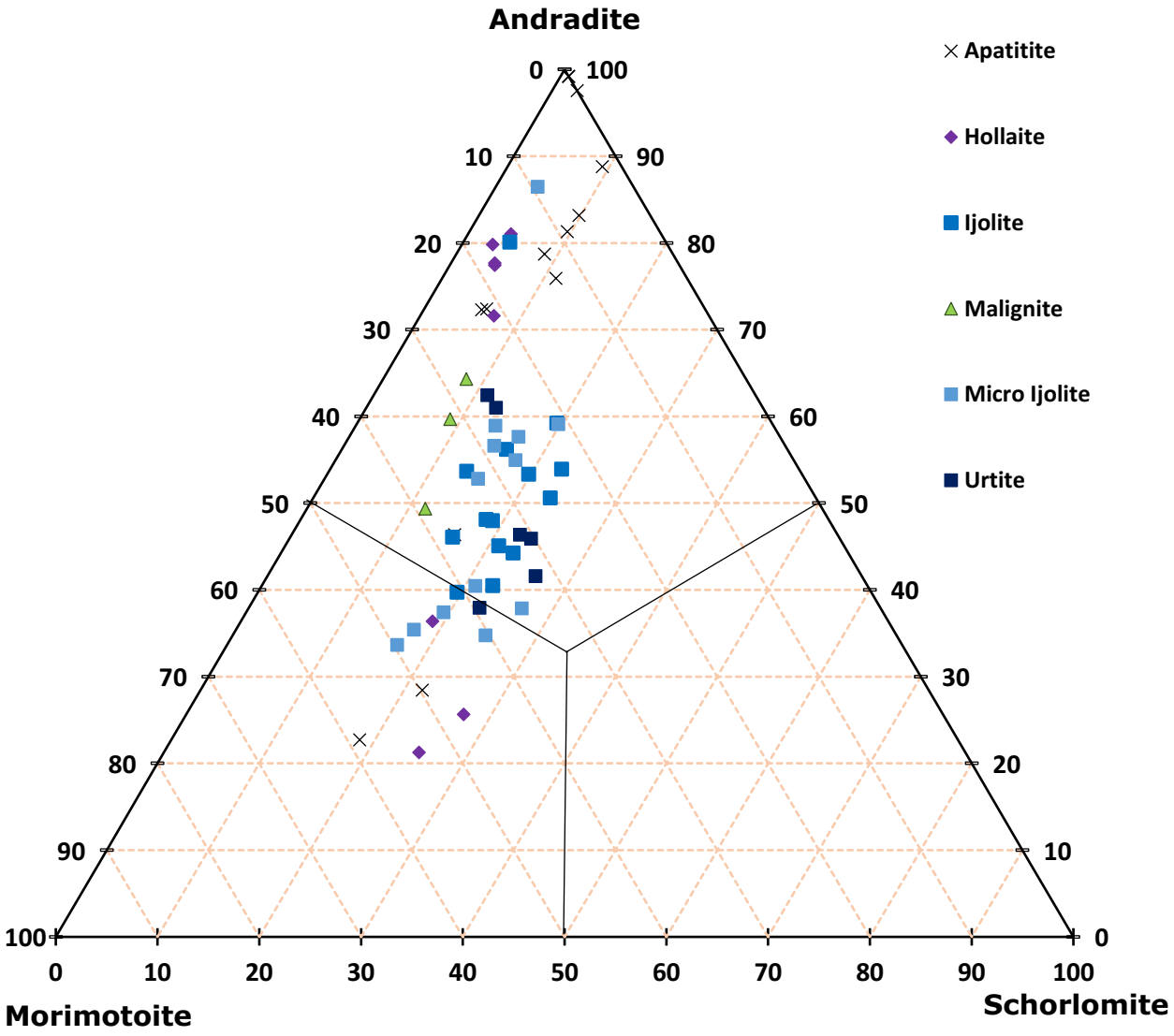

Figure 19: Garnet compositions from Prairie Lake plotted on the andradite-schorlomite-morimotoite ternary system.

The majority of garnet compositions from ijolite, micro-ijolite and urtite define a trend between 30-60 mol.% andradite, 10-30 mol.% schorlomite, and 20-50 mol.% morimotoite. Malignite garnets plot toward the andradite end of this trend, very close to those of the ijolites. Representative compositions are presented in Table 6 and 7. Ti contents in garnet at Prairie Lake vary from 2.59 to 14.92 wt.% TiO_2.

Table 6: Representative garnet compositions from the ijolite-series at Prairie Lake. End members calculated using the Excel program of Locock (2008)

Sample	**ETR-7B**	**PL-20**	**PL-76**	**PL-85**	**ETR-6A**	**PL-96A**
Rock type	Ijolite	Ijolite	Ijolite	Ijolite (Annealed)	Ijolite (Annealed)	Urtite
SiO_2	31.38	30.54	31.17	31.40	30.50	28.89
TiO_2	10.32	13.11	8.93	9.79	8.83	11.10
ZrO_2	1.22	2.49	1.74		1.34	2.58
Al_2O_3	2.30	1.65	2.38	1.53	2.47	2.28
FeO / FeO_{tot}	19.73	20.98	20.29	21.37	22.45	20.38
MnO	0.51	0.58	0.47	0.59	0.40	0.37
MgO	0.74	-	0.84	0.63	0.68	0.92
CaO	31.95	32.21	32.56	32.24	31.55	31.80
Total (calc)	98.15	101.56	98.38	97.63	98.22	98.32
final FeO	4.75	7.91	2.63	2.96	3.16	3.28
final Fe2O3	16.65	14.53	19.63	20.46	21.44	19.01
End-members:						
Kimzeyite	2.51	5.05	3.57	-	2.76	5.35
Schorlomite	6.03	14.80	7.02	9.57	8.79	15.61
Schorlomite-Al	8.94	3.04	8.23	7.63	9.54	6.08
Morimotoite	33.54	46.41	18.52	20.91	19.50	23.34
Morimotoite-Mg	2.10	0.00	7.53	5.67	-	4.36
Andradite	43.26	26.45	53.01	53.39	54.66	41.93
Calderite	1.22	1.36	1.12	1.41	0.95	0.89
Skiagite	-	2.88	-	-	0.94	
Khoharite	2.41	-	1.00%	0.76	2.86	2.44
Remainder	0	0	0	0	0	0
Total	100.01%	99.99%	100.00%	100.00%	100.00%	100.00
Recalculated into:						
Andradite	46.09	29.16	56.21	54.94	59.10	45.92
Schorlomite	15.95	19.67	16.17	17.70	19.82	23.75
Morimotoite	37.97	51.17	27.62	27.35	21.08	30.33

The most morimotoite-rich garnet is found in clinopyroxene carbonatite and apatitite. Sample WS01, a wollastonite-clinopyroxene apatitite contains anhedral garnet ranging in colour from brown- to-opaque. The garnets display a bimodal distribution, containing both almost-pure andradite (72 – 99 % An) and some morimotoite rich components with <30% An with a large composition gap between these compositions.

Table 7: Representative garnet compositions from malignite, hollaites and apatitites at Prairie Lake, end members calculated using the Excel program by Locock (2008)

Sample	PL-38	PL-86	PL-90	PL-95	WS-1-04	NP-68
Rock type	Malignite	Hollaite	Hollaite	Hollaite	Apatitite	Apatitite
SiO2	33.29	34.74	29.96	29.11	26.87	30.34
TiO2	6.51	4.05	11.50	11.86	11.41	10.68
ZrO2	0.00	b.d.	2.60	1.74	8.46	3.49
Al2O3	0.48	1.63	1.14	0.80	1.72	0.58
V2O3	0.56	b.d.	0.85	b.d.	b.d.	0.49
FeO / FeO_{tot}	23.57	24.04	18.77	19.95	16.15	19.77
MnO	0.66	0.45	0.72	0.87	0.30	0.51
MgO	b.d.	0.00	0.80	0.80	2.06	0.73
CaO	31.89	32.73	32.11	29.87	30.86	31.51
Total (calc)	96.96	97.64	98.45	95.40	97.83	98.64
final FeO	4.14	2.79	4.39	4.06	3.81	3.23
final Fe2O3	21.60	23.61	15.98	17.66	13.71	18.38
End-members:						
Kimzeyite	-	-	5.41	3.72	8.86	2.91
Schorlomite	5.38	-	16.52	18.21	14.51	13.67
Schorlomite-Al	2.42	4.13	0.32	0.41	-	-
Morimotoite	26.24	17.33	31.32	29.78	27.88	22.98
Morimotoite-Mg	-	-	8.77	4.41	18.16	9.13
Goldmanite	1.92	-	2.91	-	-	1.67
Spessartine	-	1.07	-	-	-	-
Almandine	-	0.77	-	-	-	-
Grossular	-	2.10	-	-	-	-
Andradite	61.34	74.61	32.55	35.89	17.79	39.58
Calderite	1.59	-	1.73	2.15	0.74	1.23
Skiagite	1.10	-				
Khoharite	-	-	0.47	2.02	2.90	0.04
Remainder	0	0	0	0	0	0
Total	99.99%	100.01%	100.00%	99.99%	100.01%	99.99%
Recalculated Into:						
Andradite	64.31	77.66	36.38	40.46	22.71	46.37
Schorlomite	8.18	4.30	18.82	20.99	18.52	16.01
Morimotoite	27.51	18.04	44.80	38.55	58.77	37.62

3.2.1.4 – Nepheline

Nepheline is an essential mineral in the ijolite-series rocks and normally occurs as an early-forming phase, commonly as euhedral crystals; especially in urtites. Thirteen representative compositions from five samples of different rock types were plotted on the nepheline-kalsilite-quartz ternary system. Nepheline compositions are consistent, plotting in the narrow range of $Ne_{72.5\text{-}75}Ks_{25\text{-}27}Qz_{<1.5}$ (Fig. 20). The only notable outlier is nepheline from a malignite which plots as $Ne_{70.5}Ks_{20.6}Qz_{4}$. All nephelines plot in the Morozewicz – Buerger convergence field for fully-equilibrated plutonic nepheline (Tilley, 1954). Representative nepheline compositions presented in Table 8.

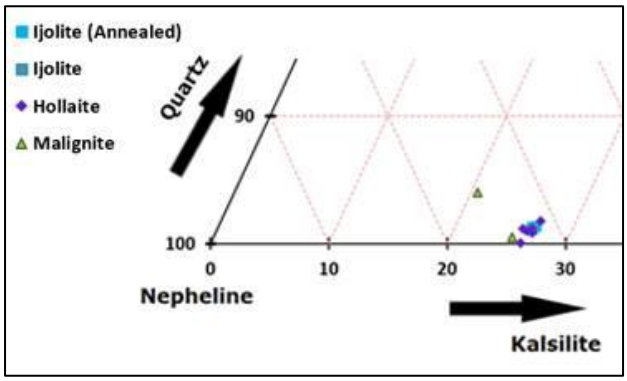

Figure 20: Nepheline compositions from Prairie Lake displayed on a nepheline-kalsilite-quartz ternary (mol. %)

Table 8: Representative nepheline compositions from Prairie Lake recalculated into nepheline-kalsilite-quartz (mol. %)

Sample	PL36	PL86	PL76	PL90	ETR7B
Rock Type	Malignite	Wollastonite Hollaite	Ijolite	Hollaite	Annealed Ijolite
SiO_2	41.2	40.77	41.75	41.79	41.82
Al_2O_3	33.91	34.11	34.01	33.83	33.29
FeO	1.19	0.84	0.86	0.77	0.92
NaO	16.09	15.5	16.08	15.75	15.76
K_2O	7.47	7.64	7.83	7.91	7.93
Total	99.86	98.86	100.53	100.05	99.72
Structural formula based on 8 oxygen:					
Si	1.007	1.004	1.013	1.017	1.023
Al	0.977	0.990	0.972	0.970	0.959
Fe	0.024	0.017	0.017	0.016	0.019
Na	0.762	0.740	0.756	0.743	0.747
K	0.233	0.240	0.242	0.246	0.247
Total	3.003	2.991	3.001	2.992	2.9951
Recalculated into Nepheline-Kalsilite-Quartz (mol. %):					
Ne	74.27	72.74	73.28	72.25	72.23
Kal	25.26	26.27	26.14	26.58	26.63
Qtz	0.48	0.99	0.58	1.16	1.14

3.2.1.3 – Biotite

Mica, which varies in colour from deep red to pale brown, is present in the majority of samples. In the ijolite series, biotite is usually a minor or trace mineral, commonly late-stage, and is found associated with apatite and calcite. It is a major constituent of the biotite pyroxenites, in which it can comprise up to 65 vol. %. In the Mg-Fe-Al ternary system, the compositions plot close to the annite phlogopite binary with some enrichment in Al (Fig. 21). There is no substitution of K by Ba. Representative compositions presented in Table 9 and 10.

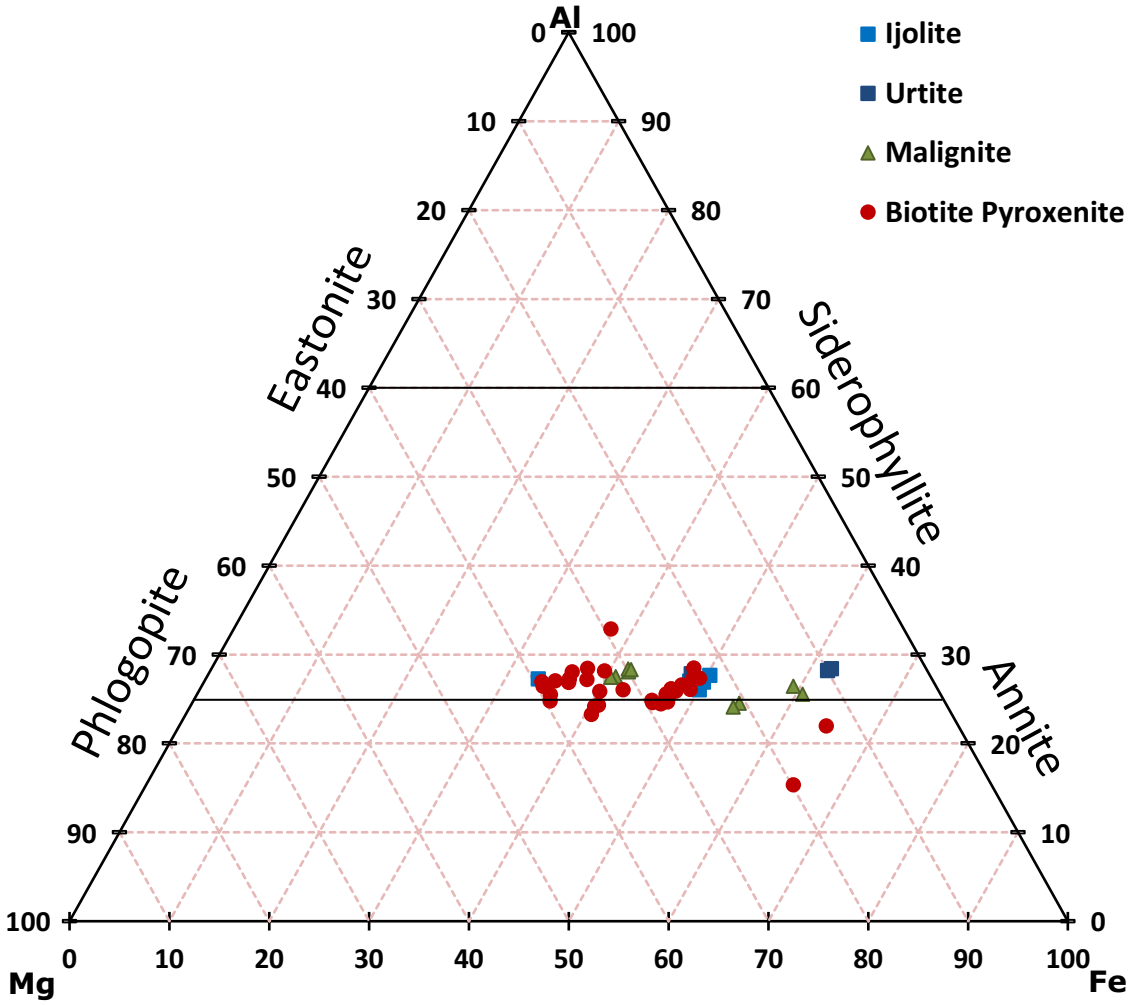

Figure 21: Mica compositions from Prairie Lake in an Al, Fe and Mg (a.p.f.u.) ternary.

Table 9: Representative compositions of micas from ijolite-series rocks and malignites from Prairie Lake

Sample	PL76		PL96A		PL67		PL46	
Rock	Ijolite		Urtite		Malignite		Porphyry Malignite	
	Ox. %	22 Ox	Ox. %	22 Ox	Ox. %	22 Ox	Ox. %	22 Ox
SiO_2	35.43	5.74	35.34	5.7	36.38	5.69	35.6	5.82
TiO_2	2.09	0.25	2.53	0.34	2.96	0.35	1.83	0.22
Al_2O_3	11.32	2.18	11.34	2.15	11.75	2.17	9.72	1.87
FeO	29.29	3.97	27.78	3.74	24.89	3.25	30.95	4.23
MnO	0.69	0.09	1.44	0.2	0.9	0.12	1.57	0.22
MgO	7.19	1.74	7.66	1.84	9.96	2.32	6.86	1.67
K_2O	9.32	1.93	9.55	1.96	9.91	1.98	9.46	1.97
Total	95.33	15.9	95.64	15.93	96.75	15.88	95.99	16

Table 10: Representative compositions of micas from biotite pyroxenites from Prairie Lake

Sample	PL38		PL48		PL51		PL55	
Rock	Biotite Pyroxenite		Biotite Pyroxenite		Biotite Pyroxenite		Biotite Pyroxenite	
	Ox. %	22 Ox	Ox. %	22 Ox	Ox. %	22 Ox	Ox. %	22 Ox
SiO_2	35.2	5.74	38.02	5.77	36.42	5.82	36.66	5.78
TiO_2	3.00	0.37	2.38	0.27	2.82	0.34	2.83	0.33
Al_2O_3	10.85	2.08	11.5	2.06	9.88	1.86	11.44	2.11
FeO	27.19	3.71	21.05	2.67	23.4	3.13	21.57	2.82
MnO	1.18	0.16	0.9	0.12	0.69	0.09	0.89	0.12
MgO	7.48	1.81	13.56	3.07	11.23	2.67	12.05	2.81
K_2O	9.46	1.97	9.96	1.93	9.87	2.01	9.79	1.95
Total	94.36	15.84	97.37	15.89	94.31	15.92	95.23	15.92

3.2.1.5 - Other minerals

A common feature in ijolite-series rocks is alteration of nepheline into a mixture of K-feldspar + zeolites especially as the ijolites grade into malignites. Cancrinite is commonly found as an alteration product of nepheline, primarily occurring as a rim when nepheline is in contact with later-stage calcite.

Apatite is found in the majority of the samples investigated, with contents varying from a trace mineral, usually associated with late-stage calcite, to <50 vol.% in apatitites. Commonly the apatite is F-bearing. Apatite in apatitite (NP68) can show zonation in BSE-images. Wollastonite is found in relatively few of the samples investigated (WS01, WS2B and PL86) predominantly occurring in wollastonite-apatite xenolith, and in apatitites.

Calcite found in the ijolites and biotite pyroxenites at Prairie Lake commonly occurs as a late-stage mineral usually interstitial between earlier-forming minerals. The majority of the calcite shows some enrichment in Sr (~1.3-1.5 wt. % SrO). Additional carbonates present include strontianite ($SrCO_3$) in malignite (WT7, Fig. 22A), pegmatitic malignite (PL42, PL46), and biotite pyroxenite (PL48) and barytocalcite $(BaCa)CO_3$ present in biotite pyroxenite (PL48). Representative carbonate compositions are presented in Table 11.

Table 11: Representative compositions of carbonate minerals from Prairie Lake

Sample	PL48		PL48		ETR7B		PL46	
Rock Type	Biotite Pyroxenite		Biotite Pyroxenite		Ijolite (Annealed)		Pegmatitic Malignite	
Mineral	Barytocalcite		Strontalcite		Calcite		Calcite	
	wt. %	6 O	wt. %	6 O	wt. %	6 O	wt. %	6 O
FeO	-	-	-	-	0.34	0.04	-	-
CaO	20.00	3.22	5.06	0.77	50.78	5.84	51.32	5.88
SrO	-	-	58.53	4.85	1.30	0.08	1.89	0.12
BaO	47.07	2.78	6.70	0.38	-	-	-	-
Σ	67.07	6.00	70.24	6.00	52.42	5.96	53.20	6.00

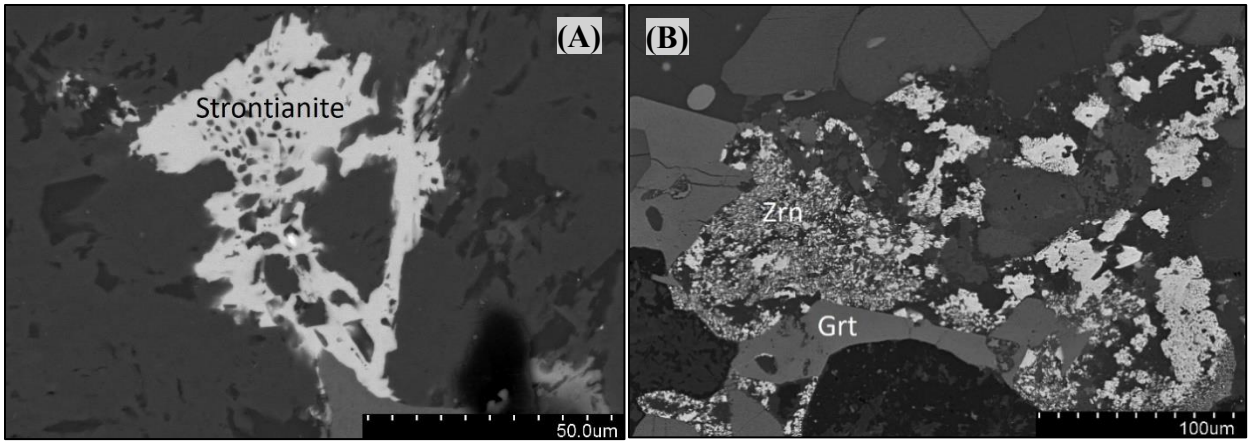

Figure 22: Trace minerals from Prairie Lake (A) BSE image of strontianite ($SrCO_3$) found in WT7; (B) zircon ($ZrSiO_4$) from WT7

Titaniferous magnetite is present in all major rock suites at Prairie Lake including ijolite series rocks, biotite pyroxenite, malignite and apatitite. Nb- and Zr- bearing trace minerals are common in much of the complex, especially in the biotite pyroxenites and malignites. Several Zr-bearing minerals occur in trace amounts in the malignites and the biotite pyroxenite, including wadeite, catapleiite, calzirtite, zircon (Fig. 22B), and baddeleyite. In biotite pyroxenite (PL48), zircon is found in close association with pyrochlore. Representative compositions for wadeite, baddeleyite and calzirtite are presented in Table 12.

Table 12: Selected Zr-bearing trace minerals: wadeite, baddeleyite, and calzirtite

Sample	PL48		PL42		PL42	
Rock Type	Biotite Pyroxenite		Pegmatitic Malignite		Pegmatitic Malignite	
	Wadeite		Baddeleyite		Calzirtite	
	wt. %	9 O	wt. %	2 O	wt. %	16 O
CaO	-	-	0.90	0.02	11.51	1.90
SiO2	44.48	2.97	-	-	-	-
TiO_2	-	-	1.98	0.03	16.80	1.88
FeO	-	-	0.85	0.01	1.29	0.16
MnO	-	-	0.36	0.01	-	-
K_2O	23.40	1.99	-	-	-	-
ZrO2	31.88	1.04	94.04	0.93	70.00	5.09
Nb_2O_5	-	-	1.86	0.02	-	-
Σ	99.77	5.99	100.00	1.02	99.60	9.03

Members of the marianoite-wöhlerite series were found in samples of biotite pyroxenite and malignite. Marianoite is more common than wöhlerite, with enrichment in Nb relative to Zr. Representative compositions are provided in Table 13.

Table 13: Representative compositions of Marianoite from the Prairie Lake carbonatite Complex

Sample	PL48		PL55		PL46	
Rock Type	Biotite Pyroxenite		Biotite Pyroxenite		Pegmatitic Malignite	
Mineral	Marianoite		Marianoite		Marianoite	
	wt. %	14 O	wt. %	14 O	wt. %	6 O
SiO_2	30.49	3.03	30.02	3.02	30.87	1.31
TiO_2	0.68	0.03	-	-	-	-
FeO	0.81	0.07	-	-	0.87	0.03
CaO	28.33	3.01	28.08	3.03	28.95	1.31
NaO	7.45	1.43	7.84	1.53	7.60	0.62
MnO	0.27	0.02	-	-	0.35	0.01
MgO	0.33	0.05	-	-	-	-
ZrO_2	14.08	0.68	14.80	0.73	14.08	0.29
Nb_2O_5	15.41	0.69	16.47	0.75	16.87	0.32
F	2.80	0.88	2.61	0.83	2.52	0.34
Σ	97.84	9.04	97.21	9.00	99.56	3.90

3.2.2 – Fen Complex

3.2.2.1 – Clinopyroxene

Clinopyroxene compositions from the Fen complex can also be represented on the Di-Hd-Ae ternary system (Fig. 23). One hundred and ninety-two compositions were collected from 13 samples, primarily members of the ijolite series together with vipetoite, a hornblende-biotite-calcite pyroxenite with accessory albite and nepheline. Representative clinopyroxene compositions from Fen are presented in Tables 14-16.

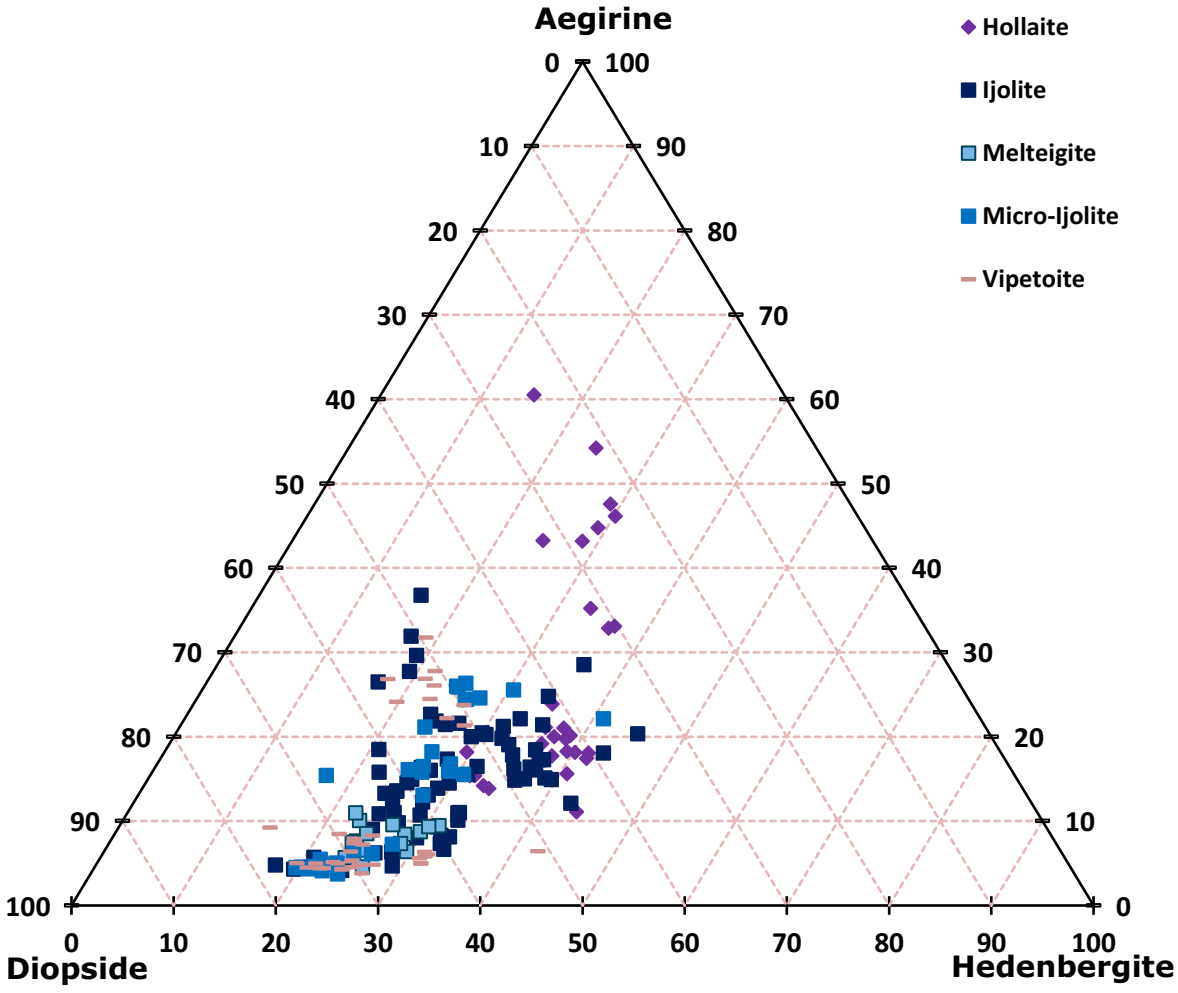

Figure 23: Clinopyroxene compositions from ijolite-series rocks and vipetoite from the Fen complex plotted on the diopside-hedenbergite-aegirine ternary.

Table 14: Representative compositions for clinopyroxenes from ijolites and micro-ijolites at Fen.

Sample	*Fen 35*	*Fen 48*	*Fen49*	*Fen 204*	*Fen 200*	*Fen 201*
Rock Type	Ijolite	Ijolite	Ijolite	Ijolite	Micro-ijolite	Micro-ijolite
SiO_2	49.59	51.55	46.99	50.33	50.86	47.94
TiO_2	0.69	0.66	0.33	0.43	0.063	b.d.
Al_2O_3	1.79	1.81	4.81	1.89	1.31	4.37
FeO	15.63	13.36	11.05	11.08	14.06	8.17
MnO	0.61	0.61	1.82	1.42	0.48	2.31
MgO	7.75	9.01	9.51	10.55	9.21	12.35
CaO	21.55	21.61	23.11	22.46	21.77	24.56
Na_2O	2.08	2.01	1.29	1.42	2.04	0.71
Total	99.69	100.62	98.91	99.58	99.793	100.41
Fe^{3+}	5.36	5.18	3.32	3.66	5.26	1.83
Fe^{2+}	10.81	9.3	8.06	7.79	9.33	6.52
Structural formula based on 6 atoms of oxygen:						
Si	1.912	1.930	1.805	1.922	1.931	1.798
Ti	0.018	0.017	0.053	0.018	-	0.065
$Al^{(IV)}$	0.081	0.066	0.195	0.078	0.059	0.193
$Al^{(VI)}$	0.006	0.014	0.023	0.007	0.011	0.009
$FE3^{(IV)}$	0.149	0.146	0.096	0.105	0.140	0.042
FE2	0.349	0.292	0.259	0.249	0.296	0.205
Mn	0.023	0.021	0.011	0.014	0.020	0
Mg	0.446	0.504	0.545	0.601	0.521	0.690
Ca	0.890	0.869	0.951	0.919	0.885	0.987
Na	0.156	0.146	0.096	0.105	0.150	0.052
Mol. % end members:						
$CaTiAl_2O_6$	1.76	1.73	5.2	1.83	1.36	6.35
$CaAl_2SiO_6$	0	1.41	2.28	0.68	0	0
$NaFeSi_2O_6$	15.45	14.71	9.5	10.49	14.89	5.04
$Ca_2Si_2O_6$	43.35	42.12	43.29	44.6	43.22	44.95
$Fe_2Si_2O_6$	17.31	14.68	12.8	12.41	14.69	9.98
$Mg_2Si_2O_6$	22.13	25.35	26.93	29.98	25.84	33.68
Recalated into aegirine-hedenbergite-diopside:						
Ae	16.38	15.52	10.68	11.01	15.52	5.45
Hd	36.7	30.98	28.78	26.06	30.61	21.61
Di	46.92	53.5	60.54	62.93	53.87	72.94

Table 15: Representative compositions of clinopyroxenes from melteigite and hollaites at Fen.

Sample	*Fen 43*	*Fen 43*	*419 (Fen)*	*419 (Fen)*	*(Fen) 418*	*Fen 405*
Rock Type	Melteigite	Melteigite	Hollaite	Hollaite	Hollaite	Hollaite
SiO_2	49.84	52.57	51.76	50.97	51.78	50.9
TiO_2	0.4	0.39	0.88	0.83	1.01	0.65
Al_2O_3	3.58	1.45	1.23	1.58	1.15	1.58
FeO	10.91	7.43	21.09	19.91	16.84	14.42
MnO	1.63	0.36	0.35	1.01	b.d.	0.51
MgO	10.96	12.96	4.18	5.06	6.94	8.98
CaO	22	23.38	14.87	17.08	20.31	21.21
Na_2O	1.18	0.97	5.51	4.33	2.61	1.86
V_2O_3	-	-	0.44	0.38	b.d.	b.d.
Total	100.5	99.51	100.31	101.15	100.64	100.11
Fe^{3+}	3.04	2.5	14.2	11.16	6.72	4.79
Fe^{2+}	8.17	5.18	8.32	9.47	10.29	10.11
Structural formula based on 6 Oxygen:						
Si	1.868	1.959	1.973	1.942	1.975	1.937
Ti	0.046	0.010	0.010	0.029	0	0.015
$Al^{(IV)}$	0.132	0.041	0.028	0.058	0.025	0.063
$Al^{(VI)}$	0.026	0.022	0.028	0.013	0.027	0.008
$FE3^{(IV)}$	0.086	0.070	0.407	0.320	0.193	0.137
FE2	0.256	0.161	0.265	0.302	0.328	0.322
Mn	0.013	0.012	0.028	0.027	0.033	0.021
Mg	0.612	0.720	0.238	0.287	0.395	0.509
Ca	0.883	0.933	0.607	0.697	0.830	0.865
Na	0.086	0.070	0.407	0.317	0.193	0.137
Mol. % end members:						
$CaTiAl_2O_6$	4.6	1.02	1.03	2.96	0	1.46
$CaAl_2SiO_6$	2.58	2.13	0.77	0.05	2.51	0.77
$NaFeSi_2O_6$	8.6	7.06	41.94	32.71	19.66	13.77
$Ca_2Si_2O_6$	40.68	45.42	30.37	34.15	41.02	42.28
$Fe_2Si_2O_6$	12.84	8.13	13.65	15.43	16.71	16.14
$Mg_2Si_2O_6$	30.69	36.25	12.23	14.7	20.1	25.57
Recalated into aegirine-hedenbergite-diopside:						
Ae	9.55	7.36	44.76	35.19	21.07	14.17
Hd	26.68	16.97	29.13	33.2	35.83	33.22
Di	63.77	75.67	26.11	31.62	43.09	52.61

Table 16: Representative compositions of clinopyroxenes from vipetoites at Fen.

Sample	*FEN 64*	*FEN 64*	*Fen 70*	*Fen 70*	*Fen 61 (groundmass)*	*Fen 61 (microcrysts)*
Rock Type	Vipetoite	Vipetoite	Vipetoite	Vipetoite	Vipetoite	Vipetoite
SiO_2	46.5	42.03	47.63	50.59	53.18	47.33
TiO_2	0	0.25	0.41	b.d.	0.33	b.d.
Al_2O_3	6.53	10.16	4.87	2.8	1.15	5.44
FeO	8.95	10.01	9.61	7.27	15.06	7.16
MnO	2.29	3.64	2.7	1.19	b.d.	2.41
MgO	11.02	9.29	10.87	12.83	8.27	12.34
CaO	23.43	23.49	23.33	23.56	17.83	24.41
Na_2O	0.91	0.72	1.34	1.13	4.08	0.63
Total	99.63	99.59	100.76	99.37	99.9	99.72
Fe^{3+}	2.34	1.86	3.45	2.91	10.51	1.62
Fe^{2+}	6.84	8.34	6.5	4.65	5.6	5.7
Structural formula based on 6 atoms of oxygen:						
Si	1.757	1.612	1.785	1.891	1.987	1.779
Ti	0.065	0.105	0.076	0.033	-	0.068
$Al^{(IV)}$	0.243	0.389	0.215	0.109	0.013	0.221
$Al^{(VI)}$	0.048	0.071	-	0.014	0.037	0.020
$FE3^{(IV)}$	0.067	0.054	0.097	0.082	0.296	0.046
FE2	0.216	0.267	0.204	0.145	0.175	0.179
Mn	-	0.008	0.013	-	0.010	-
Mg	0.621	0.531	0.607	0.715	0.461	0.691
Ca	0.949	0.965	0.937	0.943	0.714	0.983
Na	0.067	0.054	0.097	0.082	0.296	0.046
Mol. % end members:						
$CaTiAl_2O_6$	6.4	10.26	7.54	3.32	0	6.7
$CaAl_2SiO_6$	4.74	6.9	0	1.38	1.36	1.93
$NaFeSi_2O_6$	6.56	5.23	9.65	8.13	30.25	4.52
$Ca_2Si_2O_6$	41.11	38.58	42.63	44.47	35.85	44.03
$Fe_2Si_2O_6$	10.64	13.07	10.1	7.21	8.96	8.81
$Mg_2Si_2O_6$	30.55	25.96	30.09	35.48	23.58	34.01
Recalated into aegirine-hedenbergite-diopside:						
Ae	7.39	6.35	10.72	8.69	31.74	5.01
Hd	23.92	31.37	22.43	15.43	18.79	19.55
Di	68.69	62.28	66.85	75.88	49.47	75.45

Pyroxenes from ijolites, micro-ijolites and melteigite overlap in composition, plotting primarily as diopside enriched in the Ae and Hd components. Ijolites display the most compositional variability, with some examples plotting as aegirine-augite or Di-rich hedenbergite. Compositions range from diopside, $Di_{77}Hd_{18}Ae_5$, to aegirine-augite ranging from $Di_{47}Hd_{16}Ae_{37}$ to $Di_{35}Hd_{45}Ae_{20}$. Melteigite pyroxene compositions overlap the ijolite series with a tighter cluster around $Di_{65}Hd_{25}Ae_{10}$. Pyroxenes in micro-ijolites also overlap in composition with those of the ijolites but show greater variation than those of melteigites; from ~$Di_{75}Hd_{21}Ae_4$ to $Di_{44}Hd_{40}Ae_{26}$.

Clinopyroxenes in two vipetoite samples, FEN61 and FEN64, have unevolved compositions with >60mol. %Di, ~25-35 mol.% Hd, and <10mol.% Ae. FEN61 contains more evolved groundmass clinopyroxene with Ae components in excess of 20 mol.% (up to 32 mol. %), Hd between 15-30 mol.%, Di between 50-60 mol.%.

Hollaites clinopyroxene compositions continue from the end of the ijolite trend, with some overlap between evolved clinopyroxene in ijolites and unevolved clinopyroxene in hollaite. This overlap occurs from about $Di_{50}Hd_{30}Ae_{15}$ to $Di_{45}Hd_{35}Ae_{20}$, with hollaites evolving from the latter towards $Di_{20}Hd_{20}Ae_{60}$.

A general trend from unevolved ijolite to hollaite is present. The ijolites-series spread out in a roughly conical field from ~75 mol.% Di with increase in both iron and sodium and thus increasing Ae and Hd components. The hollaites represent an extension from the ijolite compositions, showing some overlap with the most enriched ijolites and displaying a mostly-linear evolution. Di-Hd contents occur in roughly equal quantities with increasing Ae component into the aegirine-augite field. These trends are presented in Fig. 24.

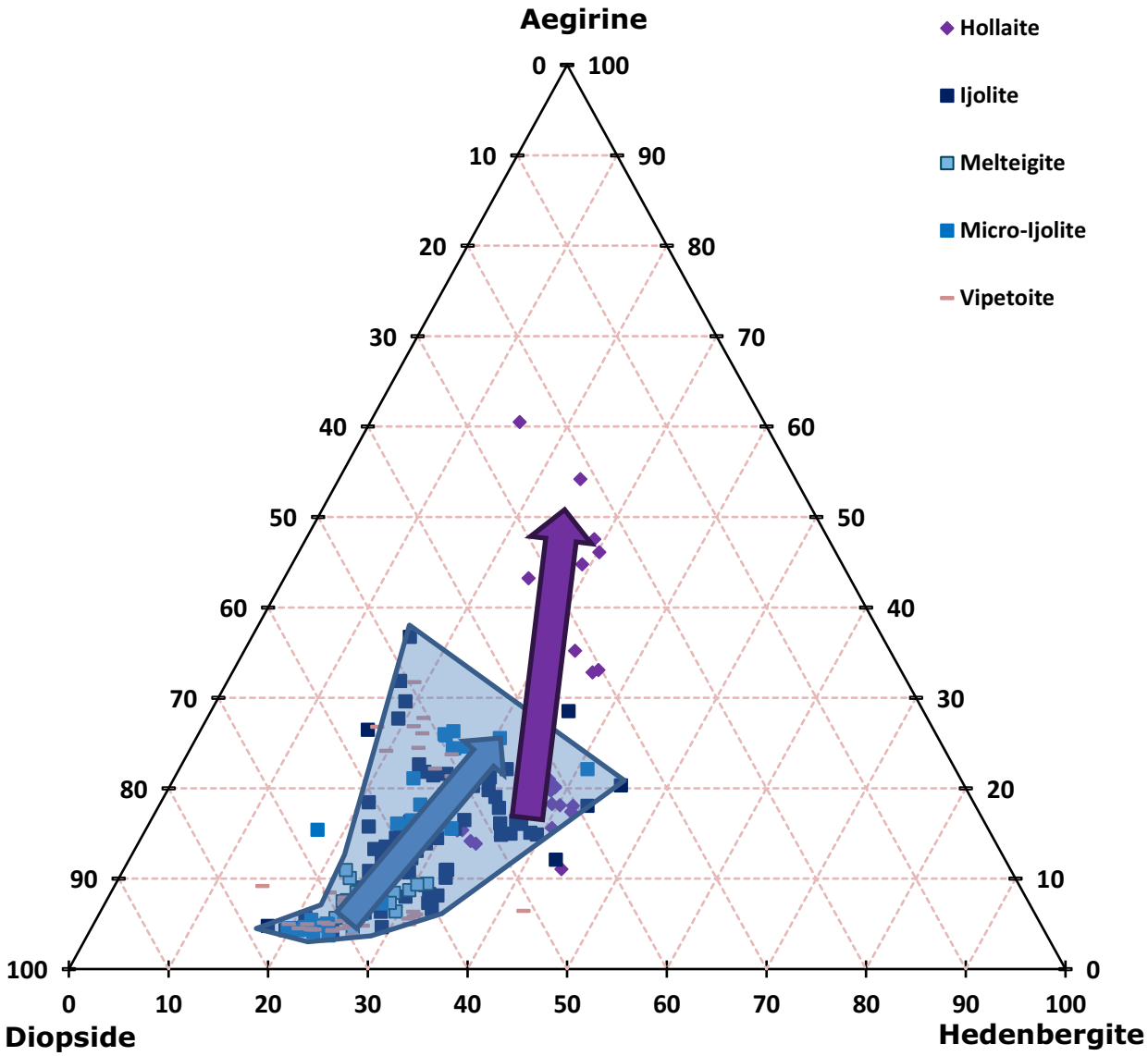

Figure 24: Evolution trends of clinopyroxene for the Fen complex. General evolution of the ijolite-series is shown in blue cumulating in the hollaite trend (purple arrow)

3.2.2.2 – Garnet

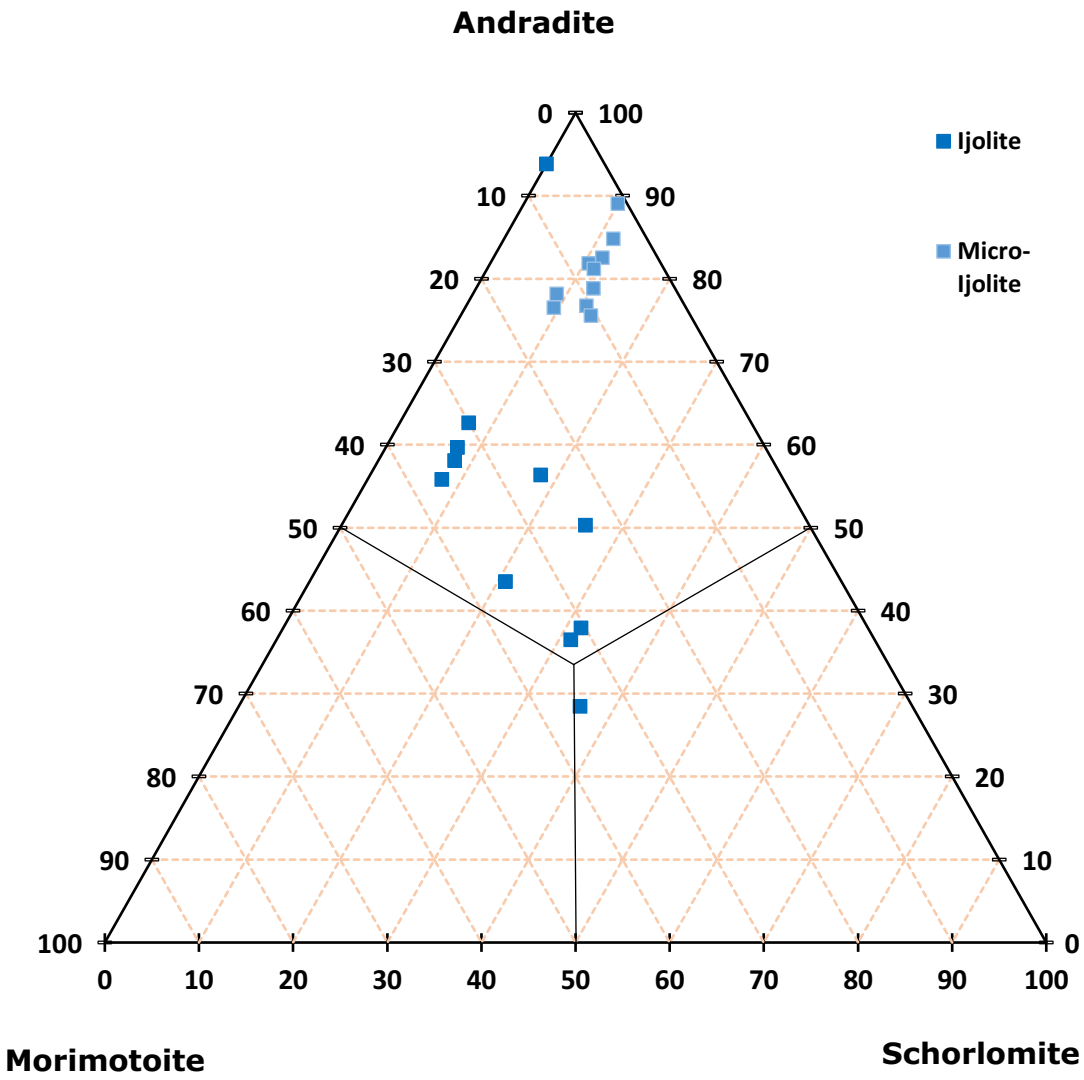

Figure 25: Garnet compositions from Fen plotted on the andradite-schorlomite-morimotoite ternary

Garnets from Fen plot in the andradite-schorlomite-morimotoite ternary system. Almost all samples plot in the andradite field with a lone outlier occurring in the ijolites towards the center of the ternary in the schorlomite field. Representative garnet compositions are presented in Table 17.

The majority of the garnets in ijolites plot in a zone between $And_{29}Sch_{36}Mor_{35}$ and $And_{63}Sch_{7}Mor_{30}$ (Fig. 25). An outlier occurs in the garnet compositions of ijolite (sample Fen35) which contains garnet with no schorlomite component, and thus approaches pure andradite.

Garnets in the micro-ijolites contain a fairly tight cluster of andradite-rich garnets (75 - 90% And) relative to the majority of garnet in ijolite at Fen, with fairly consistent schorlomite (~10%). Most of the garnet in the micro-ijolites occurring between compositions of about $An_{75}Sc_{10}Mo_{15}$ and $An_{90}Sc_{10}Mo_{0}$.

Table 17: Representative garnet compositions from the ijolites at Fen, end members calculated using the Excel program of Locock (2008)

Sample	**Fen 35**	**Fen 43**	**Fen 48**	**Fen 201**	**Fen 201**	**Fen 200**
Rock Type	Ijolite	Ijolite	Ijolite	Micro Ijolite	Micro Ijolite	Micro Ijolite
SiO_2	35.04	28.60	31.98	34.05	33.01	33.82
TiO_2	3.98	14.20	9.67	5.16	7.13	5.48
ZrO_2	b.d.	b.d.	0.66	b.d.	b.d.	b.d.
Al_2O_3	2.06	2.41	1.76	1.16	1.22	1.12
V_2O_3	b.d.	b.d.	b.d.	b.d.	b.d.	0.32
FeO / FeO_{tot}	23.45	19.66	22.19	23.85	22.61	23.10
MnO	0.49	0.48	0.67	0.36	0.38	0.34
MgO	0.37	0.96	0.71	0.36	0.35	0.43
CaO	34.51	32.38	32.76	33.43	32.82	33.12
Na_2O	b.d.	b.d.	b.d.	0.30	0.32	0.18
Total (calc)	99.90	98.69	100.40	98.67	97.84	97.91
final FeO	0.11	3.29	3.41	0.13	1.34	0.99
final Fe_2O_3	25.94	18.19	20.87	26.36	23.63	24.57
End-members:						
Kimzeyite	-	-	1.33	-	-	-
Schorlomite	-	17.75	9.48	3.17	5.49	2.97
Schorlomite-Al	-	-	7.23	5.67	6.03	5.52
M.orimotoite	0.75	23.15	23.52	0.90	9.43	6.94
NaTi garnet	-	-	-	2.41	2.60	1.46
Morimotoite-Mg	4.50	7.32	-	-	-	5.36
Goldmanite	-	-	-	-	-	1.07
Spessartine	1.13	-	-	-	-	-
Andradite	79.66	37.12	51.90	79.07	69.12	74.39
Calderite	-	1.14	1.56	-	-	-
Khoharite	-	1.57	1.88	-	-	-
Remainder	5.18	0	0	4.33	2.95	2.28
Total	91.22	88.05	96.90	95.55	95.62	99.99
Recalculated into:						
Andradite	93.8	43.5	56.3	89.0	76.7	78.2
Schorlomite	0.0	20.8	18.1	10.0	12.8	8.9
Morimotoite	6.2	35.7	25.5	1.0	10.5	12.9

3.2.3 – Mosonik

3.2.3.1 - Clinopyroxene

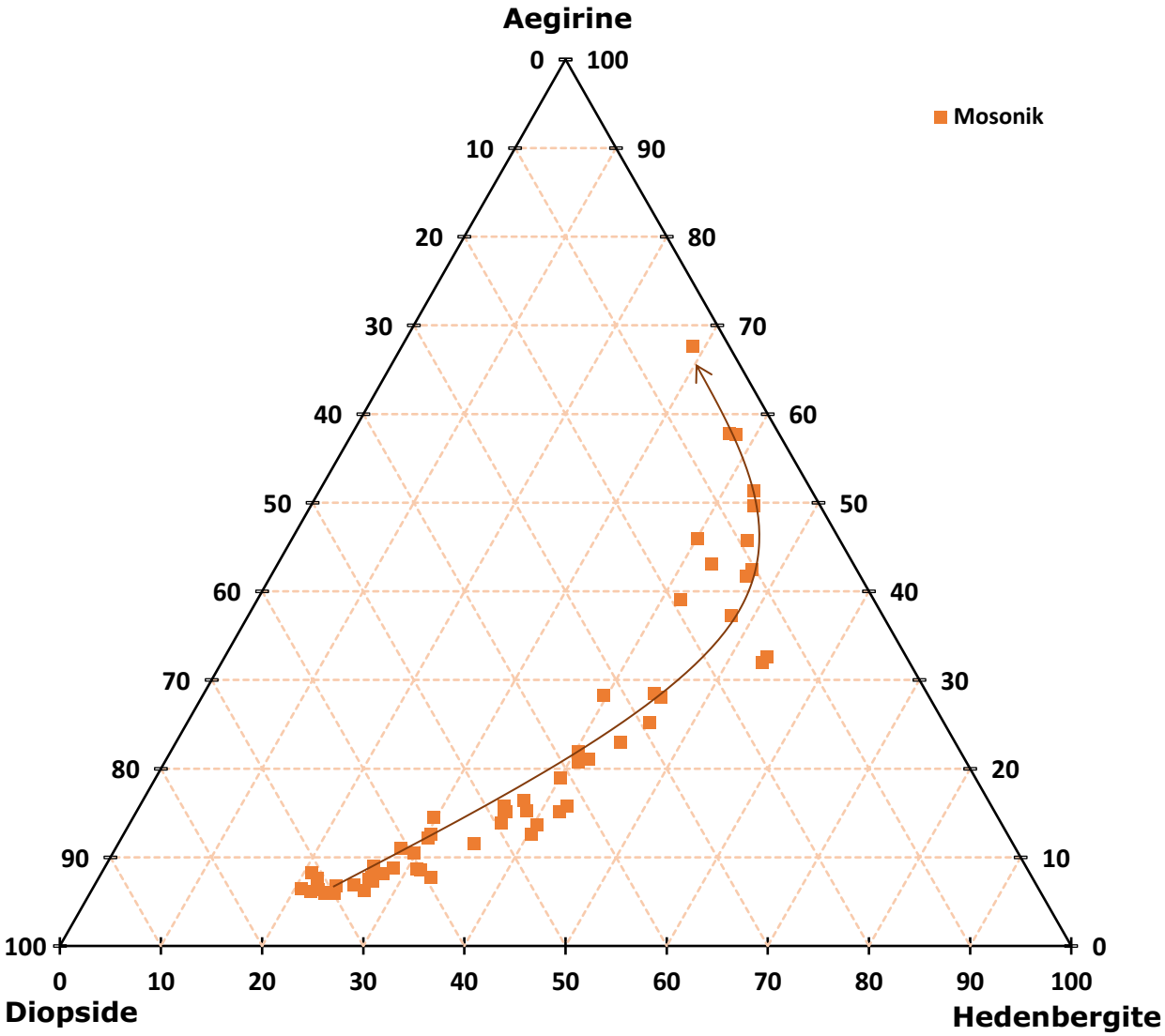

Figure 26: Clinopyroxene compositions from Mosonik29 plotted on the ternary aegirine-hedenbergite-diopside. Evolution trend is represented by the dark orange line.

Fifty-nine clinopyroxene compositions were collected from a nephelinite from Mosonik (Mosonik29) for comparison with Prairie Lake and Fen clinopyroxene compositions. From this sample, a clear curved evolution trend is clearly visible from diopside to hedenbergite-rich aegirine augite (Fig. 26); from ~$Di_{72}Hd_{22}Ae_{6}$ towards $Di_{4}Hd_{28}Ae_{68}$. This trend extends from diopside through hedenbergite-rich aegirine-augite with very little diopside component. The unevolved portion of this trend overlaps with the trends seen at Prairie Lake and Fen.

3.3 - Laser Ablation – Inductively Coupled Plasma – Mass Spectroscopy

Rocks from Prairie Lake (including Good Hope), Fen, Norway, and Mosonik, Tanzania were selected for LA-ICP-MS analysis. Twenty-two samples from Prairie Lake, eleven from Fen, two from Good hope, and two from Mosonik were chosen to represent a wide variety of different rock types (Table 18). Complete trace element data are given in Appendix 3.

Table 18: Samples selected for LA-ICP-MS and minerals examined

Sample	Rock Name	Locality	Clinopyroxene	Garnet	Apatite
ETR2	Garnet Urtite	Prairie Lake	X	X	X
ETR3	Garnet Ijolite	Prairie Lake	X	X	X
ETR7C	Garnet Micro-Ijolite	Prairie Lake	X	X	X
MT04 5-2	Garnet Ijolite	Prairie Lake	X	X	X
PL46	Porphyritic Malignite	Prairie Lake	X		X
PL49	Biotite Pyroxenite	Prairie Lake	X	X	X
PL51	Biotite Pyroxenite	Prairie Lake	X		
PL54	Biotite Pyroxenite	Prairie Lake	X		
PL55	Biotite Pyroxenite	Prairie Lake	X		X
PL59	Garnet Malignite	Prairie Lake	X	X	
PL63	Garnet Ijolite	Prairie Lake	X	X	X
PL65	Porphyry Ijolite	Prairie Lake	X		X
PL76	Garnet Ijolite	Prairie Lake	X	X	X
PL78	Garnet Ijolite	Prairie Lake	X	X	X
PL86	Wollastonite Hollaite	Prairie Lake			
PL90	Hollaite	Prairie Lake	X	X	X
PL91	Urtite	Prairie Lake	X	X	X
PL95	Mica Hollaite	Prairie Lake	X		X
PL96B	Garnet Hollaite	Prairie Lake	X	X	X
WS01	Apatitite	Prairie Lake	X		X
WT4	Garnet Ijolite	Prairie Lake	X	X	X
Val 2	Pyrochlore Apatitite	Good Hope			X
Val 3	Pyrochlore Apatitite	Good Hope			X
35	Ijolite	Fen	X		X
37	Ijolite	Fen	X		
42	Hollaite	Fen			X
43	Melteigite	Fen		X	
44	Ijolite	Fen	X		
49	Ijolite	Fen	X		
61	Vipetoite	Fen			X
204	Urtite	Fen			X
405	Titanite Hollaite	Fen			X
418	Pegmatitic Hollaite	Fen			X
421	Hollaite	Fen	X		
Mosonik11	Nephelinite	Mosonik		X	
Mosonik28	Nephelinite	Mosonik		X	X

3.3.1 – Clinopyroxene

Clinopyroxene trace element data (Sr, Y, Ba, La, Ce, Pr, Nd, Sm, Eu, Gd, Tb, Dy, Ho, Er, Tm, Yb, Lu, Ta) were collected from multiple sites of twenty samples from Prairie Lake and five from Fen. When plotted on a chondrite-normalized REE distribution diagram, trace element data from all samples show a sinusoidal pattern (Fig. 27).

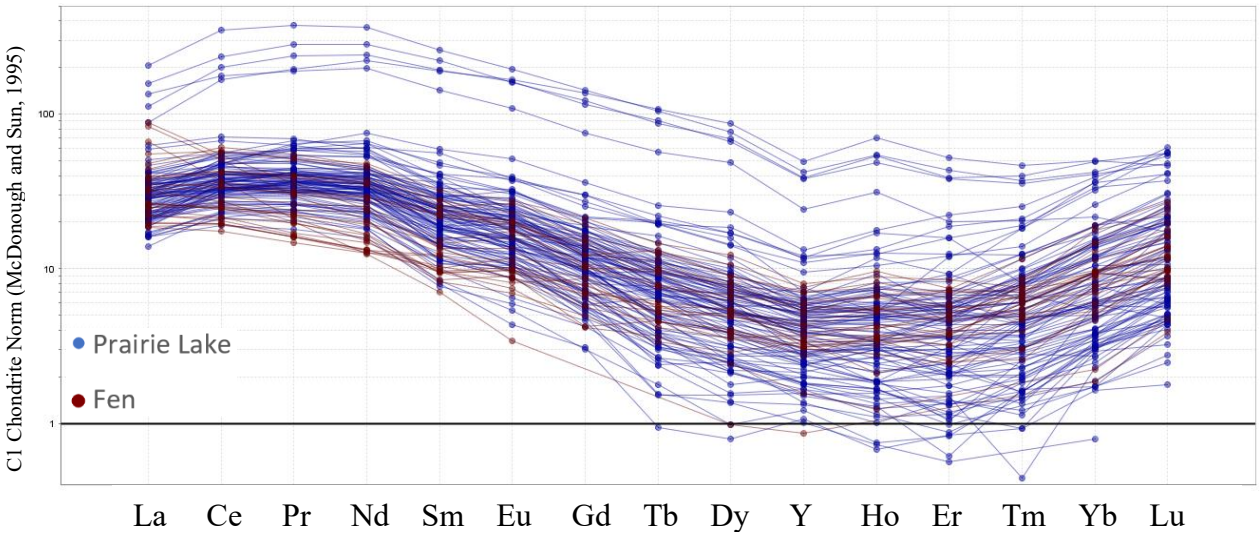

Figure 27: Chondrite-normalized clinopyroxene rare earth element data for the Prairie Lake and Fen complexes

3.3.1.1 – Prairie Lake

Prairie Lake clinopyroxene rare earth element data are shown in Fig. 28. The majority of the samples overlap somewhat with a broadly similar pattern, with a depletion in La relative to other LREE, rising to a convex maximum at Pr-Nd, followed by a steep decline reaching minima at Ho-Er before steeply rising to Lu. Whereas most of the LREE in clinopyroxenes are relatively well-constrained, the HREE display a great deal of variation.

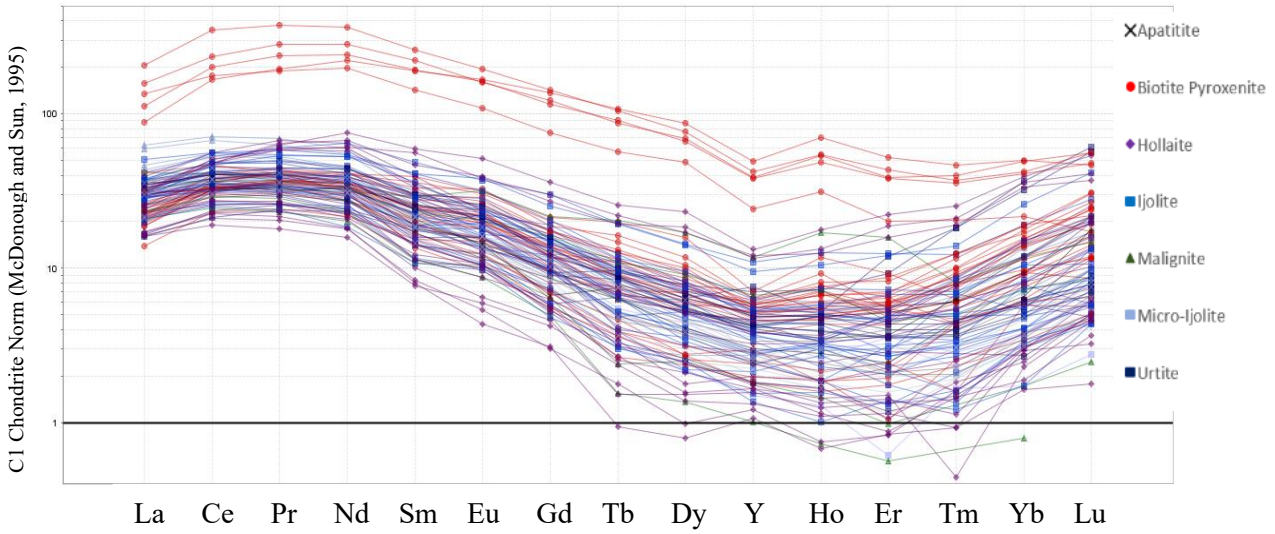

Figure 28: Chondrite-normalized clinopyroxene rare earth element data for the Prairie Lake complex sorted by rock type displaying sinusoidal patterns. Note that that some of the biotite pyroxenite cores are elevated in REE contentrelative to the other pyroxene from Prairie Lake

clustered (with the notable exception of diopside cores from biotite pyroxenite), the HREE show considerable variation.

Total REE contents vary greatly from a low of 36 ppm in ijolite (sample PL63) to 583 ppm in the diopside cores of the biotite pyroxenite (PL51). When comparing the geochemically twinned elements Y/Ho, there is a very good correlation with an R^2 value of 0.991 (Fig. 29).

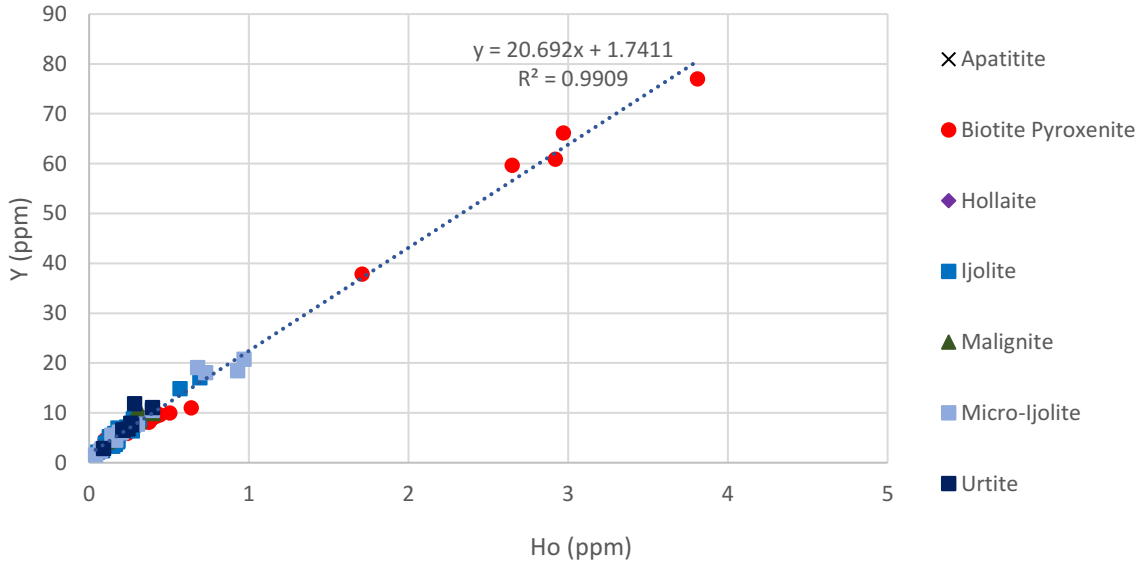

Figure 29: Y vs. Ho for clinopyroxene from different rock types from Prairie Lake. The trendline (blue)

3.3.1.1.1 – Biotite Pyroxenite

Representative data for biotite pyroxenite clinopyroxene are given in Table 19. The trace elements in clinopyroxene from the biotite pyroxenites show two distinct trends (Fig. 30): (1) a convex LREE pattern and a flattened HREE pattern with most samples having total REE contents higher than all other clinopyroxene in the complex; (2) convex LREE patterns and concave HREE patterns (with lows around 4-10x chondritic values).

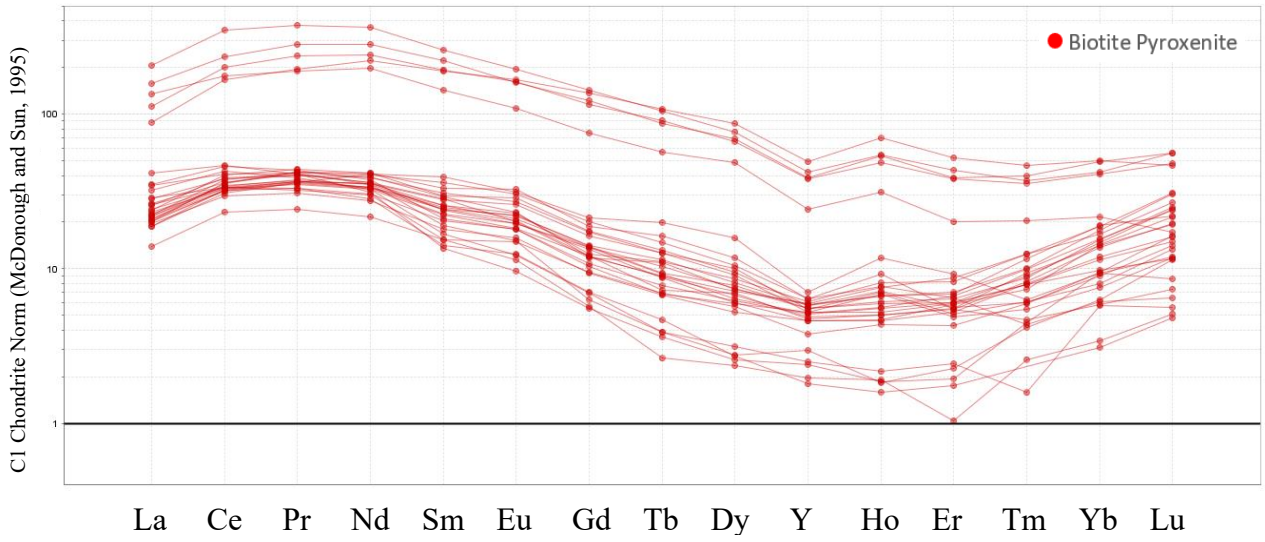

Figure 30: Clinopyroxene rare earth element data from biotite pyroxenites from Prairie Lake

Trend (1) occurs in colourless euhedral diopside cores, while trend (2) is seen in green clinopyroxene. Clinopyroxene displaying trend (2) are similar to clinopyroxene from other rock types in the complex.

Samples of the colourless diopside cores in biotite pyroxenite PL51 show trend (1) with elevation in REE (ranging from 313 – 583 ppm) in comparison to the other clinopyroxenes (>100 ppm). Two of the laser ablation analytical sites from the cores (PL51-1 and PL51-10) show the same chondrite-normalized pattern as trend (1) but is depleted in total REE relative to other cores, with contents similar to those of other clinopyroxene from the complex (66 and 57

ppm respectively). A distinguishing feature for differentiating the cores from other clinopyroxene is the HREE pattern, which flattens between Ho and Lu.

Table 19: Representative LA-ICP-MS data (ppm) for clinopyroxene (CPX) from biotite pyroxenites from Prairie Lake.

Sample	***PL51***	***PL51***	***PL51***	***PL54***	***PL49***	***PL51***
Site	CPX 1-1	CPX 1-2	CPX 2-1	CPX-1	CPX-1	CPX-4
Trend	(1) Low REE	(1) High REE	(2)	(2)	(2)	(2)
Ca	1.72E+05	1.71E+05	1.42E+05	-	1.63E+05	-
Mn	3410	2832	6550	-	6100	-
Sr	372	375	366	433	627	354.2
Y	11.04	37.9	9.62	7.6	3.08	3.76
Zr	155.1	663	863	919	357	791
Ba	1.11	b.d.	b.d.	b.d.	0.51	1.21
La	4.47	31.8	5.75	4.93	6.81	9.8
Ce	18.8	108	20.5	19.35	20.43	28.48
Pr	3.33	17.6	3.38	3.31	2.98	3.77
Nd	18.8	90.2	16.3	15.2	13.7	14.25
Sm	5.78	21.1	3.81	3.57	2.28	1.99
Eu	1.75	6.1	1.29	1.15	0.64	0.546
Gd	4.27	15	2.49	2.39	1.13	1.1
Tb	0.72	2.05	0.40	0.32	0.095	0.13
Dy	3.87	12	2.12	1.65	0.58	0.63
Ho	0.64	1.71	0.44	0.27	0.10	0.10
Er	1.48	3.2	1.31	0.87	0.17	0.31
Tm	0.16	0.51	0.31	0.20	0.06	0.11
Yb	1.51	3.47	3.03	2.2	0.55	1.5
Lu	0.21	0.42	0.76	0.48	0.13	0.29
Ta	b.d.	0.82	0.067	-	0.49	-
Tot. REE	65.79	313.16	61.89	55.90	49.66	63.02
Y/Ho	17.25	22.16	21.67	27.83	29.62	36.86
La/Yb	2.96	9.16	1.90	2.24	12.38	6.53
La/Nd	0.24	0.35	0.35	0.32	0.50	0.69
Tb/Yb	0.48	0.59	0.13	0.15	0.17	0.09

3.3.1.1.2 – Ijolites

On a chondrite-normalized REE distribution diagram (Fig. 31), clinopyroxene in members of the ijolite series (ijolites, micro-ijolites, and urtite) show a common trend of trace element abundances. They exhibit a sinusoidal pattern with maxima at Pr-Nd and minima at Ho-Er (Fig. 31). This pattern is quite similar to those seen in trend (2) from the biotite pyroxenites (Fig. 33). Representative data from ijolite series rocks is presented in Table 20.

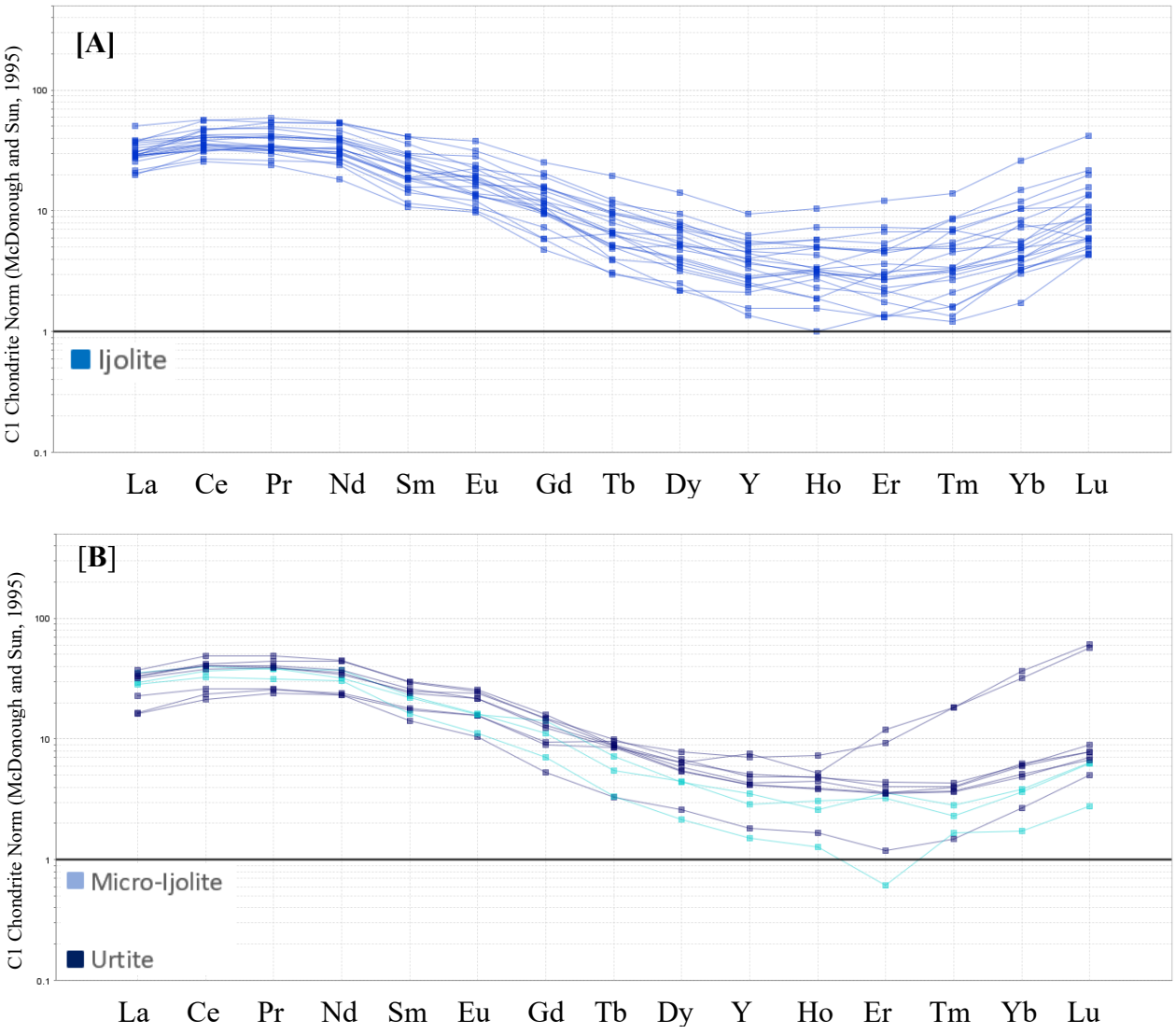

Figure 31: Chondrite-normalized clinopyroxene trace element data for ijolite series rocks from Prairie Lake. [A] Ijolites (Blue) [B] Micro-ijolite (light blue), and urtite (dark blue)

Table 20: Representative trace element abundances (ppm) of clinopyroxene from ijolite series rocks (ijolites, urtite, micro-ijolite) from Prairie Lake

Sample	ETR3	WT4	PL65	ETR7C	PL91
Site	CPX-2	CPX-2	CPX-2	CPX-1	CPX-1
Rock	Garnet Ijolite	Garnet Ijolite	Porphyry Ijolite	Garnet Micro-Ijolite	Urtite
Ca	1.86E+05	1.68E+05	-	1.70E+05	-
Mn	4000	5430	-	4110	-
Sr	562	521	395	555	587
Y	6.97	8.2	7.52	4.54	6.53
Zr	1106	314	1255	616	591
Ba	b.d.	b.d.	0.89	1.32	0.262
La	8.66	9.05	8.79	8.3	8.17
Ce	24.7	29.2	34.09	24.2	24.67
Pr	3.73	4.44	5.44	3.52	3.767
Nd	18.3	18.8	24.7	17.1	16.9
Sm	3.68	4.31	6.04	3.39	3.83
Eu	0.93	1.35	1.78	0.91	1.214
Gd	3.11	2.9	4.06	2.21	2.46
Tb	0.345	0.341	0.445	0.197	0.305
Dy	1.7	1.84	2.00	1.09	1.32
Ho	0.181	0.314	0.274	0.167	0.214
Er	0.58	1.08	0.75	0.52	0.573
Tm	0.084	0.166	0.126	0.057	0.092
Yb	1.26	1.69	1.18	0.59	0.83
Lu	0.144	0.263	0.205	0.153	0.164
Ta	0.69	0.7	-	0.55	-
Tot. REE	67.40	75.74	89.88	62.40	64.51
Y/Ho	38.51	26.11	27.45	27.19	30.51
La/Yb	6.87	5.36	7.45	14.07	9.84
La/Nd	0.47	0.48	0.36	0.49	0.48
Tb/Yb	0.27	0.20	0.38	0.33	0.37

Total REE abundances of clinopyroxene in ijolite varies between 36 ppm in PL64, to 104 ppm in MT04. Urtite clinopyroxene shows a tighter restriction from 40 ppm in ETR2 and 80 ppm in PL91. ETR7C, a micro-ijolite varies between 49 and 65 ppm.

3.3.1.1.3 – Hollaites

Clinopyroxene trace element data for four hollaite samples: (PL86, PL90, PL95, and PL96B) are shown in Table 21. The LREE patterns (Fig. 32) differ with PL95 showing a stronger convexity with higher REE contents than the flatter shape in PL86, PL90, and PL96B. Convex highs occur around Pr-Nd, and concave lows occur around Ho-Er. The MREE and HREE contents separate strongly. PL86 contains the most depleted, strongest concave shape. PL90 and PL96B containing overlapping, intermediate patterns between the others. PL95 contains the most MREE and HREE enrichment

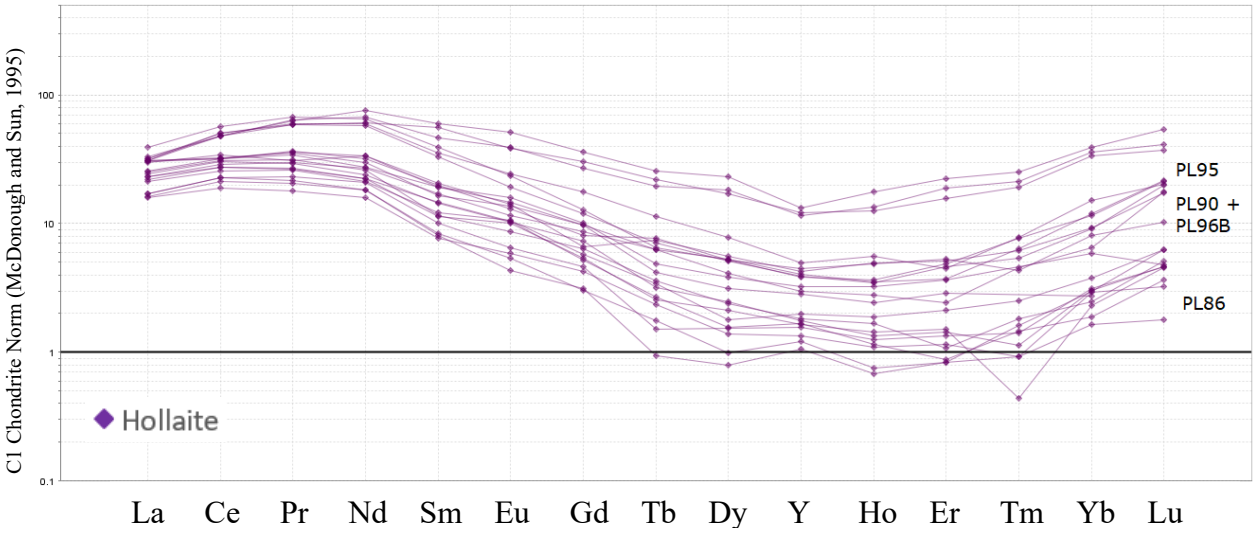

Figure 32: Chondrite-normalized clinopyroxene trace element data for hollaites from Prairie Lake

Table 21: Representative trace element data(ppm) from malignites, hollaites, and apatitite from Prairie Lake

Sample	PL59	PL46	PL95	PL96B	WS01B	PL90
Site	CPX-2	CPX-2	CPX-2	CPX-2	CPX-1	CPX-1
Rock	Garnet Malignite	Porphyritic Malignite	Mica Hollaite	Garnet Hollaite	Wollastonite Apatitite	Hollaite
Mn	-	-	7410	4320	6290	6500
Sr	525	857	357	622	734	579
Y	10.5	9.56	19.1	4.46	5.32	6.63
Zr	1812	3784	1620	469	414	710
Ba	4.1	b.d.	1	b.d.	b.d.	b.d.
La	9.82	13.98	7.55	7.36	8.83	7.11
Ce	25.2	41.17	29.2	20	25.3	21
Pr	3.42	5.83	5.42	3.26	3.76	2.84
Nd	14.6	25.2	27.9	13.6	19.1	15.4
Sm	3.39	4.33	8.3	2.42	3.6	3.05
Eu	1.15	1.354	2.15	0.77	0.85	0.8
Gd	3.21	3.6	6	1.94	2.31	1.32
Tb	0.397	0.355	0.79	0.151	0.223	0.268
Dy	2.23	1.67	4.18	0.77	1.11	1.37
Ho	0.394	0.288	0.68	0.133	0.183	0.268
Er	0.73	0.87	2.52	0.46	0.64	0.82
Tm	0.122	0.195	0.47	b.d.	0.091	0.152
Yb	1.17	2.26	5.4	0.44	0.94	1.5
Lu	0.215	0.502	0.91	b.d.	0.244	0.427
Ta	-	-	0.063	0.306	0.362	0.152
Tot. REE	66.05	101.60	101.47	51.30	67.18	56.33
Y/Ho	26.65	33.19	28.09	33.53	29.07	24.74
La/Yb	8.39	6.19	1.40	16.73	9.39	4.74
La/Nd	0.67	0.56	0.27	0.54	0.46	0.46
Tb/Yb	0.34	0.16	0.15	0.34	0.24	0.18

3.3.1.1.4 –Apatitite and Malignite

Clinopyroxene trace element data for wollastonite apatitite (WS01) shoes a shallow sinuous pattern on a chondrite-normalized diagram (Fig. 33). This trend is very similar to that seen in other clinopyroxene from the complex with a somewhat flattened, weakly convex LREE shape with a gradual depletion over the MREE with a marked increase between Er-Lu forming a concave HREE shape. Representative LA-ICP-MS data for WS01B are included in Table 22.

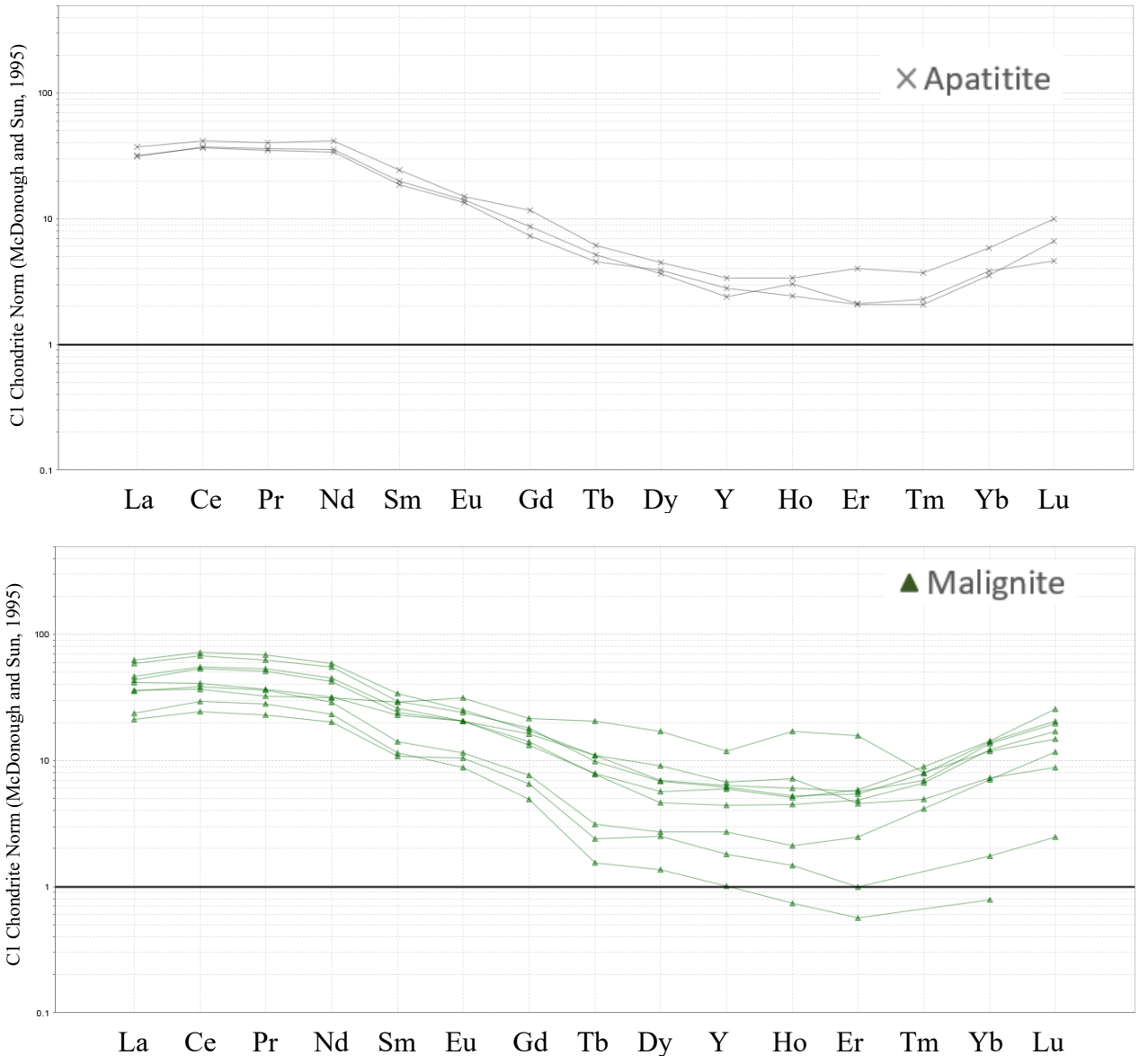

Figure 33: Chondrite-normalized clinopyroxene trace element data for (A) apatitite (grey X); and (B) malignite (green triangle) from Prairie Lake

Trace element data for malignite samples PL46 (porphyritic malignite) and PL59 (garnet malignite) shows a sinuous pattern. PL46 shows a weakly convex LREE pattern, a negative slope between Nd and Dy, flattening out between Dy and Er before rising to Lu. Five sites were analysed from a zoned pyroxene crystal from the core to the rim. The overall chondrite-normalized distributions remain mostly similar with the total REEs changing with the second and third site from the core registering REE contents >100 ppm while the first, fourth and fifth were 55 ppm, 80 ppm, and 84 ppm respectively.

3.3.1.2 – Fen

Clinopyroxene trace element data were collected for five samples from Fen, four ijolite (Fen37, Fen37, Fen44, and Fen49) and a hollaite (Fen421). The chondrite-normalized data (Fig. 34) predominantly show a shallow sinusoidal pattern predominantly with LREE highs around Ce-Pr and lows between Dy-Er. For the most part samples are well constrained with a good deal of overlap, though Fen44 and Fen37 each contain a single analytical site with anomalous HREE

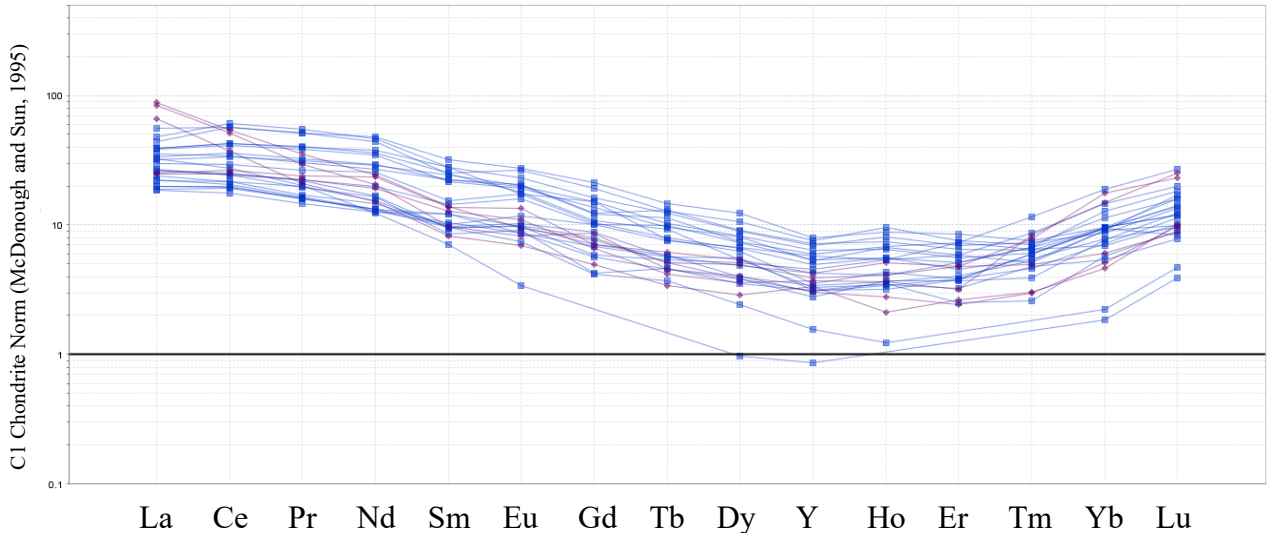

Figure 34: Chondrite-normalized trace element data for clinopyroxene from Fen

lows. Sample Fen421 contains a deviation in LREE samples which show a negative LREE slope as opposed to the convex shape seen in all other samples investigated, with the highest La seen in the Fen clinopyroxene (21 ppm).

Total REE contents vary between 31 ppm in Fen35 and 93 ppm in Fen49. Y/Ho ratios vary between 21.3 in ijolite (Fen35), and 46.1 in hollaite (Fen421) though the majority fall between 21 and 30. Y and Ho show a clear correlation when plotted on a Ho vs. Y diagram (Fig. 35), with an R^2 value of 0.92. La/Nd ratios show variation with the majority between 0.5 and 0.9, although the negative slope of some of the clinopyroxene from Fen421 results in ratios between 1.8 and 2.3. Tb/Yb ratios occur between 0.06 and 0.35.

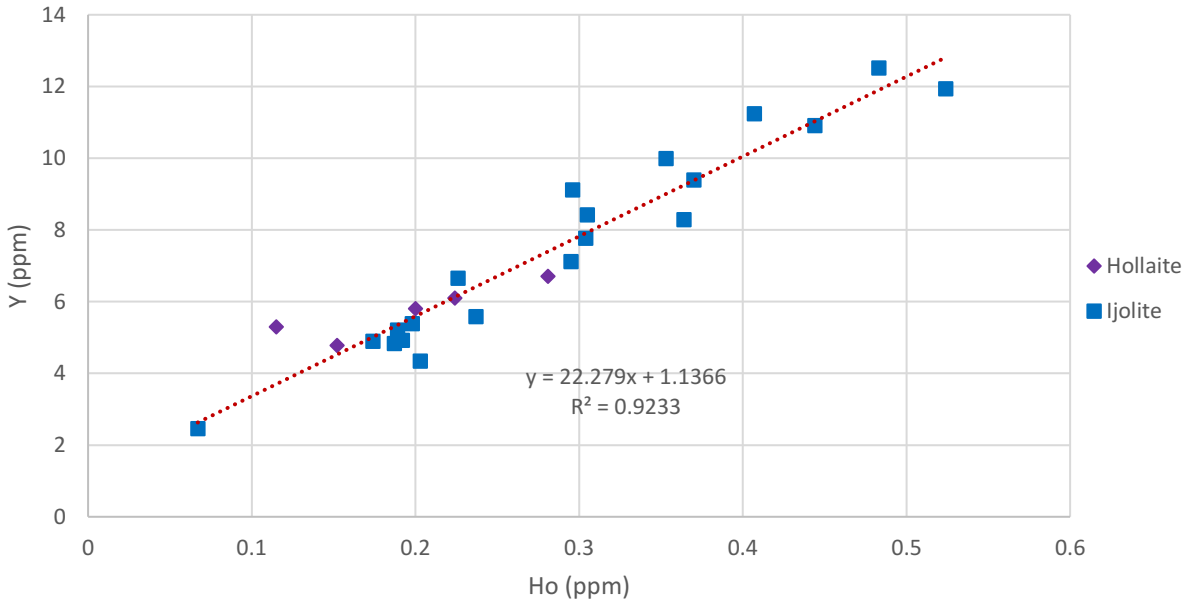

Figure 35: Ho vs. Y for clinopyroxene from Fen. Average slope is represented as red trend line

3.3.2 – Garnet

Trace element data were collected for garnets from Prairie Lake, Fen and Mosonik. The garnet trace element data shows similarities between Prairie Lake and Fen, with garnet from Mosonik deviating from that trend. On a chondrite-normalized diagram (Fig. 36), most of the garnets display a convex pattern with depleted LREE increasing and flattening in the MREE with minor depletion towards the HREE. The Y/Ho ratios for each complex are show (Fig. 37A) a consistent slope for each complex, with R^2 values of 0.9998 for Mosonik; 0.9607 for Fen; and 0.9753 for Prairie Lake (though it should be noted that the sample sizes for Mosonik and Fen are small). La/Nd ratios for Prairie Lake and Fen (Fig. 37B, Fig. 37D) show differences between the two complexes with Fen having ratios >0.1 and most of Prairie lake ≤0.1 (with the notable outliers from sample PL65 >0.25). Tb/Yb ratios (Fig. 37 C, Fig. 37D) for Prairie Lake, Fen and Mosonik between 0.38 at Mosonik and 0.74 at Fen.

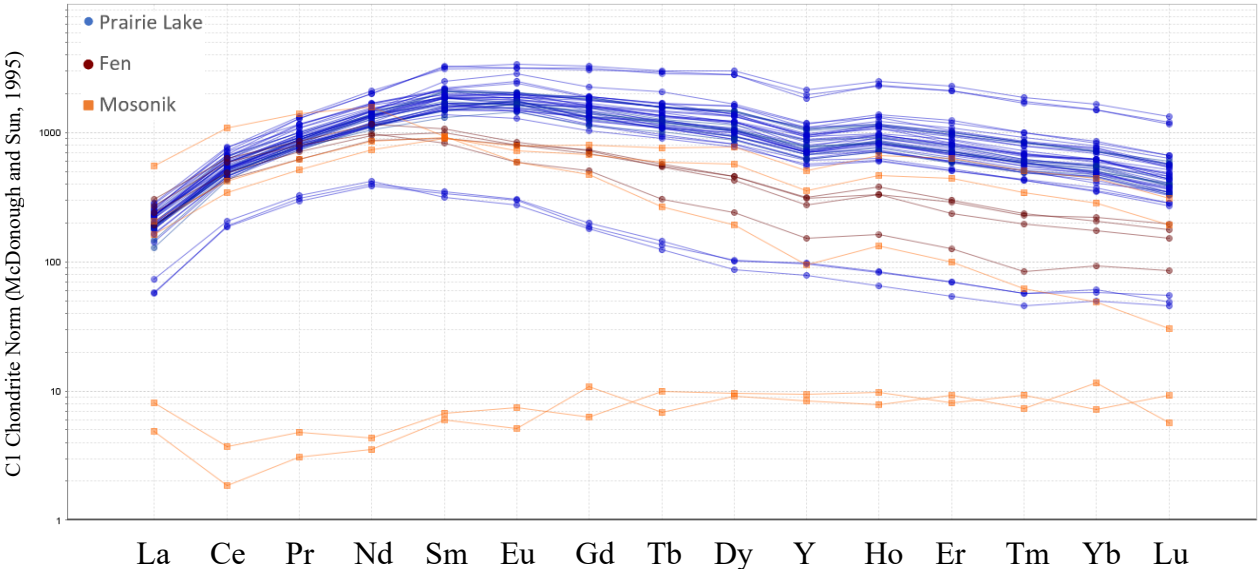

Figure 36: Chondrite-normalized garnet trace element data for Prairie Lake, Fen and Mosonik

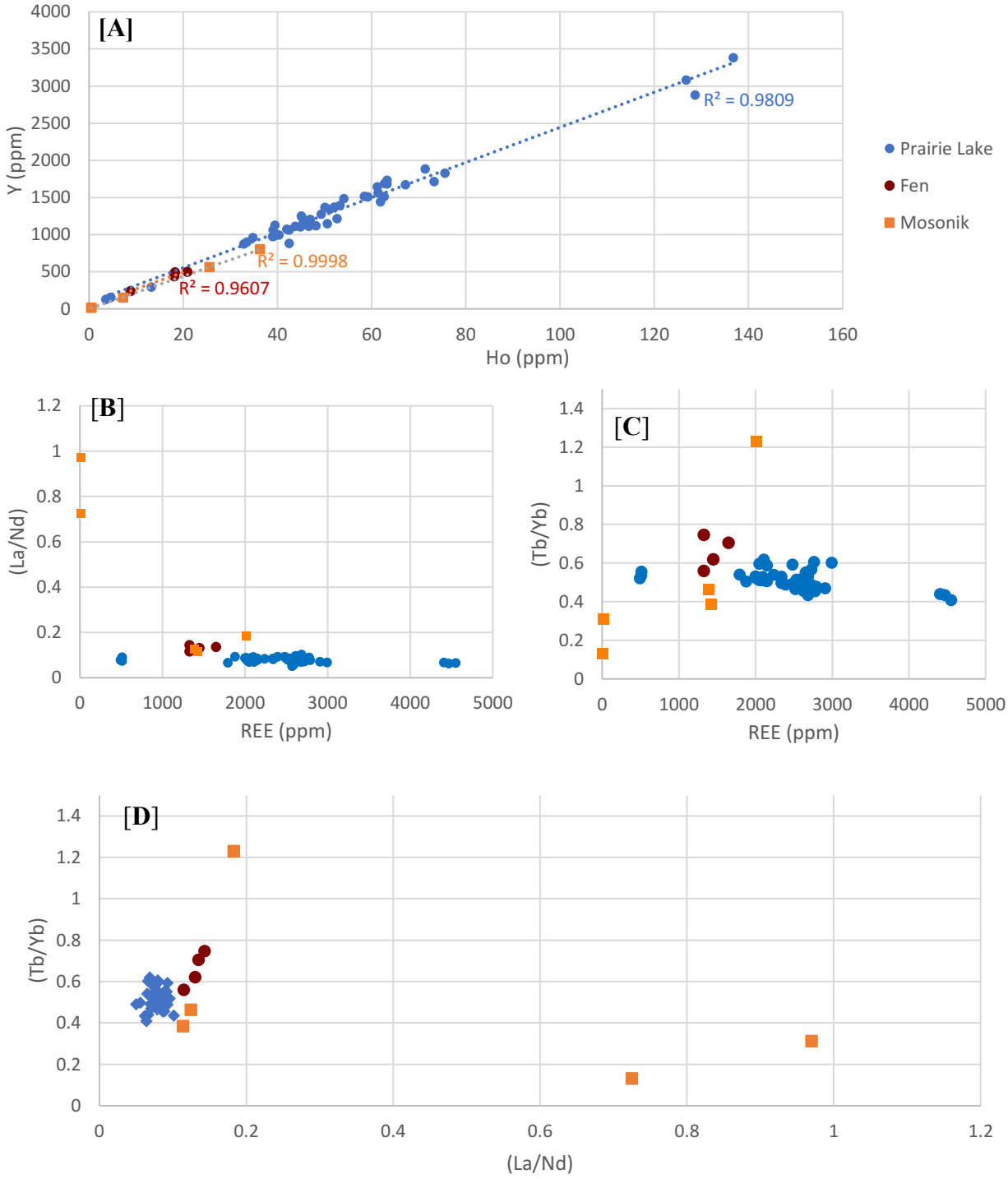

Figure 37: [A] Y plotted against Ho for Prairie Lake, Fen and Mosonik [B] (La/Nd) vs REE for garnets from Prairie Lake, Fen and Mosonik [C] Tb/Yb vs REE for garnets from Prairie Lake, Fen and Mosonik; [D] (La/Nd) vs (Tb/Yb) for garnets from Prairie Lake, Fen and Mosonik

3.3.2.1 - Prairie Lake

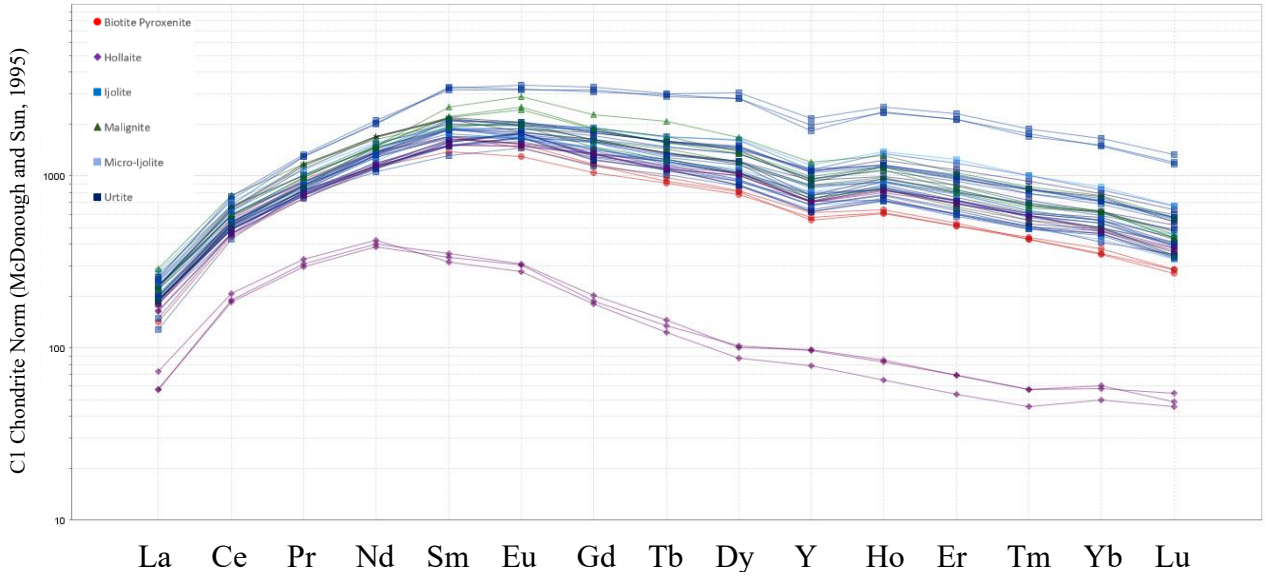

Figure 38: Chondrite-normalized LA-ICP-MS trace element data for Garnets from Prairie Lake sorted by rock type

The majority of garnets from Prairie Lake show a common, relatively restricted pattern with several notable outliers. Most samples are closely overlapping showing a depletion in LREE increasing to Sm before flattening out with weak depletion in the HREE (Fig. 38). Total REE contents vary, with most samples having abundances between 1794 ppm (PL49) and 2993ppm (PL59). Two samples have greater contents, with garnets in MT04 containing ~4500 ppm and the two analytical sites in PL65 reaching 6135 and 8336 ppm. La/Nd ratios for most Prairie Lake garnet is consistent between 0.05 and 0.10. Tb/Yb ratios show a slightly broader range of 0.41 in ijolite (MT04) to 0.61 in malignite (PL59). Zr contents vary between 928 ppm in hollaite (PL86) to 31800 ppm in PL59, however most occur within the 10000-20000 ppm range.

3.3.2.1.1 – Ijolite series rocks

Most of the garnet in the ijolite series rocks display a nearly identical convex pattern (Fig. 39). As most samples are similar in their compositions they are discussed as a group. Total REE contents range from 2000 to 3000 ppm. For most of the samples, the La/Nd ratio is constrained from 0.05 to 0.1 while the Tb/Yb ratios are ~0.5.

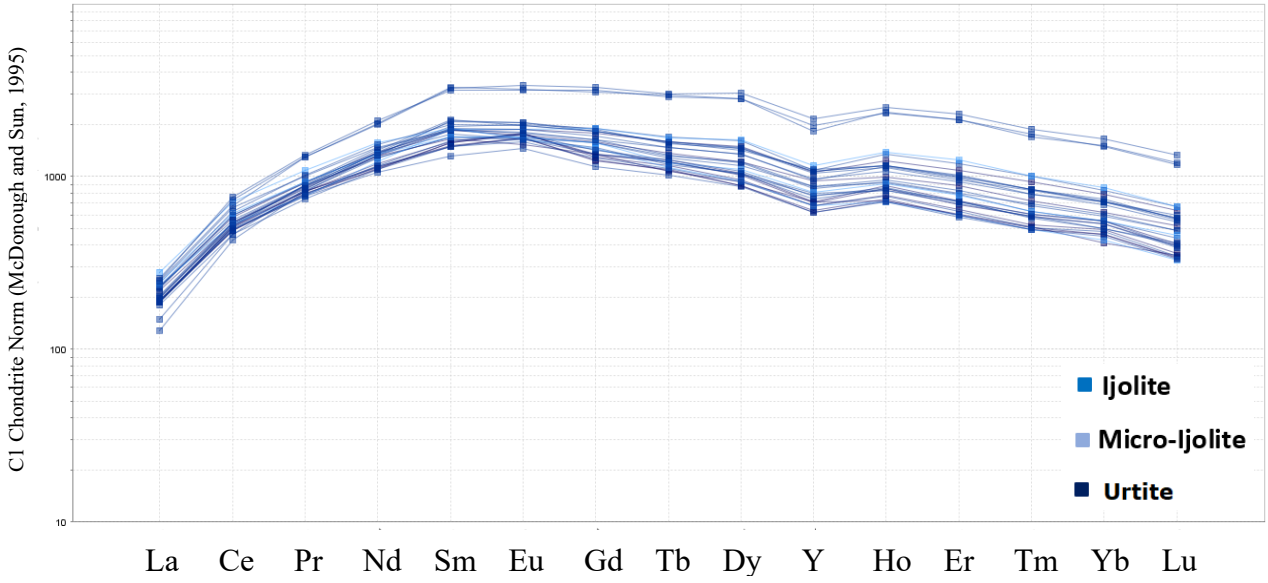

Figure 39: Chondrite-normalized LA-ICP-MS trace element data for Garnets from ijolite series rocks at Prairie Lake

The MT04 and PL65 are notable outliers from the common trend displayed by the Prairie Lake garnets. MT04, a garnet ijolite, shows a very similar pattern to other Prairie Lake garnets but differs in that the prominent enrichment in MREE and HREE. Total REE contents in MT04 are ~4500 ppm, much higher than most garnets in the complex. MT04 has similar La/Nd and Tb/Yb ratios. La/Nd ratios of 0.6 and 0.7, overlap other garnets in the complex. While the lowest Tb/Yb ratios found in the complex, 0.41 to 0.44, there is some overlap with those of other garnets; such as ETR7C which contains a similarly low Tb/Yb of 0.43.

Table 22: Representative trace element data (ppm) for garnet from ijolite series rocks at Prairie Lake

Sample	ETR2	PL91	MT04	PL78	ETR7C	PL65
Site	GRT-1	GRT-1	GRT-3	GRT-3	GRT-3	GRT-1
Rock Type	Garnet Urtite	Urtite	Garnet Ijolite	Garnet Ijolite	Garnet Micro-Ijolite	Retexturized Ijolite
Ca	2.69E+05		3.00E+05	2.70E+05	3.01E+05	-
Mn	4130	5030	6030	4200	4810	401
Sr	60.1	-	67.7	65.1	98.8	-
Y	1123	1117	2878	1248	1061	881
Zr	16800	16340	16490	14220	11470	19850
Ba	b.d.	-	b.d.	b.d.	0.88	-
La	46.8	45.6	59.7	52.8	66.3	698
Ce	330	298.6	467	364.4	439	2696
Pr	81.1	73.8	123.2	86	100.6	485
Nd	604	504	966	626	717	2562
Sm	244	230.9	466	260.3	280	666
Eu	86.5	99.5	179.2	92.6	92.9	209.4
Gd	267	268	628	294.3	291	478
Tb	38.9	45.3	104.5	42.4	40.8	64.1
Dy	229.2	258.5	694	258	231	303
Ho	39.5	48.2	128.7	45.1	39.1	42.5
Er	96.5	115.7	340	111.2	95.1	80.7
Tm	12.62	14.88	43.2	14.59	12.23	8.51
Yb	66.2	88.7	240.9	80.1	68.9	39.7
Lu	8.6	10.06	28.8	9.91	8.07	2.76
Ta	108.5	66.6	257.5	96.5	115.3	448
Tot. REE	2151	2102	4469	2338	2482	8336
Y/Ho	28.43	23.17	22.36	27.67	27.14	20.73
La/Yb	0.71	0.51	0.25	0.66	0.96	17.58
La/Nd	0.08	0.09	0.06	0.08	0.09	0.27
Tb/Yb	0.59	0.51	0.43	0.53	0.59	1.61

Sample PL65 (porphyritic ijolite) deviates from all other samples in showing a strong enrichment in LREE, and a strong depletion in HREE compared to other samples from Prairie Lake. La to Sm shows a flat convex shape before decreasing to Lu. La/Nd ratios are much higher than other garnets from Prairie Lake, up to 0.27 and 0.32. PL65 is the only sample in Prairie Lake to display a Tb/Yb ratio greater than 1.5 reaching 1.61 and 2.38.

3.3.2.1.2 – Biotite Pyroxenite, Hollaite, and Malignite

Biotite pyroxenite, hollaite, and malignite all show quite uniform patterns (Fig. 40), identical to the majority of those found in ijolite series rocks. La/Nd and Tb/Yb ratios are all within the 0.05 – 0.1 and 0.4 – 0.6 ranges respectively. Biotite pyroxenite (PL49) shows slightly below average total REE contents, 1794 ppm, though the other analytical sites do show contents above 2000 ppm. One interesting feature evident in the malignites is that some sites show a slight positive Eu anomaly with Eu* varying between 0.979 in PL90 to 1.23 in

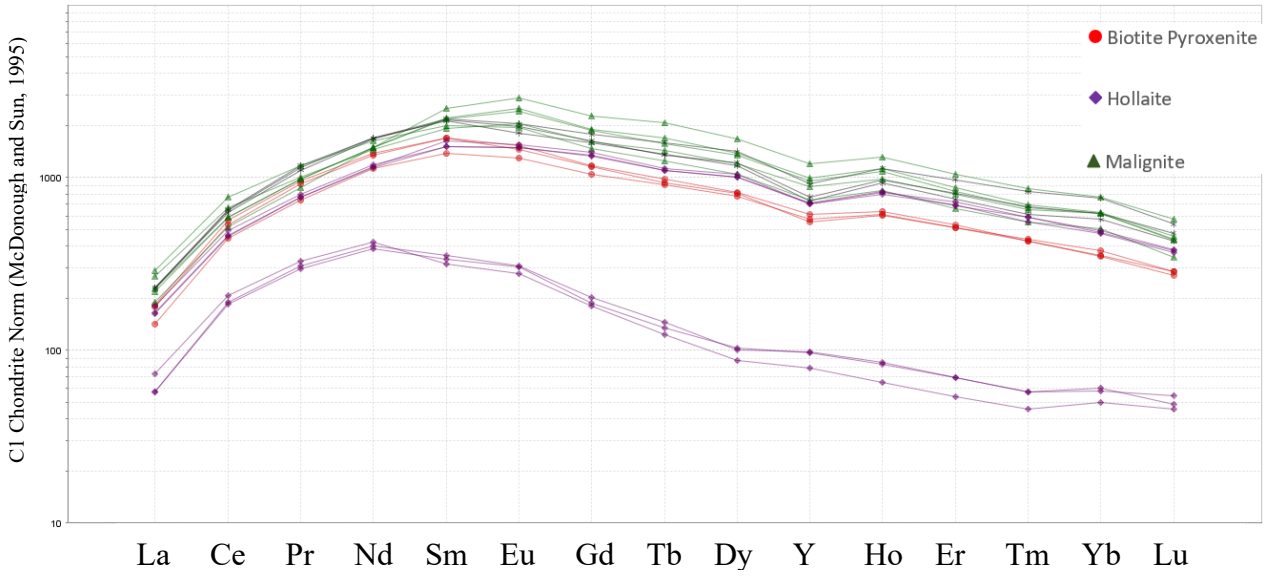

Figure 40: Chondrite-normalized LA-ICP-MS trace element data for Garnets from biotite pyroxenite, hollaite, and malignite at Prairie Lake

PL91. Representative data are displayed in Table 23. Sample NP68, an apatitite, shows the greatest deviation from other garnets in the complex, being depleted in total REE (~500 ppm) while still maintaining a similar shaped distribution pattern.

Table 23: Representative LA-ICP-MS data for garnet from biotite pyroxenite, hollaite, and malignite from Prairie Lake

Sample	**PL49**	**PL49**	**PL90**	**PL90**	**PL96B**	**PL96B**	**PL59**	**PL59**
Site	GRT-1	GRT-3	GRT-1	Grt-2	GRT-1	GRT-2	GRT-4	GRT-5
Rock Type	Biotite Pyroxenite	Biotite Pyroxenite	Hollaite	Hollaite	Garnet Hollaite	Garnet Hollaite	Garnet Malignite	Garnet Malignite
Ca	2.50E+05	2.51E+05	2.99E+05	2.98E+05	2.84E+05	2.87E+05	-	-
Mn	4410	4420	6460	6160	3890	3880	7120	7080
Sr	43.6	46.9	68.8	83.1	63	64.2	-	-
Y	957	898	1440	1213	1102	1110	1157	1506
Zr	11900	10760	17980	16710	16070	14530	3.18E+04	16500
Ba	b.d.	b.d.	b.d.	b.d.	b.d.	b.d.	-	-
La	43.1	33.6	54.5	54.3	38.5	39.1	68.3	51.7
Ce	347	272.9	401	383	281	284	474	360
Pr	88.8	68.5	109.2	102.1	71	71.3	108.6	90.7
Nd	628	516	773	765	527	524	747	684
Sm	250	203.4	325	321	240.1	224.6	294	325
Eu	86.5	73.1	115.1	110.8	87.6	84.2	110.3	136.1
Gd	234	207.7	354	326	279.4	264	293	374
Tb	35.2	32.8	57.6	48.9	40.9	39.5	44.9	57
Dy	201.1	191.6	347	300	256	246.2	257.9	332
Ho	34.8	33.5	61.9	52.7	44.9	43.8	45.7	59.2
Er	84.6	82.1	154.9	129.6	114.9	110.6	106.2	133.4
Tm	10.64	10.88	20.5	16.78	14.48	13.7	13.64	16.49
Yb	56.9	60.7	122.6	99.7	79.2	76.2	81.5	100.3
Lu	7.06	7.06	13.2	11.69	9.43	9.02	8.54	10.81
Ta	88.5	74.1	139.2	298	64.9	73.8	136.5	145
Tot. REE	2108	1794	2910	2722	2084	2030	2654	2731
Y/Ho	27.50	26.81	23.26	23.02	24.54	25.34	25.32	25.44
La/Yb	0.76	0.55	0.44	0.54	0.49	0.51	0.84	0.52
La/Nd	0.07	0.07	0.07	0.07	0.07	0.07	0.09	0.08
Tb/Yb	0.62	0.54	0.47	0.49	0.52	0.52	0.55	0.57

3.3.2.2 – Fen and Mosonik

One sample was analysed from Fen (43) with data for four analytical sites (Fig. 41). The Fen garnet shows much the same distribution pattern as found for Prairie Lake garnet. Total REE contents vary from 1327 – 1450 ppm. Y/Ho ratios show some variation from 23.78-26.75. La/Nd is limited, averaging around 0.13 ranging from 0.11-0.14. Tb/Yb ratios range from 0.56-0.75. Zr contents are between 2740 and 6800 ppm.

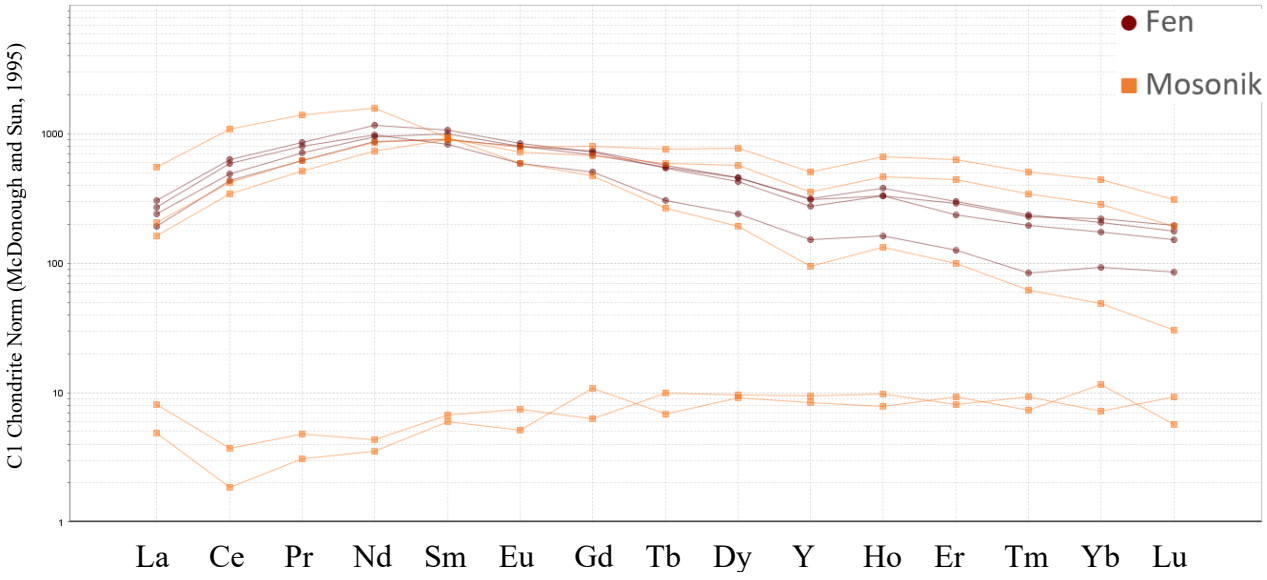

Figure 41: Chondrite-normalized LA-ICP-MS data for garnets from Fen and Mosonik

Garnet trace element data were collected from two samples from Mosonik: Mosonik11, and Mosonik28 (Fig. 41). Mosonik11 shows depleted LREE distribution pattern increasing to Nd-Sm before flattening out with a very gradual decrease; total REE contents vary from 1392 – 2014 ppm; Zr contents are between 94-102 ppm. Garnets from Mosonik28 are strongly depleted in REE (~15 ppm per analytical site) compared to all other garnets analysed in this study with a completely different pattern i.e. depleted between La and Sm before gradually rising and flattening out. Zr contents are between 998 and 2363 ppm. Representative data for garnets from Fen and Mosonik is presented in Table 24.

Table 24: Representative LA-ICP-MS data for garnet from Fen and Mosonik

Sample	Fen 43a	Fen 43b	Mosonik28	Mosonik28	Mosonik11	Mosonik11
Site	GRT-1	GRT-3	GRT-1	GRT-3	GRT-1	GRT-2
Rock Type	Ijolite	Ijolite	Nephilinite	Nephilinite	Nephilinite	Nephilinite
Ca	2.87E+05	2.92E+05	7770	6360	2.88E+05	2.85E+05
Mn	3400	3550	1221	856	3133	2596
Sr	41.9	55.1	804	604	159.2	98.9
Y	497	489	14.73	13.2	150	562
Zr	3500	6800	93.9	101.7	998	2363
Ba	b.d.	b.d.	63.4	47.8	b.d.	b.d.
La	57	45.6	1.92	1.16	132	49
Ce	301	267	2.28	1.14	672	260.3
Pr	66.8	58.3	0.445	0.285	129.9	58.2
Nd	437	397	1.98	1.6	721	393
Sm	148	133.5	1	0.89	139.9	136.4
Eu	45.1	45.2	0.42	0.29	33.7	41.2
Gd	147.5	136.8	1.26	2.14	94.9	135.3
Tb	20.77	19.9	0.361	0.245	9.71	21.36
Dy	113.5	113.6	2.36	2.25	47.9	140.7
Ho	20.9	18.28	0.532	0.43	7.25	25.6
Er	48.5	46.6	1.29	1.48	16	71.2
Tm	5.84	5.69	0.231	0.181	1.53	8.45
Yb	33.5	35.6	1.16	1.86	7.9	46.2
Lu	4.35	4.81	0.227	0.14	0.75	4.76
Ta	86.3	45.2	5.42	2.98	223.5	76
Tot. REE	1450	1328	15.47	14.09	2014	1392
Y/Ho	23.78	26.75	27.69	30.70	20.69	21.95
La/Yb	1.70	1.28	1.66	0.62	16.71	1.06
La/Nd	0.13	0.11	0.97	0.73	0.18	0.12
Tb/Yb	0.62	0.56	0.31	0.13	1.23	0.46

3.3.3 – Apatite

Trace element analysis were collected for apatite from eighteen samples from Prairie Lake, ten from Fen, two from Good Hope, and two from Mosonik (Fig. 42). All samples show REE contents well above chondritic norms with an enrichment in LREE (La … Eu) relative to HREE (Gd … Lu). Prairie Lake, Fen, and Mosonik showing an overlapping, somewhat uniform negatively sloping trend and Good Hope showing an initial depletion in LREE (relative to the other samples) before exhibiting a similar slope to the other locations from the middle REE onwards resulting in a convex shape.

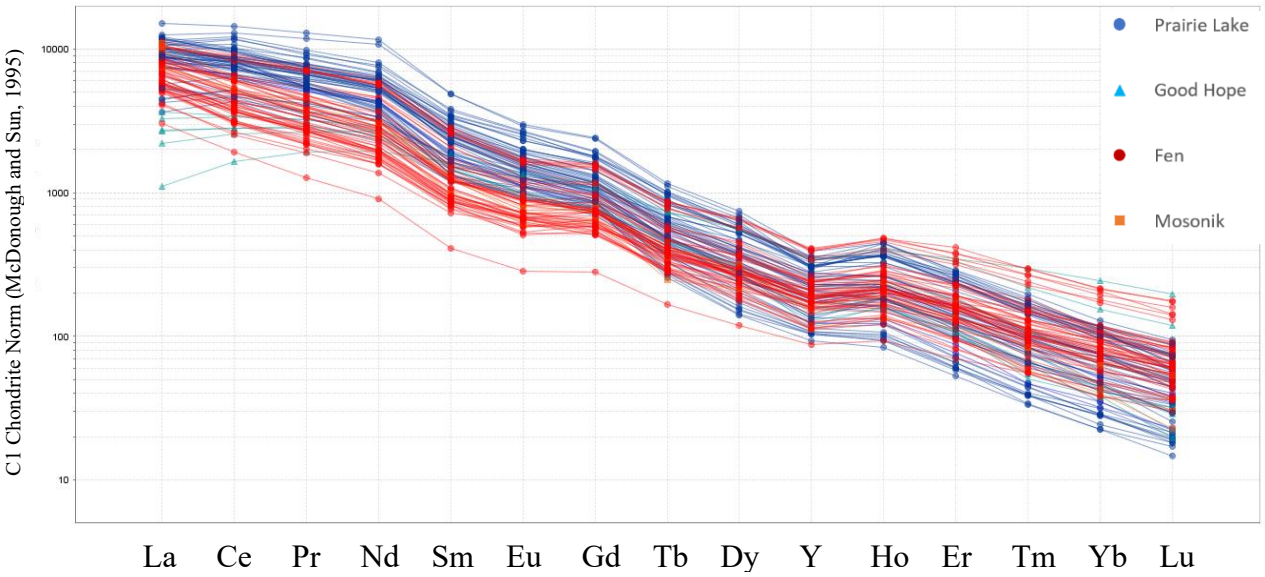

Figure 42: C1 Chondrite-normalized REE diagram for apatite from Prairie Lake (blue circles), Fen (dark-red circles), Mosonik (orange squares) and Good Hope (light-blue triangles)

While many of the features are best described on a locality-by-locality basis, some features are best highlighted by comparison. The ratio of Y/Ho (plotted as Ho vs. Y; Fig. 43A) shows an interesting feature – two trend lines and a wide variation from expected linear trend. Ce and Eu anomalies are minor, with an Eu* low of 0.68 (in Mosonik) and most between 0.8 to 1.12, and Ce* between 0.80 (Fen) to 1.31 (Prairie Lake)

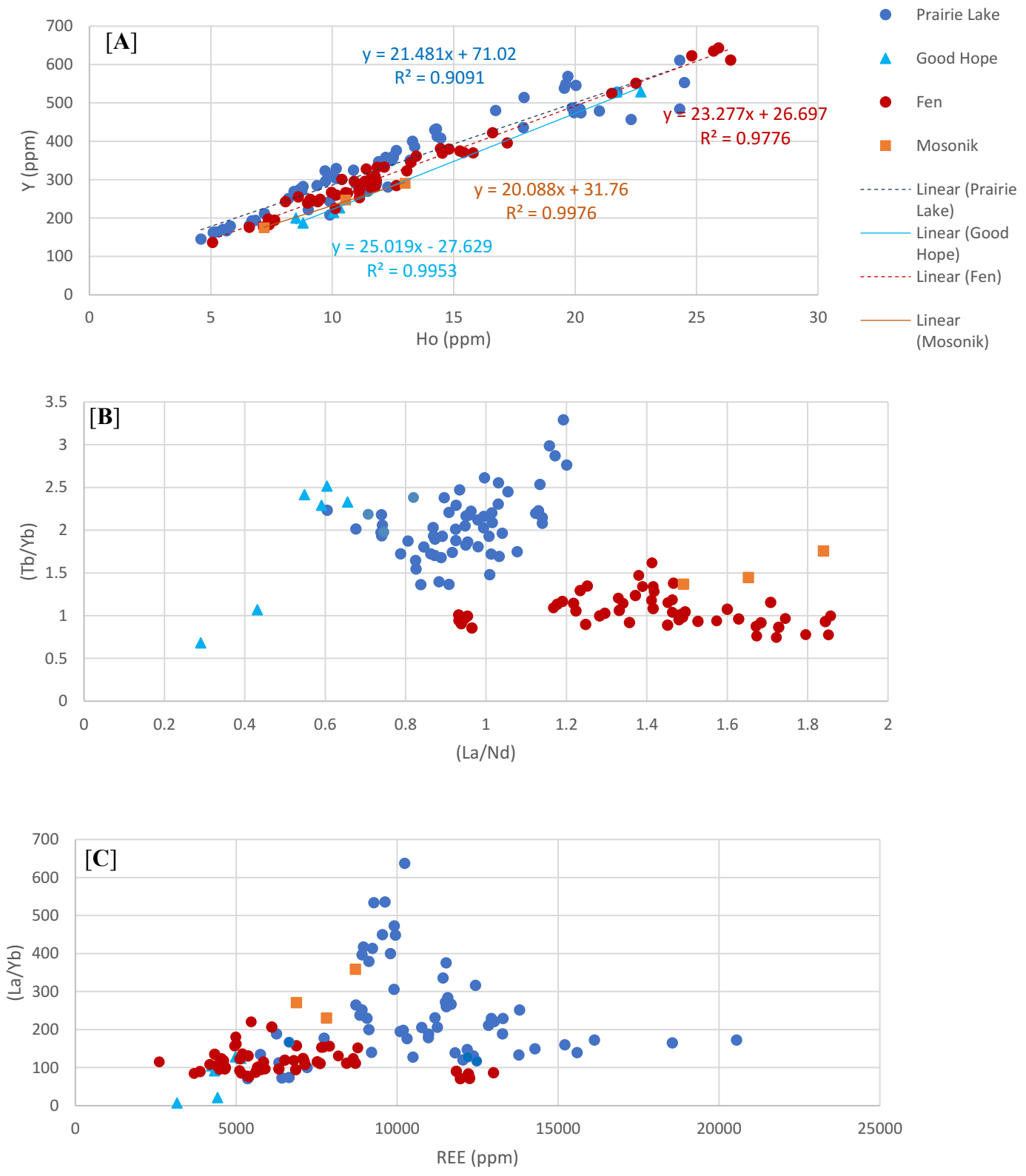

Figure 43: [A] Ho vs. Y for apatite from Prairie Lake, Fen, Mosonik, and Good Hope; [B] (La/Nd) vs (Tb/Yb) for apatite from Prairie Lake, Fen, Mosonik, and Good Hope; [C] Total REE vs La/Yb for apatite from Prairie Lake, Fen, Mosonik, and Good Hope

Total REE contents of apatite from the different complexes overlap between ~4000 - 9000 ppm with most of the apatite from Fen, Mosonik and Good Hope occurring in this range. Much of the apatite from Prairie Lake contains REE in excess of 10,000 ppm and apatite from titanite hollaite (405) from Fen has REE contents of ~12,500 ppm.

The apatite from each complex shows different slopes as indicated by La/Yb ratios. Apatite from Fen has a fairly uniform slope with La/Yb ratios ranging from 71 (in sample 405) to 207 (in sample 43), with most samples plotting between ~90 and ~130. Prairie Lake apatite shows steeper slopes on average with a wider variation; 71 (in PL55) to 637 (in PL33). Mosonik28 apatite has La/Yb above those of Fen on par with Prairie Lake, ranging from 231 to 359. Apatite from Good Hope show the greatest depletion in La/Yb ratios as a result of the LREE depletion in relation to the other complexes, ranging from as low as 6.67 (VAL-2) to 128.3 (VAL-3).

3.3.3.1 - Prairie Lake

Samples of apatite from Prairie Lake show a very uniform negatively stepping slope with a similar shape and varying REE contents on a chondrite-normalized diagram (Fig. 44), with a sample of hollaite containing a distinct outlier. Commonly there is a uniform negative slope from La – Gd before a sharp step between Gd and Tb. After this there is a concave shape from Tb – Ho (an effect of a slight Y anomaly) with a flattening occurring from Ho - Lu.

The La/Yb ratio ranges from 71 in biotite pyroxenite (PL55) to 637 in ijolite (PL63). The LREE profiles commonly have a straight negative slope. Samples PL55, PL65, PL90, and PL95 show the greatest deviation from this LREE trend. PL 55 and PL90 are depleted in relation to the common slope, while PL65 and PL95 have the lowest La/Nd (<0.8). La/Nd ratios from apatite

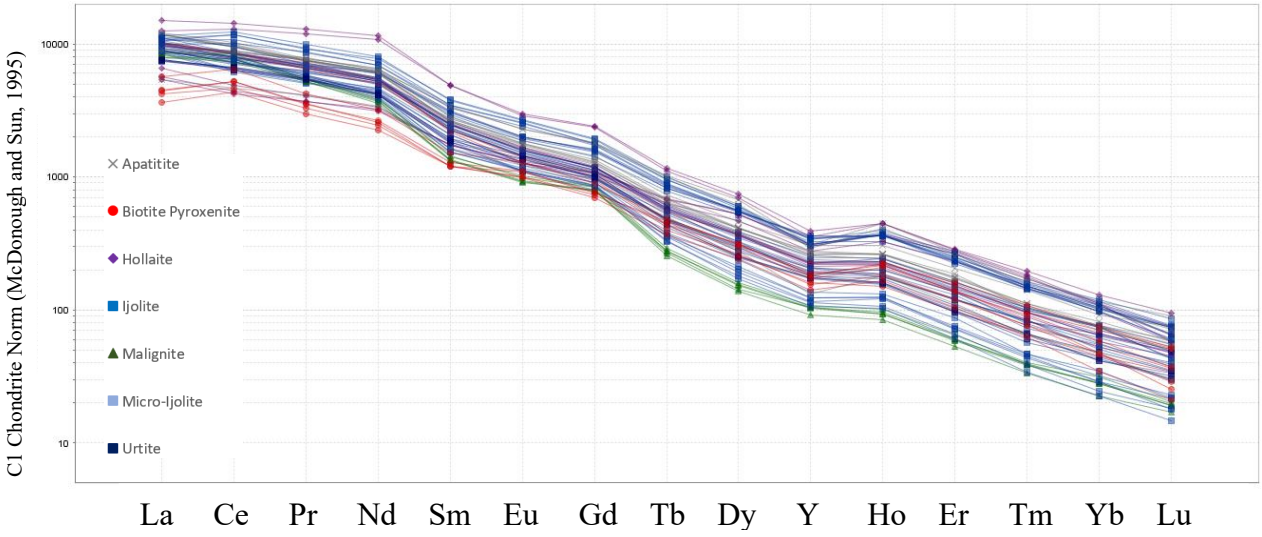

Figure 44: Chondrite-normalized LA-ICP-MS trace element data for apatite from Prairie Lake sorted by rock type

from Prairie Lake studied range from 0.6 in hollaite (PL95) to 1.2 in ijolite (PL63). Sr contents in apatite from Prairie Lake vary between 5980 ppm in biotite pyroxenite (PL55) to 8790 ppm in porphyry malignite (PL46).

3.3.3.1.1 – Biotite Pyroxenite

The two biotite pyroxenites with garnet data from Prairie Lake, PL49 and PL55, show similar chondrite-normalized patterns (Fig. 45). The LREE show the greatest difference with PL55 showing a La depletion relative to Ce not present in PL49. The LREE display the same pattern and converge at the MREE showing nearly identical patterns from Eu to Lu. The lowest REE contents from apatite occur in the biotite pyroxenites in sample PL55, 5751 ppm while the highest REE content found in apatite from the biotite pyroxenites is 11575 ppm in PL49. Representative apatite data from biotite pyroxenite is presented in Table 25.

Table 25: Representative LA-ICP-MS results (ppm) for apatite from biotite pyroxenites from Prairie Lake

Sample	**PL49**	**PL49**	**PL55**	**PL55**
Site	Ap1	Ap2	Ap2	Ap4
Rock Type	Biotite Pyroxenite	Biotite Pyroxenite	Biotite Pyroxenite	Biotite Pyroxenite
Si	6000	6290	-	-
Mn	199.8	202.1	199.9	231
Sr	8090	8520	6290	6850
Y	250.8	303	290	270
Zr	24.2	25.6	-	-
Ba	15.4	17.3	17.7	21.4
La	2429	2435	1344	1068
Ce	5190	5310	3930	3190
Pr	671	630	393	324
Nd	2443	2450	1452	1202
Sm	324	333	224.4	189.8
Eu	72.9	78.8	71.8	62.7
Gd	185.6	203.1	176.3	154.3
Tb	15.63	17.39	17.36	15.93
Dy	62.9	76.7	76	73.3
Ho	8.19	10.16	11.82	11.46
Er	15.7	19.5	22.45	21.8
Tm	1.63	1.88	2.09	2.27
Yb	7.23	8.57	7.58	9.49
Lu	0.84	0.89	0.626	0.915
Ta	0.088	0.047	b.d.	b.d.
Tot REE	11428	11575	7729	6326
Y/Ho	30.62	29.82	24.53	23.56
La/Yb	335.96	284.13	177.31	112.54
La/Nd	0.99	0.99	0.93	0.89
Tb/Yb	2.16	2.03	2.29	1.68

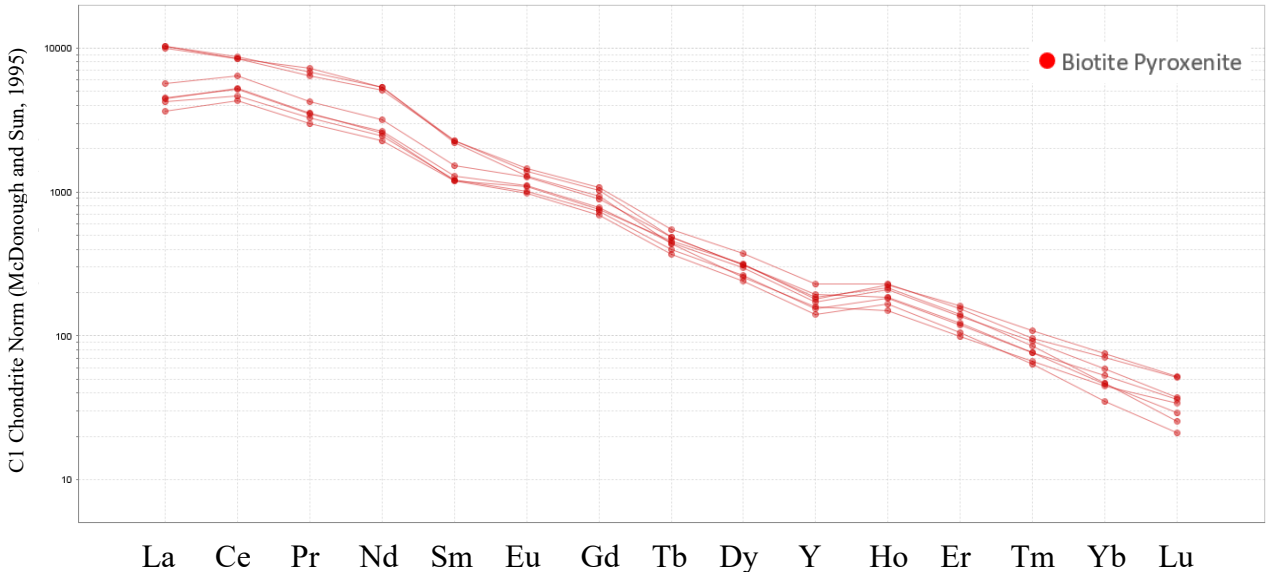

Figure 45: Chondrite-normalized LA-ICP-MS diagram for Apatite trace element data from Biotite Pyroxenites at Prairie Lake

3.3.3.1.2 – Ijolite Series

Members of the ijolite series display nearly parallel trends on a chondrite-normalized diagram (Fig. 46). Representative apatite data from ijolite-series rocks is presented in Table 26. The samples show negative slopes from La – Gd with several steps in the HREE. The HREE also display more spread. La/Nd ratios show variation from 0.73 in PL65 1.2 in PL63. Three trends are visible in the HREE; with some samples displaying high, intermediate and low contents with gaps between these profiles (especially around Ho – Er).

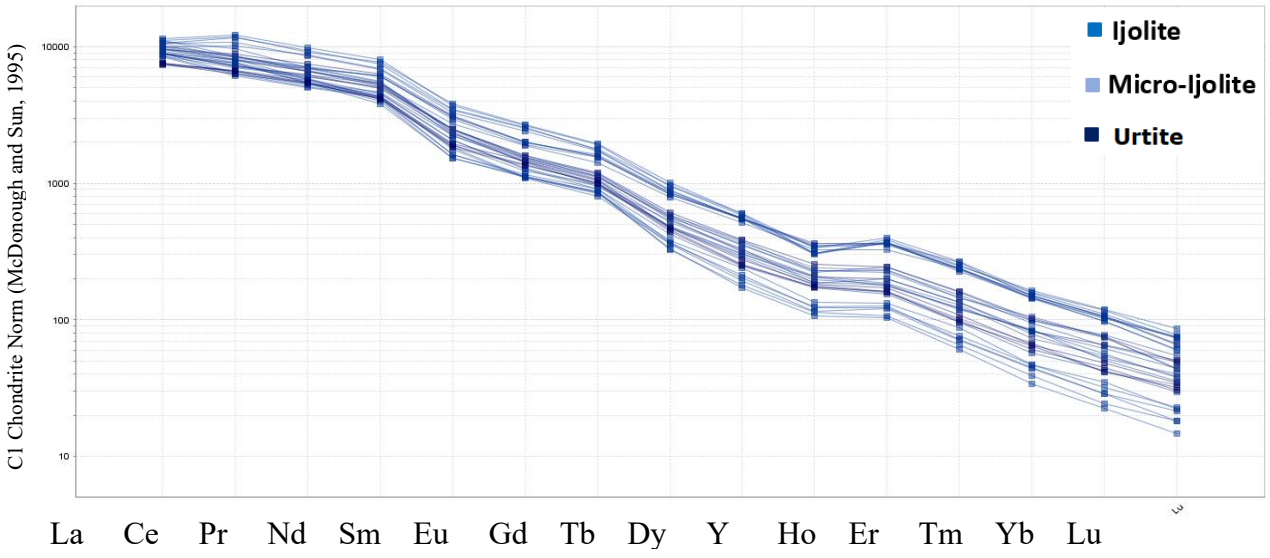

Figure 46: Chondrite-normalized LA-ICP-MS diagram for Apatite trace element data from Ijolite series rocks at Prairie Lake

ETR2, MT04, PL65, and PL76 contain apatite that display relative enrichment of REE contents, particularly the HREE relative to other members of the ijolite series. Three of these four samples display intermediate HREE contents. The only sample displaying enriched apatite being PL65. The samples showing the low HREE concentrations occur in two ijolite samples, ETR3 and PL63. The remaining ijolite series all have tightly constrained, overlapping HREE profiles.

Table 26: Representative apatite LA-ICP-MS data (ppm) for ijolite series rocks from Prairie Lake

Sample	ETR7c	PL65	PL63	PL78	PL91
Site	Ap1	Ap3	Ap3	Ap1	Ap2
Rock Type	Garnet Micro-Ijolite	Retexturized Ijolite	Garnet Ijolite	Garnet Ijolite	Urtite
Si	3680	b.d.	b.d.	4090	b.d.
Mn	167.5	295	148.5	168.1	176.7
Sr	6860	7010	8100	8170	7410
Y	351	475	180.7	282.5	285
Zr	11	b.d.	b.d.	11.53	b.d.
Ba	15.1	25.2	21.7	18.5	15.1
La	1740	2517	2086	2495	1779
Ce	4050	7180	4670	5130	4100
Pr	506	866	502	638	526
Nd	2110	3390	1737	2505	1959
Sm	331	514	226.6	350	288
Eu	83.2	143.9	63	80.6	81.5
Gd	220	350	171	199	209.1
Tb	20.4	32.4	12.81	17.34	17.06
Dy	88	135.3	47.4	70.1	67.5
Ho	13.2	19.95	6.58	8.8	9.37
Er	25.4	37.2	11.37	16.4	17.39
Tm	2.44	3.52	1.08	1.66	1.62
Yb	12.4	15.75	4.64	6.64	7.73
Lu	1.35	1.5	0.526	0.82	0.846
Ta	b.d.	b.d.	b.d.	0.033	b.d.
Tot REE	9203	15207	9540	11519	9064
Y/Ho	26.59	23.81	27.46	32.10	30.42
La/Yb	140.32	159.81	449.57	375.75	230.14
La/Nd	0.82	0.74	1.20	1.00	0.91
Tb/Yb	1.65	2.06	2.76	2.61	2.21

3.3.3.1.3 – Hollaite, Malignite, and Apatitite

Apatite trace elements from porphyritic malignite shows a somewhat different chondrite-normalized diagram to other apatite from Prairie Lake (Fig. 47). The LREE show a more convex shape, with minor La depletion relative to Ce. The sample shows strong depletion of MREE and

HREE relative to other apatite samples from the complex. Representative apatite data for hollaite, malignite and apatitite is presented in Table 27.

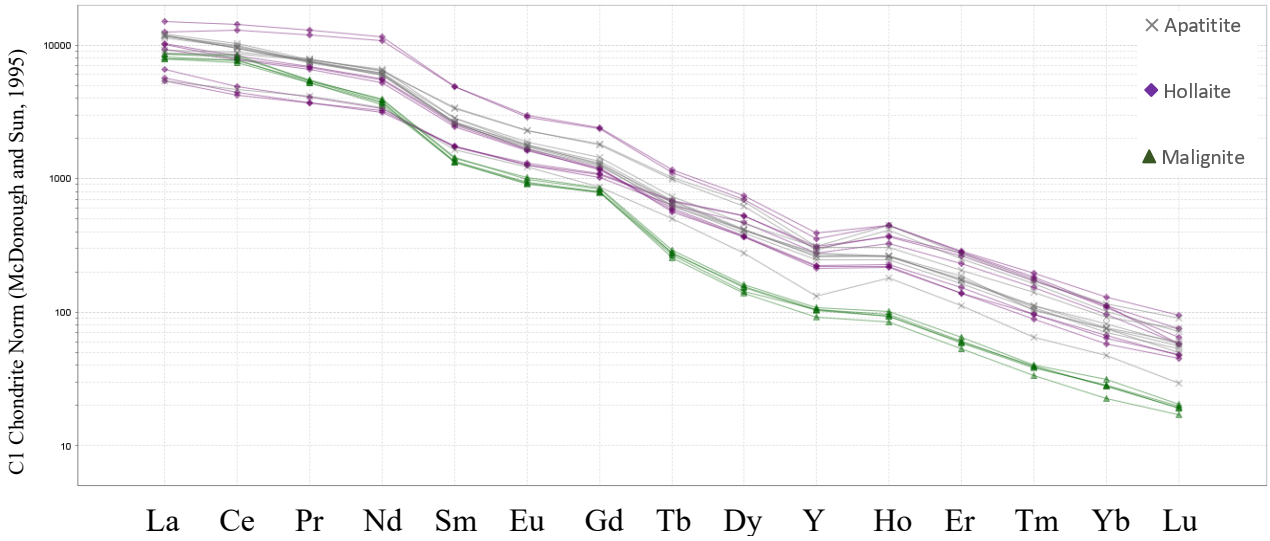

Figure 47: Chondrite-normalized LA-ICP-MS diagram for Apatite trace element data from Hollaite, Malignite, and Apatitite at Prairie Lake

Apatite data were collected from several hollaites (PL90, PL95, and PL96B), with relatively flat LREE patterns, concave patterns between Nd-Gd and Gd-Ho with flatly negative-sloped HREE from Ho-Lu.

Table 27:: Representative apatite LA-ICP-MS data for hollaite, malignite, and apatitite from Prairie Lake

Sample	PL96B	PL95	PL46	WS01A	PL90
Site	Ap1	Ap2	Ap3	Ap2	Ap2
Rock Type	Garnet Hollaite	Mica Hollaite	Porphyritic Malignite	Apatitite	Hollaite
Si	4380	4130	-	6000	2400
Mn	175.7	219.3	195	170.4	168.6
Sr	7140	6980	8280	8430	7350
Y	336	611	161.9	430	436
Zr	6.43	13.7	-	54.3	4.19
Ba	16.2	25.6	21.2	20.1	19.6
La	2423	3570	1881	2788	1549
Ce	5040	8810	4710	5750	3000
Pr	645	1202	486	690	376
Nd	2550	5280	1674	2700	1535
Sm	383	722	198.8	382	256.6
Eu	94.5	167.2	52.8	97	71.1
Gd	240	477	159.4	250.6	201.6
Tb	20.16	41.7	9.99	22.34	22.8
Dy	89.6	182	37.4	101.7	115.4
Ho	11.89	24.30	5.10	14.22	17.87
Er	22	45.8	9.32	28.5	36.9
Tm	2.18	4.83	0.95	2.75	3.79
Yb	9.31	20.7	4.55	13.2	15.4
Lu	1.10	2.32	0.484	1.42	1.41
Ta	0.064	b.d.	-	0.068	b.d.
Tot REE	11532	20550	9230	12842	7203
Y/Ho	28.26	25.14	31.75	30.24	24.40
La/Yb	260.26	172.46	413.41	211.21	100.58
La/Nd	0.95	0.68	1.12	1.03	1.01
Tb/Yb	2.17	2.01	2.20	1.69	1.48

3.3.3.2 – Fen

The apatite investigated from the Fen complex display a stepping negative slope similar to the other localities in this study with no major outliers in the pattern (Fig. 48). Representative data for apatite from Fen is presented in Table 28. Apatite from Fen shows variable La/Nd ratios from 0.93 in hollaite (405) to 1.84 in vipetoite (61) with extremely regular Tb/Yb ratios clustered around 1 (Fig. 43B).

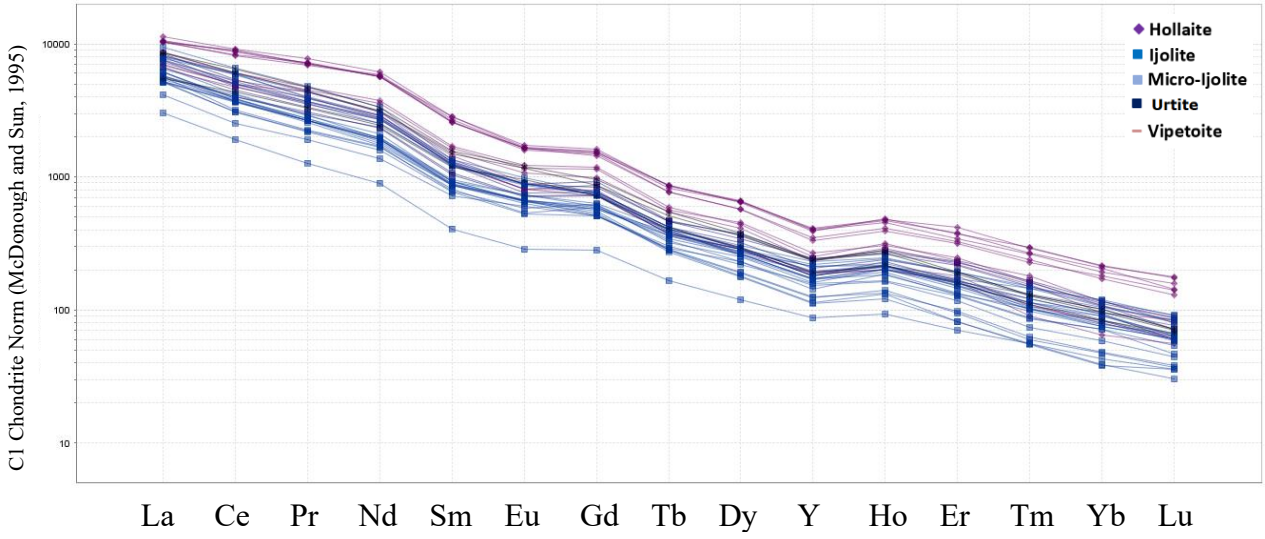

Figure 48: Chondrite-normalized LA-ICP-MS diagram for apatites from the Fen complex sorted by rock type

Perhaps most notably is the enrichment of apatite from hollaites in REE contents relative to ijolite series rocks at Fen. Apatite from hollaite contains the highest total REE contents in excess of 12,000 ppm in sample 405, showing an enrichment of ~3,000 – 4,000 ppm greater than other apatite analysed from the complex in this study. REE content in apatite from hollaites range from 6506 ppm (in 42) to 12,993 ppm (in 405). The lower end of which shows overlap with the ijolite series. The apatite in the ijolite series contains total REE contents from 3871 in ijolite (43) to 7605 in urtite (204).

Apatite data from three analytical sites were collected from one sample of vipetoite (FEN61). The apatite displays a negative LREE profile, a sharp decrease between Gd-Tb and slightly flattening before another decrease between Er-Yb. Apatite in vipetoite shows the highest La/Nd ratio from Fen, ranging from 1.6 to 1.84. Tb/Yb ratios show slightly more variation from 0.93 to 1.15. Total REE contents vary between 4331 and 5843 ppm similar to those of the ijolite series.

Table 28: RepresentativeLA-ICP-MS results for apatite from Fen samples

Sample	**204a**	**418**	**43a**	**61**	**42**	**35**	**405a**
Site	Ap1	Ap1	Ap3	Ap2	Ap2	Ap3	Ap1
Rock Type	Urtite	Hollaite	Ijolite	Vipetoite	Hollaite	Ijolite	Hollaite
Si	1520	b.d.	2420	1380	1270	1600	2400
Mn	173.9	212	96.4	72	233	148.3	180.4
Sr	6210	5020	5130	9.30E+03	4580	6430	4310
Y	285	396	182.9	328	302	270	551
Zr	7.32	0.54	8.24	1.02	b.d.	5.06	16.85
Ba	38.2	40.7	26.7	45.1	31.1	34.9	41.2
La	1319	2070	1610	1660	1660	1236	2470
Ce	2460	3730	2690	2560	3040	1880	5020
Pr	284	435	307	259	406	205	644
Nd	1057	1700	1098	900	1410	759	2650
Sm	154.4	251	142	146	212	120.3	388
Eu	40	69.4	38.6	37.2	51.3	30	89.2
Gd	143.8	234	124.8	145	152	118.1	298
Tb	13.45	21.3	10.73	13.5	15.2	12.4	27.6
Dy	70.9	108.3	49.6	66	73	64.3	141.3
Ho	12.64	17.2	7.4	11.4	11.6	11.1	22.5
Er	26.4	37.4	14.9	25.8	28.8	26.4	52.5
Tm	2.99	4.44	1.69	3.19	2.63	2.52	5.92
Yb	15	18.6	7.78	14.5	13.4	12.9	27.4
Lu	1.46	2.15	0.91	1.28	1.49	1.44	3.18
Ta	b.d.	b.d.	b.d.	b.d.	b.d.	b.d.	b.d.
Tot REE	5601	8699	6103	5843	7077	4480	11840
Y/Ho	22.55	23.02	24.72	28.77	26.03	24.32	24.49
La/Yb	87.93	111.29	206.94	114.48	123.88	95.81	90.15
La/Nd	1.25	1.22	1.47	1.84	1.18	1.63	0.93
Tb/Yb	0.90	1.15	1.38	0.93	1.13	0.96	1.01

3.3.3.3 - Good Hope and Mosonik

Apatites for two apatitite cumulate samples from Good Hope, VAL-2 and VAL-3 and one sample from Mosonik (Mosonik28) were analyzed (Fig. 49). Representative apatite LA-ICP-MS results from Good Hope and Mosonik are shown in Table 29.

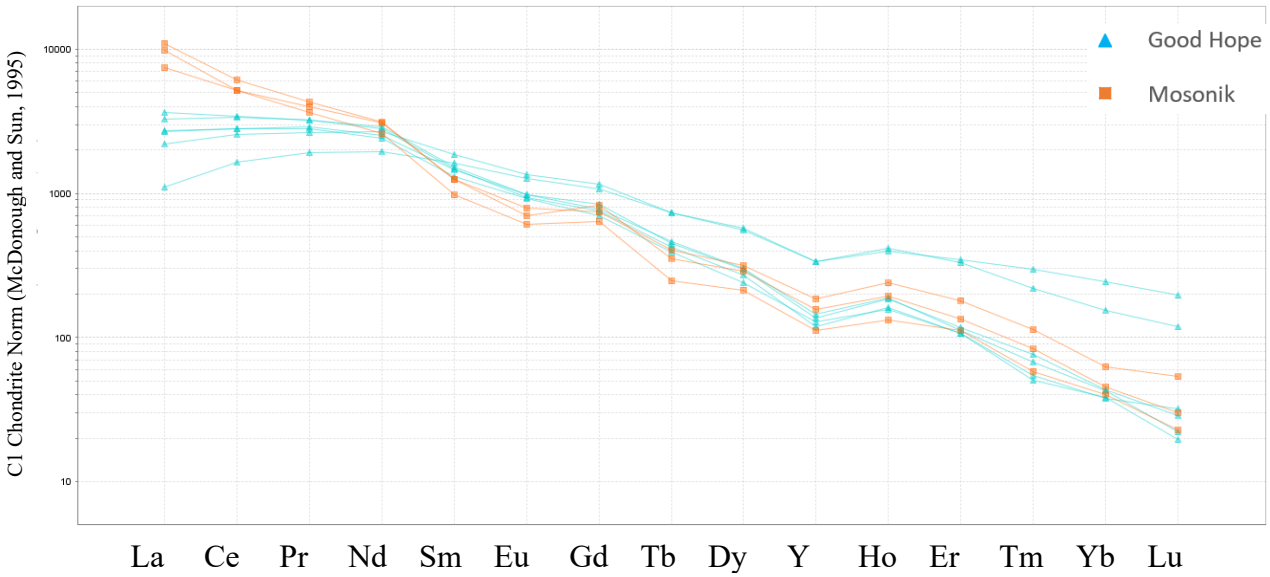

Figure 49: Chondrite-normalized LA-ICP-MS apatite trace element data for Good Hope (blue) and Mosonik (orange)

The LREE contents for apatite at Good Hope on a chondrite-normalized diagram plot as a flat to depleted pattern (notably different from the negatively sloping pattern for LREE from apatite from other complexes in this study). Sample VAL-2 shows a stronger depletion in the LREE than VAL-3 which shows a flatter shape. This is reflected in the La/Nd showing the lowest ratios in this study; below 0.7, reaching as low as 0.29. The MREE and HREE of both samples show a negative stepping slope with some apatite from VAL-2 showing relative enrichment in the LREE. Total REE contents are low relative to apatite from other sites in this study, with VAL-2 containing the lowest and highest contents from apatite at Good Hope showing variation from 3158 to 5143 ppm.

Table 29: Representative LA-ICP-MS data for apatites from Good Hope and Mosonik

Sample	Val-2	Val-3	Mosonik28	Mosonik28
Spot	Ap3	Ap1	Ap3	Ap1
Rock Type	Apatitite	Apatitite	Nephelinite	Nephilinite
Si	b.d.	b.d.	1700	1460
Mn	40.5	137.6	90	118.4
Sr	7370	8550	9.50E+03	13800
Y	529	227	175	247
Zr	0.63	b.d.	0.93	b.d.
Ba	12.8	10.7	42	29.3
La	260	631	1760	2610
Ce	1008	1720	3190	3760
Pr	178	267	339	399
Nd	895	1150	1180	1419
Sm	241	217	144	184
Eu	71.1	54.9	34.3	39.4
Gd	213	154	127	163.8
Tb	26.6	16.6	8.9	12.78
Dy	136.9	74.6	52.5	71
Ho	21.7	10.3	7.2	10.55
Er	55.3	18	17.9	21.4
Tm	7.3	1.67	1.44	2.05
Yb	39	6.87	6.5	7.28
Lu	4.8	0.54	0.56	0.74
Ta	b.d.	b.d.	b.d.	b.d.
Tot REE	3158	4322	6869	8701
Y/Ho	24.38	22.04	24.31	23.41
La/Yb	6.67	91.85	270.77	358.52
La/Nd	0.29	0.55	1.49	1.84
Tb/Yb	0.68	2.42	1.37	1.76

Apatite from Mosonik28 shows a similar shape to those of Prairie Lake and Fen (Fig. 49) showing a constant negative slope in the LREE with a negative stepping pattern for the MREE and HREE. Total REE contents show variation from 6869.3 to 8701 ppm over the three sites tested.

4 – DISCUSSION

4.1 – Mineralogy

Minerals are the record of the crystallization processes of magmas, and the variations in their major and trace element compositions provide evidence regarding the differentiation of their parental melts. In this context, with respect to alkaline rocks, the compositions of pyroxenes, garnets, micas, apatite, feldspars and feldspathoids are of particular importance in establishing differentiation trends within and between different batches of magma in an evolving plutonic magmatic system. This study focuses on the mineralogy and major and trace element composition of pyroxenes, garnets and apatite in ijolite series rocks and malignites from Prairie Lake with comparisons to ijolites from the Fen complex.

4.1.1 – Major Elements

4.1.1.1 – Clinopyroxene Compositions and Evolution Trends

4.1.1.1.1– Prairie Lake

Several distinct rock suites from the Prairie Lake complex were the focus of this investigation. These include: biotite pyroxenites (and associated CI carbonatite), ijolite-series, malignites, apatitite, and carbonatite xenolith-bearing dykes. These rock types are the result of different pulses of magma, best indicated by the pyroxenes at Prairie Lake which contain information regarding the development of the complex as illustrated by their petrography and major and trace element compositional variation. Clinopyroxenes from Prairie Lake display four evolution trends (Fig. 18 and Fig. 50) in the Di-Hd-Ae ternary system: (1) a biotite pyroxenite trend; (2) an ijolite trend; (3) the malignite trend; and (4) the apatitite trend.

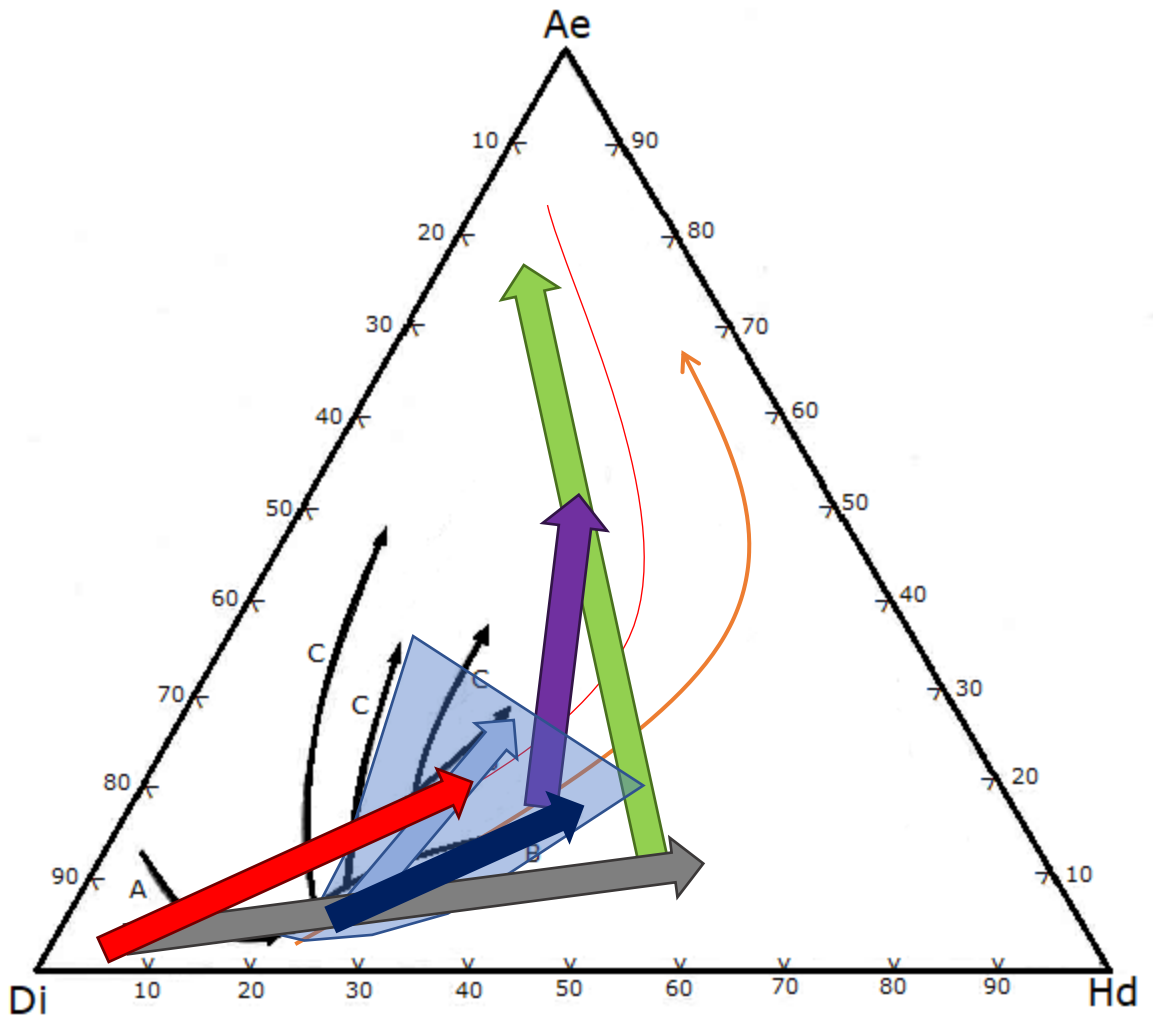

*Figure 50: Clinopyroxene evolution trends. Prairie Lake evolution trends for Biotite Pyroxenite (red arrow); ijolite-series (dark blue arrow); malignites (green arrow); and apatitite (grey arrow). General evolution of the Fen ijolite-series from this study is shown in light-blue cumulating in the Fen hollaite trend (purple arrow). Mosonik evolution trend orange line (this study). Black lines are evolution trends at Fen from Mitchell (1980); **A**. Fen damtjernite - vipetoite trend **B.** Fen aegirine - hedenbergite trend; **C**. Fen aegirine trend. (modified from Mitchell, 1980). Evolution trend from pyroxenes of the igneous complexes of eastern Uganda (red line) from Tyler and King (1967).*

The Prairie Lake evolution trends are consistent with those found in carbonatite-alkaline rock complexes elsewhere, as clinopyroxene-group minerals have been found to evolve from diopside-rich types to varieties with increasing aegirine enrichment during magma evolution (e.g. Andersen, 1988; Cooper and Reid, 1998; Reguir et al., 2012). The trends are similar to

those found for clinopyroxene at Fen in the ijolite series by Mitchell (1980). At Prairie Lake, the overlapping and different trends indicate that the complex could not have formed by simple crystallization of a single melt; hence, multiple pulses of magma are required to explain these trends. Mixing of multiple pulses of magma has previously been reported at Prairie Lake as the origin for the unique orbicular ijolites found in the complex (Zurevinski and Mitchell, 2015).

Crystals of unevolved diopside compositions, plotting close to the Di-Hd binary and with < 20 mol.% Ae, are present in biotite pyroxenite, apatitite and carbonatite xenolith-bearing dykes. In most samples they occur as xenocrysts, however in both the biotite pyroxenite and the apatitite they are encased in later stage clinopyroxene richer in Ae and Hd components. It is clear that they are formed under different conditions than most clinopyroxenes found at Prairie Lake. At Fen, clinopyroxenes of similar composition are found in the damtjernite, associated with spinels suggested to have formed under high pressure and high temperature conditions (Mitchell, 1980; Griffin, 1979). Trace element data collected for clinopyroxene from the biotite pyroxenites further supports this hypothesis, as the cores display a different REE distribution pattern to the rims (Fig. 30). The cores have higher REE contents and a flat HREE profile, whereas the rims are similar to other clinopyroxene at Prairie Lake.

The compositions of clinopyroxenes from Prairie Lake show overlapping trends (Fig. 50) with the unevolved compositions found at Mosonik (this study) and other African rift related volcanoes (Tyler and King, 1967).

The diopside-nepheline-sanidine ternary system is relevant to the origins of the ijolite series, and especially those related to malignites, as it contains the essential minerals of the ijolite series. It is however not a perfect representation as it lacks several important phases such as garnet, biotite, apatite and calcite. Experimental studies of the system by Gupta et al. (2006)

[P(H_2O) = P(Total)] has shown that at pressures of 1.0 GPa to 2GPa (depths of 30-35 km and 60-65 km, respectively; Fig. 51A) diopside is the primary mineral to crystalize from a nephelinitic magma at temperatures >670ºC. The ternary is quite different at 0.1 GPa (Fig. 51B), where nepheline and forsterite are present at temperatures >820ºC. This provides further evidence that the diopside cores probably form deeper in the complex.

4.1.1.1.2 – Fen and Mosonik

The clinopyroxenes from Fen investigated in this study show a similar evolution trend towards aegirine, overlapping with trends previously reported by Mitchell (1980) (Fig. 23; Fig. 50). The ijolites from this study are consistent with those found in the aegirine-hedenbergite trend for ijolites and urtites, and the aegirine trend for late stage urtites. This study also revealed a previously unreported trend for the hollaites, which originates from the most evolved aegirine-hedenbergite. This is because of the genetic relationship between the two, with hollaites being differentiates of ijolite –forming magmas (Mitchell and Brunfelt, 1975).

The evolution trend for clinopyroxene seen at Mosonik (Fig. 26; Fig. 50) shows overlap with both Prairie Lake and Fen compositions, but evolves quite differently from the sub-volcanic complexes, approaching the aegirine-hedenbergite binary evolving towards aegirine. This is consistent data for other nephelinite volcanoes from the East African rift (Tyler and King, 1967).

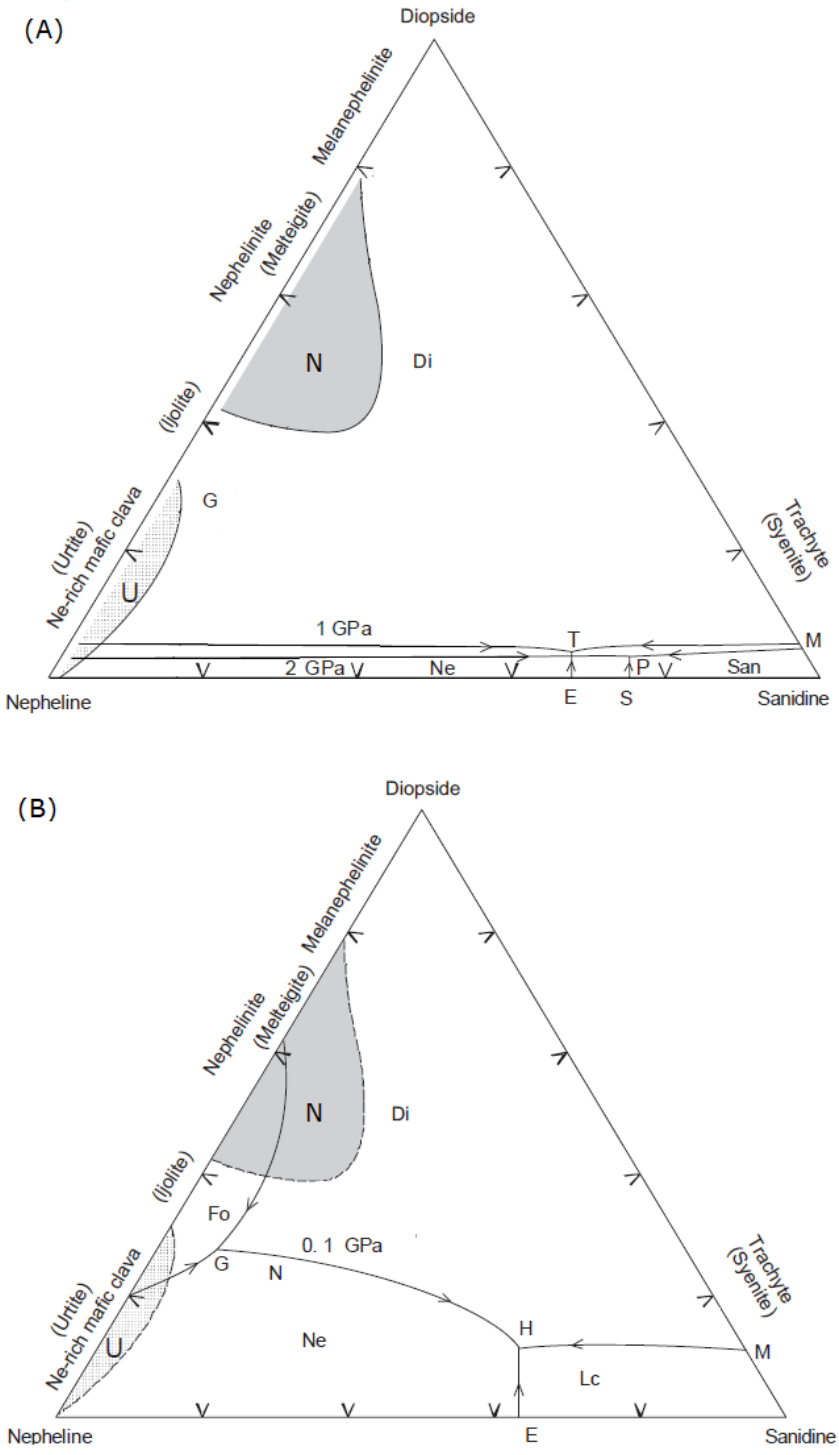

Figure 51: (A) Nepheline-Clinopyroxene-Sanidine ternary at 1GPa and 2GPa, grey field labelled N is the nephelinite field, dotted field labeled U is the urtite field (modified from Gupta et al., 2006) (B) Nepheline-Clinopyroxene-Sanidine ternary at 0.1GPA, grey field labelled N is the nephelinite field, dotted field labeled U is the urtite field (modified from Gupta et al., 2006).

4.1.1.2 – Garnet

Garnet at Prairie Lake and Fen occurs as part of the Ti-bearing andradite-schorlomite-morimotoite solid solution, consistent with garnets found in other undersaturated alkaline igneous rocks (Huggins et al., 1997a, b). At Prairie Lake, garnet is ubiquitous in the ijolite-series, where it occurs predominantly as a late stage mineral appearing opaque in thin section. Compositions of garnets from most of the ijolites together with the malignites plot in the andradite-schorlomite-morimotoite ternary system, and occur in a field between 30-60% And, 10-30% Sch, and 20-50% Mor. The REE contents of most garnets also show an identical overlapping chondrite normalized trend which may indicate that all residual melts evolve to similar compositions. While the presence of garnet is important and a characteristic feature of the ijolites, they are absent from the biotite pyroxenites. This indicates that the biotite pyroxenites are of different origin to rocks of the ijolite-suite, and probably represent cumulates from different batches of magma.

Garnet compositions from Fen are similar in being a Ti-rich and members andradite-schorlomite-morimotoite ternary solid solution series (Fig. 25). A difference from Prairie Lake is that that ijolites and micro-ijolites show quite different compositions, as opposed to overlapping at Prairie Lake. Micro-ijolites are much more andradite-rich, while ijolites plot closer to the center of the diagram towards the And-Mor boundary. At Prairie Lake, both ijolites and micro-ijolites plot closer to the center of the diagram.

4.1.2– Trace Elements

This study presents the first investigation of trace elements (Zr, Y, REE) from clinopyroxene, garnet and apatite from ijolite suite rocks in a carbonatite complex. Many previous studies investigating trace elements have provided only partial REE data (e.g. Mao et al., 2016; Hode Vuorinen et al., 2005). Other previous work has only been comparison studies contrasting the trace element content of minerals in single or very few samples from different carbonatite complexes, notably clinopyroxene, amphibole, and apatite (e.g. Chakhmouradian et al., 2017, Reguir et al., 2012). Perhaps the most relevant studies are Chen et al. (2016), which investigated trace elements in garnet from calcitic ijolite from the Oka complex, as well as Doroshkevich et al. (2015), which investigated trace elements in fluorapatite and pyrochlore from Belaya Zima. As a result of this general paucity of studies, the processes involved in trace element sequestration to particular minerals in carbonatitic and nephelinitic melts is not currently well understood.

4.1.2.1 – Clinopyroxene

Clinopyroxenes commonly contain a significant fraction of the trace element budgets of carbonatites depending on their modal abundance (Reguir et al., 2012). As such it is possible to infer that they are similarly important in carbonatite-associated ijolitic systems. Clinopyroxenes from Prairie Lake and Fen show a sinusoidal REE chondrite normalized distribution pattern similar to those found in carbonatites in general (Reguir et al., 2012).

Whereas most samples display a very similar pattern, with convex LREE and concave HREE, the colourless diopside cores found in the biotite pyroxenite display unique traits, with a flat HREE profile and total REE contents which are much higher than other pyroxenes

investigated. This is expected as the biotite pyroxenites are considered to have formed at depth under different P and T conditions.

One feature present in these rocks that has not been reported previously is the wider spread of HREE in comparison to LREE. While the LREE show a relatively constrained pattern and REE contents, with a significant overlap on a chondrite-normalized diagram, the HREE show a high degree of variability. This highlights the potential problems of using a single sample to represent an entire site. The observed variation is probably the result of late stage fluids at Prairie Lake interacting with the previously-formed clinopyroxene and re-enriching these in REE. This interaction would only be noticeable in the HREE, as the concentration is much lower than the LREE.

REE and Y partitioning into clinopyroxene has been assumed to occur at the M2 site with little to none in the M1 site (Wood and Blundy, 2014; Wood and Blundy, 2002; Blundy and Dalton, 2000); however, the discovery of sinuous REE profiles in alkali-syenitic rocks (Marks et al., 2004) and carbonatite (Reguir et al., 2012), has brought this assumption into question. Thus, Reguir et al. (2012) have proposed two-phase partitioning of the lanthanides into two different crystallographic sites and suggest that the heavy lanthanides preferentially partition into the six-coordinated M1 site and the light lanthanides into the eight-coordinated M2 site. This two-site partitioning model could help to explain the sinusoidal forms of the clinopyroxene seen in alkaline and carbonatitic rocks with preferential uptake in the M2 site as opposed to the M1 site. This model assumes that the REE distribution is not affected by late deuteric or subsolidus processes as suggested above.

4.1.2.2 – Garnet

Garnets from Prairie Lake, Fen, and Mosonik are enriched in REE (>1300 ppm) in the majority of samples. Most samples from Prairie Lake have REE contents between 2000-3000 ppm. All samples display a similar chondrite-normalized pattern of a LREE depletion, a MREE high and declining HREE (Fig. 36). This pattern is quite similar to that of garnets in the Oka calcite-ijolite (Chen et al., 2016), pyroxenite, ijolite, and nepheline syenite from Alnö (Hode Vuorinen et al., 2005).

Chen et al. (2016) concluded that the melanites contain up to 98% HREE, 85% MREEs, and 20% LREE of the calcite-ijolite whole-rock budget based on their modal distribution. HREE contents in Prairie Lake garnets are primarily between 500 and 1000 ppm, exceeding 1700 ppm in some examples.

Garnets at Prairie Lake contain Zr in excess of 10000 ppm, up to ~32000 ppm, with only one outlier, a wollastonite hollaite xenolith, PL86. Zr contents in garnet at Prairie Lake are an order of magnitude greater than those found at Oka (~1000-2000 ppm) (Chen et al., 2016). This may indicate that the nephelinite magmas that formed Prairie Lake were enriched in Zr.

Chen et al. (2016) highlight the significant effects that fractionation of melanite at Oka could have on the REE distribution of minerals co-crystallizing or later-forming than the garnet, strongly depleting the MREE and HREE budgets from the melt. This is possibly true of Prairie Lake, as garnet co-crystallizes with or forms later than clinopyroxene and prior to apatite and other late-stage minerals. With the REE contents of garnet at Prairie Lake being greater than the Oka melanites (1300-1900 ppm) it is probable that the garnets at Prairie Lake have a strong effect on the removal of heavy REE from the melt, especially in the ijolite-suite with which they are ubiquitous. Hence, deuteric melts can be expected to be enriched in LREE as noted above.

The different phases of garnet identified at Oka by Chen et al. (2016) show very similar REE patterns, with overlapping LREE and diverging HREE. The majority of garnet samples from Prairie Lake occur as a very restricted range of distribution patterns with little deviation of the LREE. One sample, MT-04, displays enriched HREE relative to the others which indicates it formed from a very different magma or under very different P-T conditions.

Sample PL86, a wollastonite hollaite differs in having much lower REE contents, and with distribution patterns not overlapping with any other samples, and Zr contents a magnitude lower than other samples at Prairie Lake (~1000 ppm). Optically, the garnet in this sample is red, and thus different from the opaque garnets seen in ijolites These differences and the presence of wollastonite, suggest that this rock did not form under the same conditions as the ijolites, a hypothesis supported by its occurrence as xenolith included in CII carbonatite.

4.1.2.3 – Apatite

The REE budget of apatite can serve as an important petrogenic indicator, especially in rocks where apatite is a common accessory or even major phase (Chakhmouradian et al., 2017; Mao et al., 2016). The apatite trace element data for Prairie Lake, Good Hope, and Fen are quite similar to that found in other carbonatite complexes as noted by Chakhmouradian et al. (2017) and Mao et al. (2016), with negatively sloping chondrite-normalized profiles. The total REE contents are high relative to other minerals investigated in this study, as a result of the affinity of apatite for REEs which vary between ~6000 to 15000 ppm at Prairie Lake, well above REE contents of both garnet and clinopyroxene. It is important to note, that apatite at in the Prairie Lake ijolites appears to predominantly form as a late-stage mineral, closely associated with interstitial garnet and calcite.

In contrast apatitites from Good Hope occur as earlier forming apatitite cumulates and consequently display different trace-element distribution patterns relative to Prairie Lake, Fen and Mosonik, with a strong depletion in LREE resulting in a convex pattern as opposed to the more linear patterns of the other samples. Chakhmouradian et al. (2017) highlights some of the effects of early crystallization of apatite where La is less compatible than Nd. Such apatite forming as an early-stage mineral that fractionates into cumulates and phoscorites will show a depletion in LREE. This is consistent with the Good Hope apatite data.

Current understanding of REE partitioning into apatite is limited by a poor understanding of the partitioning of elements from carbonate-rich melts into the mineral, with experimental studies providing conflicting results (Hammouda et al., 2010; Klemme and Dalpé, 2003). No experimental research has been directly conducted on apatite in ijolitic melts and how partitioning might differ from that in carbonatites.

The ability for the REE to substitute into two different cation sites of different geometry is one of the problems with accurately determining partitioning. REE may partition into either the Ca(1) site, which has ninefold-coordination, or the Ca(2) site, which has sevenfold-coordination (Fleet and Pan, 1995; Fleet and Pan, 1997). Chakhmouradian et al. (2017) have proposed that the accepted model of fitting apatite REE partitioning coefficients to a single curve is misleading and that instead there is preferential uptake of the LREE into the Ca(1) site and HREE into the Ca(2) site with the MREE accommodated equally well into both sites. This indicates that negative slope may be the result of lack of the HREE in the melt prior to the crystallization of apatite, perhaps by sequestration into other phases such as garnet.

One of the most interesting features of apatite analysed in this study is that Y/Ho ratios show a wide amount of variation. This is consistent with other apatite seen in other localities as

well as experimental data, which indicates Y is subtly less compatible than Ho in apatite resulting in sub-chondritic ratios in igneous apatite (Chakhmouradian et al., 2017).

Sr contents in apatite at Prairie Lake vary between ~6000-9400 ppm, lower than apatite in Mosonik (>9500 ppm) and overlapping with Fen ijolite (3850-9300 ppm) and Good Hope carbonatite (7370-9300 ppm). These are similar to Sr contents seen in apatite carbonatites worldwide (1840–22498 ppm; Mao et al., 2016; Chakhmouradian et al., 2017).

4.2 – Petrogenetic Development of the Prairie Lake Complex

The rocks at Prairie Lake represent at least four significant rock suites emplaced at the current erosion level: (1) biotite pyroxenites (together with CI carbonatites), (2) ijolite suite rocks (differentiating to hollaites and, (3) malignites), and (4) CII carbonatites. Each of these suites represents a compositionally different batch of magma. Other rock types such as wollastonite-apatitites, phoscorites, dolomite carbonatites, amphibole-pyroxene calcite carbonatites are represented by xenoliths and minor intrusions. A variety of emplacement processes are considered to have been active during formation of the complex, including magma mixing, crystal settling and differentiation, solid-state deformation and re-equilibration, and deuteric alteration.

4.2.1 – Magma Composition and Origins

A major question regarding the origins of the Prairie Lake complex is that of the source of the magma and processes involved at depth. Previous isotopic studies by Wu et al. (2017) showed that all of the rocks at Prairie Lake can be traced to a common source as evident from the identical initial Sr and Nd isotopic composition. The initial stages of development of Prairie Lake have been recorded in xenocrysts transported from depth in the biotite pyroxenite and xenolithic cumulates such as apatitites and wollastonitites. Clinopyroxene found in these rocks have the most unevolved compositions in the complex (>80 mol.% diopside).

The nature of the magma forming the silicate rocks at Prairie Lake is indicated by the consanguineous assemblage of ijolite-series rocks and carbonatites. These suggest formation from a nephelinitic magma, placing Prairie Lake in the nephelinite-clan of carbonatites as

opposed to the melilitite-clan of carbonatites as defined by Mitchell (2005), as melititolites are absent from Prairie Lake.

It is extremely unlikely that the rocks present in the complex were formed from a single batch of magma following a single channel of the ascent. Instead it is more probable that transportation involved an anastomosing series of channels at depth with cumulates forming at choke points. This cross-cutting network of channels would allow for small batches of similar magma to have slightly different evolution and crystallization sequence during emplacement at crustal levels.

4.2.2 – Biotite Pyroxenite

The biotite pyroxenites found in the northeast portion of the complex are different from members of the ijolites in the complex. The most notable difference is mineralogical, with an absence of nepheline and garnet, both characteristic of the ijolite series rocks. This, together with the significant biotite contents not seen elsewhere in the silicate rocks at Prairie Lake suggest that the biotite pyroxenites formed in a separate event to the ijolite series rocks. Further supporting this hypothesis, is the presence of xenoliths of biotite pyroxenite within the ijolite series (Mitchell, personal communication, 2019) indicating that the biotite pyroxenites were formed prior to emplacement of the ijolites.

The zoned clinopyroxene in biotite pyroxenites, with unevolved cores and evolved rims, are indicative of transport of crystals formed at depth to shallower emplacement levels (see section 4.1.1.1.1 for further discussion) The biotite pyroxenites contain trace minerals rich in REE such as marianoite-wöhlerite and wadeite. The presence of these minerals indicates that the magma parental to the biotite pyroxenites contains similar REE contents to those of the ijolite

series, or that the biotite pyroxenites came in contact with fluids containing REE, possibly residua from a malignite -forming fluid.

4.2.3 – Ijolite-series

The ijolite suite of rocks is one of the major components of the complex at the current level of exposure (Sage, 1987; Wu et al., 2017). The clinopyroxenes found in different members of the ijolite series display unique evolutionary trends, from intermediate diopside compositions following a near- linear path with increasing hedenbergite and aegirine contents (Fig. 18). This trend contains almost all members of the ijolite series, with minor outliers, suggesting common emplacement events, different to those forming the biotite pyroxenites or carbonatite dykes.

There is no geological or geophysical evidence for the presence of a large-scale magma chamber at Prairie Lake; thus, the ijolites are considered to have been formed by crystallization of repeated injections of small intrusions. As it is well known that magmatism in volcanic complexes is pulsatory, one can expect multiple intrusions of small volumes of the ijolite-forming magmas into consolidated or partially-crystallized previously emplaced batches of magma of similar but not identical composition (Emeleus and Troll, 2014). This scenario suggests also that as the magma cools, incompatible elements are concentrated into a residuum that is responsible for both primary pegmatitic malignites and extensive deuteric alteration of some of the ijolite series.

Currently, petrological hypotheses have moved away from the concept of large magma chambers to episodic intrusion of small batches of magma. The Rum complex, Northwest Scotland, is an excellent example of such processes. The complex consists of a well exposed layered suite with features similar to those seen in clastic sedimentary rocks, including layering,

graded bedding, slumping, and flame structures (Emeleus and Troll, 2014). Previous research concluded that events occurring in a magma chamber were the probable origin of these features (Wager et al., 1960., Wager and Brown, 1968). Recent research has brought this idea into question, with it becoming evident that the Rum Layered Suite was formed as the result of repeated magma intrusions with various degrees of crustal contamination into a thin, continuously growing sheet of sill-like magma (O'Driscoll et al., 2007; Emeleus and Troll, 2014).

4.2.3.1 – Sequence of Crystallization

The ijolite-series rocks at Prairie Lake are commonly altered and overprinted by a wide variety of processes. Several ijolite samples do preserve a record of the sequence of crystallization of major minerals in the ijolites. Nepheline and clinopyroxene both form subhedral-to-euhedral crystals indicating they are early liquidus phases from the parent magma. Samples ETR3 and PL64 contain tabular crystals of clinopyroxene with subhedral nepheline, indicative of clinopyroxene forming earlier. Samples PL76, and PL96B contain evidence of cotectic crystallization of clinopyroxene together with nepheline. PL81 contains euhedral-to-subhedral nepheline with later clinopyroxene. These differences record different crystallization paths along, or on either side of, the eutectic seen in Fig. 51B, which might reflect the consequences of magma mixing on bulk compositions.

Following the crystallization of clinopyroxene and nepheline is the formation of late-stage garnet, closely followed by apatite. This differentiation to Ca-P-Fe residua has not been previously emphasized in investigations of ijolite. Calcite present in the ijolites is almost exclusively interstitial, and as such, appears to be one of the last primary phases to crystalize

together with associated biotite. Nepheline in contact with late stage calcite commonly alters to cancrinite. Garnet urtites, with euhedral nepheline encased in garnet, were probably formed as floatation cumulates.

4.2.3.2 – Syn-emplacement solid-state deformation

One important conclusion of this study is recognition of the role of syn-emplacement deformation throughout most of the ijolite series rocks. The suite contains many samples in which all the crystals display rounded-to-anhedral morphologies and are most obvious in the micro-ijolites (see Fig. 10). This allotriomorphic texture is indicative of crystal annealing, or re-crystallization (Griggs et al., 1960). Annealing of an initial crystallized ijolite which would require added heat, probably from subsequent pulses of ijolite parental melts. Carbonatitic melts would be extremely unlikely as the source for this alteration as they are considered to form at lower temperatures than ijolitic melts and would thus not have the energy required for deformation. Annealing textures have been reported at Prairie Lake in the orbicular ijolites by Zurevinski and Mitchell (2015). In that case it was concluded that the orbicular ijolites were the likely result of a partially-crystallized ijolitic melt encountering a second ijolitic melt and undergoing both magma-mixing and annealing. Accordingly, it is suggested that intrusion of nephelinite magma into pre-existing ijolites results in the recrystallization of the latter. The process must have occurred at similar temperatures as there is no evidence for melting of pre-existing ijolite or formation of a new mineral assemblage

4.2.4 – Malignites

The malignites found at Prairie Lake have a direct relationship to the ijolite series rocks, as they are formed by magmatic differentiation and also by deuteric alteration of pre-existing ijolite series rocks. The clinopyroxene compositional trend in malignites trend occurs as a culmination of the ijolite series pyroxene trend, with some overlap occurring with the most evolved ijolites and the least evolved malignites.

The malignites are formed by the concentration of incompatible elements from the ijolite magma into residual fluids. Appreciable Na, Ca, and K would be needed to form the K-feldspar + zeolites. At 0.1GPa, a melt with a composition on the nepheline-clinopyroxene-sanidine ternary will differentiate and evolve towards the sanidine field and the crystallization of K-feldspar (Gupta et al., 2006). Minerals such as the marianoite-wöhlerite series, wadeite, calzirtite, strontianite, and zircon are rich in elements concentrated in the residua and can be used to characterize the fluid, which was rich in Nb, REE, Sr and Zr.

4.2.5 – Carbonatites and other rock types

While the objective of this work is not to investigate the carbonatites found at Prairie Lake, some conclusions can be made regarding their relationships to the rest of the complex. Most notably, the presence of ijolite xenoliths in the CII carbonatite (Mitchell, personal communication, 2019) indicates that emplacement occurs after formation of the ijolite-series.

Carbonatite dykes are present as xenoliths in the complex and record evidence of what is happening at depth. Present within these dykes is a diverse assemblage of antecrysts. Unevolved diopside of similar composition to the diopside cores in the biotite pyroxenite and which

probably crystallized at similar depths and P-T conditions. These pyroxenes indicate that the biotite pyroxenites are early formed cumulates from a nephelinite magma at depth. Alteration of these antecrysts is common with clinopyroxene with chlorite alteration around the mantles; euhedral and resorbed apatite, and olivine altering to chlorite and serpentine.

Apatitites display cumulate textures; however, their relationship to ijolite-series rocks is difficult to determine. The clinopyroxene compositions in apatitite display a trend overlapping with the ijolite-series but extending into the hedenbergite field while also containing diopside cores formed at depth identical to those seen it the biotite pyroxenites. Also present is resorbed wollastonite, a mineral found exclusively in xenoliths or as xenocrysts. Previous investigation of Prairie Lake by Sage (1987) recorded the presence of wollastonite ijolites although none were examined in this study. It is uncertain what relation they have with other ijolite-series rocks at the complex. They are undoubtedly formed from nephelinite magmas as wollastonite nephelinites and wollastonite ijolites are present in the recent nephelinite volcanoes of the East African Rift (e.g. Oldoinyo Lengai, Sharygin et al., 2012).

4.2.6 – Model of Formation

From this study, the following petrogenetic model is suggested (Fig. 52). A melt originating from a weakly depleted mantle source rises is emplaced at crustal levels and forms the sub-volcanic rocks seen at Prairie Lake (Wu et al., 2017). As the melt was rising through the crust, crystallization of unevolved diopside crystals occurred as recorded in the biotite pyroxenites and apatitites found in the complex. The size of many of the crystals and cumulate textures preserved in xenoliths and xenocrysts from depth indicate that cumulates were formed

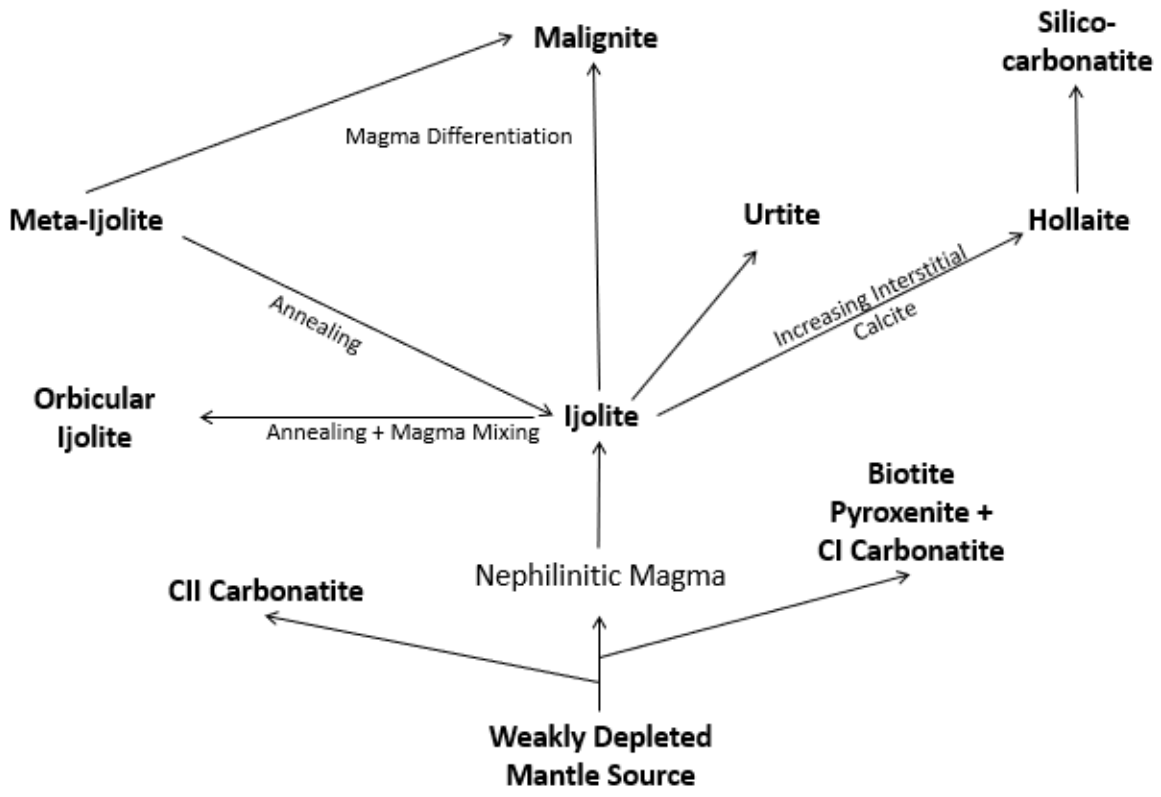

Figure 52: Petrogenetic model for the Prairie Lake carbonatite complex as indicated by the present work and Wu et al. (2017)

as the mantle-melts traveled; perhaps occurring at choke points where rising crystals would get trapped and grow further.

The most unevolved rocks at Prairie Lake are preserved as the biotite pyroxenite suite. One batch of magma transported unevolved diopside crystals from depth, which acted as nuclei for more evolved Na- and Fe-rich diopside crystallizing from the melt at the time of emplacement.

Ijolites were emplaced subsequent to the biotite pyroxenites as evidenced by the ijolite series containing xenoliths of biotite pyroxenites. The ijolite series records a very complex emplacement with evidence of crystal settling (euhedral nepheline encased in garnet in the garnet

urtites), solid-state recrystallization and deformation (the meta-ijolites), magma mixing (orbicular ijolites), magma differentiation (malignites) and deuteric metasomatism of varying intensities and styles.

As suggested above the ijolite series are the result of multiple, pulses of small volumes magma of a similar composition, and the meta-ijolites resulted from the solid-state deformation and thermal metamorphism induced by later pulses of ijolite. As the ijolite-series crystallized, incompatible elements (K, Sr, Zr, Nb, and REE) were concentrated in the residua leading to the formation of the malignites.

The calcite carbonatite of the C-II carbonatite followed the emplacement of ijolite-suite, and associated malignites. These carbonatites contain xenoliths of ijolite, wollastonite –apatititte and phoscorite. The latter are not exposed at the current level of erosion but are derived from the deeper levels of the complex. The dolomite carbonatite might represent the final stage of CII magmatism.

4.3 – Comparing Prairie Lake, Fen, and other ijolite-associated complexes

The Prairie Lake and Fen complexes exhibit many similarities, with both localities containing ijolites associated with carbonatites. Both can be classified as nephelinite-clan carbonatites (Mitchell, 2005). The ijolite series at both Fen and Prairie Lake show a similar relationship of ijolites differentiating to malignites.

The model proposed in this study for Prairie Lake is similar to that of Fen by Andersen (1988), but also has several important differences. The ijolite series in both complexes evolves towards malignitic differentiates (a.k.a. juvites or nepheline syenites at Fen). Andersen's (1988)

model for Fen describes the carbonatite being derived from the fractionation of melts into two magmas. While this is a possibility at Prairie Lake, from this study it is difficult to say with any certainty if the CII carbonatites are directly derived from an ijolite parent melt or is the result of intrusions of a later magma following the same conduit. It is evident that ijolites in some instances differentiate towards hollaites (or calcite ijolites) whereas other evolve to malignitic residua. Determination of the relationships of ijolites to CII carbonatites are beyond the scope of this study

A major difference between Prairie Lake and Fen is the role of pyroxenites. Andersen (1988) postulated that the pyroxenite at Fen "most probably originated as a pyroxene cumulate formed at an advanced stage of evolution towards nepheline syenite." In contrast the biotite pyroxenites at Prairie Lake were formed and emplaced in an event prior to the ijolite-suite. At Fen, the ijolite series is intruded by the later damtjernites and associated dolomite carbonatites and ferrocarbonatites (Saether, 1957; Andersen, 1987b). Damtjernites are not present at Prairie Lake and dolomite carbonatites occur only as a minor phase, while ferrocarbonatites occur only outside the main intrusion at Ruffle Lake.

The model for Prairie Lake also shows some similarities to that of the Belaya Zima alkaline-carbonatite complex in Russia (Doroshkevich et al., 2015). Belaya Zima displays a similar sequence of crystallization to that of Prairie Lake, the earliest crystallizing rocks being pyroxene-rich, melteigite (lacking a major mica component) in the case of Belaya Zima, and biotite pyroxenite in the case of Prairie Lake. This is followed by emplacement of ijolites and urtites, then nepheline syenites and finally carbonatite. A key difference is that clinopyroxene from Belaya Zima shows a single evolutionary trend, indicating that the different rocks (represented by nineteen samples) were formed from a single batch of magma (Doroshkevich et

al., 2015), whereas Prairie Lake displays a much more complicated evolution with several batches of magma present, and the biotite pyroxenite forming as a separate event from the ijolite-series.

The model for the Alnö complex proposed by Anderssen et al. (2013) displays several important differences with that of Prairie Lake as proposed in this study. In that model, geophysical data (reflection seismic, gravity and magnetic profiles) are used to investigate the shape of the roots of the complex to a depth of up to 6 km. It was proposed that the complex was formed in several stages beginning with the emplacement of a CO_2-bearing silicate melt in a sill-like intrusion at ~3 km depth. This melt formed radial dykes and cone-sheets of ijolites, pyroxenites and nepheline syenites causing swelling and uplift together with fenitization. Magma with significant carbonate enrichment is evacuated from the chamber causing a reduction in pressure and collapse of the roof of the magma chamber. In the final stage, the carbonatite intrudes the concentric rings around the outside of the caldera to form ring-dykes.

While some of the features are similar, such as the carbonatite emplacement following that of the ijolites and pyroxenites; perhaps the most important difference in the models for these two complexes is the importance of the magma chamber at Alnö (Anderssen et al., 2013).

The common feature between these models is that the ijolite-carbonatite association forms as complex multi-stage events tracing their origins to magmas from mantle sources (Andersen, 1987b; Andersen, 1988; Anderssen et al., 2013, Saether, 1957; Wu et al., 2017).

As nephelinites are considered to be the extrusive equivalent to the ijolite-series (Mitchell, 2005), it is logical to compare them to Prairie Lake. The clinopyroxene trends for Mosonik and nephelinites from eastern Uganda (Tyler and King, 1967) are quite similar to those

found in ijolite-series rocks (Fig. 50), however they evolve towards the Ae-Hd binary while clinopyroxene from ijolite-series rocks at Prairie Lake and Fen are mostly constrained to the diopside field. This is because the intrusive rocks at Prairie Lake and Fen only record the early stages of this trend, though the relationship is clear from the overlapping trends.

Napak is the eroded remnants of a nephelinite volcano in Uganda with the unique feature of both extrusive nephelinite with an exposed intrusive core of ijolite-carbonatite (King, 1949; Simonetti and Bell, 1994; Simonetti et al., 1996). The volcano contains several features similar to that at Prairie Lake, including the presence of ijolite and carbonatite, as well as multiple generations of clinopyroxene. Unlike Prairie Lake, mineralogical, isotopic and textural evidence supports open-system fractionation of olivine and clinopyroxene at either lower crustal or mantle levels. Napak also contains a minor (~1%) silica-saturated component of "andesitic" flows (Simonetti and Bell, 1994; Simonetti et al., 1996). One feature present at Prairie Lake that is absent at Napak is the malignites (nepheline syenites) suggesting a different evolution in the ijolite-series.

5 – CONCLUSIONS

Petrographic and mineralogical analysis of the ijolite-series rocks at Prairie Lake has provided insight into the genesis of the complex. This petrogenic model involves at least three stages of intrusion by nephelinitic melts of differing composition originating from a weakly depleted mantle source.

The first stage is biotite pyroxenites and associated coarse carbonatite veins. Unevolved diopside crystals (>80% Di in the Di-Hd-Ae ternary) with rims of more evolved clinopyroxene in the biotite pyroxenite and apatitite are evidence of diopside crystalizing at depths of ~30 km or greater that have been transported and emplaced at the current erosion level. Trace element data for the pyroxene cores in biotite pyroxenite display a unique pattern and elevated REE contents.

The second stage is primarily members of the ijolite-series. Solid state deformation results in the annealed textures of the meta-ijolites. Magma differentiation concentrating incompatible elements (including K, Zr, Sr, REE) creates the malignites (potassic nepheline syenites). Trace minerals rich in these incompatible elements such as marianoite-wöhlerite, wadeite, stronalsite, and strontianite are formed as a result of this differentiation. The third major stage is the intrusion of the CII carbonatites derived from different batches of magma.

Four clinopyroxene evolution trends are evident in the aegirine-hedenbergite-diopside ternary: (1) a biotite pyroxenite trend; (2) an ijolite trend; (3) a malignite trend; and (4) an apatitite trend. This in conjuncture with annealing processes observed in the ijolite series provide evidence for repeated intrusions of small-batches of nephelinite magma.

This study also provides the first detailed investigation of trace elements in clinopyroxene, garnet and apatite in ijolite-series rocks. Clinopyroxene displays a sinuous

chondrite-normalized distribution pattern, garnet displays a convex shape with a MREE high, and apatite exhibits a negatively sloping pattern.

Garnet is prominently found as a late-stage mineral in the ijolite-series as well as malignites but is absent in the biotite pyroxenites. Garnets are predominantly Ti-rich andradite-schorlomite-morimotoite solid solution, consistent with garnets found in other undersaturated alkaline igneous rocks. Apatite crystallization in the ijolite series closely follows garnet. Calcite is commonly the last major mineral to crystallize, present as an interstitial phase.

REFERENCES

Andersen, T. (1983) Iron ores in the Fen central complex, Telemark (S. Norway): Petrography, chemical evolution and conditions of equilibrium. Norsk Geologisk Tidsskrift 63, 73-82

Andersen, T. (1984) Secondary processes in carbonatites: Petrology of 'rodberg' (hematite-calcite-dolomite carbonatite) in the Fen complex, Telemark (South Norway). Lithos 17, 227-45

Andersen, T. (1986a) Magmatic fluids in the Fen carbonatite complex, S.E. Norway: Evidence of mid-crustal fractionation from solid and fluid inclusions in apatite. Contributions to Mineralogy and Petrology 93, 491-503

Andersen, T. (1986b) Compositional variations of some rare earth minerals from the Fen complex (Telemark, SE Norway): implications for the mobility of rare earths in a carbonatite system. Mineralogical Magazine 50, 503-509

Andersen, T. (1987a) Mantle and crustal components in a carbonatite complex, and the evolution of carbonatite magma: REE and isotopic evidence from the Fen complex, S.E. Norway. Chemical Geology: Isotope Geoscience Section 65, 147-66

Andersen, T. (1987b) A model for the evolution of hematite carbonatite based on major and trace element data from the Fen complex, S.E. Norway. Applied Geochemistry 2, 163-80

Andersen, T. (1988) Evolution of peralkaline calcite carbonatite magma in the Fen complex, S.E. Norway. Lithos 22, 99-112

Andersen, T. (1989) Carbonatite-related contact metamorphism in the Fen complex, Norway: effects and petrogenic implications. Mineralogical Magazine 53, 395-414

Andersen, T., and Qvale, H. (1986) Pyroclastic mechanisms for carbonatite intrusion: Evidence from intrusives in the Fen central complex, S.E. Norway. The Journal of Geology 94, 762-769

Andersen, T., and Sundvoll B. (1987) Strontium and neodymium isotopic composition of an early tinguaite (nepheline microsyenite) in the Fen complex, Telemark, Southeast Norway: Age and petrogenetic implications. Norges Geologiske Undersøkelse Bulletin 409, 29-34

Andersen, T., and Taylor, P.N. (1988) Pb isotope geochemistry of the Fen carbonatite complex, S.E. Norway: Age and petrogenetic implications. Geochimica Cosmochimica Acta 52, 209-215

Anderssen, M., Malehmir, A., Troll, V.R., Dehghannejad, M., Juhlin, C., and Ask, M. (2013) Carbonatite ring-complexes explained by caldera-style volcanism. Scientific Reports 3, 1667

Archibald, G.F. (1978) Exploration Report on Prairie Lake Uranium Project to October 31, 1978. Internal Company Report for New Insco Mines Ltd.

Bell, K., and Blenkinsop, J. (1980) Ages and initial 87Sr/86Sr ratios from alkalic complexes of Ontario. In: *Geoscience Research Grant Program, Summary of Research 1979–1980* (ed. Pye E. G.), 16–23. Ontario Geological Survey Miscellaneous Paper 93.

Barth, T.F.W., and Ramberg, I.B. (1966) The Fen Circular Complex. In: *Carbonatites* (Tuttle, O.F. and Gittins, J.) 225-257. New York: Interscience

Bell, K., and Blenkinsop, J. (1989) Neodymium and strontium isotope geochemistry of carbonatites. In: *Carbonatites: Genesis and Evolution* (ed. Bell, K.), 278–300. London: Unwin Hyman.

Blundy, J.D., and Dalton, J.A., (2000) Experimental comparison of trace element partitioning between clinopyroxene and melt in carbonate and silicate systems, and implications for mantle metasomatism. Contributions to Mineralogy and Petrology 139, 356–371

Bottriell, K.J. (1975) Rubidium–strontium isochron age studies of Nemegosenda and Prairie Lake. B.Sc. thesis, Carleton University, Ottawa, Canada

Bowen, N.L. (1924) The Fen area in Telmark, Norway. American Journal of Science 8, 1-11

Bowen, N.L. (1926) The carbonate rocks of the Fen area in Norway. American Journal of Science 12, 499-502

Broch, O.A. (1964) Age determination on Norwegian minerals up to March 1964. Norges Geologiske Undersøkelse 208, 84-l 13

Brögger, W.C. (1921) Die Eruptivgesteine des Kristianiagebietes. IV. Das Fengebiet in Telemark Norwegen: Norsk Videnskaps Selskrifter I, Mathematik Naturvidenskaphige Klasse I No. 9, Oslo.

Card, K.D. (1990) A review of the Superior Province of the Canadian Shield, a product of Archean accretion Precambrian Research 48, 99-156

Chakhmouradian, A.R., Reguir, E.P., Zaitsev, A.N., Christopher, C., Xu, C., Kynický, J., Mumin, A.H., and Yang, P. (2017) Apatite in carbonatitic rocks: Compositional variation, zoning, element partitioning and petrogenetic significance. Lithos 274, 188–213

Chakhmouradian, A.R., Mitchell, R.H., Burns, P.C., Mikhailova, Y., Reguir, E. P. (2008) Marianoite, a New Member of the Cuspidine Group from the Prairie Lake Silicocarbonatite, Ontario. The Canadian Mineralogist 46 (4), 1023–1032

Chen, W., Zhang, W., Simonetti, A., and Jiang, S., (2016) Mineral chemistry of melanite from calcitic ijolite, the Oka carbonatite complex, Canada: implications for multi-pulse magma mixing. Journal of Earth Science 27, 599-610

Church, A.A., and Jones, A.P. (1995) Silicate-carbonate immiscibility at Oldoinyo-Lengai. Journal of Petrology 36, 869-889

Cleaver, A. (2017) Mineralogy and Petrology of the Good Hope Carbonatite Occurrence, Marathon, ON. HBSc. thesis, Lakehead University, Thunder Bay, Ontario

Cooper, A.F., and Reid, D.L. (1998) Nepheline søvites as parental magmas in carbonatite complexe: evidence from Dicker Willem, Southwest Namibia. Journal of Petrology 39, 2123-2136

Dahlgren, S. (1983) Naturlig radioaktivitet i berggrunnen. Gammastrhlingskart. Fensfeltet, Telemark, m 1:10000. Prosjekt temakart, Telemark. Fylkeskartkontoret i Telemark, Skien.

Dahlgren, S. (1993) Late Proterozoic and Carboniferous ultramafic magmatism of carbonatitic affinity in southern Norway. Lithos, 31, 141-154

Dawson, J.B. (2009) *The Gregory Rift Valley and Neogene-Recent Volcanoes of Northern Tanzania*. Geological Society of London, London

Dawson, J.B., Smith, J.V., and Steele, I.M. (1995) Petrology and mineral chemistry of plutonic igneous xenoliths from the carbonatite volcano, Oldinyo Lengai, Tanzania. J. Petrology 36, 797-826

Deer, W.A., Howie, R.A., and Zussman, J. (2004) Rock Forming Minerals Vol. 4B – Framework Silicates: Silica Minerals, Feldspathoids and the Zeolites. 257. The Geological Society: London

Doroshkevich, A.G., Veksler, I.V., Izbrodin, I.A., Ripp, G.S., Khromova, E.A., Posokhov, V. F., Travin, A.V., and Vladykin, N.V. (2015) Stable isotope composition of minerals in the Belaya Zima plutonic complex, Russia: Implications for the sources of the parental magma and metasomatizing fluids. Journal of Asian Earth Sciences 116, 81-96

Emeleus, C.H., and Troll, V.R. (2014) The Rum Igneous Centre, Scotland. *Mineralogical Magazine* 78(4), 805–839

Ernst, R.E. and Bell, K. (2010) Large igneous provinces (LIPs) and carbonatites. Mineralogy and Petrology 98, 55–76

Fleet, M.E., and Pan, Y. (1995) Site preference of rare earth elements in fluorapatite. American Mineralogist 80, 329–335

Fleet, M.E., and Pan, Y., (1997) Site preference of rare earth elements in fluorapatite: binary (LREE + HREE)-substituted crystals. American Mineralogist 82, 870–877

Gittings, J. (1979) Problems inherent in the application of calcite-dolomite geothermometry to carbonatites. Contributions to Mineralogy and Petrology 69, 1-4

Gittins, J. (1989) The origin and evolution of carbonatite magmas. In: *Carbonatites: Genesis and Evolution*, Bell K (ed) Unwin Hyman, London, 580-600

Gittins, J., and Harmer, R E. (2003) Myth and Reality in the Carbonatite – Silicate Rock "Association." Periodico di Mineralogia 72, 19-26

Gittins, J., Macintyre, R.M., and York, D. (1967) The ages of carbonatite complexes in eastern Canada. Canadian Journal of Earth Sciences 4, 651–655

Goldshmidt, V.M., (1918) Et hittil ukjendt omraade av alkali-bergarter. Videnskaps Akademi Förhandlingar, 20 (abstract)

Grew, E., Locock, A., Mills, S.J., Galuskina, I., Galuskin, E., and Hålenius, U. (2013) Nomenclature of the garnet supergroup. American Mineralogist 98, 785-811

Griffin, W.L. (1973) Lherzolite nodules from the Fen alkaline complex, Norway. Contributions to Mineralogy and Petrology 38, 135-146

Griggs, D.T., Paterson, M.S., Heard, H.C., and Turner, F.J. (1960) Annealing recrystallization in calcite crystals and aggregates. Geological Society of America Memoirs 79, 21–3

Gupta, A.K., Chattopadhyay, S., Chattopadhyay, B., and Arima, M. (2006) Experimental study of the system diopside–nepheline–sanidine at 0.1, 1 and 2 GPa [$P(H_2O)$ =P(Total)]: Its significance in the genesis of alkali-rich basic and ultrabasic rocks. Lithos 86, 91-109

Hamilton, D.L. (1961) Nephelines as crystallization temperature indicators. Journal of Geology 69, 321-329

Hammouda, T., Chantel, J., and Devidal, J.L., (2010) Apatite solubility in carbonatitic liquids and trace element partitioning between apatite and carbonatite at high pressure Geochimica et Cosmochimica Acta 74, 7220–7235

Harmer R.E. and Gittins J. (1998) The Case for Primary, Mantle-derived Carbonatite Magma. Journal of Petrology 39, 1895-1903

Heaman, L.M., Easton, R.M., Hart, T.R., Hollings, P., MacDonald, C.A, and Smyk, M. (2007) Further refinement to the timing of Mesoproterozoic magmatism, Lake Nipigon region. Ontario Canadian Journal of Earth Sciences 44(8), 1055-1086

Hode Vuorinen, J., Hålenius, U., Whitehouse, M.J., Mansfeld, J., and Skelton, A.D.L. (2005) Compositional variations (major and trace elements) of clinopyroxene and Ti-andradite from pyroxenite, ijolite and nepheline syenite, Alnö Island, Sweden. Lithos 81(1-4), 55–77.

Högbom, A.G. (1909) The igneous rocks of Ragunda, Alnö, Rödö, and Nordingrå. Geologiska Föreningen i Stockholm Förhandlingar 31, 347-375

Huggins, F.E., Virgo, D., and Huckenholz, H.G. (1977a) Titanium-containing silicate garnets. I; The distribution of Al, Fe3+, and Ti4+ between octahedral and tetrahedral sites. American Mineralogist 62, 475–490.

Huggins, F.E., Virgo, D., Huckenholz, H.G., (1977b) Titanium-containing silicate garnets. II; The crystal chemistry of melanites and schorlomites. American Mineralogist 62, 646–665

Ivanic, T., Harte, B., Burgess, S., and Gurney, J. (2003) Factors in the formation of sinuous and humped REE patterns in garnet from mantle harzburgite assemblages. In: *Extended abstracts. 8th International Kimberlite Conference*, Victoria, BC, Canada, 5

Jennings, D.S. and Mitchell, R.H. (1969) An estimate of the temperature of carbonatite at the Fen complex, S. Norway. Lithos 2, 167-169.

King, B.C. (1949): The Napak area of southern Karamoja. Uganda. Memoir Geological Survey of Uganda 5, 1-57

Klemme, S., and Dalpé, C. (2003) Trace-element partitioning between apatite and carbonatite melt. American Mineralogist 88, 639–646

Kjarsgaard, B., Hamilton, D.L. (1988) Liquid immiscibility and the origin of alkali-poor carbonatites. Mineralogical Magazine 52, 43-55

Kwon S.T., Tilton G.R., and Grüenenfelder M.H. (1989) Lead isotope relationships in carbonatites and alkalic complexes: an overview. In: *Carbonatites: Genesis and Evolution* (ed. Bell K.), 360–87. London: Unwin Hyman.

Lawson, A.C. (1896): Malignite, a family of basic plutonic orthoclase rocks rich in alkalies and lime intrusive in the Coutchiching schists of Poohbah Lake. University of California Publications: Bulletin of the Department of Geology 1, 337-362

Le Bas, M.J. (1977) *Carbonatite – Nephilinite Volcanism.* John Wiley and Sons, London.

Le Maitre, R.W. (2002) *Igneous Rocks. A Classification and Glossary of Terms. Recommendations of the International Union of Geological Sciences Subcommission on the Systematics of Igneous Rocks*, 2nd ed. Cambridge, New York, Melbourne

Lie, A. and Østergaard, C. (2011) The Fen Carbonatite Complex, Ulefoss, South Norway: Summary of historic work and data Company Report for REE Minerals, Norway by 21st NORTH

Locock, A.J. (2008) An Excel spreadsheet to recastanalyses of garnet into end-member components, and a synopsis of the crystal chemistry of natural silicate garnets. Computers and Geosciences 34, 1769-1780

Mao, M., Rukhlov, A.S., Rowins, S.M., Spence, J., and Coogan, L.A. (2016): Apatite trace element compositions: a robust new tool for mineral exploration. Economic Geology 111, 1187–1222

Marks, M., Halama, R., Wenzel, T., and Markl, G. (2004) Trace element variations in clinopyroxene and amphibole from alkaline to peralkaline syenites and granites: implications for mineral-melt trace-element partitioning. Chemical Geology 211, 185–215

Meert, J.G., Torsvik, T.H., Eide, E.A., and Dahlgren, S. (1998) Tectonic significance of the Fen Province, S. Norway: Constraints from geochronology and paleomagnetism. The Journal of Geology 106, 553–564

Melnik, N. (1984) Textural Evidence for the Origin of the Prairie Lake Carbonatite - Alkalic Rock Complex; B.Sc. Thesis, Queen's University, Kingston, Ontario

Mitchell, R.H. and Brunfelt, A.O. (1975) Rare Earth Element Geochemistry of the Fen Alkaline Complex, Norway. Contributions to Mineralogy and Petrology 52, 247-259

Mitchell, R.H. and Crocket, J.H. (1972) Isotopic composition of strontium in rocks of the Fen complex, South Norway. Petrology 13, 83-98

Mitchell, R.H., and Platt, R.G. (1979) Nepheline-bearing rocks from the Poohbah Lake complex, Ontario: Malignites and Malignites. Contributions to Mineralogy and Petrology 69(3), 255–264

Mitchell, R.H. (1980) Pyroxenes of the Fen Alkaline Complex, Norway. American Mineralogist 65, 45-54

Mitchell, R.H. (1996) Classification of Undersaturated and Related Alkaline Rocks. In: *Mitchell, R.H. (Ed.), Undersaturated Alkaline Rocks: Mineralogy, Petrogenesis, and Economic Potential* 1-22

Mitchell, R.H. (2005) Carbonatites and Carbonatites and Carbonatites. Canadian Mineralogist 43, 2049-2068

Mitchell, R.H. (2008) Petrology of hypabyssal kimberlites: Relevance to primary magma compositions. Journal of Volcanology and Geothermal Research, 174(1-3), 1–8

Morimoto, N., Fabries, J., Ferguson, A.K., Ginzberg, L.V., Ross, M., Seifert, F.A., and Zussman, J. (1988) Nomenclature of Pyroxenes. American Mineralogist 73, 1123-1133

Nesse, W.D. (2012) *Introduction to Mineralogy* (2nd ed.) Oxford University Press, New York

Neumann, H. (1960) Apparent ages of Norwegian rocks and minerals. Nor. Geol. Tidsskr 40, 151-173

O'Driscoll, B., Donaldson, C.H., Troll, V.R., Jerram, D.J., and Emeleus, C.H. (2007) An origin for harrisitic and granular olivine in the Rum Layered Suite, NW Scotland: a Crystal Size Distribution study. Journal of Petrology 48, 253-270

Pasero, M., Kampf, A.R., Ferraris, C., Petkov, I.V., Rakovan, J., and White, T.J., (2010) Nomenclature of the apatite supergroup minerals. European Journal of Mineralogy 22, 163-179

Platt, R.G. (1996) The Ijolite Series Rocks. In: *Mitchell, R.H. (Ed.), Undersaturated Alkaline Rocks: Mineralogy, Petrogenesis, and Economic Potential* 1-22

Putrich, E., Armstrong, T., and Yassa, A. (2014) Technical Report on the Prairie Lake Property, Thunder Bay Mining Division Ontario, Canada 43-101. Report prepared for Nuinsco by P and E Mining Consultants Inc.

Ramberg, I.B. (1973) Gravity studies of the Fen Complex, Norway and their petrological significance. Contributions to Mineralogy and Petrology 38, 115-134

Reguir, E.P., Chakhmouradian, A.R., Pisiak, L., Halden, Yang, P., Xu, C., Kynický, J., Couëslan, C.G., (2012) Trace-element composition and zoning in clinopyroxene- and amphibole group minerals: implications for element partitioning and evolution of carbonatites. Lithos 128–131, 27-45

Rukhlov, A.S. and Bell, K. (2010) Geochronology of carbonatites from the Canadian and Baltic shields and the Canadian Cordillera: clues to mantle evolution. Mineralogy and Petrology 98, 11-54

Sage R.P. (1983) Geology of the Prairie Lake Carbonatite Complex. Ontario. Geological Survey Open File Report, 5412

Sage, R.P. (1987) Geology of Carbonatite—Alkalic Rock Complexes in Ontario: Prairie Lake Carbonatite Complex, District of Thunder Bay. Ministry of Northern Development and Mines, Ontario Geological Survey, Study 46

Sano, Y., Oyama, T., Terada, K., and Hidaka, H. (1999) Ion microprobe U–Pb dating of apatite. Chemical Geology 153, 249-258

Saether, E. (1957) The alkaline rock province of the Fen area in southern Norway. Det Kongelige Norske Videnskabers Selskab 1, 148

Satterly, J. (1968) Aeromagnetic Maps of Carbonatite-Alkalic Complexes in Ontario. Ontario Department of Mines and Northern Affairs, Map, (452) (revised)

Schairer, J.F. (1950) The alkali feldspar join in the system NaAlSiO4 – KAlSiO4 – SiO2. Journal of Geology 58, 512-517

Selway, J. (2017) Assessment Report for Geological Mapping Program Good Hope Niobium Property Marathon, Ontario, Canada NTS: 42E02SE. Report prepared by J-J Minerals for Plato Gold Corp.

Sharygin, V.V., Kamenetsky, V.S., Zaitsev, A.N., and Kamenetsky, M.B. (2012) Silicate–natrocarbonatite liquid immiscibility in 1917 eruption combeite–wollastonite nephelinite, Oldoinyo Lengai Volcano, Tanzania: Melt inclusion study. Lithos 152, 23-39

Simonetti, A., and Bell, K. (1994) Nd, Pb and Sr isotopic data from the Napak carbonatite - nephelinite centre, eastern Uganda: an example of open-system crystal fractionation. Contributions to Mineralogy and Petrology 115, 356-366

Simonetti, A., Shore, M., and Bell, K. (1996) Diopside phenocrysts from lavas, Napak Volcano, Eastern Uganda: Evidence for magma mixing. Canadian Mineralogist 34, 411-421

Smyth, F.H., and Adams, L.H. (1923) The system, calcium oxide-carbon dioxide. Journal of American Chemical Society 45, 1167-1184

Tilley, C. E. (1954) Nepheline-alkali feldspar parageneses. American Journal of Science 252(2), 65–75

Tyler, R.C., and King, B.C. (1967) The pyroxenes of the alkaline igneous complexes of eastern Uganda. Mineralogical Magazine and Journal of the Mineralogical Society 36(277), 5-21

Verschure, R.H., Mauer, C., Andriessen, P.A.M., Boelrljk, N.A.I.M., Hebeda, E.H., Priem, H.N.A., and Verdurmen, E.A.T. (1983) Dating explosive volcanism perforating the Pre-Cambrian basement in Southern Norway. Norges Geologiske Undersøkelse 380, 35-49

Verschure, R.H., and Mauer, C. (2005) A new Rb-Sr isotopic parameter for metasomatism, Δt, and its application in a study of pluri-fenitized gneisses around the Fen ring complex, South Norway. Norges Geologiske Undersøkelse Bulletin 445

Vulić, P., Balić-Žunić, T., Belmonte, L.J., and Kahlenberg, V. (2011) Crystal chemistry of nephelines from ijolites and nepheline-rich pegmatites: influence of composition and genesis on the crystal structure investigated by X-ray diffraction. Mineralogy and Petrology 101(3-4), 185-194

Wager, L.R., and Brown, G.M. (1968) *Layered Igneous Rock*. Oliver and Boyd, Edinburgh.

Wager, L.R., Brown, G.M., and Wadsworth, J.W. (1960) Types of igneous cumulates. Journal of Petrology 1, 73-85

Watkinson, D.H. (1971) Petrology and uranium-niobium mineralization of the alkalic rock carbonatite complex, Prairie Lake, Ontario (abstract) Canadian Mineralogist 10(5), 921

Watkinson, D.H. (1976) Petrology and uranium-niobium mineralization of the alkalic rock-carbonatite complex, Prairie Lake, Ontario (manuscript, unpublished)

Winter, J.D. (2010) *Principles of igneous and metamorphic petrology.* New York: Prentice Hall.

Wood, B.J., and Blundy, J.D. (2002) The effect of H2O on crystal-melt partitioning of trace elements. Geochimica et Cosmochimica Acta, 66(20), 3647-3656

Wood, B.J., and Blundy, J.D. (2014) Trace Element Partitioning: The Influences of Ionic Radius, Cation Charge, Pressure, and Temperature. Treatise on Geochemistry, 421-448

Woolley, A.R. (1987) *Alkaline Rocks and Carbonatites of the World Part 1: North and South America* University of Texas Press, Austin, Texas.

Wu, F., Mitchell, R.H., Li, Q., Zhang, C., and Yang, Y. (2017) Emplacement Age and Isotopic Composition of the Prairie Lake Carbonatite Complex, Northwestern Ontario. Canada Geological Magazine 154, 217-236

Wu, F.Y., Yang, Y.H., Mitchell, R.H., Bellatreccia, F., Li, Q. L., and Zhao, Z. F. (2010) In situ U–Pb and Nd–Hf– (Sr) isotopic investigations of zirconolite and calzirtite. Chemical Geology 277, 178-95

Wyllie P.J., and Huang W.L. (1976) Carbonation and melting reactions in the system CaO-MgO-SiO2-CO2 at mantle pressures with geophysical and petrological applications. Contributions to Mineralogy and Petrology 54, 79-107

Wyllie, P.J., and Tuttle, O.F. (1960) The System CaO-CO2-H2O and the Origin of Carbonatites. Journal of Petrology 1, 1-46

Zurevinski, S.E., and Mitchell, R.H. (2015) Petrogenesis of orbicular ijolites from the Prairie Lake complex, Marathon, Ontario: Textural evidence from rare processes of carbonatitic magmatism. Lithos 239, 234-244

APPENDIX 1 – Geology of Fen and Mosonik

Fen Complex

Introduction

The Fen alkaline complex is composed of carbonatites and silicate rocks together with several satellite intrusions (Barth and Ramberg, 1966). It is located at Fen in Telemark County, Norway, 119 km to the southwest of Oslo. The area has a rich history of hundreds of years of iron mining dating back to the mid-1600s, and niobium mining during the 1950s (Lie and Østergaard, 2011).

The complex may be regarded as the type locality for carbonatites, as it was where the idea of igneous carbonates was first popularized through the work of Waldemar C. Brögger. This idea was criticized by some of his contemporaries, especially those in North America such as N. L. Bowen. Because of its noteworthy history, the Fen complex has been extensively studied and provided much insight into the understanding of carbonatites today.

Regional Geology

During the Neoproterozoic, the Fen alkaline complex intruded Precambrian gneisses and gneissic granites that are part of the migmatite area of Telemark. It is located 2 km west of the Oslo Graben. To the east of the complex are amphibolites and mica schists. The emplacement of the Fen complex is coeval with faulting parallel to the margins of the Baltic Precambrian shield, and much older than the faulting in the Oslo area during the Permian (Barth and Ramberg, 1966).

The current erosion level is thought to be no further than a few kilometers beneath the surface at the time of emplacement of the complex (Saether, 1957). Overlying the complex are thick, continuous Quaternary deposits which limit the outcrop exposures (Dahlgren, 1983)

Prior Research

The following section summarizes the history of research and exploration at Fen and highlights several important papers published studying the igneous rocks at Fen. It is not meant to be all inclusive, as the rocks found at Fen are notable for having a central role in the development of our understanding of carbonatites and their relation to silicate rocks and have thus been extensively researched. This is provided to both give insight into the development of thought regarding carbonatites using Fen as a focal point while also using it as a point of comparison with Prairie Lake

Fen has a great deal of historical importance with respect to iron mining in Norway dating back to 1657. To the east of the complex is extensive deposits of iron ore in the form of rødberg (literally "red rock"), a hematite-bearing carbonatite occurring in N-S trending veins. Both open pit and underground mining has been used over the centuries at several sites in the complex. The work continued up until 1927, by which time the underground workings had reached a depth of 225m beneath the surface of Lake Norsjø (Lie and Østergaard, 2011).

The unusual nature of the rocks was first noted by Goldschmidt (1918), however they are best known from the subsequent investigation by Brögger (1921) where the complex was described, the term "carbonatite" was first used, and the concept of igneous carbonate magma

was first popularised (having previously been suggested by A.G. Högbom as the origin of the Alnö complex in his 1909 paper *The igneous rocks of Ragunda, Alnö, Rödö, and Nordingrå*).

It is of note that one of the strongest opponents to this idea was famed mineralogist N.L. Bowen (1924; 1926), who advocated an origin from silicate rocks that had underwent carbonate replacement. In Europe, Professor R. Brauns (1926) strongly supported the interpretation of Brögger (1921) which carried much weight with German-speaking geologists of the time.

The potential for an economic niobium deposit was investigated in the late 1930s by the Norwegian state. During the occupation of Norway during WW2, the Germans had a considerable interest in the potential of the deposit and conducted a great deal of research. Following the conclusion of the war, a Norwegian state-owned company was formed in 1951, Norsk Bergverk A/S. Backed by American steel industry interests, their goal was to concentrate Fe-Nb from pyrochlore-bearing søvites with an average grade of 0.35-0.4% Nb_2O_5. After extensive testing of the ore and development, mining started in 1953 quarrying near Lake Norsjø. Mining eventually went underground with a tunnel to the central parts of the søvite (calcite carbonatite) producing a good knowledge of the structures involved. Annually the mine produced around 100,000 – 150,000 tons of raw ore which was processed for iron and niobium. The mine operated for 12 years, closing in 1965 (Lie and Østergaard, 2011).

The next detailed study of Fen was conducted by Egil Saether (1957) who primarily investigated and described the textures of the rocks present. This research led to his recognition of two intervals of igneous activity at Fen. Both were marked by an intrusion of very ultrabasic magmas with associated hydrothermal activity. The first intrusion was composed of carbonatites, silicocarbonatites and members of the ijolite-urtite series along with the fluids that resulted in intense fenitization of the country rocks. The second intrusion was of the damtjernite (a variety

of lamprophyre) with successive Mg-rich carbonatitic magma resulting in alteration and metasomatization of the damtjernite (Saether, 1957).

Fen was investigated by Barth and Ramberg (1966) as a chapter in Tuttle and Gittins 1966 volume on Carbonatites. Barth and Ramberg predominantly conducted a detailed study of the petrography of samples from the Fen complex. Jennings and Mitchell (1969) used calcite-dolomite geothermometry on søvites from Fen and concluded extremely low temperatures of emplacement (280ºC and 380ºC). Andersen (1984) noted that this interpretation failed to account for reequilibration of constituent minerals, an issue first highlighted in Gittins' 1979 paper *Problems Inherent in the Application of Calcite-Dolomite Geothermometry to Carbonatites* where multiple overlooked problems with the method were brought to light.

Mitchell and Crockett (1972) determined that the $^{87}Sr/^{86}Sr$ ratio of the Fen rocks varied from 0.703 to 0.710 with the former in the calcitic carbonatite and the latter in the ankeritic ferrocarbonatite. The isotopic evidence led Mitchell and Crockett (1972) to believe that the ijolite series at Fen may have been the result of rheological processes involving the fenites.

In 1973, Ramberg published his findings of gravity studies of the complex which showed that the carbonatites probably only form a thin veneer over a much denser material (possibly damtjernite or vipetoite). Griffin (1973) conducted a study of spinel lherzolite xenoliths within the damtjernite and determined that they equilibriated at temperatures of 1200-1250ºC and pressures of 10-15 kbar indicating that at least the damtjernites have a mantle origin.

In 1975, Mitchell and Brunfelt studied the rare earth element geochemistry of the rocks at Fen and proposed that all the rocks in the complex were derived from a nephelinite rich in H_2O and CO_2., and concluded that the current exposure is the roots of a nephelinite volcano. The

ijolite series together with the calcite carbonatites (also known as søvites) are postulated to represent nephelinitic liquids undergoing immiscible fractionation at low pressures and temperature, while the damtjernites formed at high temperatures over wide range of pressures from nephelinite magmas.

Griffin and Taylor (1975) studied the damtjernites using petrography, rock chemistry, mineral (pyroxene, mica and oxide) chemistry, and Sr isotopes. They hypothesized that a carbonated hydrous mica-bearing peridotite undergoing partial melting at conditions of 1200-l250°C, 15-25 kbar which provided the origin for the damtjernites and that the carbonatites were contaminated during later intrusions.

Mitchell (1980) studied pyroxene compositions from the complex and determined that four groups are present: (1) the cores of phenocrysts in the damtjernite are Al-Na diopsides rich in $CaAl_2SiO_6$; (2) Ti-Al diopsides [the original term used in the paper "salite" is now discarded in the IMA classifications of pyroxenes; Morimoto et al., (1988)], found as zoned crystals as well as the rims of phenocrysts in damtjernite and vipetoite; (3) aegirine-hedenbergite series in the urtites, ijolites and silicocarbonates [the term aegirine is used in place of acmite; Morimoto et al., 1988]; (4) an aegirine trend in the late stage urtites. These observations in conjunction with the formation of the urtites, ijolites and silicocarbonates under much different conditions to the damtjernite and vipetoite indicate a complex evolutionary history for the complex, thus discounting fractional crystallization of a single batch of magma as the origin for the complex.

Tom Andersen of the Mineralogisk-Geologisk Museum, Norway was responsible for much of the study of Fen throughout the 1980s. His initial foray into Fen research was his 1983 investigation into the iron ores and ferrocarbonatites. The findings of Andersen's second

investigation of Fen (1984) indicate that metasomatism may play a key role in post-magmatic reequilibration of some carbonatites.

Andersen (1983) studied the iron ores and ferrocarbonatites using petrographic methods and was able to determine the presence of a primary mineral assemblage (magnetite ± pyrite ± anatase + calcite) and a secondary mineral assemblage (hematite ± goethite + calcite ± dolomite). Andersen (1984) next went into further detail of the secondary processes involved in creation of the rødberg (hematite-calcite-dolomite carbonatite) and deduced that the initial ankerite ferrocarbonatite interacted with oxidizing metasomatic fluids flowing through the surrounding country gneisses which resulted in the formation of the rødberg. This metasomatic event concentrated hematite and other insoluble phases while also partially removing some La and Sm.

In 1986, Andersen published two papers on Fen and was leading author on another. In the paper *Magmatic fluids in the Fen carbonatite complex, S.E. Norway: Evidence of mid-crustal fractionation from solid and fluid inclusions in apatite* (1986a) apatite was used as a petrogenetic indicator as it "is probably the only [mineral present in abundance in carbonatites] able to survive post-magmatic alteration without completely losing its inclusion contents." It was determined that there are three types of carbonatite magma present at Fen: (1) peralkaline calcite carbonatitic magma originating from ijolitic magmas; (2) alkaline magnesian calcite carbonatite magma which formed biotite-amphibole calcite carbonatite and dolomite carbonatite; and (3) ferrocarbonatite liquids related to the alkaline magnesian calcite carbonatite magma and/or alkaline lamprophyre magma. Apatite formed prior to the emplacement of the alkaline magnesian calcite carbonatite magma which formed biotite-amphibole calcite carbonatite and dolomite carbonatite contained inclusions of carbonates, devitrified silicate glass and fluid inclusions formed during a mid-crustal fractionation event where a carbonatitic melt and a mafic

silicate melt coexisted. Fluid inclusions present within the apatite may be divided into two categories; type (A) a more unevolved, low salinity hydrous CO_2 bearing fluid with a density of ~0.86g/cm^3, and type (B) a more saline, CO_2 free fluid showing densities between 0.7-1.0g/cm^3 that evolved during fractionation. Type B fluids also show a continuous trend of evolution toward higher salinity and densities as a result of the cooling and partitioning of the fluids.

Compositional variations of some rare earth minerals from the Fen complex (Telemark, SE Norway): implications for the mobility of rare earths in a carbonatite systems (1986b), electron microprobe analysis and X-ray diffraction were conducted on samples of ankeritic ferrocarbonatite and rødberg to investigate the REE minerals present. This included monazite, parisite, and bastnaesite together with an aluminous silicate mineral with an allanite composition and some possible synchysite. The REE distribution patterns showed changes in light REE (LREE) resulting from leaching of the LREE by fluoride-bearing fluids during re-equilibration. Andersen and Qvale (1986) investigated the pyroclastic mechanisms involved in the emplacement of ankeritic ferrocarbonatite and damtjernite and their alteration product rødberg. Analysis of field relations and microstructures indicate that the ferrocarbonatites are pyroclastic, heterogeneous intrusives containing xenoliths of the gneiss country rocks emplaced during multiple pulses of fluidized material.

Andersen published two more papers on Fen in 1987. *Mantle and crustal components in a carbonatite complex, and the evolution of carbonatite magma: REE and isotopic evidence from the Fen complex, S.E. Norway* (1987a) investigated the REE and isotopic compositions and considred,that the carbonatites may be divided into two groups: (A) Søvites, dolomite carbonatite, dyke facies ferrocarbonatites and apatite cumulates; and (B) rødberg and its parental tuffisitic ferrocarbonatite. It was determined that the carbonatites no longer reflect the

composition of their mantle source owing to a number of open-system (crustal contamination) and closed-system (fractional crystallization, liquid immiscibility, and volatile transport within the magma) processes, the latter showing strong effects on REE element distribution, and the former influencing the O, Sr and Nd isotopic systems. The O, C, Nd, and Sr isotopic systems show signs that they are influenced by a component originating from a depleted mantle source, the current composition could be explained if contamination occurred in the mid- to shallow-crust.

A model for the evolution of hematite carbonatite, based on major and trace element data from the Fen complex, S.E. Norway (Andersen, 1987b) delves into the origins of REE-rich hematite carbonatites using Fen to create a model and investigating the whole rock geochemistry and REE contents of the rocks. Andersen described the processes involved in the formation of secondary hematite-calcite-dolomite carbonatite via postmagmatic oxidation and partial dissolution of the primary ankeritic ferrocarbonatite. It was determined this was through a two-stage metasomatic process. The first below the hematite-magnetite (H-M) buffer leaching Fe^{2+} and Mg, and the second at more oxidizing conditions leaching Mg and Ca. This resulted in the formation of the iron ores at Fen.

Andersen and Taylor (1988) investigated Pb isotopes in 18 samples from Fen and determined that the $^{206}Pb/^{204}Pb$ ratio showed an extreme range from18.9 to 206 correlating with the amount of apatite in the sample as apatite fractionation might result in enrichment of U in Pb poor cumulates. The isochron plots above the Pb isotope growth curve for depleted mantle, however local crustal rocks show a similar composition and is thus evidence of crustal contamination during the differentiation of the carbonatitic magma in the middle to shallow crust.

Andersen (1988) studied the association of pyroxene søvite, the ijolite series, alkali pyroxenite, and nepheline syenite found to the West of the complex using petrography and pyroxene compositions to determine the relationships between them. Through this a petrogenetic model was created. It was determined that an ijolitic parent magma was the source of all the different rocks present. The pyroxenites were created through fractionation of the parent magma containing textural evidence of the melt beginning to fractionate into the nepheline syenite (malignite) and peralkaline carbonatite melts as immiscible liquids in the shallow crust. This was supported by the overlapping pyroxene trends of the two rocks and the identical liquidus mineral assemblages involved.

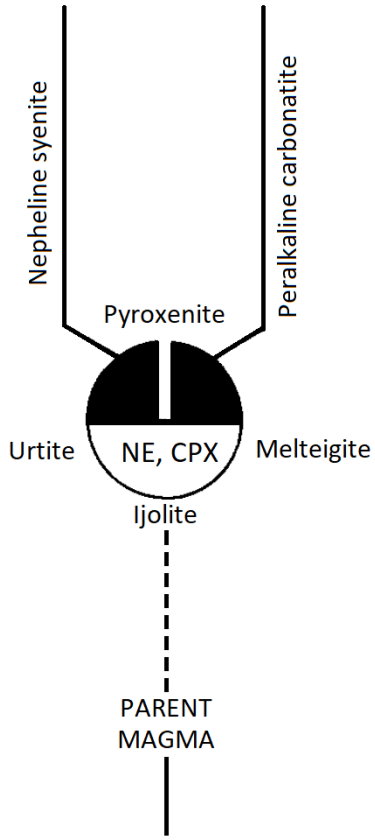

Figure: Petrogenetic model for the peralkaline rock association found at the Fen complex (Modified from Andersen, 1988)

In his final published work on the Fen complex Andersen (1989) focused on the diverse metasomatism that resulted from carbonatite intrusions. Utilizing mineral compositonsand textural evidence four types of metasomatic alteration were noted at Fen: (1) alkali metasomatism from pyroxene søvite, (2) magnesium metasomatism from søvite and dolomite carbonatite, (3) an increase in ferromagnesian components in wall-rcok søvite from granular ferrocarbonatite, and (4) chlorite pseudomorphically replacing phlogopite because of the leaching of alkalis by the heterogeneous ferrocarbonatite. Each of these processes reflecting the composition of the intruding melt.

Recent exploration work has been done by several Norwegian junior exploration companies; however no systematic exploration has been done for REE. Two companies, Thorium Norway and REE Minerals, were investigating the REE potential of the complex as of 2011 (Lie and Østergaard, 2011).

Timing of Emplacement of Fen

Age determinations of the Fen complex have placed the emplacement in the late Neoproterozoic (around 570-600Ma) and are summarized in Table 2. Research has mostly focused on the carbonatites. Currently no members of the ijolite series at Fen have been examined with regard to their timing of emplacement and their precise timing in relation to the damtjernites is currently unknown.

Table: Age determination and methods of the Fen complex

Source	Sample	Method	Age
Saether, 1957	Pyrochlore	chemical Pb	420, 579
	Columbite	chemical Pb	590
	Zircon	chemical Pb	570
Faul et al., 1959	Biotite from søvites	K-Ar	565 Ma
Neumann, 1960	Biotite from søvites	K-Ar	590 Ma
	Biotite from søvites	K-Ar	603 Ma
Broch, 1964	Biotite from carbonatite	K-Ar	565 – 585 Ma
	Biotite from damtjernite	K-Ar	573 Ma
Verschure et al., 1983	Biotite from damtjernite	K-Ar	597 ± 20 Ma
	Hornblende from damtjernite	K-Ar	564 ± 20 Ma
Andersen and Sundvall, 1986	Biotite from phonolite	Rb-Sr	550 ± 7 Ma
Andersen and Taylor, 1988	Carbonatites and associated silicate	Whole rock Pb/Pb	539 ± 14 Ma
Meert et al., 1998	Biotite/phlogopite from phonolite	$^{40}Ar/^{39}Ar$ step heating	578 ± 10 Ma
	Biotite/phlogopite from damtjernite	$^{40}Ar/^{39}Ar$ step heating	588 ± 10 Ma

The initial age determinations by Saether (1957) used a semiquantative chemical Pb method on samples of pyrochlore, columbite and zircon. The samples showed a wide range; however, the timing of the emplacement was narrowed from between 400-600 Ma. Most of the

early work on the age of Fen was done using K-Ar geochronology. Faul et al (1959), Neumann (1960), Broch (1964) and Verschure et al. (1983) all used biotite samples (with Verschure also using hornblende) from the rocks at Fen with K-Ar and were able to refine timing of emplacement to between 564 – 603 Ma.

Andersen and Sundvall (1986) conducted Rb-Sr geochronology on biotite collected via mineral separations from a phonolite dike at Fen, which provided an age of 550 ± 7 Ma. It was later noted that several of these crystals showed clear evidence of alteration, which may have resulted in too young an age due to loss of Rb or radiogenic Sr. Omitting these samples results in an age of 583 ± 41 Ma (Dahlgren, 1993). Andersen and Taylor (1988) obtained Pb/Pb isochron timing of the complex using 18 samples from carbonatites and associated silicate rocks from Fen. The samples show a wide variation in the $^{206}Pb/^{204}Pb$ ratio from 18.9 to 226 relating to the amount of apatite present in the rocks resulting in an age of 539 ± 14 Ma. This was contended by Dahlgren (1993) who noted that the age from Andersen and Taylor was strongly influenced by the presence of metamict pyrochlore in the two samples with the highest levels of uranium. This may result in the age appearing too young and when omitted results in an age of 573 ± 60 Ma.

As part of their study of paleomagnetism of the rocks of Fen, Meert et al. used the $^{40}Ar/^{39}Ar$ step heating on biotite and phlogopite samples from a damtjernite and a phonolite. This provided an average age of 583 ± 15 Ma (Meert et al., 1998).

Fen Geology

The rocks at Fen are composed of a ring complex approximately 9 km^2. The complex has a core of alkaline silicate and carbonatitic rocks that is thought to represent the roots of a nephelinite volcano from the Neoproterozoic (Mitchell and Brunfelt, 1975) with a halo of intense fenitization into the country rocks (Barth and Ramberg, 1966). Detailed descriptions of the surface geology have been written by Brögger (1921) and Saether (1957).

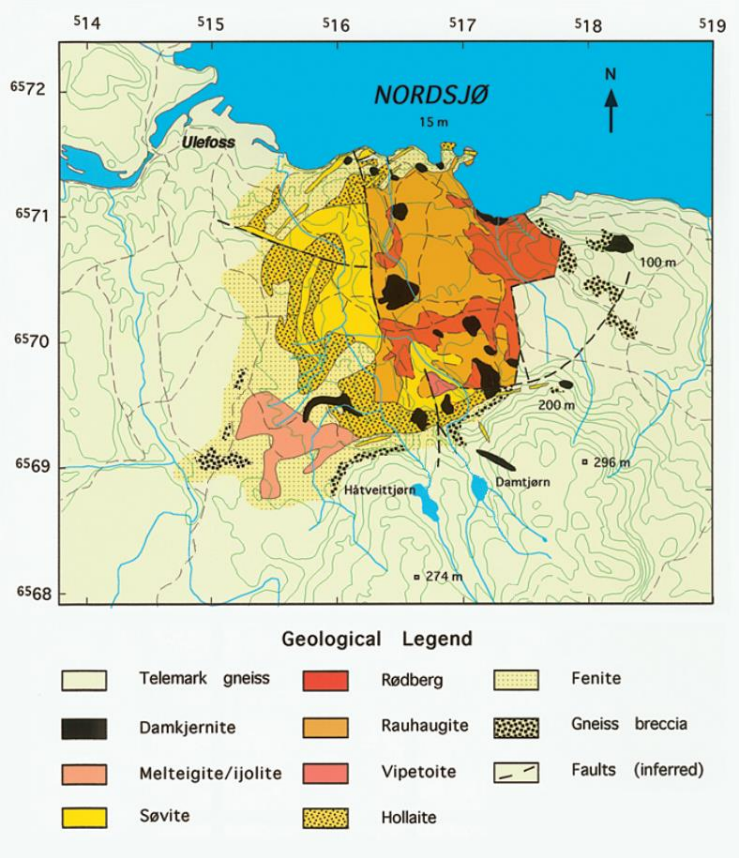

Figure: Geological Map of the Fen complex (after Verschure and Maijer, 2005)

The Fen complex extends to great depths, with gravity studies indicating that it reaches to at least 15 km below surface. The carbonatites and carbonate-silicate rocks are much less dense than the majority of the complex and are only present in major quantities within about a kilometer from the surface (Ramberg, 1973). The rocks have a mantle origin as indicated by spinel lherzolites in the damtjernite which have been shown to have equilibrated at pressures of 10-15 kbar at 1200-1250ºC (Griffin, 1975). Fen has experienced a very complex evolution showing evidence of crustal contamination, fractional crystallization, liquid immiscibility, and volatile transport as some of the processes involved (Mitchell, 1980; Andersen, 1987a)

The alkaline silicate rocks in the complex include rocks of the ijolite series, nepheline syenite and damtjernite (Saether, 1957), there are several varieties of carbonatite present in the complex including multiple types of calcite carbonatites (søvites), dolomite carbonatite, ankerite ferrocarbonatite and hematite carbonatite (rødberg) (Andersen, 1986a).

The different rocks are the result of two separate emplacement events (Saether, 1957); an earlier sequence of intrusions with an ijolitic magma source. This produced several of the different rock types found in the complex (Figure 6); pyroxenites formed as cumulates before the magma separated into the nepheline syenite and peralkaline carbonatite melts as immiscible liquids in the shallow crust (Mitchell and Brunfelt, 1975; Mitchell, 1980; Andersen, 1988).

A later sequence of intrusions brought in damtjernite producing dolomite and ferrocarbonatites associated with intense metasomatism which formed the rødberg and REE mineralization in the complex (Saether, 1957; Andersen, 1987b). An alkaline magnesian calcite carbonatite magma which formed biotite-amphibole calcite carbonatite and dolomite carbonatite associated with a silicate melt during a fractionation event in the middle crust at $T > 625^{o}C$, $P > 4$ kbars. A ferrocarbonatite liquid associated with the magnesian calcite carbonatite magma and/or the damtjernites was also involved during this time forming dykes and intrusive pyroclastic ankeritic ferrocarbonatite (Andersen, 1986a).

Mosonik Volcano

Figure: Location of Mosonik (modified from Google Maps)

Mosonik is a nephilinite-phonolite-carbonatite stratovolcano active during the Pliocene (3.12Ma). Located in Tanzania (2.61^{o}S, 35.8^{o}E) on the southern end of Lake Natron, to the North of the Ngorogoro Conservation Area. The Mosonik volcano is associated with the Gregory rift, the eastern section of the East African rift system. The volcano has a diameter of 7.5 km and a relief of 480m. The cone is cut on the north side by the north-south trending Sanjan Fault and exhibits valleys and ridges from weathering of the stratovolcano so that the summit crater is no longer evident (Dawson, 2009).

APPENDIX 2 – Mineral Compositions

Prairie Lake

Clinopyroxene compositions

Sample	**ETR-3**	**ETR-3**	**ETR-6a**	**ETR-6a**	**ETR-6a**	**ETR-6A**
Rock Type	Malignite	Malignite	Meta Micro Ijolite	Meta Micro Ijolite	Meta Micro Ijolite	Meta Micro Ijolite
Spot	1-2	1-3	1-1	1-2	1-4	1
Na_2O	0.78	0.54	1.05	0.46	0.81	0.92
MgO	10.36	12.6	9.13	10.41	10.01	9.99
Al_2O_3	3.08	1.78	4.44	3.29	3.19	1.48
SiO_2	48.88	51.86	47.9	49.36	48.75	52.12
CaO	23.3	23.88	22.91	23.54	22.29	23.96
TiO_2	1	0.52	1.64	0.78	0.82	
MnO	0.47	0.52			0.48	0.63
FeO	12.29	8.65	12.61	11.01	12.95	12.17
ZrO_2						
Total	100.16	100.35	99.68	98.85	99.3	101.27
Recalc.						
Fe^{3+}	2.01	1.39	2.71	1.19	2.09	2.37
Fe^{2+}	10.48	7.4	10.81	9.95	11.07	10.04
Total	100.36	100.49	100.59	98.98	99.51	101.51
Structural Formula						
Si	1.8645	1.9359	1.8323	1.8846	1.8752	1.956
Al(IV)	0.1355	0.0641	0.1677	0.1154	12.48	0.044
Al(VI)	0.0029	0.0142	0.0325	0.0326	0.0199	0.0214
FE3(IV)	0.0577	0.0391	0.0779	0.0341	0.0604	0.0669
FE2	0.3343	0.2309	0.3255	0.3178	0.3562	0.3148
Mn	0.0152	0.0164	0	0	0.0156	0.02
Mg	0.5892	0.7012	0.5207	0.6153	0.5741	0.5586
Ca	0.9522	0.9551	0.939	0.9629	0.9186	0.9628
Na	0.0577	0.0391	0.0779	0.0341	0.0604	0.0669
Ti	0.0287	0.0146	0.0472	0.0224	0.0237	0
End Members Based on Aegirine (Acmite)						
CaTiAl2O6	2.84	1.46	4.67	2.22	2.36	0
CaAlSiAlO6	0.29	1.42	3.22	3.23	1.97	2.15
Acmite	5.7	3.92	7.71	3.37	6	6.72
Wo	45.51	46.45	42.53	44.96	43.46	47.27
Fs	16.53	11.58	16.11	15.74	17.69	15.81
En	29.13	35.16	25.77	30.47	28.51	28.05
Recal into						
Ae	5.9	4.05	8.43	3.61	6.46	7.11
Hd	34.07	23.77	35.23	32.83	35.82	33.48
Di	60.03	72.18	56.35	63.56	57.73	59.41

Sample	**ETR-6A**	**ETR-6A**	**ETR-6A**	**ETR-7B**	**ETR-7B**	**ETR-7B**
Rock Type	Meta Micro Ijolite	Meta Micro Ijolite	Meta Micro Ijolite	Ijolite	Ijolite	Ijolite
Spot	2	3	4	1-2	1-3	2-8
Na_2O	0.81	0.65	1.25	0.93	1.04	1.04
MgO	9.41	9.68	9.58	9.85	10.11	10.08
Al_2O_3	2.77	1.64	0.74	2.87	3.35	1.9
SiO_2	50.03	51.98	53.57	48.59	49.57	51.12
CaO	23.95	23.91	23.07	22.39	22.77	22.76
TiO_2	0.77	0.39	0.3	1.14	1.1	0.67
MnO	0.49	0.6	0.75	0.44	0.63	0.54
FeO	12.6	12.11	12.66	12.04	11.99	12.26
ZrO_2						
Total	100.83	100.96	101.92	98.25	100.56	100.37
Recalc.						
Fe3+	2.09	1.67	4.51	2.4	2.68	2.68
Fe2+	10.12	10.6	8.6	9.88	9.58	9.85
Total	100.44	101.12	102.37	98.49	100.83	100.64
Structural Formula						
Si	1.9033	1.9561	1.9779	1.8819	1.8734	1.9322
Al(IV)	0.0967	0.0439	0.0221	0.1181	0.1266	0.0678
Al(VI)	0.0275	0.0289	0.0101	0.013	0.0226	0.0168
FE3(IV)	0.0597	0.0474	0.1253	0.0699	0.0762	0.0762
FE2	0.322	0.3337	0.2656	0.3203	0.3027	0.3113
Mn	0.0158	0.021	0.0235	0.0144	0.0202	0.0173
Mg	0.5337	0.5431	0.5273	0.5691	0.5697	0.568
Ca	0.9721	0.964	0.9126	0.9297	0.922	0.9217
Na	0.0597	0.0474	0.1253	0.0699	0.0762	0.0762
Ti	0.22	0.011	0.0083	0.0332	0.0313	0.019
End Members Based on Aegirine (Acmite)						
CaTiAl2O6	2.21	1.12	0.85	3.31	3.13	1.91
CaAlSiAlO6	2.76	2.21	0.56	1.3	2.26	1.69
Acmite	5.98	4.82	12.72	6.97	7.62	7.66
Wo	46.2	47.31	45.63	44.06	43.39	44.53
Fs	16.13	16.95	13.48	15.98	15.13	15.65
En	26.73	27.59	26.77	28.38	28.47	28.55
Recal into						
Ae	6.53	5.13	13.64	7.33	8.07	7.98
Hd	35.18	36.1	28.93	33.37	31.9	32.58
Di	58.3	58.76	57.43	59.3	60.03	59.45

Sample	**ETR-7B**	**ETR-7B**	**ETR-7B**	**ETR-7B**	**ETR-7B**	**ETR-7B**
Rock Type	Ijolite	Ijolite	Ijolite	Ijolite	Ijolite	Ijolite
Spot	2-9	3-2	1	2	3	4
Na_2O	2.37	0.81	0.88	0.8	0.87	0.86
MgO	8.62	10.55	9.56	10.09	9.66	9.96
Al_2O_3	0.6	2.99	2.13	1.3	2.69	1.04
SiO_2	51.81	49.54	51.63	52.9	49.49	52.72
CaO	20.13	23.33	23.57	23.94	23.07	22.76
TiO_2	0.26	1.23	0.47		0.81	
MnO	0.98	0.49	0.51	0.61	0.49	0.64
FeO	14.65	12.23	12.77	11.66	11.99	12.04
ZrO_2						
Total	99.42	101.17	101.52	101.3	99.07	100.02
Recalc.						
Fe3+	6.11	2.09	2.27	2.06	2.24	2.22
Fe2+	9.16	10.35	10.73	9.81	9.97	10.05
Total	100.04	101.38	101.75	101.51	99.29	100.25
Structural Formula						
Si	1.978	1.8677	1.9487	1.9763	1.9011	1.9788
Al(IV)	0.022	0.1323	0.0514	0.0237	0.0989	0.0212
Al(VI)	0.005	0.0006	0.0433	0.0335	0.0229	0.0248
FE3(IV)	0.1754	0.0592	0.0644	0.0579	0.0648	0.0626
FE2	0.2923	0.3264	0.3387	0.3063	0.3204	0.3153
Mn	0.0317	0.0156	0.0163	0.0193	0.0159	0.0203
Mg	0.4906	0.593	0.5379	0.562	0.5532	0.5574
Ca	0.8234	0.9424	0.9126	0.9582	0.9495	0.9555
Na	0.1754	0.0592	0.0644	0.0579	0.0648	0.0626
Ti	0.0075	0.0349	0.0133	0	0.0234	0
End Members Based on Aegirine (Acmite)						
CaTiAl2O6	0.76	3.46	1.36	0	2.34	0
CaAlSiAlO6	0.5	0.05	2.53	2.41	2.29	2.15
Acmite	17.81	5.87	6.58	5.89	6.48	6.34
Wo	41.17	45	44.71	47.53	45.19	47.31
Fs	14.84	16.19	17.31	15.58	16.03	15.97
En	24.91	29.42	27	28.58	27.68	28.23
Recal into						
Ae	18.3	6.13	6.86	6.26	6.9	6.69
Hd	30.5	32.22	35.98	33.07	34.14	33.72
Di	51.2	60.55	57.16	60.67	58.96	59.59

Sample	**NE4-2**	**NE4-2**	**NE4-2**	**NE4-2**	**NE4-2**	**PL-133**
Rock Type	Meta Micro Ijolite	Meta Micro Ijolite	Meta Micro Ijolite	Meta Micro Ijolite	Meta Micro Ijolite	Malignite
Spot	1-5	1-6	2-9	2-10	3-4	1
Na_2O	1.14	0.37	0.26	0.42	0.46	0.69
MgO	12.85	13.43	12.77	13.38	13.01	9.51
Al_2O_3	1.97	0.61	0.65	0.52	0.64	0.94
SiO_2	52.31	53.87	52.75	52.29	52.93	50.96
CaO	23.76	24.11	24.43	24.03	24.36	23.77
TiO_2	0.9	0.22	0.48	0.16	0.35	0.43
MnO	0.41	0.87	0.86	0.79	0.82	1
FeO	7.64	8.07	9.09	8.24	9.01	13.66
ZrO_2						
Total	100.98	101.55	101.29	99.83	101.58	100.96
Recalc.						
Fe3+	2.94	0.95	0.67	1.08	1.19	1.78
Fe2+	5	7.21	8.49	7.27	7.94	11.06
Total	101.28	101.64	101.36	99.94	101.7	100.14
Structural Formula						
Si	1.9254	1.9805	1.9608	1.9633	1.9588	1.9256
Al(IV)	0.0746	0.0195	0.285	0.023	0.0279	0.0419
Al(VI)	0.0109	0.007	0.0107	0.0137	0.0133	0.0325
FE3(IV)	0.0814	0.0264	0.008	0.0169	0.0197	0.0181
FE2	0.1538	0.2217	0.2638	0.2282	0.2458	0.3495
Mn	0.0128	0.0271	0.0271	0.0251	0.0257	0.032
Mg	0.7052	0.7361	0.7077	0.749	0.7178	0.5358
Ca	0.937	0.9497	0.973	0.9667	0.9659	1.0433
Na	0.0814	0.0264	0.0187	0.0306	0.033	0.0506
Ti	0.249	0.0061	0.0134	0.0045	0.009	0.0122
End Members Based on Aegirine (Acmite)						
CaTiAl2O6	2.5	0.62	1.34	0.45	0.97	1.2
CaAlSiAlO6	1.09	0.7	0	0	0	0
Acmite	8.16	2.67	1.88	3.04	3.29	4.95
Wo	45.19	47.46	48.09	47.88	47.68	50.5
Fs	7.71	11.24	13.22	11.35	12.26	17.12
En	35.36	37.3	35.47	37.27	35.8	26.24
Recal into						
Ae	8.65	2.74	1.92	3.15	3.34	5.4
Hd	16.36	22.52	26.64	22.56	24.66	67.65
Di	74.99	74.75	71.45	74.29	72	57.25

Sample	**PL-133**	**PL-133**	**PL-133**	**PL-133**	**PL-133**	**PL-133**
Rock Type	Malignite	Malignite	Malignite	Malignite	Malignite	Malignite
Spot	2	3	4	5	6	7
Na_2O	0.43	2.26	0.6	2.09	1.11	1.31
MgO	10.95	6.85	11.2	7.33	9.14	8.52
Al_2O_3	1.28	0.55	1.22	0.72	0.54	0.57
SiO_2	52.2	50.84	51.99	51.54	52.45	52.12
CaO	24.58	20.53	24.53	20.94	22.86	22.6
TiO_2	0.29	0.23	0.36	0.28	0.35	0.16
MnO	0.82	0.96	0.82	0.98	1.06	1.04
FeO	10.84	17.33	10.7	16.13	14.06	14.7
ZrO_2						
Total	101.39	99.55	101.42	100.01	101.57	101.02
Recalc.						
Fe3+	1.11	5.82	2.06	5.38	2.86	2.37
Fe2+	9.84	12.09	8.85	11.28	11.49	12.57
Total	101.5	100.13	101.63	100.54	101.86	101.26
Structural Formula						
Si	1.9533	1.9653	1.9394	1.9763	1.9755	1.9807
Al(IV)	0.0467	0.0251	0.0536	0.0237	0.024	0.0193
Al(VI)	0.0097	0.0096	0.007	0.0088	0.0005	0.0062
FE3(IV)	0.0312	0.1598	0.0509	0.1554	0.0805	0.0678
FE2	0.308	0.3909	0.2759	0.3619	0.3618	0.3994
Mn	0.026	0.0314	0.0259	0.0318	0.0338	0.0335
Mg	0.6109	0.3948	0.6229	0.4191	0.5133	0.4827
Ca	0.9854	0.8627	0.9804	0.8603	0.9225	0.9316
Na	0.0312	0.1694	0.0579	0.1554	0.0811	0.0678
Ti	0.0082	0.0067	0.0101	0.0075	0.0099	0.0089
End Members Based on Aegirine (Acmite)						
CaTiAl2O6	0.82	0.67	1.01	0.76	1.01	0.9
CaAlSiAlO6	0.98	0	0	0.88	0	0.16
Acmite	3.14	16.99	5.77	15.79	8.23	6.92
Wo	48.75	42.93	48.39	42.89	46.33	47
Fs	15.52	19.6	13.76	18.39	18.37	20.38
En	30.78	19.8	31.07	21.29	26.06	24.63
Recal into						
Ae	3.28	17.74	6.05	16.6	8.48	7.14
Hd	32.42	40.93	28.84	38.65	37.84	42.05
Di	64.3	41.34	65.11	44.76	53.68	50.82

Sample	**PL-133**	**PL-133**	**PL-20**	**PL-20**	**PL-20**	**PL-20**
Rock Type	Malignite	Malignite	Ijolite	Ijolite	Ijolite	Ijolite
Spot	8	9	1-7	1-8	1-9	2-6
Na_2O	0.92	0.8	0.84	1.25	1.11	0.7
MgO	8.59	8.55	10.16	8.11	8.8	10.51
Al_2O_3	0.89	0.79				
SiO_2	51.81	51.73	52.2	52.13	51.44	52.69
CaO	22.88	23.42	23.55	22.15	22.19	23.96
TiO_2	0.31	0.26				
MnO	0.9	1.1	0.78	1.28	1.06	
FeO	14.92	14.81	12.47	15.05	15.4	12.52
ZrO_2						
Total	101.22	101.46	100	99.97	100	100.38
Recalc.						
Fe3+	2.37	2.06		3.22	2.86	1.8
Fe2+	12.79	12.96		12.15	12.83	10.9
Total	101.46	101.67	87.53	100.29	100.29	100.56
Structural Formula						
Si	1.9675	1.9651	1.9887	2.0028	1.9823	1.9941
Al(IV)	0.0325	0.0349	0	0	0	0
Al(VI)	0.0073	0.0004	0	0	(0.0177 ?)	0
FE3(IV)	0.0677	0.0589	0.0113	0.0931	0.0652	0.0454
FE2	0.4061	0.4116	0.0507	0.3904	0.4134	0.3449
Mn	0.0289	0.0354	0.3352	0.0417	0.0346	0
Mg	0.4863	0.4842	0.0252	0.4617	0.5056	0.593
Ca	0.9309	0.9532	0.5771	0.9118	0.9162	0.9715
Na	0.0677	0.0589	0.062	0.0931	0.0829	0.0514
Ti	0.0089	0.0074	0	0	0	0
End Members Based on Aegirine (Acmite)						
CaTiAl2O6	0.9	0.75	0	0	0	0
CaAlSiAlO6	0.74	0.04	0	0	0	0
Acmite	6.86	5.97	6.21	9.54	8.29	5.11
Wo	46.32	47.87	48.12	46.79	45.79	48.28
Fs	20.56	20.84	16.78	20.01	20.66	17.14
En	24.63	24.52	28.89	23.8	25.27	29.47
Recal into						
Ae	7.05	6.17	6.37	9.82	8.3	5.19
Hd	42.29	43.11	34.41	41.18	41.25	34.86
Di	50.65	50.72	59.23	49	27.55	59.95

Sample	**PL-20**	**PL-20**	**PL34**	**PL34**	**PL34**	**PL34**
Rock Type	Ijolite	Ijolite	Ijolite	Ijolite	Ijolite	Ijolite
Spot	2-7	2-8	1	2	3	4
Na_2O	1.4	1.4	0.91	2.4	0.99	2.37
MgO	7.86	9.04	9.74	6.56	9.59	6.64
Al_2O_3			0.42	0.76	1.07	0.55
SiO_2	51.42	51.06	52.21	50.84	51.38	51.06
CaO	22.01	22.05	23.34	20.34	23.99	20.98
TiO_2			0	0	0.35	0
MnO	0.95	0.42	0.84	1.31	0.72	1.16
FeO	16.36	14.4	12.12	17.05	12.68	16.87
ZrO_2						
Total	100	98.37	99.58	99.26	100.77	99.63
Recalc.						
Fe3+	3.61	3.61	2.34	6.18	2.55	6.11
Fe2+	13.11	11.15	10.01	11.49	10.18	11.38
Total	100.36	98.73	99.81	99.88	100.82	100.25
Structural Formula						
Si	1.9862	1.9851	1.9915	1.9729	1.9494	1.9746
Al(IV)	0	0	0.0085	0.0271	0.0478	0.0251
Al(VI)	(0.0138?)	(.0149?)	0.0104	0.0077	0.0027	0.0003
FE3(IV)	0.091	0.0906	0.0673	0.1806	0.0701	0.1774
FE2	0.4236	0.3627	0.3193	0.3727	0.3232	0.3679
Mn	0.0311	0.0138	0.0271	0.0431	0.0231	0.038
Mg	0.4526	0.524	0.5539	0.3795	0.5425	0.3828
Ca	0.9109	0.9185	0.9539	0.8457	0.9752	0.8693
Na	0.1048	0.1055	0.0673	0.1806	0.0728	0.01777
Ti	0	0	0	0	0.01	0
End Members Based on Aegirine (Acmite)						
CaTiAl2O6	0	0	0	0	1	0
CaAlSiAlO6	0	0	0.86	0.78	0	0
Acmite	10.5	10.47	6.83	18.36	7.3	17.99
Wo	45.62	45.56	47.99	42.61	48.35	44
Fs	21.21	17.99	16.21	18.95	16.19	18.62
En	22.67	25.99	28.12	19.3	27.17	19.38
Recal into						
Ae	10.69	10.64	7.16	19.36	7.76	19.14
Hd	43.18	36.55	33.95	39.96	34.43	39.62
Di	46.14	52.81	58.89	40.69	57.81	41.24

Sample	**PL34**	**PL34**	**PL34**	**PL34**	**PL34**	**PL34**
Rock Type	Ijolite	Ijolite	Ijolite	Ijolite	Ijolite	Ijolite
Spot	5	6	7	8	9	10
Na_2O	2.47	1.02	1.38	1.28	0.65	1.88
MgO	6.91	10.22	8.43	8.76	10.73	7.05
Al_2O_3	0.65	0.37	0.64	0.5	0.44	0.46
SiO_2	51.86	52.16	51.82	52.4	52.3	51.51
CaO	20.77	23.85	22.81	23.33	24.6	21.69
TiO_2	0	0	0	0	0	0
MnO	1.27	0.74	0.92	1.09	0.91	0.92
FeO	17.02	12.14	14.99	13.82	11.45	16.62
ZrO_2						
Total	100.95	100.5	100.99	101.18	101.08	100.13
Recalc.						
Fe3+	6.36	2.63	3.56	3.3	1.67	4.84
Fe2+	11.29	9.78	11.79	10.85	9.94	12.26
Total	101.58	100.77	101.35	101.51	101.24	100.61
Structural Formula						
Si	1.9754	1.9743	1.9708	1.9811	1.9695	1.9824
Al(IV)	0.0246	0.0165	0.0287	0.0189	0.0195	0.0176
Al(VI)	0.0046	0.0092	0.0005	0.0034	0.011	0.0033
FE3(IV)	0.1824	0.0657	0.1012	0.0938	0.0365	0.1403
FE2	0.3598	0.3094	0.375	0.3431	0.3131	0.3946
Mn	0.041	0.0237	0.0296	0.0349	0.029	0.03
Mg	0.3924	0.5767	0.478	0.4938	0.6024	0.4045
Ca	0.8476	0.9672	0.9294	0.945	0.9925	0.8944
Na	0.1824	0.0749	0.1018	0.0938	0.0475	0.1403
Ti	0	0	0	0	0	0
End Members Based on Aegirine (Acmite)						
CaTiAl2O6	0	0	0	0	0	0
CaAlSiAlO6	0.47	0	0	0.35	0	0.33
Acmite	18.53	7.47	10.25	9.51	4.74	14.19
Wo	42.81	46.29	46.8	47.72	49.55	45.06
Fs	18.27	15.45	18.88	17.39	15.63	19.96
En	19.93	28.79	24.07	25.03	30.08	20.46
Recal into						
Ae	19.52	7.79	10.66	10.08	4.93	14.93
Hd	38.49	32.2	39.28	36.87	32.52	42.01
Di	41.99	60.01	50.07	53.05	62.56	43.06

Sample	**PL34**	**PL34**	**PL34**	**PL34**	**PL34**	**PL34**
Rock Type	Ijolite	Ijolite	Ijolite	Ijolite	Ijolite	Ijolite
Spot	11	12	13	14	15	16
Na_2O	1.03	2.4	2.31	0.66	0.61	1
MgO	10.12	6.49	7.42	11.2	10.98	9.37
Al_2O_3	0.49	0.61	0.77	0.37	0.32	0.51
SiO_2	52.31	50.92	51.58	53.19	52.78	51.77
CaO	23.94	20.84	21.13	24.69	24.66	23.74
TiO_2	0	0	0	0	0	0
MnO	0.95	1.18	1	0.93	0.92	0.82
FeO	11.8	17.31	16.17	10.72	10.19	13.1
ZrO_2						
Total	100.64	99.75	100.38	101.76	100.46	100.31
Recalc.						
Fe3+	2.65	6.18	5.95	1.7	1.57	2.58
Fe2+	9.41	11.75	10.81	9.19	8.78	10.78
Total	100.9	100.37	100.97	101.93	100.62	100.57
Structural Formula						
Si	1.9754	1.9705	1.9704	1.9796	1.9868	1.9731
Al(IV)	0.0218	0.0278	0.0296	0.0162	0.0132	0.0229
Al(VI)	0.0028	0.0017	0.0051	0.0041	0.001	0.004
FE3(IV)	0.0726	0.1784	0.1711	0.0635	0.0445	0.0699
FE2	0.2972	0.3801	0.3455	0.286	0.2763	0.3436
Mn	0.0304	0.0387	0.0324	0.0293	0.0293	0.0265
Mg	0.5698	0.3744	0.4226	0.6215	0.6162	0.5324
Ca	0.9686	0.8641	0.8648	0.9845	0.9945	0.9694
Na	0.0754	0.1801	0.1711	0.0486	0.0445	0.0739
Ti	0	0	0	0	0	0
End Members Based on Aegirine (Acmite)						
CaTiAl2O6	0	0	0	0	0	0
CaAlSiAlO6	0	0	0.51	0	0.1	0
Acmite	7.59	18.2	17.28	4.79	4.5	7.41
Wo	48.76	43.67	43.42	49.54	50.26	48.63
Fs	14.96	19.21	17.45	14.39	13.97	17.24
En	28.68	18.92	21.34	31.27	31.17	26.71
Recal into						
Ae	8	19.27	18.22	4.99	4.75	7.78
Hd	31.54	40.67	36.79	29.95	29.48	36.17
Di	60.46	40.06	45	65.07	65.77	56.05

Sample	**PL34**	**PL34**	**PL34**	**PL34**	**PL-38**	**PL-38**
Rock Type	Ijolite	Ijolite	Ijolite	Ijolite	Malignite	Malignite
Spot	17	18	19	20	1	2
Na_2O	2.01	0.54	2.48	0.71	0.93	0.93
MgO	6.87	11.23	6.78	10.81	8.39	5.64
Al_2O_3	0.46	0.34	0.65	0.32	0.7	1.06
SiO_2	51.39	52.89	51.77	52.92	51.27	48.46
CaO	21.2	24.9	20.48	24.75	23.1	20.04
TiO_2	0	0	0	0	0	0
MnO	1.01	1.06	1.18	0.81	1.17	1.15
FeO	17.11	10.48	17.16	10.94	14.07	18.76
ZrO_2						
Total	100.05	101.44	100.5	101.26	99.63	96.04
Recalc.						
Fe3+	5.18	1.39	6.39	1.83	2.4	5.54
Fe2+	12.45	8.83	11.41	9.29	11.91	13.78
Total	100.57	101.18	101.14	101.44	99.87	96.6
Structural Formula						
Si	1.9815	1.9813	1.9798	1.9815	1.9733	1.9449
Al(IV)	0.0185	0.015	0.0202	0.0141	0.0267	0.0501
Al(VI)	0.0025	0.0037	0.0091	0.0044	0.0051	0.005
FE3(IV)	0.1503	0.0355	0.1839	0.0471	0.0694	0.1623
FE2	0.4015	0.2766	0.3649	0.291	0.3835	0.4623
Mn	0.033	0.0336	0.0382	0.0257	0.0381	0.0391
Mg	0.3949	0.3272	0.3866	0.6035	0.4929	0.3375
Ca	0.8758	0.9994	0.8391	0.9929	0.9526	0.8617
Na	0.1503	0.0392	0.1839	0.0515	0.0694	0.1673
Ti	0	0	0	0	0	0
End Members Based on Aegirine (Acmite)						
CaTiAl2O6	0	0	0	0	0	0
CaAlSiAlO6	0.25	0	0.93	0	0.52	0
Acmite	15.22	3.96	18.69	5.18	7.04	16.76
Wo	44.22	50.43	42.19	49.88	48.03	43.17
Fs	20.33	13.96	18.55	14.62	19.44	23.16
En	20	31.65	19.65	30.32	24.99	16.91
Recal into						
Ae	15.87	4.16	19.66	5.45	7.34	17.3
Hd	42.41	29.33	39.01	30.76	40.55	47.81
Di	41.72	66.51	41.33	63.79	52.12	34.9

Sample	**PL-38**	**PL-38**	**PL-38**	**PL-38**	**PL-38**	**PL-38**
Rock Type	Malignite	Malignite	Malignite	Malignite	Malignite	Malignite
Spot	3	4	5	6	7	8
Na_2O	3.07	3.85	4.28	0.76	1.72	0.92
MgO	7.4	5.49	5.49	8.79	4.75	7.99
Al_2O_3	0.54	0.48	0.57	0.69	0.55	0.55
SiO_2	51.57	51.15	50.95	51.2	49.18	51.28
CaO	19.57	17.82	16.9	23.23	20.87	22.87
TiO_2	0	0	0	0	0	0
MnO	0.97	1.71	1.17	1.27	1.28	1.42
FeO	16.15	19.2	19.33	14.02	19.79	15.17
ZrO_2						
Total	99.27	99.7	98.69	99.96	98.14	100.2
Recalc.						
Fe3+	7.91	8.37	11.03	1.96	4.43	2.37
Fe2+	9.03	11.67	9.41	12.26	15.8	13.04
Total	100.06	100.54	99.8	100.16	98.58	100.44
Structural Formula						
Si	1.9788	1.9899	1.9767	1.9674	1.8403	1.9772
Al(IV)	0.0212	0.0101	0.0233	0.0314	0.1597	0.0228
Al(VI)	0.0032	0.0119	0.0028	0.0012	0.1291	0.0022
FE3(IV)	0.2284	0.2451	0.322	0.0556	0.1248	0.0688
FE2	0.2898	0.3795	0.3052	0.3955	0.4945	0.4204
Mn	0.0315	0.0563	0.0384	0.0415	0.0406	0.0464
Mg	0.4233	0.3184	0.3176	0.5056	0.265	0.4593
Ca	0.8045	0.7428	0.7025	0.9622	0.8367	0.9448
Na	0.2284	0.2451	0.322	0.0568	0.1248	0.0688
Ti	0	0	0	0	0	0
End Members Based on Aegirine (Acmite)						
CaTiAl2O6	0	0	0	0	0	0
CaAlSiAlO6	0.32	1.04	0.28	0	13.08	0.22
Acmite	23.1	25.26	32.65	5.75	12.64	7
Wo	40.52	37.75	35.48	48.67	35.83	47.99
Fs	14.66	19.55	15.48	20	25.04	21.4
En	21.41	16.4	16.1	25.57	13.42	23.38
Recal into						
Ae	24.26	25.99	34.08	5.93	14.99	7.25
Hd	30.78	40.24	32.31	21.22	55.35	44.32
Di	44.96	33.76	33.61	27.13	29.66	48.43

Sample	**PL-38**	**PL-38**	**PL-42**	**PL-42**	**PL-42**	**PL-42**
Rock Type	Malignite	Malignite	Malignite	Malignite	Malignite	Malignite
Spot	9	10	1-1	1-2	1-9	3-2
Na_2O	2.51	2.04	2.72	2.95	3.35	2.95
MgO	5.73	5.24	5.54	5.05	5.05	4.33
Al_2O_3	0.64	0.49	0.69	0.46	0.73	0.53
SiO_2	50.47	49.89	50.49	49.63	50.95	50.47
CaO	20.32	20.49	19.14	18.82	18.11	18.19
TiO_2	0	0	0.32	0.15		0.18
MnO	1.24	1.04	1.21	1.28	1.12	1.05
FeO	18.46	18.53	19.18	19.88	20.16	21.36
ZrO_2						
Total	99.37	97.72	99.29	98.22	99.47	99.06
Recalc.						
Fe3+	6.47	5.26	7.01	7.6	8.63	7.6
Fe2+	12.64	13.8	12.87	13.04	12.39	14.52
Total	100.02	98.25	99.99	98.98	100.33	99.82
Structural Formula						
Si	1.9698	1.9858	1.9699	1.9666	1.9796	1.9849
Al(IV)	0.0294	0.0142	0.0301	0.0215	0.0204	0.0151
Al(VI)	0	0.0088	0.0017	0.0119	0.0131	0.0095
FE3(IV)	0.1891	0.1574	0.2058	0.2148	0.2524	0.2249
FE2	0.4126	0.4594	0.4201	0.4321	0.4027	0.4776
Mn	0.041	0.0351	0.04	0.043	0.0369	0.035
Mg	0.3334	0.311	0.3223	0.2983	0.2925	0.2539
Ca	0.8497	0.8738	0.8001	0.799	0.7539	0.7665
Na	0.1899	0.1574	0.2058	0.2266	0.2524	0.2249
Ti	0	0	0.0094	0.0045	0	0.0053
End Members Based on Aegirine (Acmite)						
CaTiAl2O6	0	0	0.96	0.45	0	0.54
CaAlSiAlO6	0	0.89	0.17	0	1.33	0.45
Acmite	19.23	16	20.94	22.81	25.66	22.98
Wo	43.01	43.96	40.14	39.98	37.66	38.66
Fs	20.88	23.34	21.38	21.75	20.47	24.4
En	16.88	15.8	16.4	15.01	14.87	12.97
Recal into						
Ae	20.29	16.97	21.7	23.68	26.63	23.52
Hd	44.08	49.51	44.31	45.15	42.5	49.93
Di	35.62	33.52	33.99	31.17	30.87	26.55

Sample	**PL-42**	**PL-42**	**PL-42**	**PL-42**	**PL-42**	**PL-42**
Rock Type	Malignite	Malignite	Malignite	Malignite	Malignite	Malignite
Spot	3-3	1	2	3	4	5
Na_2O	3.14	1.11	1.08	0.97	1.05	1.91
MgO	4.72	6.98	6.56	6.54	6.42	5.87
Al_2O_3	0.64	1.86	1.57	1.29	1.42	0.57
SiO_2	50.18	49.84	48.19	48.47	48.84	49.61
CaO	18.14	22.52	21.67	22.04	22.22	20.04
TiO_2		0.58	0.89	0.47	0.67	0.26
MnO	1.36	1.01	0.96	1.26	1.17	1.21
FeO	22.03	16.98	16.35	16.53	17.24	17.94
ZrO_2				0.55	0.97	
Total	100.21	100.88	97.27	98.12	100	97.41
Recalc.						
Fe3+	8.09	2.86	2.78	2.5	2.73	4.92
Fe2+	14.75	14.41	13.85	14.28	14.96	13.55
Total	101.02	101.17	97.55	97.82	99.48	97.94
Structural Formula						
Si	1.9596	1.9221	1.9375	1.9373	1.9255	1.9765
Al(IV)	0.0295	0.0779	0.0611	0.0608	0.066	0.0235
Al(VI)	0.0109	0.0067	0.0014	0.002	0.0085	0.0032
FE3(IV)	0.2269	0.083	0.0828	0.0732	0.0725	0.1475
FE2	0.4819	0.4646	0.4655	0.4773	0.4933	0.4515
Mn	0.045	0.033	0.0191	0.0427	0.0391	0.0408
Mg	0.2749	0.4013	0.3932	0.3921	0.3774	0.3487
Ca	0.7593	0.9305	0.9335	0.9438	0.9386	0.8554
Na	0.2378	0.083	0.0842	0.0752	0.081	0.1475
Ti	0	0.0168	0.0269	0.0141	0.0199	0.0078
End Members Based on Aegirine (Acmite)						
CaTiAl2O6	0	1.69	2.71	1.43	2	0.79
CaAlSiAlO6	0	0.67	0	0	0	0.33
Acmite	23.88	8.36	8.47	7.6	8.14	15.04
Wo	38.12	45.67	45.61	47.01	46.14	43.04
Fs	24.19	23.4	23.42	24.14	24.78	23.02
En	13.8	20.21	19.78	19.83	18.95	17.77
Recal into						
Ae	23.91	8.75	8.93	7.96	8.51	15.57
Hd	48.45	48.96	49.37	50.53	51.84	47.64
Di	27.65	42.29	41.7	41.51	39.65	36.79

Sample	**PL-42**	**PL-42**	**PL-42**	**PL-42**	**PL-42**	**PL-42**
Rock Type	Malignite	Malignite	Malignite	Malignite	Malignite	Malignite
Spot	6	7	8	9	10	11
Na_2O	0.96	0.91	1.38	0.93	1.16	1.82
MgO	6.84	6.71	5.87	6.64	6.03	5.06
Al_2O_3	1.62	1.58	2.33	2.32	1.17	0.64
SiO_2	47.67	47.88	46.67	46.79	48.34	47.37
CaO	21.83	21.59	21.01	21.51	21.54	19.95
TiO_2	0.6	0.61	1.17	0.94	0.55	0.34
MnO	0.98	1.1	0.93	0.88	1.1	1.2
FeO	15.84	16.12	17.89	16.45	17.61	18.61
ZrO_2						
Total	96.34	96.5	97.25	96.46	97.5	94.99
Recalc.						
Fe3+	1.44	1.44	3.56	2.4	2.99	3.4
Fe2+	14.54	14.82	14.65	14.29	14.92	15.55
Total	96.48	96.64	97.57	96.7	97.8	95.33
Structural Formula						
Si	1.9345	1.9226	1.881	1.8925	1.9395	1.9678
Al(IV)	0.0655	0.0774	0.1107	0.1075	0.0553	0.0313
Al(VI)	0.012	0.0328	0.0083	0.0031	0.0052	0.0009
FE3(IV)	0.0441	0.0436	0.0995	0.0729	0.085	0.1054
FE2	0.4935	0.4977	0.4938	0.4835	0.5006	0.5402
Mn	0.0337	0.0374	0.0317	0.0301	0.0374	0.0422
Mg	0.4138	0.4017	0.3527	0.4004	0.3607	0.3134
Ca	0.9492	0.9288	0.9073	0.9321	0.9259	0.8879
Na	0.0441	0.0436	0.1078	0.0729	0.0902	0.1063
Ti	0.0183	0.0184	0.0355	0.0286	0.0166	0.0106
End Members Based on Aegirine (Acmite)						
CaTiAl2O6	1.85	1.87	3.54	2.87	1.67	1.08
CaAlSiAlO6	1.22	3.34	0	0.31	0	0
Acmite	4.46	4.43	10.76	7.32	9.09	10.82
Wo	46.53	44.62	43.48	45.17	45.83	44.65
Fs	24.99	25.31	24.63	24.25	25.23	27.49
En	20.95	20.43	17.59	20.08	18.18	15.95
Recal into						
Ae	4.63	4.73	11.3	7.62	9.48	11.08
Hd	51.87	52.72	51.74	50.53	52.82	56.28
Di	43.5	42.55	36.96	41.85	38.06	32.65

Sample	**PL-42**	**PL-42**	**PL-42**	**PL-42**	**PL-42**	**PL-42**
Rock Type	Malignite	Malignite	Malignite	Malignite	Malignite	Malignite
Spot	12	13	14	15	16	17
Na_2O	0.84	1.43	1.18	2.54	2.53	2.61
MgO	6.67	5.42	6.52	4.42	4.82	4.36
Al_2O_3	1.02	1.24	1.65	0.5	0.57	0.63
SiO_2	50.01	46.55	49.25	49.91	49.51	50.3
CaO	22.81	20.73	22.18	19.26	19.08	18.63
TiO_2	0.37	0.56	0.64	0.24	0.32	0.34
MnO	1.24	1.21	1.14	1.19	1.19	1.1
FeO	17.44	17.18	17.25	20.28	19.19	21.42
ZrO_2						
Total	100.4	94.32	99.81	98.34	97.21	99.39
Recalc.						
Fe3+	2.16	3.04	3.04	6.54	6.52	6.72
Fe2+	15.49	14.44	14.51	14.39	13.32	15.37
Total	100.61	94.62	100.11	98.99	97.86	100.06
Structural Formula						
Si	1.9482	1.944	1.9297	1.9808	1.9792	1.9779
Al(IV)	0.0468	0.056	0.0703	0.0192	0.0208	0.0221
Al(VI)	0.005	0.005	0.0058	0.0042	0.006	0.0071
FE3(IV)	0.0584	0.0955	0.0896	0.1955	0.1961	0.199
FE2	0.5047	0.5045	0.4756	0.4777	0.4454	0.5054
Mn	0.0409	0.0074	0.0378	0.04	0.0403	0.0366
Mg	0.3874	0.3499	0.3651	0.2615	0.2873	0.2556
Ca	0.952	0.9275	0.9311	0.819	0.8172	0.7849
Na	0.0634	0.0955	0.0896	0.1955	0.1961	0.199
Ti	0.0108	0.0201	0.0189	0.0072	0.0096	0.0101
End Members Based on Aegirine (Acmite)						
CaTiAl2O6	1.09	2.01	1.91	0.73	0.98	1.03
CaAlSiAlO6	0	0.5	0.59	0.43	0.16	0.2
Acmite	6.4	9.59	9.07	19.94	20.08	20.35
Wo	47.49	45.16	45.88	41.19	41.26	39.51
Fs	25.47	25.25	24.07	24.36	22.8	25.84
En	19.55	17.51	18.48	13.34	14.71	13.07
Recal into						
Ae	6.64	10.06	9.64	20.91	21.11	20.73
Hd	52.82	53.11	51.12	51.11	47.96	52.65
Di	40.54	36.84	39.24	27.98	30.93	26.63

Sample	**PL-42**	**PL-42**	**PL-42**	**PL-43**	**PL-43**	**PL-43**
Rock Type	Malignite	Malignite	Malignite	Meta Micro Ijolite	Meta Micro Ijolite	Meta Micro Ijolite
Spot	18	19	20	1	2	3
Na_2O	2.14	1.67	1.88	0.48	1.84	0.28
MgO	5.91	5.74	5.74	11.76	7.76	11.98
Al_2O_3	0.73	0.69	1.03	0.79	0.37	0.82
SiO_2	50.36	46.89	46.77	50.95	50.11	50.52
CaO	19.79	21.42	21.43	24.18	20.63	24.05
TiO_2	0.33	0.55	0.62	0.26	0.23	0.21
MnO	1.21	1.2	1.11	0.83	1.05	0.78
FeO	18.32	17.5	17.2	8.33	15.42	8.48
ZrO_2						
Total	98.79	95.66	95.78	97.58	97.41	97.12
Recalc.						
Fe3+	5.51	4.3	4.84	1.24	4.74	0.72
Fe2+	13.36	13.63	12.82	7.22	11.15	7.83
Total	99.34	96.09	96.24	97.71	97.88	97.19
Structural Formula						
Si	1.9705	1.9241	1.9119	1.9685	1.9749	1.9582
Al(IV)	0.0295	0.0334	0.0496	0.0315	0.0172	0.0375
Al(VI)	0.0042	0.0425	0.0385	0.0045	0.0079	0.0044
FE3(IV)	0.1624	0.0903	0.1105	0.036	0.1327	0.0167
FE2	0.4371	0.4677	0.439	0.2332	0.3676	0.2538
Mn	0.0401	0.0417	0.0384	0.0108	0.0351	0.0256
Mg	0.3448	0.3512	0.3498	0.6774	0.456	0.6923
Ca	0.8296	0.9417	0.9386	1.0009	0.8711	0.9987
Na	0.1623	0.1329	0.149	0.036	0.1406	0.021
Ti	0.0162	0.017	0.0191	0.0076	0.0068	0.0076
End Members Based on Aegirine (Acmite)						
CaTiAl2O6	1.51	1.63	1.86	0.76	0.69	0.76
CaAlSiAlO6	0	0	0	0.45	0	0
Acmite	16.64	13.01	14.58	3.6	14.18	2.11
Wo	41.77	45.28	44.98	49.56	43.59	49.69
Fs	22.41	22.89	21.47	11.69	18.54	12.73
En	17.67	17.19	17.11	33.95	23	34.71
Recal into						
Ae	17.19	13.96	15.89	3.8	14.58	2.18
Hd	46.29	49.14	46.81	24.64	38.13	26.24
Di	36.51	36.9	37.3	71.57	47.29	71.58

Sample	**PL-43**	**PL-43**	**PL-43**	**PL-43**	**PL-43**	**PL-43**
Rock Type	Meta Micro Ijolite	Meta Micro Ijolite	Meta Micro Ijolite	Meta Micro Ijolite	Meta Micro Ijolite	Meta Micro Ijolite
Spot	4	5	6	7	8	9
Na_2O	1.94	0.87	0.54	0.77	1.06	0.95
MgO	7.08	12.85	11.3	9.344	7.56	7.8
Al_2O_3	0.35	2.05	0.72	0.57	0.63	0.54
SiO_2	49.45	49.7	50.82	50.09	49.71	49.73
CaO	20.3	24.42	24.33	23.13	22.34	22.55
TiO_2	0.18	0.68	0.35	0.29	0.27	0.24
MnO	1.11	0.66	0.72	0.86	1.03	0.95
FeO	15.95	6.96	9.19	12.34	15.54	15.17
ZrO_2						
Total	96.36	98.19	97.97	97.394	98.14	97.93
Recalc.						
Fe3+	5	2.24	1.39	1.98	2.73	2.45
Fe2+	11.45	4.94	7.94	10.55	13.08	12.97
Total	96.86	98.41	98.11	97.584	98.41	98.18
Structural Formula						
Si	1.9735	1.8946	1.9617	1.966	1.9614	1.9641
Al(IV)	0.0165	0.0921	0.0328	0.0264	0.0293	0.0251
Al(VI)	0.0101	0.0133	0.0055	0.0076	0.0093	0.0107
FE3(IV)	0.14	0.051	0.0349	0.051	0.0718	0.0621
FE2	0.3822	0.1576	0.2563	0.3465	0.4317	0.4285
Mn	0.0375	0.0213	0.0137	0.0286	0.0344	0.0318
Mg	0.4213	0.7303	0.6503	0.5466	0.4447	0.4595
Ca	0.8765	0.9974	1.0062	0.9727	0.9444	0.9546
Na	0.1501	0.0643	0.0404	0.0586	0.0811	0.0728
Ti	0.0054	0.0189	0.0102	0.0086	0.008	0.0071
End Members Based on Aegirine (Acmite)						
CaTiAl2O6	0.54	1.86	1.01	0.86	0.8	0.71
CaAlSiAlO6	0	0	0	0	0	0
Acmite	15.12	6.33	4.03	5.88	8.15	7.29
Wo	43.87	48.13	49.71	48.41	47.03	47.49
Fs	19.25	7.75	12.79	17.4	21.68	21.47
En	21.22	35.93	32.45	27.45	22.34	23.03
Recal into						
Ae	15.74	6.75	4.27	6.16	8.47	7.57
Hd	40.08	16.55	27.06	36.41	45.08	44.6
Di	44.18	76.7	68.67	57.44	46.45	47.83

Sample	**PL-43**	**PL46**	**PL46**	**PL46**	**PL46**	**PL46**
Rock Type	Meta Micro Ijolite	Malignite	Malignite	Malignite	Malignite	Malignite
Spot	10	1	2	3	4	5
Na_2O	0.42	2.87	2.72	2.91	2.75	9.34
MgO	12.44	4.64	4.61	5.13	4.4	3.61
Al_2O_3	1.78	0.46	0.61	0.4	0.46	
SiO_2	50.35	50.14	50.05	51.3	50.04	52.79
CaO	29.63	18.87	18.46	18.82	18.59	8.42
TiO_2	0.66	0.19				0.16
MnO	0.57	1.27	1.2	1.17	1.16	0.67
FeO	6.99	20.28	20.71	20.13	19.99	22.93
ZrO_2						
Total	102.84	98.72	98.36	99.86	97.39	97.92
Recalc.						
Fe3+	1.08	7.39	6.24	5.18	7.09	24.06
Fe2+	6.02	13.63	15.1	15.47	13.61	1.28
Total	102.95	99.46	98.99	100.38	98.1	100.33
Structural Formula						
Si	1.8617	1.9778	1.9907	1.9912	1.9963	2
Al(IV)	0.0776	0.0214	0.0093	0.0088	0.0037	0
Al(VI)	0.0607	0.0008	0.0193	0.0095	0.0179	0
FE3(IV)	(-.0306)	0.2187	0.1866	0.219	0.2127	0.6874
FE2	0.186	0.4495	0.5022	0.4344	0.4542	0.0405
Mn	0.0179	0.0424	0.0404	0.0385	0.0392	0.0215
Mg	0.6858	0.2729	0.2734	0.2969	0.2617	0.2043
Ca	1.1738	0.7975	0.7867	0.7826	0.7946	0.3424
Na	0.0301	0.2195	0.1866	0.219	0.2127	0.6847
Ti	0.0184	0.0056	0	0	0	0.0046
End Members Based on Aegirine (Acmite)						
CaTiAl2O6	1.73	0.57	0	0	0	[-.19]
CaAlSiAlO6	0	0	0.96	0.9	0.38	0
Acmite	2.83	22.35	19.19	22.34	21.93	70.14
Wo	54.4	40.31	39.97	39.47	40.78	17.57
Fs	8.76	22.88	25.87	22.16	23.42	2.07
En	32.28	13.89	14.06	15.14	13.49	10.42
Recal into						
Ae	3.34	23.3	19.39	23.05	22.91	73.74
Hd	20.63	47.72	52.2	45.71	48.91	4.34
Di	76.04	28.97	28.41	31.24	28.18	21.92

Sample	**PL46**	**PL46**	**PL46**	**PL46**	**PL46**	**PL46**
Rock Type	Malignite	Malignite	Malignite	Malignite	Malignite	Malignite
Spot	6	7	8	9	10	11
Na_2O	2.92	2.83	1.43	1.41	1.6	6.57
MgO	4.91	5.13	6.71	6.24	6.69	5.7
Al_2O_3	0.64	0.47	0.52	0.91	0.62	0.2
SiO_2	51.26	50.81	51.24	50.42	51.4	52.73
CaO	19.03	18.78	22.16	21.63	21.74	13.23
TiO_2					0.36	
MnO	1.25	1.39	1.33	1.34	1.43	1.5
FeO	20.01	20.66	16.96	16.94	17.45	18.92
ZrO_2						
Total	100.02	100.07	100.35	98.89	101.29	98.85
Recalc.						
Fe3+	7.52	7.29	3.68	3.63	4.12	16.93
Fe2+	13.24	14.1	13.64	13.7	13.74	3.69
Total	100.77	100.8	100.71	99.28	101.7	100.55
Structural Formula						
Si	1.9867	1.9774	1.9806	1.9775	1.9693	1.9985
Al(IV)	0.0133	0.0216	0.0194	0.0225	0.028	0.0015
Al(VI)	0.0159	0.0009	0.0043	0.0195	0.0027	0.0074
FE3(IV)	0.2194	0.2127	0.1072	0.1072	0.1161	0.4828
FE2	0.4291	0.4589	0.4411	0.4494	0.4402	0.1169
Mn	0.041	0.0458	0.0435	0.0445	0.0464	0.0482
Mg	2837	0.2977	0.3867	0.3649	0.3821	0.3221
Ca	0.7902	0.7831	0.9177	0.9089	0.8924	0.5372
Na	0.2194	0.2136	0.1072	0.1072	0.1189	0.4828
Ti	0	0	0	0	0.104	0
End Members Based on Aegirine (Acmite)						
CaTiAl2O6	0	0	0	0	1.06	0
CaAlSiAlO6	1.36	0	0.44	2	0	0.16
Acmite	22.44	21.72	10.91	10.96	12.11	49.69
Wo	39.73	39.82	46.5	45.44	44.94	27.57
Fs	21.95	23.33	22.46	22.96	22.43	6.01
En	14.51	15.14	19.69	18.94	19.47	16.57
Recal into						
Ae	23.54	22.01	11.46	11.64	12.63	52.38
Hd	46.03	47.3	47.18	48.77	46.77	12.68
Di	30.43	30.68	41.36	39.6	40.6	34.94

Sample	**PL46**	**PL46**	**PL46**	**PL46**	**PL46**	**PL46**
Rock Type	Malignite	Malignite	Malignite	Malignite	Malignite	Malignite
Spot	11a	12	13	14	15	16
Na_2O	0.99	1.62	1.05	1.16	1.97	0.75
MgO	6.81	7.52	6.73	6.6	6.24	6.89
Al_2O_3	1.35	0.39	1.5	1.53	1.26	1.05
SiO_2	50.34	52.06	50.41	50.07	50.22	50.41
CaO	22.6	21.8	22.56	22.43	22.56	22.81
TiO_2	0.58			0.6	0.65	0.47
MnO	1.06	1.13	1.05	1.04	1.26	1.39
FeO	16.65	16.69	16.65	16.62	17.62	16.23
ZrO_2						
Total	100.38	101.21	99.95	100.05	101.78	100
Recalc.						
Fe3+	2.55	4.17	2.71	2.99	5.08	1.93
Fe2+	14.35	12.93	14.22	13.93	13.05	14.49
Total	100.63	101.62	100.23	100.35	102.29	100.19
Structural Formula						
Si	1.9591	1.9841	1.9574	1.9427	1.9225	1.9611
Al(IV)	0.0409	0.0159	0.0426	0.0573	0.0568	0.0389
Al(VI)	0.0211	0.0017	0.026	0.0126	0.0207	0.0083
FE3(IV)	0.0747	0.1197	0.0791	0.0873	0.1255	0.0566
FE2	0.4672	0.4122	0.4616	0.452	0.4179	0.4715
Mn	0.0349	0.0365	0.0345	0.0342	0.0409	0.0458
Mg	0.3951	0.4273	0.3896	0.3818	0.3561	0.3985
Ca	0.9424	0.8902	0.9385	0.9324	0.9253	0.9507
Na	0.0747	0.1197	0.079	0.0873	0.1462	0.0566
Ti	0	0	0	0.0175	0.0187	0.0137
End Members Based on Aegirine (Acmite)						
CaTiAl2O6	0	0	0	1.78	1.86	1.41
CaAlSiAlO6	2.13	0.17	2.64	1.28	0	0.85
Acmite	7.56	12.15	8.01	8.86	14.55	5.78
Wo	46.64	45.08	46.23	45.78	45.09	47.48
Fs	23.65	20.92	23.39	22.93	20.78	24.1
En	20.01	21.68	19.74	19.37	17.71	20.37
Recal into						
Ae	7.97	12.48	8.5	9.47	15.89	6.11
Hd	49.86	42.98	49.62	49.07	45.41	50.89
Di	42.17	44.55	41.88	41.45	38.7	43.01

Sample	**PL46**	**PL46**	**PL46**	**PL46**	**PL46**	**PL46**
Rock Type	Malignite	Malignite	Malignite	Malignite	Malignite	Malignite
Spot	17	18	19	20	A1	A2
Na_2O	1.22	1.21	1.11	1.04	2.69	2.64
MgO	6.68	6.41	6.46	6.52	4.54	5.12
Al_2O_3	1.56	1.64	1.75	1.06	0.76	0.58
SiO_2	48.75	48.47	49.29	50.79	49.91	50.56
CaO	22.11	22.27	22.27	22.81	18.71	19.01
TiO_2	0.77	0.73	0.79	0.54	0.33	0
MnO	1.01	0.97	1.08	1.24	1.14	1.14
FeO	16.89	17.08	17.3	17.33	19.92	19.48
ZrO_2						
Total	98.99	98.78	100.05	101.33	98	98.53
Recalc.						
Fe3+	3.14	3.12	2.86	2.68	6.93	6.8
Fe2+	14.06	14.27	14.73	14.92	13.68	13.36
Total	99.3	99.09	100.34	101.6	98.69	99.21
Structural Formula						
Si	1.9192	1.9158	1.9218	1.9537	1.9791	1.989
Al(IV)	0.0742	0.0764	0.0782	0.0463	0.0209	0.011
Al(VI)	0.0084	0.0078	0.0023	0.0018	0.0146	0.0159
FE3(IV)	0.0847	0.0849	0.0839	0.0776	0.2068	0.2014
FE2	0.463	0.4718	0.4802	0.4799	0.4534	0.4395
Mn	0.0337	0.0325	0.0357	0.0404	0.0383	0.038
Mg	0.3921	0.3777	0.3755	0.3739	0.2684	0.3003
Ca	0.9326	0.9431	0.9303	0.9401	0.7949	0.8013
Na	0.0931	0.0927	0.0839	0.0776	0.2068	0.2014
Ti	0.0228	0.0217	0.0232	0.0156	0.0098	0
End Members Based on Aegirine (Acmite)						
CaTiAl2O6	2.28	2.17	2.34	1.59	1.01	0
CaAlSiAlO6	0	0	0.23	0.18	0.12	1.12
Acmite	9.33	9.27	8.48	7.89	21.3	20.6
Wo	45.57	46.07	45.72	46.92	40.37	40.43
Fs	23.19	23.59	24.26	24.41	23.37	22.48
En	19.64	18.89	18.97	19.02	13.82	15.36
Recal into						
Ae	9.82	9.84	8.93	8.33	22.26	21.39
Hd	48.83	50.07	51.1	51.53	48.85	46.7
Di	41.35	40.09	39.97	40.15	28.89	31.91

Sample	**PL46**	**PL46**	**PL46**	**PL46**	**PL46**	**PL46**
Rock Type	Malignite	Malignite	Malignite	Malignite	Malignite	Malignite
Spot	A3	A4	A5	A6	A7	A8
Na_2O	1.9	2.85	2.81	1.99	1.12	1.34
MgO	6.3	4.4	4.25	5.92	6.14	6.52
Al_2O_3	0.58	0.57	0.64	0.51	1.06	0.39
SiO_2	50.32	49.86	49.27	50.07	50.77	51.98
CaO	20.34	18.54	18.3	20.24	22.54	21.72
TiO_2	0.39	0	0.28	0.41	0.59	0.25
MnO	6.06	1.2	1.27	1.07	1.38	1.4
FeO	17.4	20.62	20.12	17.94	17.41	16.82
ZrO_2					0.58	
Total	103.29	98.04	96.94	98.15	101.59	100.42
Recalc.						
Fe3+	4.9	7.34	7.24	5.13	2.89	3.45
Fe2+	12.99	14.01	13.61	13.33	14.81	8.71
Total	103.78	98.77	97.67	98.67	101.3	95.76
Structural Formula						
Si	1.9255	1.9821	1.979	1.9773	1.959	Calculation Error
Al(IV)	0.0262	0.0179	0.021	0.0227	0.041	
Al(VI)	0.0483	0.0088	0.0093	0.0011	0.0072	
FE3(IV)	0.0926	0.2197	0.2188	0.1524	0.0838	
FE2	0.4158	0.4658	0.457	0.4401	0.478	
Mn	0.1964	0.0404	0.0432	0.0358	0.0451	
Mg	0.3594	0.2608	0.2545	0.3486	0.3532	
Ca	0.8339	0.7896	0.7875	0.8564	0.9318	
Na	0.141	0.2197	0.2188	0.1524	0.0838	
Ti	0.112	0	0.0085	0.0122	0.0171	
End Members Based on Aegirine (Acmite)						
CaTiAl2O6	1.18	0	0.87	1.16	1.75	
CaAlSiAlO6	0	0.89	0.42	0	0.7	
Acmite	14.82	22.36	22.45	15.54	8.57	
Wo	43.25	39.75	39.76	43.09	46.45	
Fs	21.86	23.71	23.44	22.44	24.46	
En	18.89	13.28	13.06	17.77	18.07	
Recal into						
Ae	15.39	23.21	23.52	16.19	9.16	
Hd	45.39	49.23	49.12	46.77	52.24	
Di	39.23	27.56	27.36	37.04	38.6	

Sample	**PL46**	**PL46**	**PL46**	**PL46**	**PL46**	**PL46**
Rock Type	Malignite	Malignite	Malignite	Malignite	Malignite	Malignite
Spot	B1	B2	B3	B4	B5	B6
Na_2O	1.41	2.2	1.45	1.16	1.33	1.21
MgO	4.97	5.97	5.93	6.97	5.99	6.47
Al_2O_3	0.84	0.78	1.43	1.77	2.65	1.84
SiO_2	49.53	50.78	49.17	49.61	48.16	48.26
CaO	20.9	21.89	22.1	22.66	21.91	21.97
TiO_2	0	0	0.7	0.85	1.56	1.06
MnO	1.32	0.98	1.22	0.95	0.98	1.03
FeO	19.28	17.87	18.27	16.62	18.49	17.31
ZrO_2			0.48			
Total	98.25	100.47	100.75	100.59	101.07	99.15
Recalc.						
Fe3+	3.63	5.67	3.74	2.99	3.43	3.12
Fe2+	16.01	12.77	14.91	13.93	15.41	14.5
Total	98.61	101.04	100.65	100.89	101.42	99.46
Structural Formula						
Si	1.977	1.9615	1.9212	1.9174	1.8688	1.902
Al(IV)	0.023	0.0355	0.0659	0.0806	0.1212	0.0855
Al(VI)	0.0165	0.003	0.0129	0.002	0.01	0.0126
FE3(IV)	0.1091	0.1618	0.0969	0.0849	0.0901	0.0799
FE2	0.5345	0.4125	0.4871	0.4503	0.5	0.4781
Mn	0.0446	0.0321	0.0404	0.0311	0.0322	0.0344
Mg	0.2958	0.3438	0.3454	0.4016	0.3465	0.3802
Ca	0.8938	0.9059	0.9252	0.9383	0.9109	0.9277
Na	0.1091	0.1648	0.1098	0.0869	0.1001	0.0925
Ti	0	0	0.0206	0.0247	0.0455	0.0314
End Members Based on Aegirine (Acmite)						
CaTiAl2O6	0	0	2.06	2.48	4.55	3.14
CaAlSiAlO6	1.69	0	0	0	0	0
Acmite	11.14	16.54	11	8.74	9.99	9.24
Wo	44.79	45.48	45.27	45.94	43.2	44.76
Fs	27.29	20.71	24.38	22.64	24.96	23.88
En	15.1	17.26	17.29	20.19	17.3	18.99
Recal into						
Ae	11.62	17.89	11.66	9.26	10.57	9.73
Hd	56.9	44.78	51.69	47.96	52.82	50.29
Di	31.49	37.33	36.65	42.78	36.61	39.99

Sample	**PL46**	**PL46**	**PL46**	**PL46**	**PL46**	**PL46**
Rock Type	Malignite	Malignite	Malignite	Malignite	Malignite	Malignite
Spot	B1	B2	B3	B4	B5	B6
Na_2O	1.41	2.2	1.45	1.16	1.33	1.21
MgO	4.97	5.97	5.93	6.97	5.99	6.47
Al_2O_3	0.84	0.78	1.43	1.77	2.65	1.84
SiO_2	49.53	50.78	49.17	49.61	48.16	48.26
CaO	20.9	21.89	22.1	22.66	21.91	21.97
TiO_2	0	0	0.7	0.85	1.56	1.06
MnO	1.32	0.98	1.22	0.95	0.98	1.03
FeO	19.28	17.87	18.27	16.62	18.49	17.31
ZrO_2			0.48			
Total	98.25	100.47	100.75	100.59	101.07	99.15
Recalc.						
Fe3+	3.63	5.67	3.74	2.99	3.43	3.12
Fe2+	16.01	12.77	14.91	13.93	15.41	14.5
Total	98.61	101.04	100.65	100.89	101.42	99.46
Structural Formula						
Si	1.977	1.9615	1.9212	1.9174	1.8688	1.902
Al(IV)	0.023	0.0355	0.0659	0.0806	0.1212	0.0855
Al(VI)	0.0165	0.003	0.0129	0.002	0.01	0.0126
FE3(IV)	0.1091	0.1618	0.0969	0.0849	0.0901	0.0799
FE2	0.5345	0.4125	0.4871	0.4503	0.5	0.4781
Mn	0.0446	0.0321	0.0404	0.0311	0.0322	0.0344
Mg	0.2958	0.3438	0.3454	0.4016	0.3465	0.3802
Ca	0.8938	0.9059	0.9252	0.9383	0.9109	0.9277
Na	0.1091	0.1648	0.1098	0.0869	0.1001	0.0925
Ti	0	0	0.0206	0.0247	0.0455	0.0314
End Members Based on Aegirine (Acmite)						
CaTiAl2O6	0	0	2.06	2.48	4.55	3.14
CaAlSiAlO6	1.69	0	0	0	0	0
Acmite	11.14	16.54	11	8.74	9.99	9.24
Wo	44.79	45.48	45.27	45.94	43.2	44.76
Fs	27.29	20.71	24.38	22.64	24.96	23.88
En	15.1	17.26	17.29	20.19	17.3	18.99
Recal into						
Ae	11.62	17.89	11.66	9.26	10.57	9.73
Hd	56.9	44.78	51.69	47.96	52.82	50.29
Di	31.49	37.33	36.65	42.78	36.61	39.99

Sample	**PL46**	**PL46**	**PL46**	**PL46**	**PL46**	**PL46**
Rock Type	Malignite	Malignite	Malignite	Malignite	Malignite	Malignite
Spot	B7	B8	B9	B10	B11	B12
Na_2O	1.03	0.99	0.78	1.62	0.99	1.07
MgO	6.78	7.05	6.84	6.94	6.41	6.52
Al_2O_3	1.44	1.64	0.9	0.46	1.27	1.3
SiO_2	50.2	49.88	50.48	50.56	49.19	49.26
CaO	22.3	22.41	22.43	21.31	22.03	21.99
TiO_2	0.46	0.53	0.45	0	0.46	0.51
MnO	1.04	1.16	1.36	0.98	1.07	1.09
FeO	16.65	16.25	16.53	16.2	16.5	16.75
ZrO_2						
Total	99.9	99.91	99.77	98.07	97.92	98.49
Recalc.						
Fe3+	2.65	2.55	2.01	4.17	2.55	2.76
Fe2+	14.26	13.99	14.72	12.44	14.2	14.27
Total	100.16	100.2	99.97	98.48	98.17	98.77
Structural Formula						
Si	1.9503	1.9371	1.9675	1.9876	1.9533	1.9517
Al(IV)	0.0497	0.0629	0.0325	0.0124	0.0467	0.0483
Al(VI)	0.0163	0.0122	0.0089	0.0089	0.0128	0.0124
FE3(IV)	0.0776	0.0745	0.0589	0.1235	0.0762	0.0822
FE2	0.4634	0.4545	0.4799	0.4091	0.4717	0.4728
Mn	0.0342	0.0382	0.0449	0.0326	0.036	0.0366
Mg	0.3927	0.4082	0.3975	0.4068	0.3795	0.3851
Ca	0.9282	0.9324	0.9367	0.8976	0.9373	0.9165
Na	0.0776	0.0745	0.0589	0.1235	0.0762	0.0822
Ti	0.0134	0.0155	0.0132	0	0.0137	0.0152
End Members Based on Aegirine (Acmite)						
CaTiAl2O6	1.36	1.57	1.35	0	1.4	1.55
CaAlSiAlO6	1.65	1.24	0.63	0.91	1.3	1.26
Acmite	7.88	7.56	6.04	12.54	7.75	8.36
Wo	45.63	45.88	47.02	45.12	46.29	45.2
Fs	23.53	23.05	24.59	20.77	23.98	24.04
En	19.94	20.7	20.37	20.66	19.29	19.59
Recal into						
Ae	8.31	7.95	6.3	13.14	8.22	8.74
Hd	49.63	48.49	51.25	43.55	50.86	50.29
Di	42.06	43.55	42.45	43.3	40.92	40.97

Sample	**PL46**	**PL-46**	**PL-46**	**PL-46**	**PL-46**	**PL-46**
Rock Type	Malignite	Malignite	Malignite	Malignite	Malignite	Malignite
Spot	B13	1	2	Ae-3	3	4
Na_2O	1.34	3.26	2.82	10.2	3.19	2.88
MgO	6.83	5.02	5.42	2.56	5.09	5.16
Al_2O_3	0.53	0.51	0.52	0.1	0.33	0.5
SiO_2	50.73	50.07	49.65	51.18	50.33	49.64
CaO	21.57	18.74	19.14	6.94	19.15	18.49
TiO_2	0.22					
MnO	1.15	1.36	1.22	1.04	1.28	1.22
FeO	16.77	20.31	19.63	24.57	20.8	20.28
ZrO_2						
Total	99.14	99.27	98.4	96.59	100.17	98.17
Recalc.						
Fe3+	3.45	8.4	7.27	26.28	8.22	7.42
Fe2+	13.86	12.75	13.09	0.92	13.4	13.6
Total	99.68	100.11	99.13	99.22	100.99	98.91
Structural Formula						
Si	1.9793	1.9628	1.9635	1.989	1.9608	1.9624
Al(IV)	0.0207	0.0236	0.0242	0.0046	0.0152	0.0233
Al(VI)	0.0037	0.0136	0.0123	0.0065	0.024	0.0143
FE3(IV)	0.1014	0.2341	0.204	0.7621	0.2169	0.2064
FE2	0.4523	0.418	0.433	0.03	0.4367	0.4497
Mn	0.038	0.0452	0.0409	0.0342	0.0422	0.0409
Mg	0.3973	0.2934	0.3196	0.1252	0.2957	0.3041
Ca	0.9017	0.7871	0.811	0.289	0.7993	0.8043
Na	0.1014	0.2478	0.2162	0.7685	0.241	0.2207
Ti	0.0065	0	0	0	0	0
End Members Based on Aegirine (Acmite)						
CaTiAl2O6	0.66	0	0	0	0	0
CaAlSiAlO6	0.38	0	0	0	0	0
Acmite	10.32	24.85	21.67	77.59	23.93	22.08
Wo	45.39	39.47	40.63	14.59	39.7	40.22
Fs	23.03	20.96	21.69	1.51	21.96	22.49
En	20.23	14.71	16.01	6.32	14.68	15.21
Recal into						
Ae	10.66	25.83	22.32	83.21	24.76	22.65
Hd	47.56	43.58	44.69	3.24	44.87	46.14
Di	41.78	30.59	32.99	13.55	30.38	31.21

Sample	**PL-46**	**PL-46**	**PL-46**	**PL-46**	**PL-46**	**PL-46**
Rock Type	Malignite	Malignite	Malignite	Malignite	Malignite	Malignite
Spot	Ae-4	5	6	7	8	9
Na_2O	9.75	3.05	3.03	3.18	3.32	3.11
MgO	3.94	5.2	5.3	5.21	5.18	4.96
Al_2O_3	0.23	0.48	0.46	0.43	0.52	1.4
SiO_2	51.88	49.47	50.06	50.14	49.84	49.77
CaO	7.74	18.8	18.93	18.77	18.75	18.48
TiO_2						
MnO	0.56	1.37	1.25	1.38	1.24	1.26
FeO	23.53	19.86	19.98	20.16	20.15	20.31
ZrO_2						
Total	97.63	98.23	99.01	99.27	99	99.29
Recalc.						
Fe3+	25.12	7.86	7.81	8.19	8.55	8.01
Fe2+	0.93	12.79	12.96	12.79	13.25	13.1
Total	100.15	99.02	99.8	100.09	100.65	100.09
Structural Formula						
Si	1.9778	1.961	1.9659	1.965	1.9492	1.9708
Al(IV)	0.0103	0.0224	0.0213	0.0199	0.024	0.0187
Al(VI)	0.0118	0.0166	0.0129	0.0151	0.0268	0.0105
FE3(IV)	0.7089	0.2178	0.2178	0.2265	0.225	0.2283
FE2	0.0295	0.424	0.4255	0.419	0.4335	0.4338
Mn	0.0181	0.046	0.0429	0.0458	0.0411	0.0423
Mg	0.2239	0.3073	0.3103	0.3044	0.302	0.2928
Ca	31.61	0.7984	0.7965	0.788	0.7857	0.784
Na	0.7207	0.2344	0.2307	0.2416	0.2517	0.2388
Ti	0	0	0	0	0	0
End Members Based on Aegirine (Acmite)						
CaTiAl2O6	0	0	0	0	0	0
CaAlSiAlO6	0	0	0	0	0	0
Acmite	71.68	23.46	23.14	24.22	24.87	24.02
Wo	15.72	39.95	39.95	39.51	38.8	39.43
Fs	1.47	21.21	21.34	21.01	21.41	21.82
En	11.14	15.38	15.56	15.26	14.92	14.73
Recal into						
Ae	73.98	24.27	23.87	25.04	25.5	24.73
Hd	3.03	43.9	44.02	43.42	43.91	44.93
Di	22.99	31.82	32.11	31.54	30.59	30.33

Sample	**PL-46**	**PL-46**	**PL-46**	**PL-46**	**PL-46**	**PL-46**
Rock Type	Malignite	Malignite	Malignite	Malignite	Malignite	Malignite
Spot	10	HiZ1	LoZ1	HiZ2	LoZ2	HiZ3
Na_2O	3.31	2.9	1.87	3.08	10.17	3.06
MgO	4.95	4.98	2.76	5.12	2.5	4.78
Al_2O_3	0.45	0.56		0.49		0.51
SiO_2	49.64	48.94	51.25	49.05	50.74	48.66
CaO	18.45	18.51	7.61	18.46	6.57	18.32
TiO_2		0.17				0.26
MnO	1.22	1.24	1.17	1.3	0.98	1.27
FeO	20.78	20.18	24.21	19.75	25.17	20.11
ZrO_2						
Total	98.8	97.48	88.87	97.25	96.13	96.97
Recalc.						
Fe3+	8.53	7.47	25.43	7.94	26.2	7.88
Fe2+	13.11	13.46	1.33	12.61	1.59	13.02
Total	99.66	98.23	91.42	98.05	98.75	97.76
Structural Formula						
Si	1.9589	1.9586	1.9821	1.9625	1.979	1.957
Al(IV)	0.0209	0.0264	0	0.0231	0	0.0242
Al(VI)	0.0202	0.015	0.0179	0.0144	0.021	0.0188
FE3(IV)	0.233	0.21	0.7222	0.2245	0.748	0.2198
FE2	0.4325	0.4504	0.429	0.4219	0.0519	0.4378
Mn	0.0408	0.042	0.0383	0.0441	0.0324	0.0433
Mg	0.2912	0.2971	0.1591	0.3054	0.1454	0.2866
Ca	0.7801	0.7937	0.3153	0.7913	0.2745	0.7894
Na	0.2532	0.225	0.7401	0.2389	0.769	0.2386
Ti	0	0.0051	0	0	0	0.0079
End Members Based on Aegirine (Acmite)						
CaTiAl2O6	0	0.51	0	0	0	0.79
CaAlSiAlO6	0	0	0	0	0	0
Acmite	25.2	22.54	74.1	23.93	76.53	23.87
Wo	38.8	39.5	15.79	39.64	13.66	39.1
Fs	21.51	22.56	2.15	21.13	2.58	21.9
En	14.49	14.88	7.97	15.3	7.23	14.34
Recal into						
Ae	25.92	23.14	78.55	24.73	79.58	24.78
Hd	44.27	46.31	4.56	43.66	5.37	45.46
Di	29.81	30.55	16.89	31.61	15.04	29.76

Sample	**PL-46**	**PL-48**	**PL-48**	**PL-48**	**PL-48**	**PL-48**
Rock Type	Malignite	Biotite Pyroxenite	Biotite Pyroxenite	Biotite Pyroxenite	Biotite Pyroxenite	Biotite Pyroxenite
Spot	11	1-C	1-R	1-RB	2-C	2-R
Na_2O	2.99	0.35			0.47	
MgO	4.8	17	16.43	16.85	16.28	17.04
Al_2O_3	0.49					
SiO_2	49.15	55.54	53.74	51.03	54.41	55.13
CaO	18.66	25.09	24.57	25.11	24.37	25.3
TiO_2		0.29	0.19		0.34	
MnO	1.24		0.34	0.32	0.29	0.3
FeO	20.52	2.97	2.93	3.08	3.52	2.52
ZrO_2						
Total	97.85	101.24	98.2	96.39	99.68	100.29
Recalc.						
Fe3+	7.7	0.9	0	0	1.21	0
Fe2+	13.59	2.16	2.93	3.08	2.43	2.52
Total	98.62	101.33	98.2	96.39	99.8	100.29
Structural Formula						
Si	1.9618	1.9973	1.9988	1.9511	1.993	2.0979
Al(IV)	0.0231	0	0	0	0	0
Al(VI)	0.0151	0	0	0	0	0
FE3(IV)	0.2163	0.0027	0.0012	0	0.0264	0
FE2	0.4536	0.0217	0.0911	0.0985	0.0744	0.0802
Mn	0.0419	0.0649	0.0107	0.0104	0.009	0.0097
Mg	0.2857	0.9106	0.9111	0.9605	0.8891	0.6831
Ca	0.798	0.9658	0.9791	1.0286	0.9564	1.0315
Na	0.2314	0.0244	0	0	0.0334	0
Ti	0	0.0078	0.0053	0	0.0094	0
End Members Based on Aegirine (Acmite)						
CaTiAl2O6	0	0	0	0	0	(-5.61)
CaAlSiAlO6	0	0	0	0	0	0
Acmite	23.14	2.45	0	0	3.36	0
Wo	39.9	48.53	49.42	49.27	48.14	61.89
Fs	22.68	3.26	4.6	4.72	3.75	4.59
En	14.28	45.76	45.98	46.01	44.75	39.13
Recal into						
Ae	23.84	2.46	0	0	3.37	0
Hd	46.73	6.48	9.9	9.3	7.74	10.51
Di	29.43	91.05	90.91	90.7	89.16	89.49

Sample	**PL-48**	**PL-48**	**PL-48**	**PL-48**	**PL-48**	**PL-48**
Rock Type	Biotite Pyroxenite	Biotite Pyroxenite	Biotite Pyroxenite	Biotite Pyroxenite	Biotite Pyroxenite	Biotite Pyroxenite
Spot	3-C	3-R	4-C	4-R	5-C	C1C
Na_2O		0.74		1.37	0.5	
MgO	16.79	16.75	16.59	12.55	16.68	17.04
Al_2O_3						
SiO_2	55.03	55.55	55.19	51.49	54.89	55.39
CaO	24.9	24.32	24.47	21.94	24.43	25.35
TiO_2				0.63	0.28	
MnO	0.34	0.3	0.33	8.99	0.37	0.31
FeO	3.1	3.57	3.28	96.97	3.54	2.87
ZrO_2						
Total	100.16	101.23	99.86	193.94	100.69	100.96
Recalc.						
Fe3+	0	1.91	0	3.53	1.29	0
Fe2+	3.1	1.85	3.28	5.81	2.38	2.87
Total	100.16	101.42	99.86	106.31	100.82	100.96
Structural Formula						
Si	2.0054	2.0011	2.0114	1.9817	1.9911	2.0021
Al(IV)	0	0	0	0	0	0
Al(VI)	0	0	0	0	0	0
FE3(IV)	0	0.0517	0	0.0839	0.0263	0
FE2	0.0945	0.0559	0.1	0.1871	0.0722	0.0868
Mn	0.0105	0.0092	0.0102	0.0205	0.0114	0.0095
Mg	0.9123	0.8835	0.9014	0.7201	0.8994	0.9183
Ca	0.9722	0.9463	0.966	0.9047	0.9495	0.9817
Na	0	0	0	0.1022	0.0352	0
Ti	0	0	0	0	0.0076	0
End Members Based on Aegirine (Acmite)						
CaTiAl2O6	(-.28)	0	(-.58)	0	0	0
CaAlSiAlO6	0	0	0	0	0	0
Acmite	0	5.2	0	10.14	3.53	0
Wo	49.33	47.62	49.53	44.87	47.68	49.49
Fs	4.78	2.81	5.1	9.28	3.63	4.37
En	46.16	44.43	45.95	35.71	45.16	46.24
Recal into						
Ae	0	5.22	0	10.15	3.57	0
Hd	9.38	5.64	9.98	18.53	7.17	8.63
Di	90.62	89.15	90.02	71.32	89.26	91.37

Sample	**PL-48**	**PL-48**	**PL-48**	**PL-48**	**PL-48**	**PL-48**
Rock Type	Biotite Pyroxenite	Biotite Pyroxenite	Biotite Pyroxenite	Biotite Pyroxenite	Biotite Pyroxenite	Biotite Pyroxenite
Spot	C1I	C1R	loZ	1M	2M	3M
Na_2O	0.52	0.19	0.31	2.57	1.81	2.19
MgO	15.84	16.77	15.67	9.24	9.41	9.4
Al_2O_3				0.51	0.28	0.33
SiO_2	54.16	54.33	54.81	52.86	51.06	50.73
CaO	24.81	25.33	25.61	20.71	21.25	20.32
TiO_2	0.46	0.16				
MnO	0.31	0.35	0.54	0.95	0.95	1.01
FeO	3.9	2.21	4.91	14.37	12.7	13.28
ZrO_2						
Total	100	99.34	101.85	101.21	97.46	97.26
Recalc.						
Fe3+	1.34	0.49	0.8	6.62	4.66	5.64
Fe2+	2.69	1.77	3.79	8.41	8.5	8.2
Total	100.13	99.39	101.53	101.87	97.92	97.82
Structural Formula						
Si	1.9847	1.9945	1.9902	1.9775	1.9836	1.9761
Al(IV)	0	0	0	0.0225	0.0128	0.0151
Al(VI)	0.0153 (?)	.0055 (?)	[.0098]	0	0.0036	0.0087
FE3(IV)	0.0216	0.008	0.012	0.1864	0.1327	0.1567
FE2	0.0826	0.0543	0.1151	0.2632	0.2763	0.2672
Mn	0.0096	0.0109	0.0166	0.0301	0.0313	0.0333
Mg	0.8654	0.9179	0.8483	0.5154	0.545	0.5459
Ca	0.9741	0.9924	0.9963	0.8301	0.8886	0.8481
Na	0.0369	0.0135	0.0218	0.1864	0.1363	0.1654
Ti	0.0127	0.0044	0	0	0	0
End Members Based on Aegirine (Acmite)						
CaTiAl2O6	0	0	0	0	0	0
CaAlSiAlO6	0	0	0	0	0	0
Acmite	3.7	1.36	2.18	18.82	13.75	16.61
Wo	48.8	49.83	49.73	41.89	44.82	42.57
Fs	4.14	2.73	5.75	13.28	13.93	13.41
En	43.36	46.09	42.34	26.01	27.49	27.41
Recal into						
Ae	3.75	1.37	2.22	19.32	14.24	16.9
Hd	8.38	5.51	11.68	27.27	28.85	27.31
Di	87.87	93.12	86.1	53.41	56.91	55.79

Sample	**PL-48**	**PL-48**	**PL-48**	**PL-48**	**PL-48**	**PL-48**
Rock Type	Biotite Pyroxenite	Biotite Pyroxenite	Biotite Pyroxenite	Biotite Pyroxenite	Biotite Pyroxenite	Biotite Pyroxenite
Spot	C2C	C2I	C2R	HiZ	LoZ1	Loz2
Na_2O		0.42	0.35	0.19		0.33
MgO	16.45	16.08	16.97	15.75	16.03	15.9
Al_2O_3						
SiO_2	54.77	53.7	54.02	53.68	53.24	55.53
CaO	25.11	24.74	24.88	25.13	25.28	25.19
TiO_2		0.56				
MnO	0.29	0.28	0.35	0.58	0.4	0.44
FeO	3.17	3.07	2.77	3.89	2.66	3.83
ZrO_2						
Total	99.79	98.85	99.34	99.22	97.61	101.22
Recalc.						
Fe3+	0	1.08	0.9	0.49	0	0.85
Fe2+	3.17	2.1	1.96	3.45	2.66	3.06
Total	99.79	98.96	99.43	99.27	97.61	101.3
Structural Formula						
Si	2.0055	1.9848	1.9851	1.977	1.9963	2.0076
Al(IV)	0	0	0	0.023	0	0
Al(VI)	0	0	[.0149]	0.0026	0	0
FE3(IV)	0	0.0152	0.01	0.0136	0	0.0231
FE2	0.0971	149	0.0602	0.1062	0.0834	0.0927
Mn	0.009	0.0088	0.0109	0.0181	0.0127	0.0135
Mg	0.8981	0.8861	0.9297	0.8648	0.8961	0.857
Ca	0.9851	0.9797	0.9795	0.9916	1.0156	0.9757
Na	0	0.0301	0.0249	0.0136	0	0.0231
Ti	0	0.0156	0	0	0	0
End Members Based on Aegirine (Acmite)						
CaTiAl2O6	[-.28]	0	0	0	0	[-.39]
CaAlSiAlO6	0	0	0	0.26	0	0
Acmite	0	3.02	2.47	1.36	0	2.35
Wo	49.96	49.21	48.51	49.64	50.9	49.77
Fs	4.91	3.25	2.98	5.33	4.18	4.71
En	45.41	44.51	46.04	43.41	44.92	43.55
Recal into						
Ae	0	3.07	2.48	1.38	0	2.38
Hd	9.75	6.6	5.93	10.79	8.52	9.53
Di	90.25	90.33	91.59	87.83	91.48	88.1

Sample	**PL-48M**	**PL-48M**	**PL-48M**	**PL-48M**	**PL-48M**	**PL-48M**
Rock Type	Biotite Pyroxenite	Biotite Pyroxenite	Biotite Pyroxenite	Biotite Pyroxenite	Biotite Pyroxenite	Biotite Pyroxenite
Spot	1	2	3	4	5	6
Na_2O	2.37	2.89	2.24	2.44	0.96	1.41
MgO	9.57	9.24	9.72	9.63	11.96	9.9
Al_2O_3	0.38	0.27		0.26	0.37	0.55
SiO_2	53.5	51.81	52.05	53.45	53.82	52.75
CaO	20.62	20.26	20.56	20.69	23.6	21.98
TiO_2						
MnO	0.89	0.64	0.74	0.91	0.93	0.87
FeO	13.64	13.89	13.43	13.86	10.1	13
ZrO_2						
Total	100.97	99	98.74	101.24	101.74	100.46
Recalc.						
Fe3+	6.11	6.42	5.77	6.29	2.47	3.63
Fe2+	8.15	8.12	8.25	7.7	7.87	9.73
Total	101.59	99.65	99.33	101.37	101.98	100.82
Structural Formula						
Si	1.9965	2.007	1.9911	1.9975	1.9872	1.9891
Al(IV)	0.0035	(-.007)	0	0.0025	0.0128	0.0109
Al(VI)	0.0132	0.0189	0	0.0089	0.0033	0.0135
FE3(IV)	0.1715	0.1811	0.1574	0.1768	0.0687	0.1031
FE2	0.2542	0.2547	0.2637	0.2407	0.2431	0.3069
Mn	0.0281	0.0203	0.024	0.0288	0.0291	0.0278
Mg	0.5325	0.5168	0.5547	0.5366	0.6584	0.5566
Ca	0.8244	0.8143	0.8432	0.8284	0.9336	0.888
Na	0.1715	0.1811	0.1662	0.1768	0.0687	0.1031
Ti	0	0	0	0	0	0
End Members Based on Aegirine (Acmite)						
CaTiAl2O6	0	(-.36)	0	0	0	0
CaAlSiAlO6	0.36	0	0	0.26	0.34	1.11
Acmite	17.52	18.63	16.67	18.02	6.96	10.47
Wo	41.94	42.06	42.29	42.1	47.08	44.56
Fs	12.99	13.1	13.22	12.27	12.31	15.59
En	27.2	26.58	27.82	27.35	33.32	28.27
Recal into						
Ae	17.9	19.01	16.88	18.53	7.08	10.67
Hd	26.53	26.73	26.78	25.23	25.06	31.75
Di	55.57	54.25	56.34	56.24	67.86	57.59

Sample	**PL-48M**	**PL-48M**	**PL-48M**	**PL-48M**	**PL49**	**PL49**
Rock Type	Biotite Pyroxenite	Biotite Pyroxenite	Biotite Pyroxenite	Biotite Pyroxenite	Biotite Pyroxenite	Biotite Pyroxenite
Spot	7	8	9	10	Site 1-1	S1-2
Na_2O	2.05	2.28	1.21	2.28		1.99
MgO	9.76	9.61	11.47	9.65	17.46	8.72
Al_2O_3	0.43	0.44				0.39
SiO_2	53.47	53.57	52.42	5.79	55.05	51.41
CaO	21.44	20.81	22.24	20.55	25.69	20.69
TiO_2						0.25
MnO	0.99	0.96	1.2	0.96	0.26	0.59
FeO	13.3	13.99	9.41	13.49	0.97	13.74
ZrO_2						
Total	101.44	101.66	97.95	52.72	99.43	97.78
Recalc.						
Fe3+	5.28	5.87	3.12	5.87	0	5.13
Fe2+	8.55	8.7	6.6	8.2	0.97	9.13
Total	101.97	102.24	98.26	53.3	99.43	98.3
Structural Formula						
Si	1.9908	1.9881	2.0027	1.9984	2	1.9914
Al(IV)	0.0092	0.0119	0	0	0	0.0086
Al(VI)	0.0097	0.0074	0	0	0	0.0092
FE3(IV)	0.148	0.1647	0.0896	0.1658	0	0.1495
FE2	0.2661	0.2712	0.211	0.2597	0.0296	0.2956
Mn	0.0312	0.0303	0.0388	0.0308	0.008	0.0194
Mg	0.5418	0.5337	0.6533	0.5447	0.9485	0.5036
Ca	0.8553	0.8306	0.9124	0.8335	1.0028	0.8587
Na	0.148	0.1647	0.0896	0.1673	0	0.1459
Ti	0	0	0	0	0	0.0073
End Members Based on Aegirine (Acmite)						
CaTiAl2O6	0	0	(-.14)	0	[-.29]	0.44
CaAlSiAlO6	0.94	0.75	0	0	0	0
Acmite	15.04	16.7	9.17	16.97	0	15.24
Wo	42.98	41.64	46.75	42.25	50.85	43.57
Fs	13.52	13.75	10.8	13.17	1.49	15.07
En	27.52	27.06	33.42	27.61	47.95	25.68
Recal into						
Ae	15.48	16.98	9.4	17.22	0	15.75
Hd	27.84	27.97	22.12	26.73	3.02	31.16
Di	56.68	55.05	68.48	56.05	96.98	53.08

Sample	**PL49**	**PL49**	**PL49**	**PL49**	**PL49**	**PL49**
Rock Type	Biotite Pyroxenite	Biotite Pyroxenite	Biotite Pyroxenite	Biotite Pyroxenite	Biotite Pyroxenite	Biotite Pyroxenite
Spot	S1-3	S1-4	S1-5	S1-6	S1-7	S2-1
Na_2O	0.45	1.48	1.07	0.46		1.24
MgO	11.29	9.93	10.31	11.8	17.2	10.97
Al_2O_3	0.51	0.46	0.35	0.6		0.28
SiO_2	51.83	51.9	52.04	52.33	54.84	52.24
CaO	23.73	21.95	22.76	23.97	25.62	22
TiO_2		0.21	0.27			0.18
MnO	1.08	0.55	1.01	0.81	0.37	0.79
FeO	9.5	11.98	11.16	8.58	1.27	10.42
ZrO_2						
Total	98.39	98.46	98.97	98.55	99.3	98.12
Recalc.						
Fe3+	1.16	3.81	2.76	1.19	0	3.19
Fe2+	8.46	8.55	8.68	7.51	1.27	7.55
Total	98.51	98.84	99.25	98.67	99.3	98.44
Structural Formula						
Si	1.9865	1.9885	1.9873	1.9905	2	1.997
Al(IV)	0.0135	0.0115	0.0127	0.0095	0	0.003
Al(VI)	0.0096	0.0093	0.003	0.0174	0	0.0097
FE3(IV)	0.0334	0.1099	0.0792	0.0339	0	0.0919
FE2	0.2711	0.2739	0.2772	0.239	0.0388	0.2412
Mn	0.0351	0.0178	0.0327	0.0261	0.0115	0.0256
Mg	0.6452	0.5672	0.587	0.6692	0.9374	0.6252
Ca	0.9745	0.9011	0.9312	0.9768	1.0034	0.9011
Na	0.0334	0.1099	0.0792	0.0339	0	0.0919
Ti	0	0.0061	0.0078	0	0	0.0052
End Members Based on Aegirine (Acmite)						
CaTiAl2O6	0	0.58	0.65	0	[-.23]	0.15
CaAlSiAlO6	0.97	0	0	0.97	0	0
Acmite	3.4	11.17	8.08	3.46	0	9.41
Wo	49.05	45.5	47.18	49.29	50.86	46.07
Fs	13.78	13.92	14.14	12.18	1.96	12.35
En	32.8	28.83	29.95	34.1	47.41	32.02
Recal into						
Ae	3.52	11.56	8.4	3.6	0	9.59
Hd	28.54	28.8	29.38	25.37	3.98	25.17
Di	67.94	59.64	62.22	71.03	96.02	65.24

Sample	**PL49**	**PL49**	**PL49**	**PL49**	**PL49**	**PL49**
Rock Type	Biotite Pyroxenite	Biotite Pyroxenite	Biotite Pyroxenite	Biotite Pyroxenite	Biotite Pyroxenite	Biotite Pyroxenite
Spot	S2-2	S2-3	S2-4	S3-1	S3-2	S3-4
Na_2O	0.71	0.76			0.52	
MgO	9.64	9.7	15.27	15.51	11.08	14.8
Al_2O_3	0.43	0.34	0.27	0.51	0.66	1.05
SiO_2	46.09	45.7	54.16	54.23	51.24	52.34
CaO	25.57	25.47	24.97	24.93	23.25	24.51
TiO_2	4.99	4.95				0.38
MnO	0.75	0.72	0.76	0.64	1.06	0.59
FeO	8.05	8.17	4.25	3.83	9.83	4.78
ZrO_2	0.69	0.66				
Total	96.92	96.47	99.68	99.65	97.64	98.45
Recalc.						
Fe3+	1.83	1.96	0	0	1.34	0
Fe2+	6.4	6.41	4.25	3.83	8.62	4.78
Total	96.41	96.01	99.68	99.65	97.77	98.45
Structural Formula						
Si	1.832	1.8267	1.9997	1.997	1.981	1.9637
Al(IV)	0.0201	0.016	0.0003	0.0003	0.019	0.0363
Al(VI)	0.1479	0.1573	0.0114	0.0192	0.011	0.0101
FE3(IV)	[-.0932]	[-.0984]	0	0	0.039	0
FE2	0.2129	0.2142	0.1312	0.1179	0.2788	0.15
Mn	0.0252	0.0244	0.0238	0.02	0.0347	0.0187
Mg	0.5713	0.5781	0.8406	0.8515	0.6387	0.8279
Ca	1.0889	1.0908	0.9878	0.9836	0.963	0.9852
Na	0.0547	0.0589	0	0	0.039	0
Ti	0.1491	0.1488	0	0	0	0.0107
End Members Based on Aegirine (Acmite)						
CaTiAl2O6	1.01	0.8	0	0	0	1.08
CaAlSiAlO6	0	0	0.03	0.3	1.12	1.02
Acmite	5.49	5.86	0	0	3.96	0
Wo	54.14	53.9	50.38	50.13	48.34	48.61
Fs	10.68	10.66	6.7	6.03	14.16	7.56
En	28.67	28.78	42.89	43.53	32.43	41.73
Recal into						
Ae	6.52	6.92	0	0	4.08	0
Hd	25.38	25.17	13.5	12.17	29.15	15.34
Di	68.1	67.19	86.5	87.83	66.77	84.66

Sample	**PL49**	**PL49**	**PL-51**	**PL-51**	**PL-51**	**PL-51**
Rock Type	Biotite Pyroxenite	Biotite Pyroxenite	Biotite Pyroxenite	Biotite Pyroxenite	Biotite Pyroxenite	Biotite Pyroxenite
Spot	S3-5	S3-7	1C	2C	3	4
Na_2O	0.62	0.23	0.32	0.36	2.51	0.36
MgO	11.25	14.81	16.21	16.55	8.79	16.73
Al_2O_3	0.69	0.75			0.39	
SiO_2	52.61	53.44	55.31	55.18	52.71	55.3
CaO	23.62	24.79	25.43	25.43	20.66	24.32
TiO_2						
MnO	0.99	0.81	0.52	0.56	0.9	0.38
FeO	10.3	4.81	3.42	3.48	14.54	3.75
ZrO_2						
Total	100.08	99.64	101.21	101.56	100.5	100.84
Recalc.						
Fe3+	1.6	0.59	1.68	2.01	6.47	2.92
Fe2+	8.86	4.28	0.52	0.56	8.72	0.38
Total	100.24	99.7	99.99	100.65	101.15	100.39
Structural Formula						
Si	1.9832	1.9793	2.0102	1.9919	1.9874	2.0044
Al(IV)	0.0168	0.0207	0	0	0.0126	0
Al(VI)	0.0139	0.0121	0	0	0.0047	0
FE3(IV)	0.0453	0.0165	0.0225	0.0241	0.1835	0.0253
FE2	0.2794	0.1325	0.051	0.0608	0.275	0.0884
Mn	0.0316	0.0254	0.016	0.0171	0.0287	0.0117
Mg	0.6323	0.8178	0.878	0.8907	0.4941	0.8771
Ca	0.954	0.9838	0.9899	0.9865	0.8346	0.9639
Na	0.0453	0.0165	0.0225	0.0322	0.1835	0.0253
Ti	0	0	0	0	0	0
End Members Based on Aegirine (Acmite)						
CaTiAl2O6	0	0	(-.52)	0	0	(-0.22)
CaAlSiAlO6	1.41	1.22	0	0	0.48	0
Acmite	4.6	1.67	2.3	3.22	18.58	2.56
Wo	47.74	49.09	50.79	49.19	42.01	48.85
Fs	14.18	6.69	2.6	3.04	13.92	4.47
En	32.09	41.32	44.82	44.55	25.01	44.35
Recal into						
Ae	4.74	1.71	2.37	3.27	19.26	2.55
Hd	29.19	13.7	5.36	6.18	28.87	8.92
Di	66.07	84.59	92.27	90.55	51.87	88.53

Sample	**PL-51**	**PL-51**	**PL-51**	**PL-51**	**PL-51**	**PL-51**
Rock Type	Biotite Pyroxenite	Biotite Pyroxenite	Biotite Pyroxenite	Biotite Pyroxenite	Biotite Pyroxenite	Biotite Pyroxenite
Spot	5	6	7	8	9	10
Na_2O	1.13	0.36	1.51	2.42	2.33	0.31
MgO	14.05	14.68	9.85	8.7	8.78	15.48
Al_2O_3			0.36	0.44	0.28	
SiO_2	53.94	54.49	53.05	52.38	52.62	54.38
CaO	23.45	25.09	21.67	20.79	20.74	24.49
TiO_2						
MnO	0.78	0.69	0.63	0.99	0.95	0.61
FeO	7.44	5.41	13.39	14.69	15	4.38
ZrO_2						
Total	100.79	100.72	100.46	100.41	100.7	99.65
Recalc.						
Fe3+	2.91	0.93	3.99	6.24	6	1
Fe2+	4.81	4.58	9.89	9.08	10.26	3.48
Total	101.07	100.82	100.95	101.04	101.96	99.75
Structural Formula						
Si	1.9853	1.9991	1.985	1.9817	1.98	1.9995
Al(IV)	0	0	0.015	0.0183	0.0124	0
Al(VI)	(0.0147]	0	0.0273	0.0013	0.0076	0
FE3(IV)	0.066	0.0247	0.1095	0.1775	0.1624	0.0272
FE2	0.1484	0.1404	0.3094	0.2873	0.3228	0.1065
Mn	0.0243	0.0214	0.02	0.0317	0.0303	0.0189
Mg	0.771	0.803	0.5495	0.4907	0.4926	0.8455
Ca	0.9247	0.9862	0.8687	0.8427	0.8361	0.975
Na	0.0806	0.0256	0.1095	0.1775	0.17	0.0277
Ti	0	0	0	0	0	0
End Members Based on Aegirine (Acmite)						
CaTiAl2O6	0	0	0	0	0	0
CaAlSiAlO6	0	0	1.53	0.13	0	0
Acmite	8.04	2.59	11.17	17.96	17.07	2.79
Wo	46.11	49.79	43.52	42.56	41.99	49.18
Fs	7.4	7.09	15.77	14.53	16.21	5.37
En	38.45	40.54	28.01	24.82	24.73	42.65
Recal into						
Ae	8.06	2.64	11.37	18.58	17.25	2.83
Hd	14.84	14.49	31.93	30.06	32.76	10.87
Di	77.1	82.87	56.7	51.36	49.99	86.3

Sample	**PL-51**	**PL-51**	**PL-51**	**PL-51**	**PL-51**	**PL-51**
Rock Type	Biotite Pyroxenite	Biotite Pyroxenite	Biotite Pyroxenite	Biotite Pyroxenite	Biotite Pyroxenite	Biotite Pyroxenite
Spot	11	12	13	14	15	16
Na_2O	2.41	2.43		0.4	0.34	0.62
MgO	8.31	8.73	15.64	16.22	13.53	12
Al_2O_3		0.29			0.33	0.56
SiO_2	51.75	52.45	54.9	55.35	53.31	52.61
CaO	20.48	20.61	25.29	25.55	24.75	24.45
TiO_2						
MnO	0.75	0.88	0.32		0.76	0.88
FeO	15.33	15.31	3.6	3.41	7.97	8.88
ZrO_2						
Total	99.03	100.7	99.75	100.93	100.99	100
Recalc.						
Fe3+	6.21	6026	0	1.06	0.88	1.6
Fe2+	9.74	9.68	3.6	2.46	7.18	7.44
Total	99.65	6121.07	99.75	101.04	101.08	100.16
Structural Formula						
Si	1.991	1.9907	2.0128	2.0019	1.9762	1.977
Al(IV)	0	0.0093	0	0	0.0144	0.023
Al(VI)	0	0.0037	0	0	0.0093	0.0018
FE3(IV)	0.1707	0.1788	0	0.0288	0.0151	0.0452
FE2	0.3135	0.3071	0.1104	0.0744	0.2226	0.2339
Mn	0.0244	0.0026	0	0	0.0239	0.028
Mg	0.4767	0.494	0.8549	0.8746	0.7478	0.6723
Ca	0.8442	0.8381	0.9934	0.9901	0.983	0.9844
Na	0.1798	0.1788	0	0.0288	0.0244	0.0452
Ti	0	0	0.008	0	0	0
End Members Based on Aegirine (Acmite)						
CaTiAl2O6	0	0	(-.66)	(-.09)	0	0
CaAlSiAlO6	0	0.37	0	0	0	0.19
Acmite	18.03	17.88	0	2.88	2.44	4.56
Wo	42.34	41.71	51.21	49.66	49.09	49.55
Fs	15.72	15.35	5.65	3.73	11.12	11.8
En	23.91	24.69	43.79	43.83	37.35	33.91
Recal into						
Ae	18.54	18.25	0	2.94	2.46	4.75
Hd	32.32	31.34	11.43	7.61	22.38	24.58
Di	49.15	50.41	88.57	89.45	75.16	70.68

Sample	**PL-51**	**PL-55**	**PL-55**	**PL-55**	**PL-55**	**PL-55**
Rock Type	Biotite Pyroxenite	Biotite Pyroxenite	Biotite Pyroxenite	Biotite Pyroxenite	Biotite Pyroxenite	Biotite Pyroxenite
Spot	17	1	2	3	4	5
Na_2O	2.3	0.59	1.04	0.86	1.25	1.43
MgO	8.71	14.4	12.65	11.99	11.04	10.61
Al_2O_3	0.29		0.51	0.46	0.32	0.35
SiO_2	53.29	54.38	53.63	53.46	52.44	52.88
CaO	21.58	24.45	23.37	23.96	22.93	22.54
TiO_2				0.33	0.42	0.24
MnO	1.14	0.97	1.11	0.87	0.74	0.83
FeO	14.56	5.49	7.18	8.57	10.49	11.52
ZrO_2						
Total	101.87	100.28	99.49	100.5	99.63	100.4
Recalc.						
Fe3+	5.93	1.52	2.68	2.22	3.22	3.68
Fe2+	9.23	4.12	4.77	6.58	7.59	8.2
Total	102.47	100.43	99.76	100.73	99.95	100.76
Structural Formula						
Si	1.9885	2.002	1.9985	1.9942	1.9799	1.9869
Al(IV)	0.0115	0	0.0015	0.0058	0.0142	0.0131
Al(VI)	0.0013	0	0.0209	0.0145	0.0059	0.0024
FE3(IV)	0.1664	0.0421	0.0751	0.0622	0.0856	0.1042
FE2	0.288	0.1269	0.1486	0.2051	0.2397	0.2578
Mn	0.036	0.0302	0.035	0.0275	0.0237	0.0105
Mg	0.4846	0.7904	0.7028	0.6668	0.6214	0.5944
Ca	0.8628	0.9644	0.933	0.9576	0.9275	0.9074
Na	0.1664	0.0421	0.0751	0.0622	0.0915	0.1042
Ti	0	0	0	0	0.0119	0.0124
End Members Based on Aegirine (Acmite)						
CaTiAl2O6	0	0	0	0	0.72	0.66
CaAlSiAlO6	0.13	0	0.16	0.59	0	0
Acmite	16.9	4.29	7.76	6.35	9.25	10.55
Wo	43.75	49.13	48.11	48.57	46.51	45.62
Fs	14.62	6.46	7.68	10.47	12.11	13.06
En	24.61	40.23	36.3	34.03	31.4	30.1
Recal into						
Ae	17.72	4.39	8.11	6.66	9.6	10.89
Hd	30.67	13.23	16.04	21.96	25.16	26.96
Di	51.61	82.38	75.85	71.38	65.23	62.15

Sample	**PL-55**	**PL-55**	**PL-55**	**PL-55**	**PL-55**	**PL-67**
Rock Type	Biotite Pyroxenite	Biotite Pyroxenite	Biotite Pyroxenite	Biotite Pyroxenite	Biotite Pyroxenite	Hollaite
Spot	6	7	8	9	10	1
Na_2O	1.38	1.26	1.72		0.33	4.04
MgO	8.61	9.32	8.84	15.48	14.38	6.02
Al_2O_3	0.56	0.37	0.65			0.72
SiO_2	51.55	52.48	51.88	54.46	54.13	51.52
CaO	22.49	22.7	21.97	25.51	24.84	17.67
TiO_2	0.47	0.53	0.26			
MnO	1.04	0.83	0.89	0.92	0.81	0.84
FeO	14.2	13.33	14.2	4.07	5.7	18.36
ZrO_2						0.66
Total	100.3	100.82	100.41	100.44	100.19	99.83
Recalc.						
Fe3+	3.56	3.25	4.43	4.07	0.85	10.42
Fe2+	11	10.61	10.21	0.92	4.93	9
Total	100.66	101.35	100.85	101.36	100.27	100.23
Structural Formula						
Si	1.9677	1.9794	1.9709	1.9985	2.002	1.9804
Al(IV)	0.0252	0.0164	0.0282	0	0	0.0196
Al(VI)	0.0071	0.0042	0.0009	0	0	0.013
FE3(IV)	0.0951	0.0879	0.1258	0	0.0237	0.3011
FE2	0.3512	0.3346	0.3244	0.1249	0.1526	0.2894
Mn	0.0336	0.0265	0.0286	0.0286	0.0191	0.0273
Mg	0.49	0.5241	0.5007	0.8469	0.7929	0.345
Ca	0.9198	0.9173	0.8942	1.003	0.9843	0.7265
Na	0.1021	0.0921	0.1267	0	0.0237	0.3011
Ti	0.0141	0.015	0.0074	0	0	0
End Members Based on Aegirine (Acmite)						
CaTiAl2O6	1.27	0.84	0.75	0	0	0
CaAlSiAlO6	0	0	0	0	0	1.32
Acmite	10.33	9.36	12.8	0	2.39	30.47
Wo	45.87	46.18	44.78	50.79	49.86	36.1
Fs	17.76	17	16.38	6.32	7.72	14.65
En	24.78	26.62	25.29	42.89	40.12	17.46
Recal into						
Ae	10.83	9.69	13.31	0	2.44	32.18
Hd	37.23	35.19	34.09	12.85	15.75	30.94
Di	51.95	55.12	52.6	87.15	81.81	36.88

Sample	**PL-67**	**PL-67**	**PL-67**	**PL-67**	**PL-67**	**NP-68**
Rock Type	Hollaite	Hollaite	Hollaite	Hollaite	Hollaite	Apatitite
Spot	2	3	4	5	6	1
Na_2O	2.79	3.19	3.04	3.14	5.76	0.42
MgO	7.15	6.24	7.41	7.43	5.81	12.07
Al_2O_3	0.58	0.7	0.75	0.53	0.7	1.01
SiO_2	50.4	50.62	51.99	52.26	52.7	52.82
CaO	19.07	18.37	19.57	19.86	14.98	24.32
TiO_2						0.75
MnO	0.87	0.98	0.86	0.86	0.81	0.6
FeO	15.87	17.82	16.16	16.79	19.32	9.02
ZrO_2	0.38					
Total	97.11	97.92	99.78	100.87	100.08	101.01
Recalc.						
Fe3+	7.19	8.22	7.83	8.09	14.84	1.08
Fe2+	9.4	10.42	9.11	9.51	5.97	8.05
Total	97.45	98.74	100.56	101.68	101.57	101.12
Structural Formula						
Si	1.9852	1.9802	1.9865	1.9762	1.9843	1.9602
Al(IV)	0.0148	0.0198	0.0135	0.0236	0.0157	0.0398
Al(VI)	0.0121	0.0125	0.0203	0	0.0153	0.0044
FE3(IV)	0.2131	0.242	0.2252	0.2301	0.4205	0.0302
FE2	0.3097	0.341	0.2912	0.3008	0.1878	0.2497
Mn	0.029	0.0325	0.0117	0.0275	0.0258	0.0189
Mg	0.4199	0.3639	0.4221	0.4189	0.3262	0.6678
Ca	0.8048	0.7699	0.8012	0.8046	0.6043	0.9749
Na	0.2131	0.242	0.2252	0.2302	0.4205	0.0302
Ti	0	0	0	0	0	0.0209
End Members Based on Aegirine (Acmite)						
CaTiAl2O6	0	0	0	0	0	2.02
CaAlSiAlO6	1.23	1.27	1.36	0	1.55	0
Acmite	21.6	24.55	22.77	23.2	42.59	3.06
Wo	40.19	38.42	39.81	40.54	29.83	48.41
Fs	15.7	17.3	14.72	15.15	9.51	12.66
En	21.29	18.46	21.34	21.11	16.52	33.85
Recal into						
Ae	22.6	25.55	24	24.24	45	3.19
Hd	32.85	36.01	31.02	31.66	20.1	26.35
Di	44.54	38.43	44.98	44.1	34.9	70.46

Sample	**NP-68**	**NP-68**	**NP-68**	**NP-68**	**NP-68**	**NP-68**
Rock Type	Apatitite	Apatitite	Apatitite	Apatitite	Apatitite	Apatitite
Spot	2	3	1-C	1-R	2-C	2-R
Na_2O	0.64	1.15	0.66	0.74	0.58	0.48
MgO	11.51	10.36	16.23	12.18	16.35	11.58
Al_2O_3	2.21	0.42	0.22	1.43	0.07	1.27
SiO_2	51.61	54.14	54.06	51.38	54.93	51.89
CaO	24.34	22.96	23.57	22.67	23.96	22.82
TiO_2	1.15		0.09	0.64	0.19	0.63
MnO	0.36	0.84	0.49	1	0.45	0.78
FeO	9.61	11.79	4.69	9.96	3.48	10.55
ZrO_2						
Total	101.43	101.66	100.01	100	100.01	100
Recalc.						
Fe3+	1.65	2.96	1.7	1.91	1.49	1.24
Fe2+	8.13	9.12	3.16	3.84	2.14	9.44
Total	101.6	101.95	100.18	95.79	100.16	100.13
Structural Formula						
Si	1.9154	2.0069	1.984	1.9809	2.0012	1.957
Al(IV)	0.0846	[-0.0069]	0.0095	0.0191	(-.0012)	0.043
Al(VI)	0.012	0.0252	0.0065	0.459	0.0042	0.0134
FE3(IV)	0.0461	0.0827	0.0405	0.0553	0.0413	0.0351
FE2	0.2522	0.2828	0.097	0.124	0.0655	0.2976
Mn	0.0113	0.0264	0.0152	0.0327	0.014	0.0249
Mg	0.6369	0.5726	0.888	0.7001	0.8946	0.6511
Ca	0.9678	0.9119	0.9189	0.9364	0.9263	0.9221
Na	0.0461	0.0827	0.047	0.0553	0.0413	0.0351
Ti	0.0321	0	0.0025	0.0186	0.0052	0.0179
End Members Based on Aegirine (Acmite)						
CaTiAl2O6	3.22	[-0.36]	0.25	1.01	-0.06	1.82
CaAlSiAlO6	1.21	0	0	0	0	0.74
Acmite	4.62	8.57	4.7	5.88	4.19	3.57
Wo	46.34	47.45	45.81	49.29	47.09	45.62
Fs	12.65	14.66	4.85	6.59	3.33	15.14
En	31.95	29.68	44.39	37.23	45.45	33.12
Recal into						
Ae	4.92	8.81	4.87	6.29	4.18	3.77
Hd	26.97	30.15	9.37	14.1	6.53	30.19
Di	68.1	61.04	85.76	79.61	89.2	66.04

Sample	**NP-68**	**NP-68**	**NP-68**	**NP-68**	**PL-76**	**PL-76**
Rock Type	Apatitite	Apatitite	Apatitite	Apatitite	Ijolite	Ijolite
Spot	3-C	3-R	4-C	4-R	1	2
Na_2O	1.3	0.52	0.4	0.68	0.68	0.69
MgO	16.43	11.54	17.66	11.88	10.08	10.16
Al_2O_3	0.05	1.55	0.04	1.22	2.6	1.82
SiO_2	53.51	51.66	54.21	51.78	50.16	50.24
CaO	22.87	22.69	23.9	22.7	23.73	23.33
TiO_2	0.24	0.26	0.12	0.36	0.67	0.37
MnO	0.2	0.7	0.5	1	0.53	0.72
FeO	5.38	11.06	3.14	10.38	12.08	12.6
ZrO_2						
Total	99.98	99.98	99.97	100	100.53	99.93
Recalc.						
Fe3+	3.35	1.34	1.03	1.75	1.75	1.78
Fe2+	2.37	9.88	2.21	8.8	10.5	11
Total	100.32	100.14	100.07	100.17	100.7	100.11
Structural Formula						
Si	1.9662	1.9448	1.8583	1.9524	1.9019	1.9135
Al(IV)	0.0022	0.0552	0.1417	0.0476	0.0981	0.0817
Al(VI)	0.0316	0.0143	0.1023	0.0066	0.0181	0.0048
FE3(IV)	0.061	0.0383	0.0266	0.0497	0.05	0.0462
FE2	0.0727	0.03142	0.0634	0.2776	0.3331	0.3504
Mn	0.0062	0.0225	0.0145	0.0319	0.017	0.0232
Mg	0.9001	0.654	0.9026	0.6678	0.5698	0.6019
Ca	0.9004	0.9241	0.8778	0.917	0.964	0.952
Na	0.0926	0.0383	0.0266	0.0497	0.05	0.051
Ti	0	0.0074	0.0031	0.0102	0.0191	0.0106
End Members Based on Aegirine (Acmite)						
CaTiAl2O6	0	0.75	0.31	1.03	1.91	1.05
CaAlSiAlO6	0	1.43	10.22	0.66	1.81	0
Acmite	9	3.85	2.66	5.02	4.99	5.05
Wo	43.74	45.33	38.57	45.5	46.25	46.68
Fs	3.53	15.78	3.17	14.03	16.62	17.37
En	43.73	32.85	45.07	33.75	28.43	29.84
Recal into						
Ae	9.33	4.07	3.33	5.23	5.25	5.13
Hd	6.78	31.13	6.35	27.82	34.95	34.9
Di	83.9	64.8	90.32	66.94	59.8	59.69

Sample	**PL-76**	**PL-76**	**PL-76**	**PL78**	**PL78**	**PL78**
Rock Type	Ijolite	Ijolite	Ijolite	Meta Micro Ijolite	Meta Micro Ijolite	Meta Micro Ijolite
Spot	3	4	5	1-1	1-3	3-3
Na_2O	0.74	0.75	0.64	0.57	0.79	0.75
MgO	10.43	10.18	10.12	10.85	9.66	9.47
Al_2O_3	1.54	1.67	1.61	1.97	2.21	2.36
SiO_2	51.71	51.19	51.28	50.29	47.99	49.07
CaO	23.36	24.08	23.83	23.88	22.81	23.76
TiO_2	0.42	0.38	0.44	0.69	0.75	0.67
MnO	0.9	0.73	0.71	0.68	0.58	0.81
FeO	12.05	12.02	12.51	12.58	13.45	14.67
ZrO_2						
Total	101.15	101	101.14	101.51	98.24	101.56
Recalc.						
Fe3+	1.91	1.93	1.65	1.47	2.04	1.93
Fe2+	10.33	10.46	11.03	11.26	11.62	12.93
Total	101.34	101.37	101.31	101.66	98.45	101.75
Structural Formula						
Si	1.9437	1.9299	1.9353	1.8971	1.8805	1.8717
Al(IV)	0.0563	0.0701	0.0647	0.0876	0.1021	0.1061
Al(VI)	0.012	0.0041	0.0069	0.0154	0.0175	0.0222
FE3(IV)	0.0539	0.0548	0.0468	0.0263	0.0426	0.0333
FE2	0.3249	0.3298	0.348	0.3553	0.3807	0.4125
Mn	0.0287	0.0233	0.0227	0.0217	0.0192	0.0262
Mg	0.5845	0.5722	0.5694	0.6102	0.5643	0.5386
Ca	0.9408	0.9726	0.9635	0.9651	0.9576	0.971
Na	0.0539	0.0548	0.0468	0.0417	0.06	0.0555
Ti	0.0119	0.0108	0.0125	0.0196	0.0221	0.0192
End Members Based on Aegirine (Acmite)						
CaTiAl2O6	1.2	1.08	1.25	1.93	2.16	1.87
CaAlSiAlO6	1.21	0.41	0.69	0	0	0
Acmite	5.44	5.48	4.7	4.1	5.87	5.41
Wo	46.27	47.91	47.35	46.5	45.75	46.38
Fs	16.39	16.5	17.45	17.47	18.62	20.1
En	29.49	28.62	28.56	30.01	27.6	26.24
Recal into						
Ae	5.6	5.73	4.86	4.22	6.03	5.51
Hd	33.72	34.47	36.09	35.24	37.86	40.68
Di	60.68	59.8	50.62	60.54	56.11	53.51

Sample	**PL78**	**PL85**	**PL85**	**PL85**	**PL85**	**PL85**
Rock Type	Meta Micro Ijolite	Meta Micro Ijolite	Meta Micro Ijolite	Meta Micro Ijolite	Meta Micro Ijolite	Meta Micro Ijolite
Spot	3-6	2-4	3-4	5-1	7-1	7-4
Na_2O	1.04	0.76	0.59	0.62	0.94	0.7
MgO	10.03	9.51	9.8	11.36	10.41	10.19
Al_2O_3	1.93	0.77	1.68	1.02	1.65	2.36
SiO_2	49.7	51.74	48.39	51.56	50.6	49.63
CaO	23.64	23.75	22.23	23.89	23.17	23.38
TiO_2	0.62	0	0.71	0.69	1.12	1.12
MnO	0.69	1.05	0.83	0.44	0.5	0.76
FeO	14.42	13.31	12.73	10.26	11.47	11.14
ZrO_2						
Total	102.07	100.89	96.96	99.84	99.86	99.28
Recalc.						
Fe3+	2.68	1.96	1.52	1.6	2.42	1.8
Fe2+	12.01	11.55	11.36	8.82	9.29	9.52
Total	102.34	101.09	97.11	100	100.1	99.46
Structural Formula						
Si	1.8793	1.9654	1.9135	1.9501	1.9218	1.9007
Al(IV)	0.086	0.0345	0.0783	0.0455	0.0739	0.0993
Al(VI)	0.0347	0.0001	0.0082	0.0045	0.0044	0.0072
FE3(IV)	0.0415	0.0558	0.037	0.041	0.0649	0.052
FE2	0.3797	0.3668	0.3757	0.279	0.2951	0.3048
Mn	0.0221	0.0338	0.0278	0.0141	0.0161	0.0247
Mg	0.5654	0.5386	0.5778	0.6406	0.5895	0.5818
Ca	0.9577	0.9666	0.9418	0.9681	0.9428	0.9593
Na	0.0762	0.056	0.0452	0.0455	0.0692	0.052
Ti	0.0176	0	0.0211	0.0196	0.032	0.0323
End Members Based on Aegirine (Acmite)						
CaTiAl2O6	1.7	0	2.1	1.96	3.2	3.24
CaAlSiAlO6	0	0	0	0	0	0.72
Acmite	7.36	5.64	4.51	4.55	6.93	5.23
Wo	45.35	48.72	45.88	47.46	45.59	46.24
Fs	18.32	18.49	18.72	13.96	14.77	15.32
En	27.28	27.15	28.79	32.06	29.51	29.25
Recal into						
Ae	7.5	5.82	4.68	4.71	7.26	5.54
Hd	37.16	38.16	37.56	28.91	30.94	32.47
Di	55.34	56.02	57.76	66.37	61.8	61.99

Sample	**PL85**	**PL-86**	**PL-86**	**PL-86**	**PL-86**	**PL-86**
Rock Type	Meta Micro Ijolite	Hollaite	Hollaite	Hollaite	Hollaite	Hollaite
Spot	7-5	1	2	3	4	5
Na_2O	0.66	0.6	1.79	0.58	1.79	1.12
MgO	10.51	10.7	6.15	11.31	6.1	7.93
Al_2O_3	0.99	1.33	0.58	1.18	0.76	0.66
SiO_2	50.55	49.7	50.83	52.48	50.31	51.03
CaO	23.26	23.01	20.69	24.04	20.93	22.6
TiO_2		0.4				
MnO	0.66	0.71	1.2	0.77	0.98	0.96
FeO	10.78	11.01	18.06	11.22	18.44	14.46
ZrO_2						
Total	97.41	97.46	99.3	101.58	99.31	98.76
Recalc.						
Fe3+	1.7	1.55	4.61	1.49	4.61	2.89
Fe2+	9.25	9.68	13.91	9.88	14.29	11.86
Total	97.58	97.68	99.76	101.73	99.77	99.05
Structural Formula						
Si	1.9658	1.942	1.9855	1.958	1.9976	1.9839
Al(IV)	0.0342	0.058	0.0145	0.042	0.0024	0.0161
Al(VI)	0.0112	0.0033	0.0122	0.0099	0.0319	0.0141
FE3(IV)	0.0498	0.0455	0.1356	0.042	0.1325	0.0844
FE2	0.3008	0.3163	0.4544	0.3081	0.4564	0.3857
Mn	0.0217	0.007	0.0397	0.0243	0.0285	0.0316
Mg	0.6094	0.6234	0.3582	0.6291	0.3473	0.4596
Ca	0.9691	0.9633	0.8659	0.961	0.8564	0.9413
Na	0.0498	0.0455	0.1356	0.042	0.1325	0.0844
Ti	0	0.0118	0	0	0	0
End Members Based on Aegirine (Acmite)						
CaTiAl2O6	0	1.17	0	0	0	0
CaAlSiAlO6	1.12	0.33	1.24	0.99	0.24	1.43
Acmite	5	4.53	13.82	4.21	13.75	8.57
Wo	48.14	47.2	43.52	47.75	44.31	47.08
Fs	15.12	15.74	23.16	15.47	23.68	19.58
En	30.62	31.03	18.26	31.58	18.02	23.34
Recal into						
Ae	5.18	4.61	14.3	4.28	14.16	9.08
Hd	31.34	32.11	47.93	31.47	48.75	41.48
Di	63.48	63.28	37.78	64.25	37.1	49.44

Sample	**PL-86**	**PL-86**	**PL-86**	**PL-86**	**PL-86**	**PL-90**
Rock Type	Hollaite	Hollaite	Hollaite	Hollaite	Hollaite	Hollaite
Spot	6	7	8	9	10	1
Na_2O	0.59	0.46	0.58	2.02	1.88	1.25
MgO	10.67	10.07	10.15	6.08	6.15	8.58
Al_2O_3	1.13	1.21	1.13	0.55	0.5	1.04
SiO_2	51.4	49.74	51	51.18	51.07	51.88
CaO	23.72	20.38	23.91	20.09	21.06	23.03
TiO_2						0.53
MnO	0.78	0.87	0.77	1.26	1.34	0.74
FeO	10.76	11.52	11.97	18.09	17.97	11.69
ZrO_2						
Total	99.05	94.25	99.51	99.27	99.97	98.74
Recalc.						
Fe3+	1.52	1.49	1.49	5.2	4.84	3.22
Fe2+	9.39	10.18	10.63	13.41	13.61	8.79
Total	99.2	94.4	99.66	99.79	100.45	99.06
Structural Formula						
Si	1.9694	1.9412	1.9549	1.9923	1.9825	1.9867
Al(IV)	0.0306	0.0557	0.0451	0.0077	0.0175	0.0133
Al(VI)	0.0204	0.0031	0.006	0.0176	0.0054	0.0336
FE3(IV)	0.0438	0.0408	0.0431	0.1528	0.1415	0.0928
FE2	0.3009	0.3321	0.3406	0.4373	0.4419	0.2816
Mn	0.0253	0.0288	0.025	0.0416	0.0441	0.024
Mg	0.6095	0.5859	0.5801	0.3536	0.3559	0.4899
Ca	0.9614	0.9998	0.982	0.8396	0.8759	0.9449
Na	0.0438	0.0439	0.0431	0.1528	0.1415	0.0928
Ti	0	0	0	0	0	0.0153
End Members Based on Aegirine (Acmite)						
CaTiAl2O6	0	0	0	0	0	0.7
CaAlSiAlO6	2.07	0	0.6	0.79	0.55	0
Acmite	4.43	4.38	4.32	15.72	14.42	9.73
Wo	47.52	49.85	48.93	42.8	44.37	49.16
Fs	15.2	16.56	17.07	22.5	22.52	14.75
En	30.78	29.22	29.08	18.19	18.14	25.67
Recal into						
Ae	4.59	4.56	4.47	16.19	15.06	10.74
Hd	31.54	34.52	35.34	46.34	47.04	32.58
Di	63.87	60.91	60.19	37.47	37.89	56.68

Sample	**PL-90**	**PL-90**	**PL-90**	**PL-90**	**PL-90**	**PL-90**
Rock Type	Hollaite	Hollaite	Hollaite	Hollaite	Hollaite	Hollaite
Spot	2	3C	3R	4C	4R	4Z
Na_2O	0.97	0.93	1.4	1.59	1.82	0.96
MgO	9.8	9.77	7.63	8.82	6.81	9.87
Al_2O_3	0.98	0.9	1.1	0.85	0.91	0.86
SiO_2	52.9	52.95	52.4	53.18	52.05	52.95
CaO	23.33	23.84	22.41	22.21	21.51	23.87
TiO_2	0.41		0.45		0.34	
MnO	0.76	0.69	0.71	0.92	0.83	0.9
FeO	12.77	12.41	15.8	13.23	17.06	12.55
ZrO_2						
Total	101.92	101.49	101.9	100.8	101.33	101.96
Recalc.						
Fe3+	2.5	2.4	3.61	4.07	4.69	2.47
Fe2+	10.52	10.25	12.55	9.57	12.84	10.32
Total	102.17	101.73	102.26	101.21	101.8	102.2
Structural Formula						
Si	1.972	1.9812	1.9825	1.9979	1.9777	1.982
Al(IV)	0.028	0.0188	0.0175	0.0021	0.0223	0.018
Al(VI)	0.0151	0.0209	0.0316	0.0355	0.0184	0.0067
FE3(IV)	0.0701	0.0675	0.1027	0.1151	0.1341	0.0697
FE2	0.328	0.3208	0.3972	0.3006	0.408	0.3232
Mn	0.024	0.0219	0.0228	0.0293	0.0267	0.0285
Mg	0.5447	0.545	0.4022	0.494	0.3858	0.5508
Ca	0.9318	0.9557	0.9084	0.894	0.8756	0.9573
Na	0.0701	0.0675	0.1027	0.1151	0.1341	0.0697
Ti	0.0115	0	0.0128	0	0.0097	0
End Members Based on Aegirine (Acmite)						
CaTiAl2O6	1.17	0	0.91	0	1	0
CaAlSiAlO6	0.51	1.91	0	0.22	0.3	0.68
Acmite	7.15	6.83	10.69	11.98	13.75	7.05
Wo	46.67	47.43	46.81	46.43	44.25	48.07
Fs	16.72	16.24	20.67	15.65	20.92	16.34
En	27.77	27.59	20.93	25.72	19.78	27.86
Recal into						
Ae	7.44	7.23	11.38	12.65	14.45	7.38
Hd	34.79	34.38	44.03	33.04	43.97	34.25
Di	57.77	58.39	44.58	54.31	41.58	58.37

Sample	**PL-90**	**PL-90**	**PL-90**	**PL-90**	**PL-90**	**PL-95**
Rock Type	Hollaite	Hollaite	Hollaite	Hollaite	Hollaite	Hollaite
Spot	5	6	7	8	9	1
Na_2O	0.76	1.99	1.71	0.83	1.72	2.04
MgO	10.15	6.99	9.06	10.19	1.87	7.92
Al_2O_3	0.81	0.95	0.78	0.6	0.81	1.87
SiO_2	53.33	52.2	53.54	53.23	51.8	50.15
CaO	23.96	21.27	22.23	23.66	21.33	20.15
TiO_2		0.51				0.38
MnO	0.87	0.8	0.88	0.67	0.77	1.02
FeO	11.6	17.26	13.34	11.54	17.16	14.62
ZrO_2						
Total	101.48	101.97	101.54	100.72	95.46	98.15
Recalc.						
Fe3+	1.96	5.13	4.41	2.14	4.95	5.26
Fe2+	9.84	12.65	9.38	14.62	12.71	9.89
Total	101.68	102.49	101.99	105.94	95.96	98.68
Structural Formula						
Si	1.9899	1.9806	1.9953	1.9467	1.9815	1.9461
Al(IV)	0.0101	0.0194	0.0047	0.0259	0.0185	0.0539
Al(VI)	0.0255	0.0007	0.0296	0.0257	0.0181	0.0317
FE3(IV)	0.055	0.1464	0.1236	0.0314	0.1424	0.1535
FE2	0.307	0.4013	0.2922	0.447	0.4066	0.321
Mn	0.0275	0.0257	0.0278	0.0208	0.0249	0.0355
Mg	0.5647	0.3954	0.5038	0.5556	0.3918	0.4582
Ca	0.9579	0.8646	0.8876	0.9271	0.8742	0.8378
Na	0.055	0.1464	0.1236	0.589	0.1424	0.1535
Ti	0	0.0146	0	0	0	0.0111
End Members Based on Aegirine (Acmite)						
CaTiAl2O6	0	0.99	0	0	0	1.13
CaAlSiAlO6	1.03	0	0.48	0	1.83	3.22
Acmite	5.64	14.91	12.77	5.75	14.42	15.61
Wo	48.62	43.53	45.63	45.28	43.34	40.42
Fs	15.75	20.43	15.1	21.83	20.58	16.32
En	28.96	20.13	26.02	27.14	19.83	23.3
Recal into						
Ae	5.93	15.52	13.44	5.97	15.14	16.46
Hd	33.13	42.55	31.79	41.92	43.22	34.41
Di	60.94	41.93	54.77	52.11	41.65	49.13

Sample	**PL-95**	**PL-95**	**PL-95**	**PL-95**	**PL-95**	**PL-95**
Rock Type	Hollaite	Hollaite	Hollaite	Hollaite	Hollaite	Hollaite
Spot	2	3	4	5	6	7
Na_2O	2.11	2.11	2.79	2.64	2	2.03
MgO	8.82	7.94	8.29	8.45	7.93	7.65
Al_2O_3	1	0.83	0.54	0.37	0.81	0.84
SiO_2	52.15	51.73	52.46	52.54	51.33	53.45
CaO	21.12	20.53	19.54	19.19	20.94	21.44
TiO_2	0.62	0.26	0.2	0.15		
MnO	0.88	0.98	0.87	1.25	1.13	1.25
FeO	14.02	15.48	14.69	14.48	14.35	15.91
ZrO_2						
Total	100.72	99.86	99.38	99.07	98.49	102.57
Recalc.						
Fe3+	5.44	8.01	7.19	6.8	5.15	5.23
Fe2+	9.13	8.27	8.22	8.36	9.71	11.2
Total	101.27	100.66	100.1	99.75	99	103.09
Structural Formula						
Si	1.9638	1.9527	1.9945	1.9902	1.9914	1.9786
Al(IV)	0.0362	0.0369	0.0055	0.0098	0.0086	0.0214
Al(VI)	0.0082	0.0104	0.0187	0.0157	0.0083	0.0159
FE3(IV)	0.1541	0.2172	0.2057	0.1939	0.1504	0.1485
FE2	0.2875	0.2611	0.2614	0.2648	0.3151	0.3534
Mn	0.0281	0.0313	0.0248	0.0401	0.047	0.0399
Mg	0.4952	0.4468	0.4699	0.4772	0.4587	0.4302
Ca	0.8521	0.8303	0.796	0.8032	0.8704	0.8665
Na	0.1541	0.2276	0.2057	0.1939	0.1504	0.1485
Ti	0.0176	0.0074	0.0057	0.0043	0	0
End Members Based on Aegirine (Acmite)						
CaTiAl2O6	1.79	0.74	0.28	0.44	0	0
CaAlSiAlO6	0.11	0	0	0.13	0.85	1.62
Acmite	15.71	22.75	21.19	20	15.4	15.13
Wo	42.49	41.13	40.86	41.15	44.13	43.33
Fs	14.66	13.05	13.47	13.66	16.13	18
En	25.25	22.33	24.21	24.62	23.48	21.92
Recal into						
Ae	16.45	24.33	21.95	20.72	16.28	15.93
Hd	30.69	27.9	27.9	28.29	34.1	37.92
Di	52.87	47.77	50.15	50.99	49.63	46.16

Sample	**PL-96A**	**PL-96A**	**PL-96A**	**PL-96A**	**PL-96A**	**PL-96A**
Rock Type	Urtite	Urtite	Urtite	Urtite	Urtite	Urtite
Spot	1L	2L	3L	4L	1E	2E
Na_2O	3.7	3.25	4.6	4.76	0.8	0.76
MgO	8.16	8.51	6.67	6.41	10.52	10.91
Al_2O_3	0.67	0.8	0.54	0.57	3.77	2.92
SiO_2	53.25	51.67	51.07	52.04	48.79	50.68
CaO	18.6	19.44	16.03	16.68	23.81	24.06
TiO_2					1.44	0.96
MnO	0.99	0.77	1.2	1.13	0.38	0.3
FeO	15.81	15.24	17.7	17.86	11.52	11.15
ZrO_2						
Total	101.18	99.68	97.81	99.45	101.03	101.74
Recalc.						
Fe3+	9.53	8.37	11.85	12.26	2.06	1.96
Fe2+	7.23	7.71	7.04	6.82	9.67	10.19
Total	102.13	100.52	99	100.67	101.24	102.74
Structural Formula						
Si	1.9844	1.9626	1.9776	1.9808	1.8399	1.9522
Al(IV)	0.0156	0.0358	0.0224	0.0192	0.1601	0.0478
Al(VI)	0.0138	0.0016	0.0022	0.0064	0.0075	0.0848
FE3(IV)	0.2673	0.2378	0.3454	0.3513	0.0585	0.0568
FE2	0.2254	0.2448	0.2278	0.2172	0.3048	0.3282
Mn	0.0312	0.0248	0.0394	0.0364	0.0121	0.0098
Mg	0.4534	0.4819	0.3851	0.3638	0.5915	0.3968
Ca	0.7426	0.7911	0.6651	0.6802	0.962	0.993
Na	0.2673	0.2393	0.3454	0.3513	0.0585	0.0568
Ti	0	0	0	0	0.0408	0.0278
End Members Based on Aegirine (Acmite)						
CaTiAl2O6	0	0	0	0	4.04	2.58
CaAlSiAlO6	1.4	0	0.23	0.65	0.74	0
Acmite	27.14	23.98	35.05	35.66	5.78	6.12
Wo	37	39.63	33.63	34.2	45.15	52.23
Fs	11.44	12.26	11.56	11.03	15.06	17.69
En	23.02	24.14	19.54	18.46	29.23	21.39
Recal into						
Ae	28.26	24.78	36.04	37.68	6.13	7.26
Hd	23.82	25.34	23.77	23.3	31.92	41.98
Di	47.92	49.89	40.19	39.02	61.95	50.76

Sample	**PL-96A**	**PL-96A**	**PL-96A**	**PL-96A**	**PL-96A**	**PL-96A**
Rock Type	Urtite	Urtite	Urtite	Urtite	Urtite	Urtite
Spot	3E	4E	1Z	2Z	3Z	4Z
Na_2O	0.75	0.73	0.88	0.62	1.33	0.91
MgO	11.27	10.78	8.48	10.22	9.69	8.8
Al_2O_3	2.48	2.85	2.16	1.45	0.64	2.2
SiO_2	51.34	50.65	50.48	51.56	52.1	50.08
CaO	24.66	23.41	23.59	24.37	23.19	23.56
TiO_2	1.11	1.02	0.48			0.41
MnO	0.33	0.4	0.64	0.85	0.98	0.72
FeO	10.36	11.66	15.05	11.62	12.67	14.72
ZrO_2						
Total	102.3	101.5	101.76	100.69	100.6	101.4
Recalc.						
Fe3+	1.93	1.88	2.27	1.6	2.34	2.34
Fe2+	8.82	9.97	13.01	10.18	10.56	12.61
Total	102.69	101.69	101.99	100.85	100.83	101.63
Structural Formula						
Si	1.8955	1.8869	1.914	1.9488	1.9809	1.9332
Al(IV)	0.1045	0.1131	0.086	0.0502	0.0191	0.0668
Al(VI)	0.0034	0.012	0.0105	0.0144	0.0096	0.0258
FE3(IV)	0.0537	0.0527	0.0647	0.0455	0.0671	0.0631
FE2	0.2724	0.3105	0.4125	0.322	0.3358	0.377
Mn	0.0103	0.0126	0.0206	0.0272	0.0316	0.0218
Mg	0.6203	0.5987	0.4794	0.5762	0.5493	0.469
Ca	0.9754	0.9543	0.9583	0.9874	0.9447	0.9789
Na	0.0537	0.0527	0.0647	0.0455	0.0671	0.0631
Ti	0.0308	0.0286	0.0137	0	0	0.011
End Members Based on Aegirine (Acmite)						
CaTiAl2O6	3.07	2.84	1.37	0	0	1.11
CaAlSiAlO6	0.33	1.19	1.05	1.45	0.97	2.6
Acmite	5.34	5.25	6.46	4.57	6.8	6.35
Wo	46.84	45.47	46.62	48.87	47.38	47.39
Fs	13.55	15.45	20.59	16.17	17.01	18.96
En	30.87	29.79	23.92	28.94	27.83	23.59
Recal into						
Ae	5.67	5.48	6.76	4.82	7.05	6.94
Hd	28.78	32.28	43.12	34.12	35.27	41.47
Di	65.55	62.24	50.11	61.06	57.69	51.59

Sample	**PL-96A**	**PL-96A**	**PL-96A**	**PL-96A**	**PLL-01B**	**PLL-01B**
Rock Type	Urtite	Urtite	Urtite	Urtite	Xenolith Dike	Xenolith Dike
Spot	5 in Gt	6 in Gt	7 in Gt	8 in Gt	1C	1R
Na_2O	0.46	1.63	1.18	0.86	0.57	0.69
MgO	12.32	11.9	11.89	10.72	15.86	15.53
Al_2O_3	2.57	1.54	1.4	2.82	0.62	1.37
SiO_2	50.84	53.07	52.74	50.12	53.81	52.41
CaO	24.65	23.11	24.03	24.17	24.04	24.13
TiO_2	1.09	0.44		0.99	0.45	0.75
MnO	0.36	0.46	0.6	0.47		
FeO	9.15	9.57	10.04	11	5.22	5.03
ZrO_2						
Total	101.44	101.72	101.88	101.15	100.57	99.91
Recalc.						
Fe3+	1.19	4.2	3.04	0.93	1.47	1.78
Fe2+	8.08	5.79	7.3	10.17	3.9	3.43
Total	101.56	102.14	102.18	101.25	100.72	100.09
Structural Formula						
Si	1.889	1.9467	1.9465	1.8917	1.9745	1.9302
Al(IV)	0.111	0.0533	0.0535	0.1083	0.0255	0.0595
Al(VI)	0.0015	0.0132	0.0074	0.0193	0.0013	0.0103
FE3(IV)	0.0331	0.1159	0.0844	0.0263	0.0406	0.039
FE2	0.2512	0.1776	0.2254	0.3209	0.1196	0.1057
Mn	0.0113	0.0143	0.0188	0.015	0	0
Mg	0.6825	0.6508	0.6526	0.6032	0.8403	0.8528
Ca	0.9813	0.9082	0.9502	0.9774	0.9451	0.9522
Na	0.0331	0.1159	0.0844	0.0263	0.0405	0.0493
Ti	0.0305	0.0121	0	0.0281	0.0124	0.0208
End Members Based on Aegirine (Acmite)						
CaTiAl2O6	3.03	1.22	0	2.81	1.24	2.05
CaAlSiAlO6	0.15	1.33	0.74	1.93	0.06	0
Acmite	0.329	11.63	8.42	2.63	4.06	4.85
Wo	47.15	44.28	47.03	46.46	46.62	45.88
Fs	12.48	8.91	11.25	16.03	5.98	5.2
En	33.9	32.64	32.56	30.14	42.03	42.01
Recal into						
Ae	3.43	12.28	8.77	2.77	4.17	5.02
Hd	25.98	18.81	23.42	33.76	11.94	10.47
Di	70.59	68.91	67.8	63.47	83.89	84.51

Sample	**PLL-01B**	**PLL-01B**	**PLL-01B**	**PLL-01B**	**PLL-01B**	**PLL-01B**
Rock Type	Xenolith Dike	Xenolith Dike	Xenolith Dike	Xenolith Dike	Xenolith Dike	Xenolith Dike
Spot	2	3	4	5	6a (asym zoning)	6b
Na_2O	0.66	0.64	0.93	0.81	0.95	0.65
MgO	15.54	15.48	13.75	14.59	13.89	15.17
Al_2O_3	0.57	0.44	1.79	1.48	0.88	0.46
SiO_2	53.2	53.26	52.02	51.95	52.46	52.81
CaO	23.88	24.11	22.83	23.29	21.94	23.51
TiO_2	0.24	0.44	0.82	0.82	0.46	0.3
MnO						
FeO	5.36	5.24	7.91	6.14	8.09	5.33
ZrO_2						
Total	99.45	99.61	100.05	99.08	98.67	98.23
Recalc.						
Fe3+	1.7	1.65	2.4	2.09	2.45	1.67
Fe2+	3.83	3.76	5.35	4.26	5.89	3.81
Total	99.62	99.78	99.89	99.29	98.92	98.38
Structural Formula						
Si	1.967	1.9667	1.9329	1.9289	1.9675	1.9664
Al(IV)	0.0248	0.0191	0.0671	0.0653	0.0325	0.0202
Al(VI)	0.0081	0.0141	0.0113	0.0059	0.0064	0.0134
FE3(IV)	0.0392	0.0317	0.067	0.0529	0.0691	0.0335
FE2	0.1184	0.116	0.1664	0.1334	0.1847	0.1187
Mn	0	0	0	0	0	0
Mg	0.8566	0.8522	0.7617	0.8139	0.7767	0.8699
Ca	0.946	0.9539	0.9089	0.9337	0.8816	0.9379
Na	0.0473	0.0458	0.067	0.0588	0.0691	0.0469
Ti	0.0067	0.0122	0.0229	0.0231	0.013	0.0084
End Members Based on Aegirine (Acmite)						
CaTiAl2O6	0.66	0.95	2.29	2.28	1.3	0.83
CaAlSiAlO6	0	0	1.13	0	0.64	0
Acmite	4.68	4.53	6.68	5.81	6.91	4.63
Wo	46.45	46.67	43.62	45.04	43.1	45.82
Fs	5.86	5.73	8.3	6.6	9.23	5.85
En	42.36	42.12	37.99	40.26	38.83	42.88
Recal into						
Ae	4.8	4.63	7.12	6.06	7.42	4.81
Hd	11.56	11.43	16.65	13.23	17.78	11.43
Di	83.64	83.95	76.23	80.71	74.8	83.76

Sample	**PLL-01L**	**PLL-01L**	**PLL-01L**	**PLL-01L**	**PLL-01L**	**PLL-01L**
Rock Type	Xenolith Dike	Xenolith Dike	Xenolith Dike	Xenolith Dike	Xenolith Dike	Xenolith Dike
Spot	1C	1R	2	3	4	5
Na_2O	0.48	0.45	0.36	0.56	0.8	0.8
MgO	16.73	14.76	15.73	14.38	16.22	16.36
Al_2O_3	0.84	3.53	2.81	4.97	0.91	0.89
SiO_2	53.19	48.75	51.39	48.13	53.24	53.7
CaO	24.33	23.7	24.41	24.18	24.02	23.94
TiO_2	0.64	2	1.56	2.5	0.47	0.49
MnO						
FeO	4.64	6.58	5.91	6.67	5.35	3.44
ZrO_2						
Total	100.85	99.77	102.17	101.39	101.01	99.62
Recalc.						
Fe3+	1.24	1.16	0.93	1.44	2.06	2.06
Fe2+	3.54	5.54	4.68	5.37	3.5	3.59
Total	100.99	99.89	101.87	101.53	101.22	101.83
Structural Formula						
Si	1.9383	1.8213	1.8688	1.7743	1.939	1.947
Al(IV)	0.0361	0.1576	0.1204	0.2159	0.0391	0.0295
Al(VI)	0.0256	0.0211	0.0108	0.0097	0.0219	0.0236
FE3(IV)	0.0083	0.0115	0.0146	0.0303	0.0346	0.0327
FE2	0.1078	0.173	0.1422	0.1656	0.1065	0.1087
Mn	0	0	0	0	0	0
Mg	0.909	0.8221	0.8528	0.7904	0.8808	0.8843
Ca	0.9499	0.9486	0.951	0.9531	0.9377	0.93
Na	0.0339	0.0326	0.0254	0.04	0.0565	0.0562
Ti	0.0175	0.0562	0.0427	0.0693	0.0129	0.0134
End Members Based on Aegirine (Acmite)						
CaTiAl2O6	1.71	5.44	4.18	6.73	1.26	1.3
CaAlSiAlO6	0	0	0	0	0	0
Acmite	3.31	3.16	2.49	3.89	5.51	5.49
Wo	45.44	43.22	44.54	42.93	45.1	44.74
Fs	5.25	8.38	6.97	8.05	5.19	5.31
En	44.3	39.81	51.82	38.4	45.95	43.16
Recal into						
Ae	3.51	3.52	2.72	4.33	5.76	5.78
Hd	10.23	16.77	13.9	16.57	10.16	10.31
Di	86.26	79.71	83.38	79.09	84.08	83.91

Sample	**WS-2D**	**WS-2D**	**WS-2D**	**WS-2D**	**WS-2D**	**WS-2E**
Rock Type	Apatitite	Apatitite	Apatitite	Apatitite	Apatitite	Apatitite
Spot	1	2	3	4	5	1R
Na_2O	0.73	0.74	0.62	0.79	0.99	1.06
MgO	9.84	9.78	8.87	8.06	7.53	5.55
Al_2O_3	1.57	1.43	1.36	0.82	2.06	0.84
SiO_2	51.1	50.95	50.62	51.39	49.59	49.34
CaO	24.06	23.87	23.36	21.37	23.55	23.11
TiO_2	0.52	0.47	0.78	0.12	0.33	0.31
MnO	0.8	0.87	0.83	0.87	0.9	1.28
FeO	13.06	13.03	13.89	15.37	16.13	18.59
ZrO_2						
Total	101.68	101.14	100.33	98.79	101.08	100.08
Recalc.						
Fe3+	1.88	1.91	1.6	2.04	2.55	2.73
Fe2+	11.37	10.3	12.45	13.54	13.83	16.13
Total	101.87	100.32	100.49	99	101.33	100.35
Structural Formula						
Si	1.9257	1.9409	1.9464	1.9937	1.8938	1.9432
Al(IV)	0.0697	0.0591	0.0536	0.0063	0.0946	0.039
Al(VI)	0.0046	0.0051	0.0081	0.0312	0.0115	0.0178
FE3(IV)	0.0488	0.0547	0.0462	0.0594	0.0633	0.0631
FE2	0.3582	0.3283	0.4004	0.4392	0.4509	0.5313
Mn	0.0255	0.0281	0.0267	0.0286	0.0297	0.0427
Mg	0.5529	0.5554	0.5085	0.4662	0.4376	0.3259
Ca	0.9714	0.9742	0.9706	0.8966	0.9834	0.9751
Na	0.0533	0.0547	0.0462	0.0594	0.0748	0.0809
Ti	0.0147	0.0135	0.0081	0.0035	0.0097	0.0092
End Members Based on Aegirine (Acmite)						
CaTiAl2O6	1.47	1.36	0.81	0.33	0.95	0.92
CaAlSiAlO6	0	0.51	0.81	0	0	0
Acmite	5.32	5.5	4.65	6.18	7.37	8.08
Wo	47.74	48.13	48.01	46.44	47.94	48.22
Fs	17.88	16.53	20.14	22.83	22.2	26.52
En	27.59	27.97	25.58	24.23	21.54	16.27
Recal into						
Ae	5.53	5.82	4.84	6.24	7.77	8.63
Hd	37.15	34.98	41.92	45.49	46.81	56.64
Di	57.32	59.19	53.24	48.28	45.24	34.47

Sample	**WS-2E**	**WS-2E**	**WS-2E**	**WS-2E**	**WS-2E**	**WS-2E**
Rock Type	Apatitite	Apatitite	Apatitite	Apatitite	Apatitite	Apatitite
Spot	2C	2R	3Ca	3Cb	3R	4lz
Na_2O	0.81	1.03	0.88	0.56	1.26	0.61
MgO	6.89	6.39	10.5	8.89	5.91	9.6
Al_2O_3	1.1	0.9	1.09	1.3	0.91	1.12
SiO_2	49.21	49.3	52.52	50.39	50.3	51.23
CaO	23.59	23.41	25.26	24.79	23.05	24.27
TiO_2	0.32	0.17	0.26	0.29	0.22	0.23
MnO	1.06	1.09	0.76	1	1.22	0.98
FeO	16.4	17.35	11.67	12.78	18.32	12.32
ZrO_2						
Total	99.38	99.64	102.94	100	101.19	100.36
Recalc.						
Fe3+	2.09	2.65	2.27	1.44	3.25	1.57
Fe2+	14.52	14.96	9.72	11.48	15.39	10.91
Total	99.59	99.9	103.26	100.14	101.51	100.52
Structural Formula						
Si	1.9212	1.9399	1.9421	1.9388	1.9462	1.9527
Al(IV)	0.0506	0.0417	0.0475	0.0589	0.0417	0.0473
Al(VI)	0.0282	0.0183	0.0104	0.0023	0.0121	0.003
FE3(IV)	0.0331	0.0602	0.0527	0.0395	0.0828	0.0451
FE2	0.4741	0.4924	0.3006	0.3694	0.5001	0.3476
Mn	0.0351	0.0363	0.0238	0.0326	0.0402	0.0316
Mg	0.401	0.3749	0.5789	0.51	0.3424	0.5456
Ca	0.9876	0.9869	1.0008	1.0219	0.9597	0.9911
Na	0.0613	0.0786	0.0631	0.0418	0.0949	0.0451
Ti	0.0311	0.005	0.0072	0.0084	0.0064	0.0066
End Members Based on Aegirine (Acmite)						
CaTiAl2O6	2.52	0.5	0.72	0.84	0.64	0.66
CaAlSiAlO6	0	0	0	0	0	0.31
Acmite	6.1	7.79	6.27	4.19	9.5	4.54
Wo	47.84	48.7	49.34	50.85	47.7	49.47
Fs	23.59	24.42	14.93	18.53	25.02	17.52
En	19.95	18.59	28.75	25.94	17.13	27.5
Recal into						
Ae	6.55	8.31	6.69	4.53	10.13	4.8
Hd	50.63	52.06	31.89	40.1	53.35	37.05
Di	42.82	39.64	61.42	55.36	36.53	58.14

Sample	**WS-2E**	**WS-2E**	**WS-2E**	**WS-2E**	**WS-2E**	**WS-2E**
Rock Type	Apatitite	Apatitite	Apatitite	Apatitite	Apatitite	Apatitite
Spot	4hz	5lz	5hz	6lz	6hz	7lz
Na_2O	1.02	0.96	0.79	0.91	0.96	1
MgO	7.72	8.28	7.37	9.33	7.25	9.59
Al_2O_3	1.02	1.42	0.67	1.21	0.96	0.74
SiO_2	51.01	48.91	48.38	50.87	52.27	50.88
CaO	23.74	23.59	22.53	24.58	24.46	23.99
TiO_2	0.21	0.38	0.32	0.39	0.16	0.4
MnO	0.74	0.74	1.03	0.76	0.99	0.92
FeO	15.44	13.88	15.04	12.96	15.78	12.47
ZrO_2						
Total	100.9	98.16	96.13	101.01	102.83	99.99
Recalc.						
Fe3+	2.63	1.19	2.04	2.34	2.47	2.47
Fe2+	13.08	12.01	13.21	10.85	13.55	10.24
Total	101.17	97.48	96.34	101.24	103.07	100.23
Structural Formula						
Si	1.9545	1.9378	1.9544	1.931	1.9664	1.97
Al(IV)	0.0455	0.0622	0.0319	0.0542	0.0336	0.03
Al(VI)	0.0005	0.0041	0.0137	0.0147	0.009	0.0038
FE3(IV)	0.0758	0.0353	0.0481	0.0542	0.0702	0.0721
FE2	0.419	0.398	0.4462	0.3451	0.4272	0.3317
Mn	0.024	0.0248	0.0352	0.0245	0.0316	0.0171
Mg	0.441	0.4861	0.4439	0.5291	0.4074	0.5536
Ca	0.9746	1.0014	0.9751	1.0016	0.9878	0.9537
Na	0.0758	0.0353	0.0619	0.0671	0.0702	0.0721
Ti	0.0061	0.022	0.0097	0.0112	0.0045	0.0047
End Members Based on Aegirine (Acmite)						
CaTiAl2O6	0.61	2.22	0.97	1.1	0.46	0.47
CaAlSiAlO6	0.05	0.41	0	0	0.91	0.38
Acmite	7.61	3.56	6.19	6.64	7.1	7.24
Wo	48.58	49.91	48.3	49.01	49.29	47.46
Fs	21.03	20.08	22.33	17.07	21.62	16.66
En	22.13	24.52	22.21	26.18	20.61	27.8
Recal into						
Ae	8.1	3.84	6.5	7.13	7.75	7.53
Hd	44.77	43.29	46.87	36.66	47.22	34.65
Di	47.13	52.87	46.63	56.21	45.03	57.82

Sample	**WS-2E**	**WS-2E**	**WS-2E**	**WS-2E**	**WS-2E**	**WS-2E**
Rock Type	Apatitite	Apatitite	Apatitite	Apatitite	Apatitite	Apatitite
Spot	7hz	8lz	8hz	9lz	9hz	10lz
Na_2O	1.09	0.86	1.22	0.76	0.96	0.84
MgO	6.13	9.58	5.32	8.63	6.68	9.06
Al_2O_3	0.91	0.81	1.24	1.88	1.16	1.47
SiO_2	49.74	51.07	49.69	48.07	49.81	50.23
CaO	22.65	24.47	22.19	23.4	23.47	24.12
TiO_2	0.52	0.2	0.3	0.48	0.27	0.28
MnO	1.09	0.61	1.36	0.55	0.99	0.75
FeO	16.56	12.39	18.69	13.15	16.67	13.25
ZrO_2						
Total	98.69	99.99	100.01	96.92	100.01	100
Recalc.						
Fe3+	2.81	2.22	3.14	1.96	2.47	2.16
Fe2+	14.33	10.4	15.26	11.39	13.84	11.3
Total	99.27	100.22	99.72	97.12	99.65	100.21
Structural Formula						
Si	1.9861	1.9452	1.9567	1.9151	1.9433	1.9188
Al(IV)	0.0139	0.0364	0.0433	0.0849	0.0507	0.0662
Al(VI)	0.0289	0.0185	0.0142	0.0027	0.0028	0.015
FE3(IV)	0.0844	0.045	0.0931	0.0582	0.0728	0.0472
FE2	0.4786	0.3311	0.5026	0.3763	0.4531	0.3611
Mn	0.0369	0.0197	0.0454	0.0184	0.0328	0.0243
Mg	0.3649	0.544	0.3123	0.5084	0.3898	0.5502
Ca	0.8834	0.9986	0.9362	0.9906	0.9841	0.9872
Na	0.0844	0.0635	0.0931	0.0582	0.0728	0.0622
Ti	0.0156	0.0175	0.0089	0.0143	0.0079	0.008
End Members Based on Aegirine (Acmite)						
CaTiAl2O6	0.73	1.73	0.91	1.42	0.8	0.79
CaAlSiAlO6	0	0	1.45	0.27	0.28	0
Acmite	8.87	6.29	9.5	5.8	7.35	6.13
Wo	46.06	48.61	46.57	48.47	49.07	48.21
Fs	25.15	16.41	25.64	18.73	22.84	17.78
En	19.18	26.96	15.93	25.31	19.65	27.09
Recal into						
Ae	9.09	6.77	10.26	6.17	7.95	6.39
Hd	51.58	35.28	55.35	39.91	49.48	37.09
Di	39.33	57.96	34.4	53.92	42.56	56.52

Sample	**WS-2E**
Rock Type	Apatitite
Spot	10hz
Na_2O	1.17
MgO	6.03
Al_2O_3	1.03
SiO_2	49.23
CaO	22.69
TiO_2	0.37
MnO	1.13
FeO	18.84
ZrO_2	
Total	100.49
Recalc.	
Fe3+	3.01
Fe2+	15.73
Total	100.39
Structural Formula	
Si	1.9334
Al(IV)	0.0477
Al(VI)	0.019
FE3(IV)	0.0701
FE2	0.5165
Mn	0.0376
Mg	0.3531
Ca	0.9547
Na	0.0891
Ti	0.0109
End Members Based on Aegirine (Acmite)	
CaTiAl2O6	1.09
CaAlSiAlO6	0
Acmite	8.85
Wo	46.88
Fs	25.65
En	17.54
Recal into	
Ae	9.29
Hd	53.88
Di	36.83

Garnet compositions

Sample	PL-86	PL-86	PL-86	PL-86	PL-86	PL-38	PL-38
Analysis (wt. %)	1	2	3	4	5	1	2
SiO2	35.58	34.74	35.27	34.40	34.00	33.29	31.42
TiO2	3.58	4.05	3.52	4.10	5.51	6.51	8.94
ZrO2						0.00	1.59
Al2O3	1.81	1.63	1.55	1.48	1.49	0.48	0.81
V2O3						0.56	0.00
FeO / FeOtot	24.63	24.04	25.16	24.06	23.87	23.57	22.17
MnO	0.56	0.45	0.50	0.55	0.48	0.66	0.69
MgO	0.28	0.00	0.00	0.00	0.00		
CaO	33.22	32.73	32.37	32.30	32.56	31.89	31.32
Total (calc)	99.66	97.64	98.37	96.89	97.91	96.96	96.94
Recalculated (wt. %)							
final FeO	2.14	2.79	3.36	2.88	3.41	4.14	5.71
final Fe2O3	25.00	23.61	24.23	23.54	22.74	21.60	18.29
Total	102.17	100.00	100.80	99.25	100.19	99.13	98.77
End-members							
Kimzeyite							3.35%
Schorlomite	0.00%	0.00%	0.00%	0.00%	0.00%	5.38%	10.09%
Schorlomite-Al	4.02%	4.13%	2.88%	4.27%	7.08%	2.42%	0.78%
Morimotoite	14.07%	17.33%	16.34%	17.58%	20.69%	26.24%	36.40%
Morimotoite-Mg	0.00%	0.00%	0.00%	0.00%	0.00%	0.00%	0.00%
Goldmanite						1.92%	
Spessartine	1.30%	1.07%	1.18%	1.32%	0.30%		
Pyrope	1.14%						
Almandine	0.20%	0.77%	2.37%	0.95%			
Grossular	2.10%	2.10%	1.19%	0.85%			
Andradite	77.18%	74.61%	76.04%	75.03%	69.99%	61.34%	46.07%
Calderite					0.84%	1.59%	1.68%
Skiagite					1.10%	1.10%	1.63%
Khoharite							
Remainder	0.00%	0.00%	0.00%	0.00%	0.00%	0.00%	0.00%
Total	100.01%	100.01%	100.00%	100.00%	100.00%	99.99%	100.00%
Recal Into:							
Andradite	81.01%	77.66%	79.82%	77.45%	71.59%	64.31%	49.36%
Schorlomite	4.22%	4.30%	3.02%	4.41%	7.24%	8.18%	11.65%
Morimotoite	14.77%	18.04%	17.15%	18.15%	21.16%	27.51%	39.00%
Quality Index	Superior	Superior	Superior	Superior	Superior	Superior	Superior

Sample	PL-38	PL-96A	PL-96A	PL-96A	PL-96A	PL-96A	PL-96A-1
Analysis (wt. %)	3	1	2	3	4	5	1
SiO2	32.74	28.88	28.89	32.14	32.20	29.07	29.76
TiO2	7.16	10.77	11.10	7.17	7.73	12.56	12.60
ZrO2	0.54	2.52	2.58	1.24	1.05	1.73	1.71
Al2O3	0.60	2.15	2.28	0.78	0.93	2.18	2.19
V2O3	0.45						
FeO / FeOtot	23.14	20.17	20.38	23.33	23.47	20.34	19.43
MnO	0.76	0.42	0.37	0.51	0.78	0.36	0.00
MgO		0.85	0.92	0.52	0.33	0.99	0.94
CaO	31.51	31.54	31.80	31.86	32.17	32.40	32.49
Total (calc)	96.90	97.30	98.32	97.55	98.66	99.63	99.12
Recalculated (wt. %)							
final FeO	4.76	3.34	3.28	3.34	3.47	3.43	4.62
final Fe2O3	20.42	18.70	19.01	22.21	22.22	18.80	16.46
Total	98.94	99.17	100.23	99.77	100.88	101.52	100.77
End-members							
Kimzeyite	1.13%	5.28%	5.35%	2.58%	2.16%	3.54%	3.51%
Schorlomite	6.47%	14.93%	15.61%	9.19%	9.62%	17.39%	13.99%
Schorlomite-Al	1.90%	5.61%	6.08%	1.34%	2.46%	7.23%	7.35%
Morimotoite	29.47%	24.03%	23.34%	23.81%	24.51%	24.03%	32.47%
Morimotoite-Mg	0.00%	4.56%	4.36%	1.08%	0.37%	5.92%	4.58%
Goldmanite	1.55%						
Andradite	56.05%	42.45%	41.93%	58.94%	57.77%	38.88%	35.71%
Calderite	1.84%	1.02%	0.89%	1.23%	1.86%	0.85%	
Skiagite	1.57%						
Khoharite		2.11%	2.44%	1.84%	1.26%	2.15%	2.40%
Remainder	0.00%	0.00%	0.00%	0.00%	0.00%	0.00%	0.00%
Total	99.98%	99.99%	100.00%	100.01%	100.01%	99.99%	100.01%
Recal Into:							
Andradite	59.70%	46.35%	45.92%	62.46%	60.98%	41.61%	37.95%
Schorlomite	8.91%	22.43%	23.75%	11.16%	12.75%	26.35%	22.68%
Morimotoite	31.39%	31.22%	30.33%	26.38%	26.26%	32.05%	39.37%
Quality Index	Superior	Superior	Superior	Superior	Superior	Superior	Superior

Sample	PL-76	PL-76	PL-76	PL-76	PL-76	PL-43	PL-43
Analysis (wt. %)	1	2	3	4	5	1	2
SiO2	30.10	31.17	29.59	29.49	30.10	28.92	29.01
TiO2	10.39	8.93	11.67	12.16	11.31	13.44	11.57
ZrO2	2.03	1.74	1.65	1.77	1.95	1.78	2.26
Al2O3	2.18	2.38	2.31	1.89	2.31	1.02	1.32
V2O3							
FeO / FeOtot	19.43	20.29	19.68	19.45	19.68	19.74	18.67
MnO	0.43	0.47	0.50	0.35	0.45	0.62	0.60
MgO	0.93	0.84	0.76	0.97	0.78	0.85	0.85
CaO	32.24	32.56	32.42	32.36	32.72	32.53	31.28
Total (calc)	97.73	98.38	98.58	98.44	99.30	98.90	95.56
Recalculated (wt. %)							
final FeO	3.12	2.63	3.44	3.69	3.54	3.89	4.22
final Fe2O3	18.12	19.63	18.04	17.51	17.94	17.62	16.06
Total	99.54	100.35	100.38	100.19	101.10	100.67	97.17
End-members							
Kimzeyite	4.21%	3.57%	3.40%	3.66%	3.99%	3.68%	4.83%
Schorlomite	11.01%	7.02%	13.44%	15.62%	12.30%	22.17%	16.05%
Schorlomite-Al	6.72%	8.23%	8.11%	5.78%	7.43%	1.42%	1.99%
Morimotoite	22.23%	18.52%	24.35%	26.15%	24.82%	27.60%	30.90%
Morimotoite-Mg	8.82%	7.53%	6.76%	8.57%	7.12%	10.75%	9.31%
Andradite	44.98%	53.01%	41.81%	38.16%	42.40%	32.98%	34.84%
Calderite	1.03%	1.12%	1.19%	0.84%	1.07%	1.11%	1.48%
Skiagite							
Khoharite	0.99%	1.00%	0.94%	1.23%	0.88%		0.60%
Remainder	0.00%	0.00%	0.00%	0.00%	0.00%	0.28%	0.00%
Total	99.99%	100.00%	100.00%	100.01%	100.01%	99.99%	100.00%
Recal Into:							
Andradite	47.97%	56.21%	44.26%	40.48%	45.07%	34.75%	37.43%
Schorlomite	18.91%	16.17%	22.81%	22.70%	20.97%	24.85%	19.38%
Morimotoite	33.12%	27.62%	32.93%	36.83%	33.95%	40.40%	43.19%
Quality Index	Superior	Superior	Superior	Superior	Superior	Superior	Superior

Sample	PL-95	PL-95	PL-95	PL-90	PL-90	PL-90	ETR-7B
Analysis (wt. %)	1	2	3	1	2	3	1
SiO2	28.72	29.11	28.61	28.72	28.84	29.96	32.54
TiO2	11.62	11.86	11.83	14.73	14.92	11.50	9.14
ZrO2	4.48	1.74	4.62	0.91	1.00	2.60	1.09
Al2O3	0.87	0.80	0.79	1.06	0.89	1.14	2.12
V2O3				0.66	0.28	0.85	
FeO / FeOtot	18.91	19.95	18.10	18.87	18.89	18.77	20.64
MnO	0.81	0.87	0.79	0.72	0.52	0.72	0.50
MgO	0.77	0.80	0.77	0.70	0.73	0.80	0.75
CaO	29.40	29.87	29.49	31.89	31.27	32.11	32.89
Total (calc)	96.19	95.40	95.65	98.26	97.34	98.45	99.67
Recalculated (wt. %)							
final FeO	4.72	4.06	4.58	5.29	6.60	4.39	3.79
final Fe2O3	15.77	17.66	15.03	15.09	13.66	15.98	18.73
Total	97.77	97.17	97.16	99.77	98.71	100.05	101.55
End-members							
Kimzeyite	4.51%	3.72%	4.11%	1.90%	2.11%	5.41%	2.20%
Schorlomite	14.16%	18.21%	13.60%	21.96%	20.97%	16.52%	4.75%
Schorlomite-Al	0.00%	0.41%	0.00%	3.44%	2.42%	0.32%	8.15%
Morimotoite	34.69%	29.78%	33.84%	37.80%	47.65%	31.32%	26.25%
Morimotoite-Mg	3.44%	4.41%	6.50%	6.08%	2.48%	8.77%	4.96%
Goldmanite				2.26%	0.97%	2.91%	
Spessartine							
Pyrope							
Almandine							
Grossular							
Andradite	28.68%	35.89%	27.36%	23.88%	19.83%	32.55%	51.08%
Calderite	2.01%	2.15%	1.97%	1.74%	1.27%	1.73%	1.17%
Skiagite							
Khoharite	2.22%	2.02%	1.22%	0.94%	2.31%	0.47%	1.44%
Remainder	0.00%	0.00%	0.00%	0.00%	0.00%	0.00%	0.00%
Total	100.00%	99.99%	100.01%	100.00%	100.01%	100.00%	100.00%
Recal Into:							
Andradite	35.42%	40.46%	33.65%	25.63%	21.24%	36.38%	53.66%
Schorlomite	17.49%	20.99%	16.73%	27.26%	25.06%	18.82%	13.55%
Morimotoite	47.09%	38.55%	49.62%	47.10%	53.70%	44.80%	32.79%
Quality Index	Superior	Superior	Superior	Superior	Superior	Superior	Superior

Sample	ETR-7B	ETR-6A	PL-68	PL-20	PL-20	PL-20	PL-20
Analysis (wt. %)	2	1	Big GNT	1--3	1--4	1--5	1--6
SiO2	30.82	32.17	30.34	29.87	34.87	30.54	32.12
TiO2	11.91	8.25	10.68	13.80	3.44	13.11	6.03
ZrO2	1.86	1.04	3.49	1.63		2.49	5.38
Al2O3	2.02	2.63	0.58	1.10	1.48	1.65	1.79
V2O3			0.49				
FeO / FeOtot	19.60	20.63	19.77	21.21	27.87	20.98	22.83
MnO	0.43	0.63	0.51	0.63	0.69	0.58	0.60
MgO	0.98	0.64	0.73				
CaO	32.69	32.40	31.51	31.75	32.12	32.21	31.27
Total (calc)	100.31	98.39	98.64	99.99	100.47	101.56	100.02
Recalculated (wt. %)							
final FeO	4.59	3.21	3.23	7.77	2.94	7.91	6.30
final Fe2O3	16.68	19.36	18.38	14.94	27.71	14.53	18.37
Total	101.98	100.33	100.48	101.49	103.25	103.02	101.86
End-members							
Kimzeyite	3.77%	2.13%	2.91%	3.36%		5.05%	8.93%
Schorlomite	12.11%	2.18%	13.67%	18.26%	0.00%	14.80%	2.93%
Schorlomite-Al	6.12%	10.87%	0.00%	2.12%	6.96%	3.04%	0.00%
Morimotoite	31.86%	22.47%	22.98%	47.00%	7.32%	46.41%	32.55%
Morimotoite-Mg	6.10%	3.46%	9.13%	0.00%	0.00%	0.00%	0.00%
Goldmanite			1.67%				
Spessartine					0.20%		
Pyrope							
Almandine							
Grossular							
Andradite	37.02%	55.89%	39.58%	25.12%	79.84%	26.45%	47.97%
Calderite	1.01%	1.49%	1.23%	1.50%	1.40%	1.36%	1.43%
Skiagite				2.64%	4.28%	2.88%	4.02%
Khoharite	2.01%	1.51%	0.04%				
Remainder	0.00%	0.00%	0.00%	0.00%	0.00%	0.00%	0.00%
Total	100.00%	100.00%	99.99%	100.00%	100.00%	99.99%	100.00%
Recal Into:							
Andradite	39.72%	58.91%	46.37%	27.16%	84.83%	29.16%	57.48%
Schorlomite	19.56%	13.76%	16.01%	22.03%	7.39%	19.67%	3.51%
Morimotoite	40.73%	27.33%	37.62%	50.81%	7.78%	51.17%	39.01%
Quality Index	Superior	Superior	Superior	Superior	Superior	Superior	Superior

Sample	PL-20	PL-20	PL-20	ETR-6A	NE4-2	NE4-2	NE4-2
Analysis (wt. %)	2--4	2--5	2--12	1--3	1--1	1--2	3--3
SiO2	33.72	34.91	37.03	30.50	32.88	36.08	28.73
TiO2	5.47	4.77		8.83	9.38	2.59	13.36
ZrO2	3.04	0.58		1.34	0.18		
Al2O3			22.88	2.47	1.92	2.93	1.43
V2O3							
FeO / FeOtot	25.58	27.43	1.40	22.45	22.13	24.19	19.63
MnO	0.63	0.56		0.40	0.68	0.49	0.56
MgO				0.68	0.77	0.45	1.04
CaO	31.86	32.12	37.82	31.55	33.61	33.45	31.62
Total (calc)	100.30	100.37	99.13	98.22	101.55	100.18	96.37
Recalculated (wt. %)							
final FeO	5.56	4.65	0.00	3.16	2.74	1.32	3.44
final Fe2O3	22.25	25.31	1.56	21.44	21.55	25.42	17.99
Total	102.53	102.90	99.29	100.37	103.71	102.73	98.17
End-members							
Kimzeyite				2.76%	0.36%		
Schorlomite	2.37%	4.29%		8.79%	7.33%	0.00%	18.88%
Schorlomite-Al	0.00%	0.00%		9.54%	8.83%	3.69%	7.27%
Morimotoite	29.77%	21.13%		19.50%	18.59%	8.43%	24.80%
Morimotoite-Mg	0.00%	0.00%	0.00%	0.00%	6.39%	0.00%	9.56%
Goldmanite							
Spessartine						1.12%	
Pyrope						1.81%	
Almandine						0.17%	
Grossular			92.20%			7.21%	
Andradite	57.08%	68.40%	1.23%	54.66%	55.97%	77.57%	36.86%
Calderite	1.49%	1.31%		0.95%	1.56%		1.36%
Skiagite	3.07%	3.70%		0.94%			
Khoharite				2.86%	0.98%		1.27%
Remainder	0.00%	0.00%	6.57%	0.00%	0.00%	0.00%	0.00%
Total	100.00%	100.00%	100.00%	100.00%	100.01%	100.00%	100.00%
Recal Into:							
Andradite	63.98%	72.91%	N/A	59.10%	57.64%	86.49%	37.86%
Schorlomite	2.66%	4.57%	N/A	19.82%	16.64%	4.11%	26.86%
Morimotoite	33.37%	22.52%	N/A	21.08%	25.72%	9.40%	35.29%
Quality Index	Superior	Superior	Poor	Superior	Superior	Superior	Superior

Sample	WS-1-04	WS-1-04	WS-1-04	WS-1-04	WS-1-04	WS-1-04	WS-1-04
Analysis (wt. %)	1--11	2--2	2--3	2--4	2--5	2--8	3--5
SiO2	31.78	26.87	33.31	26.69	34.13	34.40	34.93
TiO2	5.77	11.41	4.89	11.79	4.64	0.24	5.08
ZrO2		8.46	2.24	7.81	1.08		0.13
Al2O3	1.62	1.72	1.37	1.85	1.73	1.74	2.23
V2O3							
FeO / FeOtot	20.93	16.15	23.13	16.31	24.40	26.73	21.66
MnO	1.72	0.30	0.27	0.34			0.22
MgO	0.44	2.06	1.16	1.86	0.96	0.78	1.00
CaO	33.49	30.86	32.03	30.41	33.39	32.60	33.19
Total (calc)	95.75	97.83	98.40	97.72	100.33	96.49	98.44
Recalculated (wt. %)							
final FeO	0.00	3.81	2.16	3.02	1.12	0.00	1.89
final Fe2O3	23.26	13.71	23.31	14.77	25.87	29.71	21.98
Total	98.25	99.20	100.74	99.20	102.92	99.47	100.65
End-members							
Kimzeyite		8.86%	4.58%	9.52%	2.15%		0.26%
Schorlomite	5.92%	14.51%	3.44%	16.85%	2.07%	0.00%	0.00%
Schorlomite-Al	8.17%	0.00%	2.19%	0.00%	6.19%	0.76%	5.39%
Morimotoite		27.88%	15.14%	22.02%	7.69%	0.00%	13.03%
Morimotoite-Mg	5.61%	18.16%	4.47%	16.48%	4.35%	0.00%	7.77%
Goldmanite							
Spessartine							0.51%
Pyrope						2.03%	1.52%
Almandine							
Grossular						1.32%	3.17%
Andradite	68.94%	17.79%	66.18%	21.98%	75.09%	92.88%	68.34%
Calderite		0.74%	0.64%	0.84%			
Skiagite							
Khoharite		2.90%	3.35%	1.76%	2.45%		
Remainder	11.36%	0.00%	0.00%	0.81%	0.00%	3.01%	0.00%
Total	100.00%	100.01%	99.99%	99.99%	99.99%	100.00%	99.99%
Recal Into:							
Andradite	N/A	22.71%	72.39%	28.42%	78.72%	99.19%	72.29%
Schorlomite	N/A	18.52%	6.16%	21.79%	8.66%	0.81%	5.70%
Morimotoite	N/A	58.77%	21.45%	49.79%	12.62%	0.00%	22.00%
Quality Index	Poor	Superior	Superior	Superior	Superior	Fair	Superior

Sample	~~WS-1-04~~	WS-1-04	WS-1-04	WS-1-04	WS-1-04	WS-1-04	WS-1-04
Analysis (wt. %)	~~3--6~~	4--5	4--8	4--9	5--8	5--9	6--5
SiO2	~~35.51~~	33.33	34.61	35.03	34.50	34.51	34.01
TiO2	~~1.68~~	5.53	3.40	3.73	4.28	4.55	0.73
ZrO2	~~0.14~~	1.12	0.09	0.18			
Al2O3	~~12.66~~	1.93	3.14	11.27	1.76	1.95	1.01
V2O3							
FeO / FeOtot	~~9.38~~	22.59	22.46	10.98	25.39	24.84	26.81
MnO	~~0.49~~	0.22	0.35	0.36	0.18		
MgO	~~0.34~~	1.17	0.77	0.16	0.63	0.67	0.85
CaO	~~34.85~~	33.82	33.73	35.67	33.79	33.81	31.48
Total (calc)	~~95.05~~	99.71	98.75	97.38	100.53	100.33	94.89
Recalculated (wt. %)							
final FeO	~~0.00~~	0.00	0.00	0.00	0.51	0.85	0.00
final Fe2O3	~~10.42~~	25.11	24.96	12.20	27.65	26.66	29.80
Total	~~96.14~~	102.25	101.28	98.64	103.30	103.00	97.88
End-members							
Kimzeyite	~~0.28%~~	2.24%	0.18%	0.35%			
Schorlomite		3.74%	0.00%		1.21%	0.11%	0.00%
Schorlomite-Al	~~4.59%~~	7.10%	8.08%	8.33%	8.44%	9.36%	2.36%
Morimotoite		0.00%	0.00%		3.45%	5.77%	0.00%
Morimotoite-Mg	~~1.15%~~	12.51%	1.63%	1.92%	3.45%	3.16%	0.00%
Pyrope			0.27%				1.13%
Grossular	~~56.11%~~		6.63%	44.90%			
Andradite	~~32.06%~~	73.65%	76.93%	37.05%	81.64%	79.94%	94.18%
Calderite					0.41%		
Skiagite							
Khoharite		0.22%			1.40%	1.66%	1.25%
Remainder	~~5.80%~~	0.38%	4.70%	7.45%	0.00%	0.00%	1.08%
Total	~~99.99%~~	99.99%	100.01%	100.00%	100.00%	100.00%	100.00%
Recal Into:							
Andradite	~~N/A~~	75.93%	88.79%	N/A	83.14%	81.29%	97.56%
Schorlomite	~~N/A~~	11.18%	9.33%	N/A	9.83%	9.63%	2.44%
Morimotoite	~~N/A~~	12.90%	1.88%	N/A	7.03%	9.08%	0.00%
Quality Index	~~Poor~~	Superior	Fair	Poor	Superior	Superior	Good

Sample	WS-1-04	ETR-7B	ETR-7B	ETR-7B	ETR-7B	PL-85	PL-85
Analysis (wt. %)	6--6	1--1	2--5	2--6	3--3	2--1	2--2
SiO2	34.77	31.38	34.96	36.06	29.90	31.40	32.65
TiO2	0.23	10.32	4.86	1.08	10.25	9.79	9.17
ZrO2		1.22			1.95		
Al2O3	0.42	2.30	0.89	0.79	2.00	1.53	1.73
V2O3							
FeO / FeOtot	27.31	19.73	24.05	25.57	19.57	21.37	21.58
MnO	0.33	0.51	0.19	0.45	0.62	0.59	0.50
MgO	1.64	0.74	0.31	0.10	0.69	0.63	0.73
CaO	31.21	31.95	32.44	32.53	31.37	32.24	32.62
Total (calc)	95.91	98.15	98.14	96.58	96.46	97.63	99.05
Recalculated (wt. %)							
final FeO	0.00	4.75	1.83	1.78	3.55	2.96	3.37
final Fe2O3	30.35	16.65	24.70	26.44	17.80	20.46	20.24
Total	98.98	99.82	100.62	99.23	98.24	99.68	101.08
End-members							
Kimzeyite		2.51%			4.10%		
Schorlomite	0.64%	6.03%	0.00%		10.76%	9.57%	5.81%
Schorlomite-Al	0.09%	8.94%	4.35%		6.07%	7.63%	8.47%
Morimotoite	0.00%	33.54%	12.74%	6.87%	25.64%	20.91%	23.40%
Morimotoite-Mg	0.00%	2.10%	1.91%	0.00%	5.43%	5.67%	4.25%
Spessartine			0.02%	1.07%			
Pyrope				0.42%			
Almandine				0.23%			
Grossular				2.22%			
Andradite	93.69%	43.26%	76.35%	84.15%	44.41%	53.39%	54.73%
Calderite		1.22%	0.43%		1.51%	1.41%	1.17%
Skiagite							
Khoharite	2.41%	2.41%	0.65%		1.15%	0.76%	1.60%
Remainder	3.17%	0.00%	0.00%	5.04%	0.00%	0.00%	0.00%
Total	100.00%	100.01%	100.00%	100.00%	99.99%	100.00%	99.99%
Recal Into:							
Andradite	99.23%	46.09%	80.07%	N/A	48.11%	54.94%	56.62%
Schorlomite	0.77%	15.95%	4.56%	N/A	18.23%	17.70%	14.77%
Morimotoite	0.00%	37.97%	15.36%	N/A	33.66%	27.35%	28.61%
Quality Index	Fair	Superior	Superior	Poor	Superior	Superior	Superior

Sample	PL-85	PL-78	PL-78	PL-78	PL-78
Analysis (wt. %)	5--2	1--2	2--3	3--5	4--3
SiO2	32.60	30.73	30.67	30.68	30.41
TiO2	9.58	9.80	9.05	11.22	10.46
ZrO2	0.59	1.62	1.15	1.04	1.31
Al2O3	1.40	1.98	2.28	2.25	2.54
V2O3					
FeO / FeOtot	22.34	21.99	21.72	21.65	21.36
MnO	0.60	0.47	0.56	0.53	0.48
MgO	0.61	0.87	0.69	0.78	0.84
CaO	32.82	32.16	32.37	33.22	32.89
Total (calc)	100.54	99.62	98.49	101.37	100.29
Recalculated (wt. %)					
final FeO	4.20	3.28	2.22	2.90	2.41
final Fe2O3	20.16	20.80	21.68	20.84	21.06
Total	102.56	101.71	100.67	103.46	102.40
End-members					
Kimzeyite	1.19%	3.30%	2.36%	2.08%	2.64%
Schorlomite	8.78%	11.90%	9.66%	13.38%	11.79%
Schorlomite-Al	5.62%	6.45%	8.95%	8.79%	9.74%
Morimotoite	28.96%	22.89%	15.59%	19.86%	16.71%
Morimotoite-Mg	1.68%	2.00%	4.48%	4.99%	5.35%
Andradite	50.44%	49.41%	56.24%	48.16%	50.98%
Calderite	1.40%	1.11%	1.33%	1.23%	1.12%
Skiagite					
Khoharite	1.94%	2.94%	1.39%	1.51%	1.67%
Remainder	0.00%	0.00%	0.00%	0.00%	0.00%
Total	100.01%	100.00%	100.00%	100.00%	100.00%
Recal Into:					
Andradite	52.83%	53.33%	59.25%	50.60%	53.91%
Schorlomite	15.08%	19.81%	19.61%	23.29%	22.77%
Morimotoite	32.09%	26.86%	21.14%	26.11%	23.33%
Quality Index	Superior	Superior	Superior	Superior	Superior

Nepheline compositions

Sample	PL86	PL86	PL86	PL36	PL36	PL76	PL76	PL90	PL90	PL90	ETR7B	ETR7B	ETR7B
Site	1	2	3	1	2	1	3	1	2	3	1	2	3
Si	41.88	40.77	41.36	41.52	41.2	41.71	41.75	41.65	41.79	42.05	41.67	41.82	41.87
Al	35.09	34.11	34.85	33.77	33.91	34.67	34.01	33.24	33.83	33.57	33.09	33.29	33.31
Fe	0.75	0.84	0.8	1.24	1.19	0.88	0.86	0.88	0.77	0.87	0.9	0.92	1.01
Ca	0.6	b.d.	b.d.	b.d.	b.d.	b.d.	b.d.	b.d.	b.d.	b.d.	b.d.	b.d.	b.d.
Na	15.45	15.5	16.17	14.67	16.09	16.1	16.08	15.36	15.75	15.96	15.58	15.76	15.71
K	7.45	7.64	7.83	7.26	7.47	7.91	7.83	7.97	7.91	8.07	7.93	7.93	7.87
Total	101.22	98.86	101.01	98.46	99.86	101.27	100.53	99.1	100.05	100.52	99.17	99.72	99.77
Si	1.0044	1.0039	0.9986	1.0212	1.0067	1.0045	1.0126	1.023	1.0171	1.0207	1.0241	1.0225	1.0218
Al	0.9918	0.9899	0.9917	0.9789	0.9765	0.984	0.9721	0.9636	0.9704	0.9603	0.9585	0.9593	0.9603
Fe	0.015	0.0173	0.0162	0.0255	0.0243	0.0177	0.0174	0.0181	0.0157	0.0177	0.0185	0.0188	0.0207
Ca	0.0154												
Na	0.7184	0.74	0.757	0.6996	0.7623	0.7517	0.7561	0.7314	0.7432	0.7511	0.7424	0.7471	0.7451
K	0.2279	0.24	0.2412	0.2278	0.2329	0.243	0.2423	0.2497	0.2456	0.2499	0.2486	0.2474	0.2456
Recalculated into nepheline-kalsilite-quartz													
Ne	73.03	72.74	73.8	70.46	74.27	73.24	73.28	71.21	72.25	72.39	71.85	72.23	72.22
Kal	25.8	26.27	26.18	20.55	25.26	26.36	26.14	27.07	26.58	26.81	26.79	26.63	26.51
Qtz	1.17	0.99	0.02	4	0.48	0.4	0.58	1.72	1.16	0.8	1.35	1.14	1.27

Mica compositions

Sample	PL34	PL34	PL34	PL34	PL34	PL76	PL76	PL96A	PL96A	PL96A	PL67	PL67	PL67	PL67
Rock	Ijolite	Ijolite	Ijolite	Ijolite	Ijolite	Ijolite	Ijolite	Urtite	Urtite	Urtite	Malignite	Malignite	Malignite	Malignite
Mg	7.7	7.46	7.54	7.6	7.22	7.19	13.08	7.66	3.19	3.03	9.96	10.48	9.62	10.54
Al	10.76	10.6	10.62	10.44	10.66	11.32	11.41	11.34	11.42	11.45	11.75	11.58	11.55	11.4
Si	35.13	35.2	35.04	35.38	35.25	35.43	37.16	35.34	33.12	32.86	36.38	36.82	36.83	37.27
K	9.53	9.55	9.38	9.78	9.62	9.32	9.47	9.55	9.26	9.22	9.91	9.83	9.92	9.91
Ti	3.46	3.49	3.45	3.65	3.3	2.09	2.34	2.53	2.34	2.25	2.96	2.73	4.21	3.13
Mn	0.96	0.95	0.87	0.84	0.9	0.69	1.21	1.44	1.2	1.22	0.9	0.74	0.98	0.84
Fe	27.38	27.73	27.35	28.26	27.92	29.29	19.68	27.78	35.39	35.39	24.89	24.32	23.99	23.7
Ba	b.d.	b.d.	b.d.	b.d.	b.d.	b.d.	b.d.	b.d.	b.d.	b.d.	b.d.	b.d.	b.d.	b.d.
	94.92	94.98	94.25	95.95	94.87	95.33	94.35	95.64	95.92	95.42	96.75	96.5	97.1	96.79
22Ox														
Mg	1.86	1.8	1.83	1.82	1.75	1.74	3.04	1.84	0.8	0.76	2.32	2.44	2.22	2.43
Al	2.06	2.03	2.04	1.98	2.04	2.18	2.1	2.15	2.26	2.28	2.17	2.13	2.11	2.08
Si	5.69	5.71	5.72	5.7	5.73	5.74	5.8	5.7	5.55	5.55	5.69	5.74	5.71	5.78
K	1.97	1.97	1.95	2.01	2	1.93	1.88	1.96	1.98	1.99	1.98	1.96	1.96	1.96
Ti	0.42	0.43	0.42	0.44	0.4	0.25	0.27	0.34	0.29	0.29	0.35	0.32	0.49	0.36
Mn	0.13	0.13	0.12	0.11	0.12	0.09	0.16	0.2	0.17	0.17	0.12	0.1	0.13	0.11
Fe	3.71	3.76	3.75	3.81	3.8	3.97	2.57	3.74	4.96	4.99	3.25	3.17	3.11	3.07
Ba	0	0	0	0	0	0	0	0	0	0	0	0	0	0

Sample	PL67	PL46	PL46	PL46	PL46	PL51	PL51	PL51	PL51	PL51	PL55	PL55	PL55	PL55
Rock	Malignite	Por. Malig	Por. Malig	Por. Malig	Por. Malig	Biotite Pyroxenite	B.P.	B.P.	B.P.	B.P.	B.P.	B.P.	B.P.	B.P.
Mg	9.57	4.36	4.41	6.49	6.86	11.23	11.78	10.48	11.11	11.63	11.36	10.81	12.24	12.05
Al	11.6	10.21	10.35	9.73	9.72	9.88	10.17	10.94	10.69	9.5	11.29	11.94	11.35	11.44
Si	35.43	34.54	35.14	35.47	35.6	36.42	37.92	37.06	36.77	37.04	37.19	36.88	37.25	26.66
K	9.46	9.04	9.22	9.41	9.46	9.87	9.98	9.85	9.84	9.74	9.78	10.11	9.83	9.79
Ti	3.08	1.64	2.98	1.5	1.83	2.82	2.36	3.14	3.01	2.29	3.38	3.54	2.94	2.83
Mn	0.78	0.93	1.23	1.43	1.57	0.69	0.87	0.85	0.91	0.87	0.77	0.8	0.83	0.89
Fe	24.35	34.37	32.71	30.72	30.95	23.4	24.07	25.1	23.46	23.32	22.38	23.59	21.87	21.57
Ba	b.d.	b.d.	b.d.	b.d.	b.d.	b.d.	b.d.	b.d.	b.d.	b.d.	b.d.	b.d.	b.d.	b.d.
	94.27	95.09	96.04	94.75	95.99	94.31	97.15	97.42	95.79	94.39	96.15	97.67	96.31	85.23
22Ox														
Mg	2.29	1.09	1.08	1.6	1.67	2.67	2.72	2.42	2.6	2.76	2.62	2.48	2.82	2.81
Al	2.19	2.02	2	1.9	1.87	1.86	1.86	2	1.98	1.78	2.06	2.16	2.07	2.11
Si	5.68	5.79	5.77	5.87	5.82	5.82	5.87	5.75	5.77	5	5.76	5.67	5.75	5.78
K	1.93	1.93	1.93	1.99	1.97	2.01	1.97	1.95	1.97	1.98	1.93	1.98	1.94	1.95
Ti	0.37	0.21	0.37	0.19	0.22	0.34	0.27	0.37	0.36	0.27	0.39	0.41	0.34	0.33
Mn	0.11	0.13	0.17	0.2	0.22	0.09	0.11	0.11	0.12	0.12	0.1	0.1	0.11	0.12
Fe	3.26	4.8	4.49	4.25	4.23	3.13	3.12	3.26	3.08	3.11	2.9	3.03	2.82	2.82
Ba	0	0	0	0	0	0	0	0	0	0	0	0	0	0

Sample	PL55	PL48	PL48	PL48	PL48	PL48	PL48	PL48	PL48	PL48	PL38	PL38	PL38	PL38
Rock	B.P.	B.P.	B.P.	B.P.	B.P.	B.P.	B.P.	B.P.	B.P.	B.P.	B.P.	B.P.	B.P.	B.P.
Mg	11.18	13.04	4.24	6.33	12.1	13	13.64	13.56	13.56	10.31	7.42	8.75	7.4	8.06
Al	11.87	10.37	8.89	6.19	12.08	11.75	11.88	11.19	11.5	14.6	11.01	10.28	11.42	10.69
Si	36.48	36.67	36.34	36.25	36.3	37.29	37.49	37.67	38.02	33.56	35.83	37.06	35.15	35.87
K	9.8	9.47	6.37	9.06	9.5	9.85	9.82	9.89	9.96	7.7	9.56	9.62	9.57	9.42
Ti	3.35	1.96			2.38	2.17	1.37	1.88	2.38	0.8	3.51	2.88	3.47	3.02
Mn	0.83	0.9	1.38	1.51	0.77	0.91	0.91	0.79	0.9	0.9	1.16	1.3	1.17	1.18
Fe	22.14	21.05	37.02	37.01	22.05	21.57	20.95	21.94	21.05	23.67	28.14	26.69	27.34	27.15
Ba	b.d.	b.d.	0.39	b.d.	0.2	0.48	b.d.	b.d.	b.d.	2.1	b.d.	b.d.	b.d.	b.d.
	95.65	93.46	94.63	96.35	95.38	97.02	96.06	96.92	97.37	93.64	96.63	96.58	95.52	95.39
22Ox														
Mg	2.6	3.09	1.06	1.59	2.82	2.98	3.13	3.1	3.07	2.49	1.76	2.06	1.77	1.93
Al	2.18	1.94	1.76	1.23	2.22	2.13	2.15	2.02	2.06	2.79	2.07	1.91	2.17	2.02
Si	5.69	5.83	6.1	6.09	5.67	5.73	5.77	5.78	5.77	5.44	5.71	5.86	5.66	5.76
K	1.95	1.92	1.36	1.94	1.89	1.93	1.93	1.94	1.93	1.59	1.94	1.94	1.96	1.93
Ti	0.39	0.23			0.28	0.25	0.16	0.2	0.27	0.1	0.42	0.34	0.42	0.36
Mn	0.11	0.12	0.02	0.22	0.1	0.12	0.12	0.1	0.12	0.12	0.16	0.17	0.16	0.16
Fe	2.89	2.8	5.2	5.2	2.88	2.77	2.7	2.81	2.67	3.21	3.75	3.53	3.68	3.65
Ba	0	0	0.03	0	0.01	0.03	0	0	0	0.13	0	0	0	0

Sample	PL38	PL38	PL38	PL38	PL38	PL38	PL38	PL38	PL38	PL38	PL38
Rock	B.P.	B.P.	B.P.	B.P.	B.P.	B.P.	B.P.	B.P.	B.P.	B.P.	B.P.
Mg	7.48	8.44	8.45	8.61	8.06	9.3	9.1	8.84	8.77	8.56	9.3
Al	10.85	10.11	10.51	10.63	10.73	9.88	9.84	10.39	9.86	10.61	9.97
Si	35.2	36.42	36.81	36.62	36.66	37.8	37.15	37.24	37.18	37.05	37.29
K	9.46	9.44	9.76	9.69	9.77	9.87	9.59	9.78	9.73	10.02	9.82
Ti	3	3.38	3.14	2.67	2.88	2.68	2.75	2.6	3.03	2.56	2.68
Mn	1.18	1.17	1.3	1.19	1.1	1.28	1.1	1.2	1.14	1.25	1.2
Fe	27.19	26.4	27.38	27.18	28.41	26.09	26.7	26.98	29.83	26.96	26.02
Ba	b.d.	b.d.	b.d.	b.d.	b.d.	b.d.	b.d.	b.d.	b.d.	b.d.	b.d.
	94.36	95.36	97.35	96.59	97.61	96.9	96.23	97.03	99.54	97.01	96.28
22Ox											
Mg	1.81	2.01	1.98	2.03	1.89	2.18	2.15	2.07	2.07	2.01	2.19
Al	2.08	1.91	1.95	1.99	1.99	1.83	1.84	1.93	1.84	1.97	1.86
Si	5.74	5.83	5.8	5.8	5.78	5.93	5.89	5.86	5.88	5.84	5.9
K	1.97	1.93	1.96	1.99	1.96	1.98	1.94	1.96	1.96	2.02	1.98
Ti	0.37	0.43	0.37	0.32	0.34	0.32	0.33	0.31	0.36	0.3	0.32
Mn	0.16	0.16	0.17	0.16	0.15	0.17	0.15	0.16	0.15	0.17	0.16
Fe	3.71	3.53	3.6	3.6	3.75	3.43	3.54	3.55	3.55	3.56	3.44
Ba	0	0	0	0	0	0	0	0	0	0	0

Fen

Clinopyroxene compositions

Sample	***FEN 64***	***FEN 64***	***FEN 64***	***FEN 64***	***FEN 64***	***FEN 64***
Spot	*1*	*2*	*3*	*4*	*5*	*6*
Na	1.27	0.56	0.6	0.91	1.05	0.72
Mg	13.64	11.36	11.3	11.02	11.41	9.29
Al	1.3	6.19	6.45	6.53	6.59	10.16
Si	53.07	46.44	45.99	46.5	46.55	42.03
Ca	23.25	23.96	23.99	23.43	23.2	23.49
Mn	0.31	0.21	0.28	0	0.2	0.25
Ti	0.54	1.9	1.75	2.29	2.21	3.64
Fe	7.31	8.56	8.85	8.95	8.85	10.01
Zr						
V2O5						
Recal						
Fe3+	3.27	1.44	1.55	2.34	2.71	1.86
Fe2+	4.75	7.26	7.46	6.84	6.42	8.34
Structural Formula						
Si	1.9458	1.7669	1.7536	1.7573	1.7506	1.6115
Al(IV)	0.0542	0.2331	0.2464	0.2427	0.2494	0.3885
Al(VI)	0.002	0.0444	0.0434	0.0482	0.0427	0.0706
FE3(IV)	0.0903	0.0413	0.0444	0.0667	0.0766	0.0535
FE2	0.1455	0.231	0.2378	0.2162	0.2018	0.2674
Mn	0.0096	0.0068	0.0009	0	0.0064	0.0081
Mg	0.7456	0.6444	0.6424	0.6209	0.6398	0.5311
Ca	0.9133	0.9767	0.98	0.9487	0.9348	0.965
Na	0.0903	0.0413	0.0444	0.0667	0.0766	0.0535
K	0	0	0	0		0
Ti	0.0149	0.0544	0.0502	0.0651	0.0625	0.1049
End Members Based on Acmite						
CaTiAl2O6	1.49	5.35	4.91	6.4	6.14	10.26
CaAlSiAlO6	0.2	4.37	4.25	4.74	4.2	6.9
Acmite	9.02	4.06	4.34	6.56	7.53	5.23
Wo	44.78	43.17	43.4	41.11	40.77	38.58
Fs	7.27	11.36	11.64	10.64	9.92	13.07
En	37.25	31.69	31.45	30.55	31.44	25.96
Recal into						
Ae	9.2	4.51	4.8	7.39	8.45	6.35
Hd	14.83	25.2	25.72	23.92	21.95	31.37
Di	75.97	70.29	69.48	68.69	69.6	62.28

Sample	***FEN 64***	***FEN 64***	***FEN 64***	***FEN 64***	***FEN 64***	***FEN 64***
Spot	*7*	*8*	*9*	*10*	*11*	*12*
Na	0.66	0.58	0.43	1	0.56	0.63
Mg	9.25	9.6	10.39	10.44	12.16	12.16
Al	9.51	9.42	9.34	8.42	5.45	3.11
Si	41.37	43.15	43	44.58	47.8	47.88
Ca	23.3	24.32	24	23.91	24.24	24.31
Mn	0.18	0.22	0.14	0.17	0.19	0.16
Ti	3.53	3.53	3.74	2.8	1.96	1.76
Fe	9.89	9.9	8.05	9.24	7.91	7.77
Zr						
V2O5						
Recal						
Fe3+	1.7	1.49	1.11	2.58	1.44	1.62
Fe2+	8.36	8.56	7.05	7.1	6.66	6.31
Structural Formula						
Si	1.619	1.6364	1.6431	1.6781	1.7905	1.8424
Al(IV)	0.381	0.3636	0.3569	0.3219	0.2095	0.141
Al(VI)	0.0577	0.0574	0.0637	0.0517	0.0311	0.0166
FE3(IV)	0.0501	0.0426	0.0319	0.073	0.0407	0.0304
FE2	0.2736	0.2713	0.2254	0.2236	0.2087	0.203
Mn	0.006	0.0071	0.0045	0.0054	0.006	0.0052
Mg	0.5397	0.5428	0.5919	0.5859	0.6791	0.6976
Ca	0.977	0.9881	0.9826	0.9643	0.9728	1.0022
Na	0.0501	0.0426	0.0319	0.073	0.0407	0.047
K	0	0	0		0	0
Ti	0.1039	0.1007	0.1075	0.0793	0.0552	0.0509
End Members Based on Acmite						
CaTiAl2O6	10.13	9.84	10.56	7.73	5.44	4.97
CaAlSiAlO6	5.62	5.61	6.26	5.04	3.07	0
Acmite	4.88	4.17	3.13	7.12	4.01	4.59
Wo	39.74	40.58	39.87	40.64	43.71	46.45
Fs	13.33	13.26	11.08	10.9	10.29	9.91
En	26.3	26.53	29.09	28.57	33.48	34.07
Recal into						
Ae	5.8	4.98	3.78	8.27	4.39	4.96
Hd	31.69	31.67	26.53	25.33	22.47	21.42
Di	62.51	63.35	69.69	66.4	73.14	73.62

Sample	***FEN 64***	***FEN 64***	***FEN 64***	***FEN 64***	***FEN 64***	***FEN 64***
Spot	*13*	*14*	*15*	*16*	*17*	*18*
Na	0.59	0.59	0.58	0.88	0.99	0.66
Mg	10.86	9.77	6	10.98	11.13	9.72
Al	7.98	9.02	9.6	6.94	6.57	9.73
Si	45.03	43.83	43.37	46.92	47.05	43.13
Ca	24.35	24.19	24.16	23.54	23.83	24.11
Mn	0.28	0.27	0.18	0.4	0.29	0.18
Ti	2.57	2.64	9.29	2.47	2.38	3.44
Fe	9.07	10.08	10.21	9.22	9.2	10.4
Zr						
V2O5						
Recal						
Fe3+	1.52	1.52	1.49	2.27	2.55	1.7
Fe2+	7.7	8.71	8.87	7.18	6.9	8.58
Structural Formula						
Si	1.6963	1.6659	1.6031	1.7468	1.7505	1.6292
Al(IV)	0.3037	0.3341	0.3969	0.2532	0.2495	0.3708
Al(VI)	0.0506	0.07	0.0213	0.0513	0.0385	0.0624
FE3(IV)	0.0431	0.0435	0.0416	0.0635	0.0714	0.0483
FE2	0.2426	0.2769	0.274	0.2235	0.2148	0.271
Mn	0.0089	0.0087	0.0056	0.0126	0.0091	0.0058
Mg	0.6099	0.5537	0.3307	0.6095	0.6174	0.5474
Ca	0.9828	0.9851	0.9568	0.939	0.9499	0.9758
Na	0.0431	0.0435	0.0416	0.0635	0.0714	0.0483
K	0	0	0	0	0	0
Ti	0.0728	0.0755	0.2582	0.0691	0.0666	0.0977
End Members Based on Acmite						
CaTiAl2O6	7.12	7.37	21.54	6.85	6.56	9.53
CaAlSiAlO6	4.95	6.84	0	5.08	3.8	6.08
Acmite	4.21	4.25	4.51	6.29	7.04	4.71
Wo	42.02	41	41.14	40.53	41.61	39.77
Fs	11.87	13.52	14.87	11.07	10.58	13.22
En	29.83	27.03	17.94	30.18	30.41	26.69
Recal into						
Ae	4.81	4.97	6.43	7.2	7.9	5.59
Hd	27.09	31.68	42.4	24.9	23.77	31.26
Di	68.1	63.34	51.16	67.9	68.32	63.14

Sample	***FEN 64***	***FEN 64***	***419 (Fen)***	***419 (Fen)***	***419 (Fen)***	***419 (Fen)***
Spot	*19*	*20*	*1*	*2*	*3*	*4*
Na	0.92	0.7	5.51	5.84	6.78	5.8
Mg	11.06	9.54	4.18	3.75	3.51	3.88
Al	7.45	10.59	1.23	1.25	1.25	1.26
Si	45.93	41.86	51.76	52.25	52.38	52
Ca	23.96	23.81	14.87	14.17	12.55	14.13
Mn	0.25	0.33	0.88	0.66	0.73	0.86
Ti	2.92	3.39	0.35	0.38	0.26	0.45
Fe	9.03	10.34	21.09	21.78	22.75	22.24
Zr				0.5		0.62
V2O5			0.44	0.38	0.55	0.45
Recal						
Fe3+	2.37	1.8	14.2	15.05	17.47	14.94
Fe2+	6.9	8.72	8.32	8.24	7.03	8.79
Structural Formula						
Si	1.7104	1.5941	1.9725	1.9824	1.9788	1.9697
Al(IV)	0.2896	0.4059	0.0275	0.0176	0.0212	0.0303
Al(VI)	0.0373	0.0694	0.0277	0.0382	0.0344	0.026
FE3(IV)	0.0664	0.0517	0.4071	0.4296	0.4966	0.426
FE2	0.2148	0.2776	0.265	0.2615	0.2221	0.2785
Mn	0.0079	0.0106	0.0284	0.0212	0.0234	0.0276
Mg	0.614	0.5417	0.2375	0.2121	0.1977	0.2191
Ca	0.9559	0.9715	0.6071	0.576	0.508	0.5735
Na	0.0664	0.0517	0.4071	0.4296	0.4966	0.426
K	0	0	0	0	0	0
Ti	0.0818	0.0971	0.01	0.0108	0.0074	0.0128
End Members Based on Acmite						
CaTiAl2O6	8.03	9.42	1.03	0.92	0.76	1.32
CaAlSiAlO6	3.67	6.74	0.77	0	0.67	0.48
Acmite	6.52	5.02	41.94	44.81	51.33	43.9
Wo	41.09	39.06	30.37	29.58	25.54	28.65
Fs	10.55	13.47	13.65	13.63	11.48	14.35
En	30.15	26.29	12.23	11.06	10.22	11.29
Recal into						
Ae	7.42	6.03	44.76	47.56	54.19	46.12
Hd	23.99	31.84	29.13	28.95	24.24	30.16
Di	68.59	62.13	26.11	23.49	21.57	23.72

Sample	***419 (Fen)***	***419 (Fen)***	***419 (Fen)***	***419 (Fen)***	***419 (Fen)***	***419 (Fen)***
Spot	*5*	*6*	*7*	*8*	*9*	*10*
Na	7.65	5.44	4.33	4.1	4.13	5.38
Mg	4.03	5.28	5.06	5.04	4.92	4.61
Al	1.01	1.29	1.58	1.48	1.45	1.38
Si	53.37	52.49	50.97	51.45	50.65	51.82
Ca	11.13	15.19	17.08	17.37	17.27	15.55
Mn	0.58	0.68	0.83	0.98	0.87	0.68
Ti	0.3	0.48	1.01	0.95	0.99	0.48
Fe	22.13	19.77	19.91	19.97	20.17	20.68
Zr	0.45	0.48			0.4	
V2O5	0.38	0.45	0.38	0.37	0.4	
Recal						
Fe3+	19.71	14.02	11.16	10.56	10.64	13.82
Fe2+	4.39	7.16	9.47	10.46	10.59	8.21
Structural Formula						
Si	1.9922	1.9711	1.9417	1.9471	1.9382	1.96
Al(IV)	0.0078	0.0289	0.0583	0.0529	0.0618	0.04
Al(VI)	0.0367	0.0282	0.0126	0.0131	0.0036	0.0215
FE3(IV)	0.5537	0.3961	0.3198	0.3008	0.3064	0.3945
FE2	0.1372	0.2248	0.3017	0.3312	0.339	0.2596
Mn	0.0183	0.0216	0.0268	0.0314	0.0282	0.0218
Mg	0.2243	0.2956	0.2874	0.2844	0.2807	0.26
Ca	0.4451	0.6111	0.6971	0.7043	0.708	0.6302
Na	0.5537	0.3961	0.3168	0.3008	0.3064	0.3945
K	0	0	0	0	0	0
Ti	0.0084	0.0136	0.0289	0.027	0.0285	0.0137
End Members Based on Acmite						
CaTiAl2O6	0.41	1.4	2.96	2.72	2.89	1.39
CaAlSiAlO6	0	0.19	0.05	0	0.36	1.29
Acmite	57074	40.85	32.71	30.89	31.07	40.15
Wo	23.01	30.73	34.15	34.8	34.27	30.73
Fs	7.51	11.59	15.43	17	17.19	13.21
En	11.69	15.25	14.7	14.6	14.23	13.23
Recal into						
Ae	60.5	43.22	35.19	32.83	33.08	43.16
Hd	14.99	24.53	33.2	36.14	36.61	28.4
Di	24.51	26.48	31.62	31.08	30.31	28.44

Sample	***Fen49***	***Fen49***	***Fen49***	***Fen49***	***Fen49***	***Fen49***
Spot	*1*	*2*	*3*	*4*	*5*	*6*
Na	0.82	1.01	1.14	1.03	1.29	0.8
Mg	9.67	9.45	9.51	9.72	9.51	10.74
Al	6.9	7.02	6.56	5.13	4.81	4.35
Si	45.05	44.82	45.16	46.71	46.99	48.5
Ca	24.1	24.24	24.14	23.6	23.11	24.94
Mn	0.38	0.35	0	0.41	0.33	0
Ti	3.07	2.89	3.25	2.17	1.82	1.86
Fe	11.37	11.37	11.49	12.06	11.05	10.08
Zr						
V2O5						
Recal						
Fe3+	2.11	2.6	2.94	2.65	3.32	2.06
Fe2+	9.47	9.03	8.85	9.67	8.06	8.23
Structural Formula						
Si	1.7046	1.6997	1.7078	1.7743	1.8053	1.8165
Al(IV)	0.2954	0.3003	0.2922	0.2257	0.1947	0.1835
Al(VI)	0.0123	0.0135	0.0002	0.0004	0.0231	0.0085
FE3(IV)	0.0602	0.0743	0.0836	0.0759	0.0961	0.0581
FE2	0.2996	0.2863	0.2798	0.3072	0.2589	0.2576
Mn	0.0122	0.0112	0	0.0132	0.0107	0
Mg	0.5455	0.5343	0.5362	0.5505	0.5447	0.5997
Ca	0.977	0.9849	0.9781	0.9605	0.9512	1.0008
Na	0.0602	0.0743	0.0836	0.0759	0.0961	0.0581
K	0	0	0	0	0	0
Ti	0.0874	0.0824	0.2924	0.062	0.0526	0.0524
End Members Based on Acmite						
CaTiAl2O6	8.55	8.04	9	6.09	5.2	5.15
CaAlSiAlO6	1.21	1.31	0.02	0.39	2.28	0.84
Acmite	5.89	7.25	8.14	7.45	9.5	5.71
Wo	42.96	43.37	43.11	43.94	43.29	46.18
Fs	14.67	13.97	13.62	15.09	12.8	12.66
En	26.71	26.06	26.11	27.04	26.93	29.47
Recal into						
Ae	6.64	8.3	9.29	8.13	10.68	6.35
Hd	33.1	32	31.1	32.91	28.78	28.14
Di	60.26	59.71	59.61	58.96	60.54	65.51

Sample	***Fen49***	***Fen49***	***Fen49***	***Fen49***	***Fen49***	***Fen49***
Spot	*7*	*8*	*9*	*10*	*11*	*12*
Na	0.78	0.59	2.08	2.22	1.94	2.21
Mg	10.94	10.94	7.85	7.55	7.72	7.61
Al	4.07	3.53	1.84	2.01	1.92	1.79
Si	49.04	48.13	50.49	50.95	50.57	50.72
Ca	24.9	24.73	21.36	21.62	21.66	21.76
Mn	0.24	0.34	0.76	0.49	0.65	0.7
Ti	1.65	1.84	0.45	0.59	0.45	0.45
Fe	9.92	9.92	16.05	16.34	16.06	16.16
Zr						
V2O5						
Recal						
Fe3+	2.01	1.52	5.36	5.72	5	5.69
Fe2+	7.71	8.55	11.23	11.19	11.56	11.04
Structural Formula						
Si	1.8342	1.8301	1.9223	1.921	1.9245	1.9221
Al(IV)	0.1658	0.1582	0.0777	0.079	0.0755	0.0779
Al(VI)	0.0136	0.0117	0.0049	0.0103	0.0106	0.002
FE3(IV)	0.0566	0.0318	0.1535	0.1623	0.1431	0.1624
FE2	0.2412	0.2719	0.3575	0.3529	0.368	0.3498
Mn	0.0076	0.011	0.0245	0.0156	0.021	0.0225
Mg	0.6101	0.6202	0.4456	0.4244	0.438	0.43
Ca	0.9978	1.0075	0.8713	0.8733	0.8831	0.8835
Na	0.0566	0.0435	0.1535	0.1623	0.1431	0.1624
K	0	0	0	0	0	0
Ti	0.0464	0.0526	0.0129	0.0167	0.129	0.0128
End Members Based on Acmite						
CaTiAl2O6	4.59	5.16	1.29	1.67	1.29	1.28
CaAlSiAlO6	1.35	0	0.49	1.03	1.06	0.2
Acmite	5.59	4.27	15.36	16.21	14.32	16.21
Wo	46.37	46.82	42.69	42.27	43.01	43.37
Fs	11.93	13.34	17.88	17.63	18.41	17.46
En	30.17	30.41	22.29	21.2	21.91	21.47
Recal into						
Ae	6.23	4.65	16.05	17.27	15.08	17.24
Hd	26.57	29.07	37.37	37.56	38.77	37.13
Di	67.2	66.29	46.58	45.17	46.15	45.64

Sample	***Fen49***	***Fen49***	***Fen49***	***Fen 43***	***Fen 43***	***Fen 43***
Spot	*13*	*14*	*15*	*1*	*2*	*3*
Na	2.6	1.27	0.89	0.55	1.02	0.7
Mg	8.24	10.68	9.51	11.27	9.85	11.58
Al	1.81	2.41	7.31	6.28	7.14	6.04
Si	51.25	51.21	43.48	45.77	45.44	46.48
Ca	21.02	23.9	23.67	23.35	22.56	23.55
Mn	0.53	0.59	0	0.26	0	0
Ti	0.59	0.63	3.22	2.54	2.99	2.5
Fe	15.09	11.11	11.18	8.88	10.87	8.63
Zr						
V2O5						
Recal						
Fe3+	6.7	3.27	2.29	1.42	2.63	1.8
Fe2+	9.06	8.17	9.12	7.6	8.51	7.03
Structural Formula						
Si	1.9279	1.9037	1.6795	1.7493	1.7265	1.7597
Al(IV)	0.0721	0.0963	0.3205	0.2507	0.2735	0.2403
Al(VI)	0.0082	0.0093	0.0123	0.0322	0.0462	0.0292
FE3(IV)	0.1896	0.0915	0.0667	0.0408	0.0751	0.0514
FE2	0.2851	0.2538	0.2945	0.2431	0.2702	0.2225
Mn	0.0169	0.0186	0	0.0084	0	0
Mg	0.4621	0.5919	0.5477	0.6422	0.558	0.6536
Ca	0.8472	0.9519	0.9796	0.9561	0.9184	0.9553
Na	0.1896	0.0915	0.0667	0.0408	0.0751	0.0514
K	0	0	0	0	0	0
Ti	0.0167	0.0176	0.0935	0.073	0.0854	0.0712
End Members Based on Acmite						
CaTiAl2O6	1.67	1.75	9.08	7.2	8.42	7
CaAlSiAlO6	0.82	0.92	1.19	3.17	4.55	2.87
Acmite	18.98	9.12	6.47	4.02	7.41	5.05
Wo	41.15	46.08	42.4	41.96	38.79	42.02
Fs	14.26	12.64	14.29	11.99	13.32	10.94
En	23.12	29.48	26.58	31.66	27.51	32.13
Recal into						
Ae	20.24	9.77	7.33	4.57	8.72	5.65
Hd	30.43	27.08	32.4	26.2	29.79	23.95
Di	49.33	63.15	60.26	69.23	61.5	70.38

Sample	***Fen 43***	***Fen 43***	***Fen 43***	***Fen 43***	***Fen 43***	***Fen 43***
Spot	*4*	*5*	*6*	*7*	*8*	*9*
Na	0.76	1.06	1.18	1.01	1.35	1.19
Mg	10.29	10.44	10.96	11.76	11.79	9.73
Al	7.12	5.55	3.58	2.78	2.22	4.78
Si	45.51	47.68	49.84	50.9	51.58	46.7
Ca	23.25	23.12	22	23.33	22.61	22.77
Mn	0.34	0.3	0.4	0.41	0.49	0
Ti	2.88	2.21	1.63	0.9	0.81	2.07
Fe	10.25	10.82	10.91	9.73	10.42	11.89
Zr						
V2O5						
Recal						
Fe3+	1.96	2.73	3.04	2.6	3.48	3.07
Fe2+	8.49	8.36	8.17	7.39	7.29	9.13
Structural Formula						
Si	1.7226	1.786	1.8676	1.8965	1.9122	1.7949
Al(IV)	0.2774	0.214	0.1324	0.1035	0.0878	0.2051
Al(VI)	0.0402	0.031	0.0258	0.0186	0.0092	0.0114
FE3(IV)	0.0558	0.077	0.0857	0.073	0.097	0.0887
FE2	0.2687	0.262	0.2562	0.2302	0.226	0.2935
Mn	0.0109	0.0095	0.0127	0.0129	0.0154	0
Mg	0.5807	0.583	0.6123	0.6533	0.6517	0.5576
Ca	0.9429	0.9278	0.8833	0.9313	0.8971	0.9376
Na	0.0558	0.077	0.0857	0.073	0.097	0.0887
K	0	0	0	0	0	0
Ti	0.082	0.0622	0.0459	0.0252	0.0226	0.0598
End Members Based on Acmite						
CaTiAl2O6	8.09	6.16	4.6	2.52	2.26	5.87
CaAlSiAlO6	3.97	3.07	2.58	1.85	0.92	1.12
Acmite	5.51	7.62	8.6	7.28	9.7	8.71
Wo	40.51	41.32	40.68	44.28	43.28	42.53
Fs	13.26	12.97	12.84	11.48	11.29	14.41
En	28.66	28.86	30.69	32.59	32.56	27.37
Recal into						
Ae	6.36	8.44	9.55	7.63	10.07	9.44
Hd	29.62	28.38	26.68	24.07	23.16	31.23
Di	64.02	63.17	63.77	68.3	66.77	59.33

Sample	***Fen 43***	***Fen 43***	***Fen 43***	***Fen 43***	***Fen 43***	***Fen 43***
Spot	*10*	*11*	*12*	*13*	*14*	*15*
Na	1.43	1.16	0.85	0.93	0.96	1.11
Mg	11.32	9.94	11.52	11.72	11.11	11.5
Al	2.1	5.03	2.74	2.83	3.69	3.16
Si	50.87	47.1	50.33	50.22	49.1	50.54
Ca	22.57	22.4	23.28	22.22	23.25	22.99
Mn	0.42	0.34	0.38	0.31	0.31	0
Ti	0.63	2.13	0.73	0.73	1.49	1
Fe	10.07	11.58	9.4	9.36	11.04	10.12
Zr						
V2O5						
Recal						
Fe3+	3.68	2.99	2.19	2.4	2.47	2.86
Fe2+	6.75	8.89	7.43	7.2	8.81	7.55
Structural Formula						
Si	1.9196	1.7962	1.9047	1.9106	1.8437	1.8887
Al(IV)	0.0804	0.2038	0.0953	0.0894	0.1563	0.1113
Al(VI)	0.013	0.0223	0.0269	0.0375	0.007	0.0279
FE3(IV)	0.1046	0.0858	0.0624	0.0686	0.0699	0.0804
FE2	0.2132	0.2835	0.2351	0.2292	0.2768	0.2358
Mn	0.0134	0.011	0.0122	0.01	0.0099	0
Mg	0.6369	0.5652	0.65	0.6648	0.622	0.6407
Ca	0.9125	0.9153	0.9439	0.9057	0.9354	0.9205
Na	0.1046	0.0858	0.0624	0.0686	0.0699	0.0804
K	0	0	0	0	0	0
Ti	0.0179	0.0611	0.0208	0.0209	0.0421	0.0281
End Members Based on Acmite						
CaTiAl2O6	1.79	6.05	2.08	2.09	4.16	2.79
CaAlSiAlO6	1.3	2.21	2.69	3.76	0.69	2.77
Acmite	10.45	8.5	6.23	6.88	6.91	7.99
Wo	44.02	41.2	44.78	42.47	43.81	42.93
Fs	10.64	14.04	11.75	11.49	13.68	11.71
En	31.8	27.99	32.48	33.32	30.75	31.82
Recal into						
Ae	10.96	9.35	6.58	7.49	7.31	8.51
Hd	22.33	30.29	24.82	23.72	28.55	24.62
Di	33.71	60.37	68.6	68.79	64.15	66.87

Sample	*Fen 70*	*Fen 70*	*Fen 70*	*Fen 70*	*Fen 70*	*Fen 70*
Spot	*1*	*2*	*3*	*4*	*5*	*6*
Na	0.72	0.76	0.84	1.25	1.34	0.91
Mg	12.25	11.37	10.28	10.55	10.87	11.01
Al	4.92	5.92	7.36	4.73	4.87	5.76
Si	48.25	47.44	45.92	47.93	47.63	47.09
Ca	25.26	24.71	24.11	23.63	23.33	23.59
Mn	0	0.36	0.35	0.52	0.41	0.39
Ti	1.93	2.15	2.34	2.5	2.7	2.11
Fe	7.9	8.73	9.39	9.59	9.61	8.79
Zr						
V2O5						
Recal						
Fe3+	1.86	1.96	2.16	3.22	3.45	2.34
Fe2+	6.23	6.97	7.44	6.69	6.5	6.68
Structural Formula						
Si	1.7934	1.7671	1.7296	1.7984	1.7849	1.7807
Al(IV)	0.2066	0.2329	0.2704	0.2016	0.2151	0.2193
Al(VI)	0.0089	0.027	0.0563	0.0076	0	0.0374
FE3(IV)	0.0519	0.0549	0.0613	0.0909	0.0974	0.0667
FE2	0.1937	0.2171	0.2344	0.21	0.2038	0.2113
Mn	0	0.0114	0.0112	0.0165	0.013	0.0125
Mg	0.6789	0.6314	0.5773	0.5902	0.6073	0.6207
Ca	1.0059	0.9861	0.9729	0.95	0.9367	0.9558
Na	0.0519	0.0549	0.0613	0.0909	0.0974	0.0667
K	0	0	0	0	0	0
Ti	0.0539	0.0602	0.0663	0.0705	0.0761	0.06
End Members Based on Acmite						
CaTiAl2O6	5.28	5.93	6.53	7.02	7.54	5.94
CaAlSiAlO6	0.87	2.66	5.54	0.76	0	3.71
Acmite	5.07	5.4	6.04	9.05	9.65	6.61
Wo	46.11	44.25	41.89	43.37	42.63	42.52
Fs	9.47	10.68	11.55	10.45	10.1	10.47
En	3319	31.08	28.44	29.36	30.09	30.75
Recal into						
Ae	5.61	6.08	7.03	10.2	10.72	7.42
Hd	20.95	24.03	26.85	23.56	22.43	23.51
Di	73.44	69.9	66.12	66.23	66.85	69.07

Sample	***Fen 70***	***Fen 70***	***Fen 70***	***Fen 70***	***(Fen) 418***	***(Fen) 418***
Spot	*7*	*8*	*9*	*10*	*Core 1*	*Core 2*
Na	0.74	1.13	0.64	0.94	1.41	2.45
Mg	11.78	12.83	11.44	12.48	7.47	7.39
Al	4.98	2.8	5.79	3.31	1.76	1.1
Si	47.39	50.59	47.59	49.75	49.58	51.67
Ca	23.41	23.56	23.93	23.61	22.39	20.93
Mn	0.26	0	0	0.3	0.96	1.03
Ti	1.83	1.19	2.1	1.18	0.68	0.18
Fe	7.75	7.27	7.85	6.88	16.24	16.48
Zr						
V2O5						
Recal						
Fe3+	1.98	2.91	1.65	4.42	3.63	6.31
Fe2+	6.03	4.65	6.37	4.7	12.97	10.8
Structural Formula						
Si	1.8098	1.8906	1.7951	1.8791	1.9125	1.9572
Al(IV)	0.1902	0.1094	0.2049	0.1209	0.08	0.0428
Al(VI)	0.034	0.0139	0.0525	0.0265	0.0075	0.0063
FE3(IV)	0.0548	0.0819	0.0468	0.0688	0.098	0.1799
FE2	0.1927	0.1453	0.2008	0.1485	0.4184	0.3421
Mn	0.0084	0	0	0.0096	0.0314	0.033
Mg	0.6707	0.7148	0.6434	0.7028	0.4296	0.4174
Ca	0.9579	0.9433	0.9671	0.9555	0.9254	0.8494
Na	0.0548	0.0819	0.0468	0.0688	0.1055	0.1799
K	0	0	0	0	0	0
Ti	0.0526	0.0334	0.0596	0.0335	0.0197	0.0051
End Members Based on Acmite						
CaTiAl2O6	5.21	3.32	5.91	3.34	1.97	0.52
CaAlSiAlO6	3.37	1.38	5.2	2.64	0	0.64
Acmite	5.43	8.13	4.64	6.87	10.52	18.17
Wo	43.19	44.47	42.39	44.68	45.19	42.32
Fs	9.55	7.21	9.96	7.41	20.88	17.28
En	33.25	35.48	31.9	35.06	21.44	21.08
Recal into						
Ae	5.97	8.69	5.25	7.48	11.06	19.15
Hd	20.99	15.43	22.54	16.14	43.88	36.42
Di	73.04	75.88	72.21	76.38	45.06	44.43

Sample	***(Fen) 418***	***(Fen) 418***	***(Fen) 418***	***Fen 35***	***Fen 35***	***Fen 35***
Spot	*Core 3*	*Core 4*	*Core 5*	*1*	*2*	*3*
Na	2.61	2.31	2.57	1.74	1.75	1.81
Mg	6.94	6.98	6.81	10.12	10.19	9.53
Al	1.15	0.98	1.29	1.07	1.1	1.39
Si	51.78	51.1	51.2	51.77	51.55	51
Ca	20.31	20.81	20.26	22.7	22.53	22.23
Mn	1.01	0.56	0.98	0.45	0.58	0.6
Ti	0	0	0	0	0	0.52
Fe	16.84	16.9	17.37	12.75	12.85	13.23
Zr						
V2O5						
Recal						
Fe3+	6.72	5.95	6.62	4.48	4.51	4.66
Fe2+	10.29	11.54	11.41	8.72	8.79	9.03
Structural Formula						
Si	1.9754	1.969	1.9583	1.9505	1.9453	1.9325
Al(IV)	0.0246	0.031	0.0417	0.0475	0.0489	0.0621
Al(VI)	0.0271	0.0135	0.0164	0.002	0.0058	0.0054
FE3(IV)	0.1931	0.1726	0.1906	0.1251	0.1222	0.1276
FE2	0.3283	0.372	0.365	0.2746	0.2775	0.2863
Mn	0.0326	0.0183	0.0317	0.0144	0.0185	0.0193
Mg	0.3947	0.401	0.3883	0.5685	0.5733	0.5384
Ca	0.8301	0.8591	0.8302	0.9163	0.9109	0.9025
Na	0.1931	0.1726	0.1906	0.1271	0.128	0.133
K	0	0	0	0	0	0
Ti	0	0	0	0	0	0.0148
End Members Based on Acmite						
CaTiAl2O6	0	0	0	0	0	1.48
CaAlSiAlO6	2.51	1.35	1.66	0	0	0
Acmite	19.66	17.34	19.24	12.62	12.69	13.25
Wo	41.02	42.48	41.08	45.51	45.14	44.21
Fs	16.71	18.69	18.42	13.64	13.75	14.26
En	20.1	20.14	19.6	28.23	28.41	26.81
Recal into						
Ae	21.07	18.25	20.19	13.1	13.08	13.89
Hd	35.83	39.34	38.67	28.31	28.35	28.89
Di	43.09	42.41	41.14	58.59	58.57	56.22

Sample	***Fen 35***	***Fen 35***	***Fen 35***	***Fen 35***	***Fen 35***	***Fen 35***
Spot	*4*	*5*	*6*	*7*	*8*	*9*
Na	1.21	2.49	1.18	2.08	1.93	1.89
Mg	11.53	8.11	11.51	7.75	8.08	10.14
Al	1.16	1.66	1.84	1.79	1.89	1.07
Si	52.25	50.82	51.99	49.59	49.81	51
Ca	23.8	20.79	23.85	21.55	21.66	22.31
Mn	0.43	0.6	0.31	0.69	0.58	0.63
Ti	0.52	0	0.69	0.61	0.68	0.51
Fe	10.57	15.86	10.37	15.63	15.48	12.13
Zr						
V2O5						
Recal						
Fe3+	3.12	6.42	3.04	5.36	4.97	4.87
Fe2+	7.76	10.09	7.63	10.81	11.01	7.75
Structural Formula						
Si	1.9404	1.9356	1.9232	1.9124	1.9107	1.9365
Al(IV)	0.0508	0.0644	0.0768	0.0814	0.0854	0.0479
Al(VI)	0.0088	0.0101	0.0034	0.0063	0.0038	0.0156
FE3(IV)	0.0783	0.1839	0.0846	0.1492	0.1397	0.1235
FE2	0.2411	0.3213	0.2362	0.3485	0.3531	0.246
Mn	0.0135	0.0194	0.0097	0.0225	0.0188	0.0203
Mg	0.6384	0.4605	0.6348	0.4456	0.4621	0.574
Ca	0.947	0.8484	0.9472	0.8904	0.8902	0.9076
Na	0.0871	0.1839	0.0846	0.1555	0.1435	0.1391
K	0	0	0	0	0	0
Ti	0.0145	0	0.192	0.0177	0.0196	0.0146
End Members Based on Acmite						
CaTiAl2O6	1.44	0	1.91	1.76	1.95	1.44
CaAlSiAlO6	0	1.01	0.34	0	0	0
Acmite	8.65	18.31	8.43	15.45	14.27	13.77
Wo	46.27	41.75	45.95	43.35	43.27	44.2
Fs	11.97	16	11.76	17.31	17.55	12.18
En	31.68	22.93	31.61	22.13	22.97	28.41
Recal into						
Ae	9.01	19.04	8.86	16.38	14.97	14.51
Hd	24.95	33.27	24.71	36.7	36.83	25.56
Di	66.04	47.69	66.43	46.92	48.2	59.84

Sample	***Fen 35***	***Fen 35***	***Fen 61 (groundmass)***	***Fen 61 (groundmass)***	***Fen 61 (groundmass)***	***Fen 61 (groundmass)***
Spot	*10*	*11*	*1*	*2*	*3*	*4*
Na	2.3	2.54	3.33	2.78	4.08	3.53
Mg	8.05	8.41	8.56	8.63	8.27	9.53
Al	1.55	1.57	1.17	1.07	1.15	1.34
Si	51.06	50.93	52.25	53.11	53.18	52.69
Ca	21.19	21.15	19.41	20.9	17.83	19.32
Mn	0.71	0.56	0.48	0.49	0.33	0.45
Ti	0.71	0.46	0	0	0	0
Fe	15.58	14.74	14.37	14.83	15.06	13.54
Zr						
V2O5						
Recal						
Fe3+	5.93	6.54	8.58	7.16	10.51	9.1
Fe2+	10.25	8.58	6.65	8.38	5.6	5.36
Structural Formula						
Si	1.9302	1.9338	1.9717	1.9723	1.9867	1.9612
Al(IV)	0.0691	0.0662	0.0283	0.0277	0.0133	0.0388
Al(VI)	0.0007	0.0041	0.0237	0.0191	0.0374	0.02
FE3(IV)	0.1679	0.187	0.2436	0.2002	0.2955	0.2547
FE2	0.324	0.2725	0.2098	0.2604	0.175	0.1667
Mn	0.0227	0.018	0.0153	0.0154	0.0104	0.0142
Mg	0.4537	0.4761	0.4816	0.4778	0.4606	0.5289
Ca	0.8582	0.8604	0.7848	0.8315	0.7137	0.7705
Na	0.1686	0.187	0.2436	0.2002	0.2955	0.2547
K	0	0	0	0	0	0
Ti	0.0202	0.0131	0	0	0	0
End Members Based on Acmite						
CaTiAl2O6	2.03	1.31	0	0	0	0
CaAlSiAlO6	0	0.41	2.39	1.92	1.36	2
Acmite	16.91	18.7	24.52	20.13	30.25	25.53
Wo	42.04	42.16	38.3	40.84	35.85	37.61
Fs	16.25	13.62	10.56	13.09	8.96	8.35
En	22.76	23.8	24.23	24.02	23.58	26.5
Recal into						
Ae	17.82	19.99	26.06	21.33	31.74	26.81
Hd	34.24	29.12	22.44	27.75	18.79	17.54
Di	47.95	50.89	51.5	50.92	49.47	55.65

Sample	***Fen 61 (groundmass)***	***Fen 61 (groundmass)***	***Fen 61 (groundmass)***	***Fen 61 (groundmass)***	***Fen 61 (groundmass)***	***Fen 61 (groundmass)***
Spot	*5*	*6*	*7*	*8*	*9*	*10*
Na	3.12	3.5	3.14	3.1	2.86	3.57
Mg	8.5	8.81	8.79	9.37	8.75	8.45
Al	0.99	1.13	1	1.21	0.95	1.4
Si	52.8	53.53	53.34	53.51	53.09	52.72
Ca	19.67	18.88	19.23	20.29	20.17	18.89
Mn	0.58	0.4	0.35	0.48	0.54	0.47
Ti	0	0	0	0	0	0
Fe	15.32	14.91	14.07	13.07	14.3	14.74
Zr						
V2O5						
Recal						
Fe3+	8.04	9.02	8.09	7.99	7.37	9.2
Fe2+	8.09	6.4	6.79	5.88	7.67	6.64
Structural Formula						
Si	1.9745	1.9866	1.9965	1.9793	1.985	1.9722
Al(IV)	0.0255	0.0134	0.0035	0.0207	0.015	0.0278
Al(VI)	0.0182	0.036	0.0406	0.0321	0.0269	0.0339
FE3(IV)	0.2262	0.2518	0.2279	0.2223	0.2073	0.2589
FE2	0.2529	0.1985	0.2125	0.182	0.2398	0.2022
Mn	0.0184	0.0126	0.0111	0.015	0.0171	0.0149
Mg	0.4739	0.4875	0.4905	0.5167	0.4878	0.4713
Ca	0.7881	0.7507	0.7712	0.8041	0.808	0.7571
Na	0.2262	0.2518	0.2279	0.2223	0.2073	0.2589
K	0	0	0	0	0	0
Ti	0	0	0	0	0	0
End Members Based on Acmite						
CaTiAl2O6	0	0	0	0	0	0
CaAlSiAlO6	1.83	1.37	0.36	2.1	1.52	2.82
Acmite	22.79	25.78	23.57	22.59	21.1	26.2
Wo	38.78	37.74	39.7	39.8	40.35	36.9
Fs	12.74	10.16	10.99	9.25	12.2	10.23
En	23.87	24.95	25.37	26.25	24.82	23.85
Recal into						
Ae	23.74	26.85	24.48	24.14	22.18	27.77
Hd	26.54	21.17	22.83	19.76	25.65	21.69
Di	49.73	51.98	52.69	56.1	52.17	50.54

Sample	***Fen 61 (microcrysts)***	***Fen 61 (microcrysts)***	***Fen 61 (microcrysts)***	***Fen 61 (microcrysts)***	***Fen 61 (microcrysts)***	***Fen 61 (microcrysts)***
Spot	*1*	*2*	*3*	*4*	*5*	*6*
Na	0.65	0.56	0.63	0.66	0.53	0.79
Mg	12.13	12.11	12.34	11.99	11.65	11.18
Al	4.94	6.03	5.44	4.75	5.51	7.39
Si	47.39	45.5	47.33	48.37	45.8	45.65
Ca	24.26	23.93	24.41	24.1	23.69	24.08
Mn	0.2	0	0	0	0	0
Ti	2.16	2.93	2.41	2.41	2.47	3.3
Fe	8.63	7.31	7.16	8.38	8.36	8.79
Zr						
V2O5						
Recal						
Fe3+	1.67	1.44	1.62	1.7	1.37	2.04
Fe2+	7.12	6.01	5.7	6.85	7.07	6.92
Structural Formula						
Si	1.7829	1.7394	1.7787	1.8055	1.7642	1.7051
Al(IV)	0.2171	0.2606	0.2213	0.1945	0.2358	0.2949
Al(VI)	0.002	0.0111	0.0197	0.0145	0.0143	0.0304
FE3(IV)	0.0474	0.0415	0.0459	0.0478	0.0396	0.0572
FE2	0.2241	0.1922	0.1791	0.2138	0.2278	0.2161
Mn	0.0064	0	0	0	0	0
Mg	0.6804	0.6902	0.6914	0.6673	0.669	0.6226
Ca	0.9779	0.9801	0.9829	0.9638	0.9777	0.9636
Na	0.0474	0.0415	0.0459	0.0478	0.0396	0.0572
K	0	0	0	0	0	0
Ti	0.0611	0.0842	0.0681	0.0676	0.0715	0.0927
End Members Based on Acmite						
CaTiAl2O6	5.99	8.25	6.7	6.69	7.02	9.09
CaAlSiAlO6	0.19	1.08	1.93	1.43	1.4	2.98
Acmite	4.65	4.07	4.52	4.72	3.88	5.61
Wo	44.84	43.36	44.03	43.59	43.73	41.21
Fs	10.98	9.42	8.81	10.57	11.17	10.59
En	33.35	33.82	34.01	32.99	32.8	30.52
Recal into						
Ae	4.98	4.49	5.01	5.14	4.25	6.39
Hd	23.54	20.8	19.55	23.02	24.32	24.12
Di	71.48	74.71	75.45	71.84	71.43	69.49

Sample	***Fen 61 (microcrysts)***	***Fen 61 (microcrysts)***	***Fen 61 (microcrysts)***	***Fen 61 (microcrysts)***	***Fen 43***	***Fen 43***
Spot	*7*	*8*	*9*	*10*	*1*	*2*
Na	0.66	0.57	0.57	0.52	0.86	0.9
Mg	11.27	12.41	12.29	11.3	10.39	10.32
Al	7.18	5.32	5.45	7.89	5.99	6.73
Si	45.68	48.46	47.36	44.68	47.69	46.02
Ca	24.52	24.66	24.37	24.21	23.44	23.55
Mn	0	0	0	0	0.33	0
Ti	3.59	2.44	2.46	3.74	2.43	2.77
Fe	8.65	7.97	7.89	8.3	10.32	10.13
Zr						
V2O5						
Recal						
Fe3+	1.7	1.47	1.47	1.34	2.22	2.32
Fe2+	7.12	6.65	6.57	7.09	8.33	8.04
Structural Formula						
Si	1.702	1.7873	1.774	1.679	1.7795	1.7373
Al(IV)	0.298	0.2127	0.226	0.321	0.2205	0.2627
Al(VI)	0.0173	0.0185	0.0145	0.0285	0.0429	0.0368
FE3(IV)	0.0477	0.0408	0.0414	0.0379	0.0622	0.0659
FE2	0.2218	0.2051	0.2058	0.223	0.2598	0.2539
Mn	0	0	0	0	0.0104	0
Mg	0.6261	0.6824	0.6863	0.6331	0.578	0.5809
Ca	0.9788	0.9745	0.978	0.9748	0.9371	0.9525
Na	0.0477	0.0408	0.0414	0.0379	0.0622	0.0659
K	0	0	0	0	0	0
Ti	0.1006	0.0677	0.0693	0.1057	0.0682	0.0786
End Members Based on Acmite						
CaTiAl2O6	9.86	6.67	6.8	10.36	6.78	7.73
CaAlSiAlO6	1.7	1.83	1.43	2.79	4.27	3.62
Acmite	4.67	4.02	4.06	3.71	6.19	6.48
Wo	42.2	43.76	43.9	41.19	41.09	41.15
Fs	10.88	10.1	10.1	10.93	12.92	12.48
En	30.69	33.62	33.7	31.02	28.75	28.55
Recal into						
Ae	5.32	4.39	4.43	4.31	7	7.31
Hd	24.77	22.09	22.04	24.32	28.84	28.19
Di	69.9	73.52	73.52	70.77	64.16	64.49

Sample	***Fen 43***	***Fen 43***	***Fen 43***	***Fen 43***	***Fen 43***	***Fen 43***
Spot	*3*	*4*	*5*	*6*	*7*	*8*
Na	0.88	1.03	0.76	0.97	1.37	1.04
Mg	10.19	9.83	10.22	12.96	11.82	11.22
Al	6.51	5.48	5.89	1.45	3.29	3.22
Si	46.39	47.76	46.33	52.57	50.65	49.21
Ca	23.28	23.03	22.93	23.38	22.11	22.4
Mn	0	0.28	0.31	0.39	0.26	0.3
Ti	2.63	2.32	2.4	0.36	0.68	1.18
Fe	10.28	11.66	10.73	7.43	8.21	9.1
Zr						
V2O5						
Recal						
Fe3+	2.27	2.65	1.96	2.5	3.53	2.68
Fe2+	8.24	9.27	8.97	5.18	5.03	6.69
Structural Formula						
Si	1.7541	1.7909	1.7684	1.9587	1.9091	1.8868
Al(IV)	0.2459	0.2091	0.2316	0.0413	0.0909	0.1132
Al(VI)	0.0443	0.0331	0.0334	0.0224	0.0552	0.0323
FE3(IV)	0.0645	0.0749	0.0562	0.0701	0.1001	0.0773
FE2	0.2606	0.2908	0.2863	0.1614	0.1587	0.2145
Mn	0	0.0089	0.01	0.0123	0.0083	0.0097
Mg	0.5745	0.5496	0.5816	0.7199	0.6642	0.6414
Ca	0.9431	0.9253	0.9377	0.9333	0.8929	0.9202
Na	0.0645	0.0749	0.0562	0.0701	0.1001	0.0773
K	0	0	0	0	0	0
Ti	0.0748	0.0654	0.0689	0.0101	0.0193	0.034
End Members Based on Acmite						
CaTiAl2O6	7.38	6.5	6.82	1.02	1.94	3.41
CaAlSiAlO6	4.37	3.29	3.31	2.13	5.27	3.23
Acmite	6.37	7.44	5.57	7.06	10	7.74
Wo	40.67	41.05	41.35	45.42	41.32	42.76
Fs	12.86	14.44	14.17	8.13	7.98	10.74
En	28.35	27.29	28.79	36.25	33.42	32.12
Recal into						
Ae	7.26	8.31	6.31	7.36	10.87	8.3
Hd	28.94	31.73	30.9	16.97	17.19	22.98
Di	63.8	59.97	62.79	75.67	71.95	68.72

Sample	***Fen 43***	***Fen 43***	***Fen 43***	***Fen 43***	***Fen 43***	***Fen 43***
Spot	*9*	*10*	*11*	*12*	*13*	*14*
Na	1.01	1.12	0.69	1.06	1.04	1.13
Mg	10.08	10.4	11.36	9.36	11.85	9.36
Al	5.71	4.87	5.52	6.88	2.99	4.84
Si	47.4	48.24	47.69	45.06	51.72	48.44
Ca	22.93	22.94	23.71	23.1	23.28	23.11
Mn	0.45	0.31	0.25	0.27	0.3	0
Ti	2.31	2.03	2.34	2.99	1.25	1.92
Fe	10.83	10.65	8.89	10.93	9.49	11.94
Zr						
V2O5						
Recal						
Fe3+	2.6	2.89	1.78	2.73	2.68	2.91
Fe2+	8.49	8.05	7.29	8.47	7.08	9.32
Structural Formula						
Si	1.7847	1.814	1.7887	1.7231	1.899	1.8255
Al(IV)	0.2153	0.186	0.2113	0.2769	0.101	0.1745
Al(VI)	0.0381	0.0298	0.0326	0.0332	0.0283	0.0405
FE3(IV)	0.0737	0.0817	0.0502	0.0786	0.074	0.0826
FE2	0.2673	0.2533	0.2287	0.2709	0.2174	0.2937
Mn	0.0144	0.0099	0.0079	0.0087	0.0093	0
Mg	0.5659	0.5831	0.6352	0.5336	0.6487	0.5259
Ca	0.925	0.9242	0.9528	0.9464	0.9158	0.9331
Na	0.0737	0.0817	0.0502	0.0786	0.074	0.0826
K	0	0	0	0	0	0
Ti	0.0654	0.0574	0.066	0.086	0.0345	0.0544
End Members Based on Acmite						
CaTiAl2O6	6.51	5.71	6.55	8.48	3.46	5.41
CaAlSiAlO6	3.79	2.96	3.24	3.27	2.85	4.02
Acmite	7.34	8.12	4.98	7.75	7.43	8.2
Wo	40.89	41.62	43.37	40.81	42.8	41.64
Fs	13.3	12.59	11.34	13.36	10.91	14.59
En	28.16	28.99	31.51	26.32	32.55	26.13
Recal into						
Ae	8.24	8.9	5.55	8.9	7.99	9.15
Hd	29.44	27.59	25	30.68	23.09	32.56
Di	62.33	63.52	69.45	60.42	68.92	58.29

Sample	***Fen 204***	***Fen 204***	***Fen 204***	***Fen 204***	***Fen 204***	***Fen 204***
Spot	*1*	*2*	*3*	*4*	*5*	*6*
Na	1.42	2.05	2.77	1.56	1.77	1.97
Mg	10.55	9.4	8.86	10.43	10.44	10.14
Al	1.89	1.71	1.33	2.04	1.72	1.78
Si	50.33	50.11	51.48	50.5	51.14	50.85
Ca	22.46	21.23	20.12	22.14	22.05	21.83
Mn	0.43	0.5	0.62	0.42	0.52	0.55
Ti	1.42	0.54	0.37	0.81	0.63	0.54
Fe	11.08	12.94	14.17	11.15	11.69	12.45
Zr						
V2O5						
Recal						
Fe3+	3.66	5.28	7.14	4.02	4.56	5.08
Fe2+	7.79	7.59	7.75	7.53	7.59	7.88
Structural Formula						
Si	1.9218	1.9332	1.9503	1.9202	1.9286	1.9206
Al(IV)	0.0782	0.0668	0.0497	0.0798	0.0714	0.0792
Al(VI)	0.0069	0.0109	0.0097	0.0116	0.005	0.0002
FE3(IV)	0.1051	0.1533	0.2035	0.115	0.1294	0.1441
FE2	0.2487	0.2448	0.2455	0.2395	0.2393	0.249
Mn	0.0139	0.0163	0.0199	0.0135	0.0166	0.0176
Mg	0.6006	0.5407	0.5004	0.5913	0.587	0.571
Ca	0.9189	0.8775	0.8167	0.902	0.8909	0.8834
Na	0.1051	0.1533	0.2035	0.115	0.1294	0.1443
K	0	0	0	0	0	0
Ti	0.0184	0.0157	0.0105	0.0232	0.0179	0.0153
End Members Based on Acmite						
CaTiAl2O6	1.83	1.57	1.06	2.32	1.79	1.53
CaAlSiAlO6	0.68	1.09	0.98	1.17	0.51	0
Acmite	10.49	15.36	20.45	11.51	12.95	14.37
Wo	44.6	42.63	40.03	43.41	43.42	43.25
Fs	12.41	12.26	12.34	11.19	11.97	12.4
En	29.98	27.08	25.15	29.6	29.37	28.45
Recal into						
Ae	11.01	16.33	21.43	12.16	13.54	14.96
Hd	26.06	26.07	25.86	25.33	25.04	25.82
Di	62.93	57.59	52.71	62.51	61.42	59.22

Sample	***Fen 204***	***Fen 204***	***Fen 204***	***Fen 204***	***Fen 204***	***Fen 204***
Spot	*7*	*8*	*9*	*10*	*11*	*12*
Na	2.07	1.4	2.08	1.77	2.94	2.07
Mg	9.83	10.83	9.61	10.44	9.05	10.59
Al	1.61	2.36	1.63	1.69	1.39	1.71
Si	50.71	50.49	50.93	51.37	52.05	52.24
Ca	21.2	22.67	21.26	22.05	19.81	21.32
Mn	0.43	0.41	0.49	0.52	0.51	0.52
Ti	0.58	0.74	0.59	0.63	0.4	0.53
Fe	12.32	10.64	12.98	13.05	13.99	11.56
Zr						
V2O5						
Recal						
Fe3+	5.33	3.61	5.36	4.56	7.57	5.33
Fe2+	7.52	7.39	8.16	7.59	7.17	6.76
Structural Formula						
Si	1.9357	1.9094	1.9337	1.9323	1.9555	1.9463
Al(IV)	0.0643	0.0906	0.0663	0.0677	0.0445	0.0537
Al(VI)	0.0081	0.0146	0.0066	0.0073	0.0171	0.0214
FE3(IV)	0.1532	0.1027	0.1531	0.1291	0.2142	0.1495
FE2	0.2401	0.2339	0.259	0.2386	0.2254	0.2106
Mn	0.0139	0.0131	0.0158	0.0166	0.0162	0.0164
Mg	0.5594	0.6106	0.544	0.5855	0.5069	0.5882
Ca	0.867	0.9186	0.8648	0.8887	0.7974	0.851
Na	0.1532	0.1027	0.1531	0.1291	0.2142	0.1495
K	0	0	0	0	0	0
Ti	0.0166	0.021	0.0168	0.0178	0.0113	0.0148
End Members Based on Acmite						
CaTiAl2O6	1.67	2.1	1.69	1.79	1.14	1.5
CaAlSiAlO6	0.82	1.46	0.66	0.73	1.72	2.15
Acmite	15.34	10.24	15.33	12.93	21.56	15.06
Wo	42.16	44.06	42.12	43.26	38.72	41.05
Fs	12.02	11.67	12.97	11.96	11.35	10.61
En	28	30.47	27.23	29.33	25.52	29.63
Recal into						
Ae	16.08	10.84	16.01	13.54	22.63	15.77
Hd	25.2	24.69	27.09	25.04	23.81	22.21
Di	58.72	64.47	56.9	61.42	53.56	62.02

Sample	***Fen 204***	***Fen 204***	***Fen 204***	***Fen 204***	***Fen 204***	***Fen 204***
Spot	*13*	*14*	*15*	*16*	*17*	*18*
Na	1.71	3.54	3.8	2.39	2.87	3.23
Mg	10.5	8.75	8.58	10.22	9.13	9
Al	1.82	1.21	1.25	1.6	1.2	1.19
Si	50.78	52.02	52.08	52.44	51.57	51.74
Ca	22.15	18.61	18.11	20.9	19.82	19.25
Mn	0.54	0.54	0.5	0.62	0.68	0.64
Ti	0.55	0.3	0.4	0.28	0.28	0.35
Fe	11.13	14.01	14.45	11.8	14.2	13.23
Zr						
V2O5						
Recal						
Fe3+	4.41	9.12	9.79	6.16	7.39	8.32
Fe2+	7.17	5.8	5.64	6.26	7.55	4.74
Structural Formula						
Si	1.9276	1.9674	1.9648	1.957	1.9517	1.9749
Al(IV)	0.0724	0.0326	0.0352	0.043	0.0483	0.0251
Al(VI)	0.009	0.0213	0.0204	0.0273	0.0052	0.0288
FE3(IV)	0.1259	0.2596	0.278	0.1729	0.2106	0.239
FE2	0.2275	0.1835	0.1779	0.1953	0.2388	0.1513
Mn	0.0174	0.0173	0.016	0.0196	0.0218	0.0207
Mg	0.5942	0.4934	0.4826	0.5686	0.5152	0.5122
Ca	0.9008	0.7541	0.732	0.8356	0.8037	0.7872
Na	0.1259	0.2596	0.278	0.1729	0.2106	0.239
K	0	0	0	0	0	0
Ti	0.0157	0.0085	0.0113	0.0079	0.008	0.01
End Members Based on Acmite						
CaTiAl2O6	1.57	0.86	1.15	0.79	0.8	1.03
CaAlSiAlO6	0.9	1.57	1.26	2.76	0.52	0.52
Acmite	12.59	26.3	28.19	17.46	21.14	24.59
Wo	43.83	36.98	35.91	40.41	39.68	39.72
Fs	11.38	9.3	9.02	9.86	11.99	7.79
En	29.73	24.99	24.47	28.71	25.86	26.35
Recal into						
Ae	13.28	27.72	29.62	18.46	21.83	26.48
Hd	24.01	19.2	18.96	20.85	24.76	16.77
Di	62.71	52.68	51.42	60.69	53.41	56.75

Sample	***Fen 204***	***Fen 204***	***Fen 200***	***Fen 200***	***Fen 200***	***Fen 200***
Spot	*19*	*20*	*1*	*2*	*3*	*4*
Na	4.11	4.6	0.8	2.15	2.79	2.45
Mg	8.52	7.72	11.33	10.26	9.43	9.74
Al	1.38	1.49	3.44	0.57	0.51	0.63
Si	51.82	51.21	48.56	52.57	52.88	52.48
Ca	17.25	16.78	23.81	22.24	21.04	21.3
Mn	0.49	0.6	0.26	0.42	0.48	0.45
Ti	0.54	0.38	1.88	0	0	0
Fe	14.7	15.26	9.76	12.7	13.83	13.89
Zr						
V2O5						
Recal						
Fe3+	10.59	11.85	2.06	5.54	7.19	6.31
Fe2+	5.17	4.6	7.86	7.72	7.36	8.17
Structural Formula						
Si	1.9586	1.9534	1.8404	1.9663	1.9751	1.9665
Al(IV)	0.0414	0.0466	0.1537	0.0251	0.0225	0.0278
Al(VI)	0.0201	0.0204	0.006	0.0085	0.0024	0.0057
FE3(IV)	0.3012	0.3402	0.0528	0.1474	0.1996	0.1723
FE2	0.1635	0.1466	0.249	0.2413	0.2299	0.256
Mn	0.0157	0.0194	0.0083	0.0133	0.0152	0.0143
Mg	0.4801	0.439	0.6402	0.5722	0.5251	0.5441
Ca	0.6985	0.6858	0.9668	0.8913	0.842	0.8551
Na	0.3012	0.3402	0.0588	0.1559	0.202	0.178
K	0	0	0	0	0	0
Ti	0.0153	0.0109	0.0588	0	0	0
End Members Based on Acmite						
CaTiAl2O6	1.56	1.1	5.29	0	0	0
CaAlSiAlO6	1.09	2.05	0	0	0	0
Acmite	30.57	34.31	5.8	15.46	20.19	17.7
Wo	34.13	33	45.05	44.2	42.07	42.52
Fs	8.29	7.39	12.28	11.97	11.49	12.73
En	24.36	22.14	31.58	28.37	26.24	27.05
Recal into						
Ae	31.88	36.75	6.2	16.08	21.11	18.2
Hd	17.3	15.83	26.26	24.9	24.02	26.17
Di	50.82	47.42	67.54	59.02	54.87	55.63

Sample	***Fen 200***	***Fen 200***	***Fen 200***	***Fen 200***	***Fen 200***	***Fen 200***
Spot	*5*	*6*	*7*	*8*	*9*	*10*
Na	2.14	0.95	2.18	2.23	2.12	2.04
Mg	9.67	11.1	9.89	9.44	10.1	9.21
Al	1.13	3.07	0.85	0.79	0.78	1.31
Si	51.33	48.97	52.32	51.88	52.78	50.86
Ca	21.14	23.39	21.69	21.26	22.03	21.77
Mn	0.5	0.33	0.44	0.45	0.43	0.063
Ti	0.32	1.7	0	0.27	0	0.48
Fe	14.01	10.65	13.1	14.03	13.14	14.06
Zr						
V2O5						
Recal						
Fe3+	5.51	2.45	5.62	5.75	5.46	5.26
Fe2+	9.05	8.45	8.05	8.86	8.22	9.33
Structural Formula						
Si	1.9432	1.8531	1.966	1.9596	1.9663	1.9307
Al(IV)	0.0504	0.1369	0.034	0.0352	0.0337	0.0586
Al(VI)	0.0063	0.01	0.0036	0.0052	0.0005	0.0107
FE3(IV)	0.1507	0.0597	0.1588	0.1581	0.1531	0.1395
FE2	0.2865	0.2673	0.2528	0.2799	0.2562	0.2962
Mn	0.016	0.0106	0.014	0.0144	0.0136	0.0203
Mg	0.5458	0.6263	0.5541	0.5316	0.561	0.5213
Ca	0.8575	0.9483	0.8732	0.8604	0.8793	0.8854
Na	0.1571	0.0697	0.1588	0.1633	0.1531	0.1501
K	0	0	0	0	0	0
Ti	0.0091	0.0484	0	0.0077	0	0
End Members Based on Acmite						
CaTiAl2O6	0.91	4.77	0	0.76	0	1.36
CaAlSiAlO6	0	0	0.36	0	0.05	0
Acmite	15.61	6.87	15.87	16.28	15.29	14.89
Wo	42.14	44.34	43.45	42.5	43.87	43.22
Fs	14.23	13.17	12.63	13.95	12.79	14.69
En	27.11	30.85	27.68	26.5	28	25.84
Recal into						
Ae	15.88	7.24	16.45	16.75	15.78	15.52
Hd	28.96	27.75	26.18	28.71	26.41	30.61
Di	55.17	65.01	57.37	54.54	57.81	53.87

Sample	***Fen 200***	***Fen 200***	***Fen 201***	***Fen 201***	***Fen 201***	***Fen 201***
Spot	*11*	*12*	*1*	*2*	*3*	*4*
Na	1.74	0.8	0.6	3.38	0.71	3.4
Mg	10.25	11.48	12.67	8.35	12.35	8.43
Al	0.83	3.56	4.87	0.95	4.37	1.21
Si	52.6	49.25	46.98	51.41	47.94	52.47
Ca	22.67	23.97	24.16	19.45	24.56	19.41
Mn	0.51	0.18	0	0.48	0	0.6
Ti	0	1.89	2.57	0.17	2.31	0
Fe	12.85	9.84	7.89	15.29	8.17	15.47
Zr						
V2O5						
Recal						
Fe3+	4.48	2.06	1.55	8.71	1.83	8.76
Fe2+	8.62	7.99	6.5	7.45	6.52	7.59
Structural Formula						
Si	1.9649	1.8427	1.7732	1.955	1.7977	1.9618
Al(IV)	0.0351	0.157	0.2166	0.0426	0.1931	0.0382
Al(VI)	0.0015	0.0003	0.0101	0.0025	0.0092	0.0151
FE3(IV)	0.126	0.0578	0.0338	0.2467	0.0424	0.2465
FE2	0.2692	0.2499	0.2051	0.237	0.2046	0.2372
Mn	0.0161	0.0057	0	0.0155	0	0.019
Mg	0.5709	0.6404	0.713	0.4734	0.6904	0.4699
Ca	0.9073	0.9609	0.977	0.7924	0.9867	0.7775
Na	0.126	0.058	0.0439	0.2492	0.0516	0.2465
K	0	0	0	0	0	0
Ti	0	0.0532	0.0729	0.0049	0.0651	0
End Members Based on Acmite						
CaTiAl2O6	0	5.26	7.1	0.48	6.35	0
CaAlSiAlO6	0.15	0	0	0	0	1.52
Acmite	12.6	5.74	4.27	24.84	5.04	24.74
Wo	45.27	44.93	43.97	39.26	44.95	38.26
Fs	13.45	12.37	9.98	11.82	9.98	11.9
En	28.53	31.7	34.68	23.6	33.68	23.58
Recal into						
Ae	13.05	6.12	4.63	25.97	5.45	25.85
Hd	27.86	26.35	21.31	24.7	21.61	24.88
Di	59.09	67.53	74.06	49.33	72.94	49.28

Sample	***Fen 201***	***Fen 201***	***Fen 201***	***Fen 201***	***Fen 201***	***Fen 201***
Spot	*5*	*6*	*7*	*8*	*10*	*11*
Na	0.53	0.78	3.26	3.42	0.66	2.86
Mg	12.42	11.34	7.3	8.16	12.24	6.2
Al	5.4	5.5	1.05	1.16	3.45	1.44
Si	46.4	45.52	50.47	51.87	49.12	50.35
Ca	23.51	23.65	19.19	19.35	24.34	19.37
Mn	0	0	0.64	0.5	0.2	0.69
Ti	2.71	2.56	0	0	2.08	0.52
Fe	7.43	8.97	16.58	15.59	8.68	18.91
Zr						
V2O5						
Recal						
Fe3+	1.37	2.01	8.4	8.81	1.7	7.37
Fe2+	6.2	7.16	9.05	7.66	7.12	12.28
Structural Formula						
Si	1.7692	1.7523	1.9541	1.9601	1.8366	1.937
Al(IV)	0.2308	0.2477	0.0459	0.0399	0.152	0.063
Al(VI)	0.01118	0.0018	0.0021	0.0118	0.0114	0.0023
FE3(IV)	0.0392	0.0582	0.2447	0.2506	0.0365	0.2133
FE2	0.1977	0.2305	0.2921	0.2421	0.2226	0.3951
Mn	0	0	0.021	0.016	0.0063	0.0225
Mg	0.706	0.6508	0.4214	0.4597	0.6823	0.3556
Ca	0.9604	0.9754	0.7961	0.7834	0.9751	0.7984
Na	0.0392	0.0582	0.2447	0.2506	0.0478	0.2133
K	0	0	0	0	0	0
Ti	0.0777	0.0741	0	0	0.0585	0.015
End Members Based on Acmite						
CaTiAl2O6	7.65	7.23	0	0	5.75	1.51
CaAlSiAlO6	1.16	0.17	0.21	1.18	0	0.23
Acmite	3.86	5.68	24.46	25.08	4.7	21.41
Wo	42.86	43.9	39.68	38.62	45.06	39.19
Fs	9.73	11.25	14.6	12.12	10.94	19.82
En	34.74	31.76	21.06	23.01	33.54	17.84
Recal into						
Ae	4.31	6.2	25.54	26.31	5.02	22.13
Hd	20.94	24.54	30.49	25.42	23.37	40.98
Di	74.76	69.27	43.98	48.27	71.61	36.89

Sample	***Fen 201***	***Fen 201***	***Fen 201***	***Fen 201***	***Fen 201***	***Fen 201***
Spot	*12*	*13*	*14*	*15*	*16*	*17*
Na	0.58	3.23	3.14	3.22	0.58	0.47
Mg	12.74	8.45	8.25	8.13	11.92	11.98
Al	5.58	0.98	0.94	1.02	4.62	5.68
Si	46.71	51.99	52.23	51.41	46.26	45.97
Ca	24.32	19.55	20.16	19.26	22.69	24.23
Mn	0	0.42	0.57	0.47	0	0
Ti	2.67	0	0	0	2.52	3.22
Fe	7.25	15.61	15.13	15.86	8.08	8.25
Zr						
V2O5						
Recal						
Fe3+	1.49	8.32	8.09	8.3	1.49	1.21
Fe2+	5.91	8.12	7.85	8.39	6.74	7.16
Structural Formula						
Si	1.7568	1.9628	1.968	1.9612	1.7973	1.7407
Al(IV)	0.2432	0.0372	0.032	0.0388	0.2027	0.2535
Al(VI)	0.0041	0.0064	0.0097	0.0071	0.0088	0.0058
FE3(IV)	0.0423	0.2364	0.2294	0.2382	0.0437	0.0287
FE2	0.1857	0.2564	0.2474	0.2678	0.2188	0.2287
Mn	0	0.0134	0.0182	0.0152	0	0
Mg	0.7144	0.4756	0.4635	0.4624	0.6905	0.6763
Ca	0.98	0.7908	0.8139	0.7872	0.9445	0.983
Na	0.0423	0.2364	0.2294	0.2382	0.0437	0.0345
K	0	0	0	0	0	0
Ti	0.0755	0	0	0	0.0736	0.0917
End Members Based on Acmite						
CaTiAl2O6	7.39	0	0	0	7.28	8.96
CaAlSiAlO6	0.4	0.64	0.98	0.71	0.87	0
Acmite	4.14	23.62	0.2302	23.81	4.32	3.37
Wo	44.04	39.18	40.34	38.99	42.6	43.55
Fs	9.09	12.81	12.41	13.38	10.81	11.08
En	34.94	23.76	23.25	23.11	34.12	33.04
Recal into						
Ae	4.49	24.41	24.4	24.59	4.82	3.73
Hd	19.71	26.48	26.31	27.66	22.91	24.17
Di	75.8	49.11	49.29	47.75	72.27	72.1

Sample	***Fen 201***	***Fen 201***	***Fen 201***	***Fen 405***	***Fen 405***	***Fen 405***
Spot	*18*	*19*	*20*	*1*	*2*	*3*
Na	0.64	0.53	3.32	1.94	1.74	1.86
Mg	11.98	12.37	8.05	8.77	8.53	8.98
Al	5.02	5.08	0.98	1.68	1.91	15.8
Si	47.19	47.35	51.6	50.29	49.09	50.9
Ca	24.26	24.47		21.7	21.6	21.21
Mn	0.27	0	0.44	0.6	0.74	0.65
Ti	2.33	2.74	0	0.48	0.74	0.51
Fe	8.5	7.98	15.95	13.67	13.9	14.42
Zr						
V2O5						
Recal						
Fe3+	1.65	1.37	8.55	5	4.48	4.79
Fe2+	7.02	6.75	8.25	9.17	9.87	10.11
Structural Formula						
Si	1.7787	1.7739	1.9637	1.9306	1.9108	1.9368
Al(IV)	0.2213	0.2243	0.0363	0.0694	0.0876	0.0632
Al(VI)	0.0017	0.0018	0.0077	0.0066	0.0016	0.0077
FE3(IV)	0.0468	0.0367	0.245	0.1444	0.1297	0.1372
FE2	0.2212	0.2115	0.2627	0.2945	0.3211	0.3216
Mn	0.0086	0	0.0142	0.0195	0.0244	0.0209
Mg	0.6732	0.6909	0.4568	0.502	0.495	0.5094
Ca	0.9797	0.9822	0.7833	0.8925	0.9008	0.8647
Na	0.0468	0.0385	0.245	0.1444	0.1313	0.1372
K	0	0	0	0	0	0
Ti	0.066	0.0772	0	0.0139	0.0217	0.0146
End Members Based on Acmite						
CaTiAl2O6	6.49	7.57	0	1.39	2.16	1.46
CaAlSiAlO6	0.17	0	0.77	0.66	0	0.77
Acmite	4.6	3.78	24.49	15.45	13.12	13.77
Wo	44.81	44.39	38.77	43.64	43.93	42.28
Fs	10.87	10.37	13.13	14.74	16.05	16.14
En	33.08	33.89	22.83	25.12	24.74	25.57
Recal into						
Ae	4.97	4.09	15.4	15.35	13.86	14.17
Hd	23.5	22.48	17.24	31.3	33.9	33.22
Di	71.53	73.43	47.36	53.35	52.25	52.61

Sample	***Fen 405***	***Fen 405***	***Fen 48***	***Fen 48***	***Fen 48***	***Fen 48***
Spot	*4*	*5*	*1*	*2*	*3*	*4*
Na	2.26	1.93	1.42	1.55	1.95	1.9
Mg	8.44	8.62	9.5	7.52	8.4	7.57
Al	1.65	1.73	2.47	1.32	1.63	1.66
Si	50.81	50.5	50.42	51.34	51.77	50.73
Ca	21.2	20.98	22.73	21.04	21.65	21.32
Mn	0.62	0.6	0.42	0.62	0.63	0.61
Ti	0.5	0.6	0.88	0.46	0.4	0.57
Fe	13.77	13.72	13.01	16.32	15.46	16.09
Zr						
V2O5						
Recal						
Fe3+	5.82	4.97	3.66	3.99	5.02	4.9
Fe2+	8.53	9.25	9.72	12.73	10.94	11.68
Structural Formula						
Si	1.9417	1.9422	1.9023	1.9666	1.9416	1.9383
Al(IV)	0.0583	0.0578	0.0977	0.0334	0.0584	0.0617
Al(VI)	0.0161	0.0206	0.0121	0.0262	0.0137	0.0131
FE3(IV)	0.1675	0.1439	0.1039	0.1151	0.1418	0.1408
FE2	0.2726	0.2974	0.3066	0.4077	0.3431	0.3734
Mn	0.0201	0.0195	0.0134	0.0201	0.02	0.0197
Mg	0.4809	0.4943	0.5344	0.4295	0.4697	0.4312
Ca	0.868	0.8645	0.9188	0.8635	0.87	0.8728
Na	0.1675	0.1439	0.1039	0.1151	0.1418	0.1408
K	0	0	0	0	0	0
Ti	0.0144	0.0174	0.025	0.0133	0.0113	0.0164
End Members Based on Acmite						
CaTiAl2O6	1.45	1.75	2.49	1.36	1.13	1.65
CaAlSiAlO6	1.62	2.08	1.21	0.7	1.37	1.32
Acmite	16.86	14.52	10.36	11.8	14.24	14.16
Wo	42.16	41.7	43.98	43.23	42.44	42.41
Fs	13.72	15	15.3	20.9	17.23	18.78
En	24.2	24.92	26.66	22.01	23.59	21.69
Recal into						
Ae	18.18	15.38	10.99	12.09	14.85	14.89
Hd	29.6	31.78	32.45	42.81	35.94	39.5
Di	52.22	52.83	56.56	45.1	49.2	45.62

Sample	***Fen 48***	***Fen 48***	***Fen 48***	***Fen 48***	***Fen 48***	***Fen 48***
Spot	*5*	*6*	*7*	*8*	*9*	*10*
Na	2.01	1.32	2.79	2.14	2.23	1.41
Mg	9.01	9.72	8.62	8.8	6.25	9.49
Al	1.81	2.5	1.67	1.87	1.61	2.9
Si	51.55	50.55	52.05	51.59	50.64	50.32
Ca	21.61	22.75	20.41	21.54	21.06	23
Mn	0.66	0.57	0.57	0.55	0.84	0.5
Ti	0.61	0.77	0.51	0.62	0.55	1.01
Fe	13.36	13	14.88	14.43	17.48	12.91
Zr						
V2O5						
Recal						
Fe3+	5.18	3.4	7.19	5.51	5.75	3.63
Fe2+	9.3	9.94	8.11	9.47	12.31	9.64
Structural Formula						
Si	1.934	1.9021	1.9444	1.9311	1.9417	1.8867
Al(IV)	0.066	0.0979	0.0556	0.0689	0.0583	0.1133
Al(VI)	0.014	0.013	0.0179	0.0136	0.0144	0.0149
FE3(IV)	0.1462	0.0963	0.2021	0.1553	0.1658	0.1025
FE2	0.2918	0.3128	0.2534	0.2964	0.3947	0.3023
Mn	0.021	0.0182	0.018	0.0174	0.0273	0.159
Mg	0.504	0.5453	0.4801	0.4911	0.3573	0.5305
Ca	0.8686	0.9172	0.8169	0.8638	0.8652	0.9239
Na	0.1462	0.0963	0.2021	0.1553	0.1658	0.1025
K	0	0	0	0	0	0
Ti	0.0172	0.0218	0.0143	0.0175	0.0159	0.0285
End Members Based on Acmite						
CaTiAl2O6	1.73	2.18	1.44	1.75	1.6	2.84
CaAlSiAlO6	1.41	1.3	1.8	1.36	1.46	1.48
Acmite	14.71	9.62	20.34	15.59	16.75	10.22
Wo	42.12	44.06	39.49	41.79	42.19	43.92
Fs	14.68	15.62	12.75	14.87	19.95	15.08
En	25.35	27.23	24.16	24.64	18.05	26.46
Recal into						
Ae	15.52	10.09	21.6	16.47	18.06	10.96
Hd	30.98	32.77	27.09	31.44	43.01	32.32
Di	53.5	57.14	51.32	52.09	38.93	59.72

Sample	***(Fen) 421***	***(Fen) 421***	***(Fen) 421***	***(Fen) 421***	***(Fen) 421***	***(Fen) 421***
Spot	*1*	*2*	*3*	*4*	*5*	*6*
Na	2.21	2.26	2.28	2.59	1.99	2.53
Mg	6.75	6.58	7.39	7.22	7.26	6.96
Al	1.26	1.37	1.3	1.18	1.06	1.33
Si	51.49	50.74	51.47	51.33	51.64	51.88
Ca	20.43	20.47	20.88	20.27	21.44	20.22
Mn	0.88	0.88	0.93	0.79	0.98	0.86
Ti	0.5	0.57	0.53	0.54	0.33	0.47
Fe	17.39	17.31	16.68	17.2	16.65	17.3
Zr						
V2O5						
Recal						
Fe3+	5.69	5.82	5.87	6.67	5.13	6.52
Fe2+	12.27	12.07	11.39	11.2	12.04	11.43
Structural Formula						
Si	1.9618	1.9503	1.9475	1.9479	1.9604	1.9583
Al(IV)	0.0382	0.0497	0.0525	0.0521	0.0396	0.0417
Al(VI)	0.0184	0.0124	0.0054	0.0007	0.0078	0.0175
FE3(IV)	0.1633	0.1684	0.1673	0.1906	0.1465	0.1852
FE2	0.3908	0.388	0.3605	0.3553	0.3821	0.3609
Mn	0.0284	0.0286	0.0298	0.0254	0.0315	0.0275
Mg	0.3834	0.3771	0.4169	0.4085	0.4109	0.3917
Ca	0.834	0.843	0.8464	0.8241	0.872	0.8177
Na	0.1633	0.1684	0.1673	0.1906	0.1465	0.1852
K	0	0	0	0	0	0
Ti	0.0143	0.0165	0.0151	0.0154	0.0094	0.0133
End Members Based on Acmite						
CaTiAl2O6	1.46	1.67	1.52	1.55	0.95	1.36
CaAlSiAlO6	0.98	1.25	0.55	0.07	0.79	1.53
Acmite	16.67	17.07	16.9	19.2	14.83	18.81
Wo	41.36	41.25	41.74	40.71	43.28	40.09
Fs	19.95	19.66	18.22	17.9	19.35	18.33
En	19.58	19.1	21.07	20.58	20.8	19.89
Recal into						
Ae	17.41	18.04	17.71	19.97	15.59	19.74
Hd	41.69	41.56	38.16	37.23	40.67	38.49
Di	40.9	40.39	44.13	42.8	43.74	41.77

Sample	***(Fen) 421***	***(Fen) 421***	***(Fen) 421***	***(Fen) 421***	***Fen 37***	***Fen 37***
Spot	*7*	*8*	*9*	*10*	*1*	*2*
Na	2.24	2.67	2.5	3.05	0.55	2.01
Mg	6.7	6.83	6.66	6.82	12.84	7.88
Al	1.27	1.31	1.27	1.33	3.71	1.7
Si	50.97	51.99	52.33	52.04	49.37	50.35
Ca	20.94	19.84	19.86	19.99	23.72	20.42
Mn	0.96	1.02	0.94	0.99	0	0.62
Ti	0.96	0.32	0.17	0.37	1.02	0.77
Fe	16.72	17.29	16.97	17.47	7.17	14.83
Zr						
V2O5						
Recal						
Fe3+	5.77	6.88	6.44	7.86	1.42	5.18
Fe2+	11.53	11.1	11.17	10.4	5.89	10.17
Structural Formula						
Si	1.9456	1.9655	1.9847	1.9524	1.8695	1.9452
Al(IV)	0.0544	0.0345	0.0153	0.0476	0.1305	0.0548
Al(VI)	0.0027	0.0238	0.0415	0.0112	0.0351	0.0226
FE3(IV)	0.1658	0.1957	0.1838	0.2219	0.0404	0.1506
FE2	0.368	0.3509	0.3544	0.3263	0.1867	0.3286
Mn	0.031	0.0327	0.0302	0.0315	0	0.0203
Mg	0.3813	0.385	0.3766	0.3815	0.7249	0.4539
Ca	0.8564	0.8036	0.807	0.8035	0.9624	0.8452
Na	0.1658	0.1957	0.1838	0.2219	0.0404	0.1506
K	0	0	0	0	0	0
Ti	0.0276	0.0091	0.0048	0.0104	0.029	0.0224
End Members Based on Acmite						
CaTiAl2O6	2.77	0.93	0.51	1.06	2.88	2.28
CaAlSiAlO6	0	1.67	0.58	1.13	3.48	1.03
Acmite	16.88	20.01	19.19	22.45	4	15.35
Wo	42.88	39.78	41.57	39.56	44.49	41.44
Fs	18.73	17.94	18.5	16.51	9.25	16.75
En	19.41	19.68	19.65	19.3	35.91	23.14
Recal into						
Ae	18.12	21.01	20.09	23.87	4.3	16.14
Hd	40.21	37.67	38.74	35.1	19.6	35.22
Di	41.67	41.32	41.17	41.04	76.1	48.65

Sample	*Fen 37*	*Fen 37*	*Fen 37*	*Fen 37*	*Fen 37*	*Fen 37*
Spot	*3*	*4*	*5*	*6*	*7*	*8*
Na	0.61	1.54	2.36	1.83	1.02	0.73
Mg	13.12	9.72	7.55	9.17	10.32	12.23
Al	4	3	1.87	1.56	1.71	3.86
Si	49.64	49.37	50.38	50.74	51.83	49.7
Ca	23.93	21.6	20.32	20.88	21.85	23.87
Mn	0	0.42	0.67	0.48	0.47	0
Ti	1.71	1.48	0.76	0.63	0.47	1.78
Fe	6.71	11.79	16.21	12.95	11.16	7.89
Zr						
V2O5						
Recal						
Fe3+	1.57	3.97	6.08	4.72	2.63	1.88
Fe2+	5.3	8.22	10.74	8.71	8.8	6.2
Structural Formula						
Si	1.851	1.8856	1.9262	1.9515	1.9696	1.8554
Al(IV)	0.149	0.1144	0.0738	0.0485	0.0304	0.1446
Al(VI)	0.0268	0.0206	0.0105	0.0222	0.0462	0.0253
FE3(IV)	0.0441	0.114	0.1749	0.1365	0.0752	0.0528
FE2	0.1651	0.2625	0.3434	0.2801	0.2795	0.1935
Mn	0	0.0136	0.0217	0.0156	0.0151	0
Mg	0.7294	0.5535	0.4304	0.5258	0.5847	0.6807
Ca	0.956	0.8839	0.8324	0.8604	0.8896	0.9548
Na	0.0441	0.114	0.1749	0.1365	0.0752	0.0528
K	0	0	0	0	0	0
Ti	0.0479	0.0425	0.0219	0.0182	0.0134	0.05
End Members Based on Acmite						
CaTiAl2O6	4.76	4.27	2.2	1.85	1.4	4.97
CaAlSiAlO6	2.66	2.07	1.05	1.23	0.37	2.52
Acmite	4.38	11.45	17.6	13.86	7.82	5.26
Wo	43.77	41.22	40.24	42.15	45.43	43.76
Fs	8.2	13.19	17.27	14.22	14.55	9.63
En	36.23	27.8	21.65	26.7	30.44	33.87
Recal into						
Ae	4.77	12.26	18.44	14.48	8	5.7
Hd	17.58	28.23	36.19	29.72	29.76	20.87
Di	77.65	59.51	45.37	55.8	62.24	73.43

Sample	***Fen 37***	***Fen 37***	***Fen 37***	***Fen 37***	***Fen 37***	***Fen 37***
Spot	*9*	*10*	*11*	*12*	*13*	*14*
Na	2.52	2.57	0.53	2.69	2.5	2.78
Mg	7.94	8.1	12.37	7.78	5.54	7.36
Al	1.48	2.35	3.04	1.44	1.55	1.68
Si	52	50.45	51.06	51.38	49.06	50.94
Ca	19.91	19.5	23.77	19.56	18.47	19.04
Mn	0	0.58	0	0.58	0.65	0.68
Ti	0.6	0.92	1.25	0.55	0.61	0.55
Fe	15.35	14.68	8.74	15.54	18.77	16.02
Zr						
V2O5						
Recal						
Fe3+	6.49	6.62	1.37	6.93	6.44	7.16
Fe2+	9.51	8.72	7.51	9.3	12.97	9.57
Structural Formula						
Si	1.9696	1.9262	1.8956	1.9588	1.9505	1.9541
Al(IV)	0.0304	0.0738	0.1044	0.0412	0.0495	0.0459
Al(VI)	0.0357	0.0319	0.0286	0.0235	0.0231	0.0301
FE3(IV)	0.1851	0.1902	0.0382	0.1988	0.1927	0.2068
FE2	0.3012	0.2785	0.2332	0.2966	0.4314	0.3072
Mn	0	0.0188	0	0.0187	0.0219	0.0221
Mg	0.4484	0.4611	0.6847	0.4422	0.3284	0.4209
Ca	0.808	0.7977	0.9455	0.7989	0.7867	0.7826
Na	0.1851	0.1902	0.0381	0.1988	0.1927	0.2068
K	0	0	0	0	0	0
Ti	0.0171	0.0264	0.0349	0.0158	0.0182	0.0159
End Members Based on Acmite						
CaTiAl2O6	1.56	2.69	3.48	1.61	1.86	1.62
CaAlSiAlO6	0	2.14	2.86	0.99	1.33	1.45
Acmite	19.05	19.36	3.81	20.28	19.63	21.16
Wo	40.81	38.18	44.03	39.44	38.48	38.51
Fs	15.5	14.17	11.64	15.13	21.97	15.72
En	23.08	23.46	34.16	22.55	16.73	21.54
Recal into						
Ae	19.8	20.46	4.15	21.21	20.32	22.12
Hd	32.22	29.95	24.35	31.63	45.24	32.86
Di	47.98	49.59	71.5	47.16	34.44	45.03

Sample	***Fen 37***	***Fen 37***	***Fen 37***	***Fen 37***	***Fen 37***	***Fen 37***
Spot	*15*	*16*	*17*	*18*	*19*	*20*
Na	0.59	2.17	2.67	3.35	0.58	3.08
Mg	12.7	8.89	7.01	5.43	12.76	6.63
Al	3.05	2.64	1.59	2.44	3.43	1.5
Si	50.7	51.15	50.34	49.24	50.8	51.02
Ca	23.84	20.74	19.4	17.76	24.04	18.77
Mn	0	0.42	0.58	0.68	0	0.57
Ti	1.23	0.51	0.54	0.69	1.49	0.51
Fe	8.01	13.2	16.42	17.93	7.45	17.03
Zr						
V2O5						
Recal						
Fe3+	1.52	5.59	6.88	8.63	1.49	7.94
Fe2+	6.64	8.17	10.23	9.76	6.11	9.89
Structural Formula						
Si	1.89	1.9326	1.9495	1.935	1.8811	1.9605
Al(IV)	0.11	0.0674	0.0505	0.065	0.1189	0.0395
Al(VI)	0.024	0.0501	0.022	0.048	0.0308	0.0284
FE3(IV)	0.0426	0.159	0.2005	0.2552	0.0416	0.2295
FE2	0.2071	0.2581	0.3313	0.3209	0.1891	0.3178
Mn	0	0.0134	0.019	0.0226	0	0.0186
Mg	0.7058	0.5008	0.4047	0.3181	0.7045	0.3798
Ca	0.9522	0.8396	0.8049	0.7478	0.9538	0.7728
Na	0.0426	0.159	0.2005	0.2552	0.0416	0.2295
K	0	0	0	0	0	0
Ti	0.0345	0.0145	0.0157	0.0204	0.0415	0.0147
End Members Based on Acmite						
CaTiAl2O6	3.43	1.47	1.59	2.1	4.14	1.51
CaAlSiAlO6	2.39	3.91	1.93	2.49	3.07	1.03
Acmite	4.25	16.14	20.28	26.29	4.16	23.49
Wo	44.49	39.94	38.96	36.21	44.01	38.28
Fs	10.31	13.11	16.76	16.52	9.44	16.26
En	35.14	25.43	20.48	16.38	35.17	19.44
Recal into						
Ae	4.55	17.32	21.41	28.54	4.51	24.75
Hd	21.65	28.12	35.38	35.88	20.2	34.28
Di	73.8	54.56	43.22	35.58	75.28	40.97

Garnet compositions

Sample	Fen 48	Fen 48	Fen 48	Fen 48	Fen 48	Fen 201	Fen 201
Analysis **(wt. %)**	1	2	3	4	5	1	2
SiO_2	32.47	32.17	32.87	31.46	31.98	33.01	34.05
TiO_2	9.60	9.53	8.60	10.40	9.67	7.13	5.16
ZrO_2	0.40	0.55	0.82	0.53	0.66		
Al_2O_3	1.53	1.67	1.67	1.58	1.76	1.22	1.16
V_2O_3							
FeO / FeO_{tot}	22.55	22.21	23.11	21.95	22.19	22.61	23.85
MnO	0.58	0.53	0.53	0.59	0.67	0.38	0.36
MgO	0.48	0.51	0.44	0.45	0.71	0.35	0.36
CaO	32.89	32.47	32.90	32.36	32.76	32.82	33.43
Na_2O						0.32	0.30
Total (calc)	100.50	99.64	100.94	99.32	100.40	97.84	98.67
Recalculated (wt. %)							
final FeO	4.11	4.31	4.05	4.42	3.41	1.34	0.13
final Fe_2O_3	20.49	19.89	21.19	19.48	20.87	23.63	26.36
final MnO	0.58	0.53	0.53	0.59	0.67	0.38	0.36
final Mn_2O_3	0.00	0.00	0.00	0.00	0.00	0.00	0.00
Total	102.55	101.63	103.07	101.27	102.49	100.20	101.31
End-members							
Kimzeyite	0.80%	1.12%	1.64%	1.08%	1.33%		
Schorlomite	0.00%	0.00%	0.00%	0.00%	9.48%	5.49%	3.17%
Schorlomite-Al	6.63%	7.07%	6.44%	6.71%	7.23%	6.03%	5.67%
Morimotoite	28.38%	29.55%	26.44%	30.88%	23.52%	9.43%	0.90%
Morimotoite-Mg	0.00%	0.00%	0.00%	0.00%	0.00%	0.00%	0.00%
Goldmanite							
Spessartine							
Andradite	51.81%	50.77%	55.09%	47.45%	51.90%	69.12%	79.07%
Calderite	1.35%	1.25%	1.23%	1.39%	1.56%		
Skiagite		0.16%	0.45%	0.02%			
Khoharite	1.77%	2.11%	1.80%	1.87%	1.88%		
Remainder	0.00%	0.00%	0.00%	0.00%	0.00%	2.95%	4.33%
Total	90.74%	92.03%	93.09%	89.40%	96.90%	93.02%	93.14%
Recal into:							
An	59.7%	58.1%	62.6%	55.8%	56.3%	76.7%	89.0%
Sc	7.6%	8.1%	7.3%	7.9%	18.1%	12.8%	10.0%
Mo	32.7%	33.8%	30.1%	36.3%	25.5%	10.5%	1.0%
Quality Index	Superior	Superior	Superior	Superior	Superior	Good	Fair

Sample	Fen 201	Fen 201	Fen 201	Fen 200	Fen 200	Fen 200	Fen 200
Analysis (wt. %)	3	4	5	1	2	3	4
SiO2	33.6	33.63	33.56	32.99	32.65	33.15	33.57
TiO2	5.5	6.76	5.9	5.2	6.06	5.13	5.13
ZrO2							
Al2O3	1.08	1.14	1.02	1.28	1.1	1.28	1.34
V2O3	0.62			0.32	0.23	0.29	0.3
FeO / FeOtot	23.41	23.44	23.57	22.98	22.65	23.35	23.54
MnO	0.42	0.42	0.33	0.35	0.3	0.26	0.35
MgO	0.26	0.25	0.25	0.35	0.32	0.44	0.46
CaO	33.5	33.63	33	33.13	32.85	33.24	33.12
Na2O	0.29	0.35	0.39	0.31	0.22	0.28	
Total (calc)	98.68	99.62	98.02	96.91	96.38	97.42	97.81
Recalculated (wt. %)							
final FeO	0	0.71	0.57	0	0.51	0	1.15
final Fe2O3	26.02	25.26	25.56	25.54	24.6	25.95	24.88
final MnO	0.39	0.42	0.33	0	0.3	0	0.35
final Mn2O3	0.03	0	0	0.38	0	0.29	0
Total	101.29	102.15	100.58	99.5	98.84	100.05	100.3
End-members							
Kimzeyite							
Schorlomite	0.0513	0.0593	0.0467	0.0444	0.0553	0.0455	0.0263
Schorlomite-Al	0.0529	0.0553	0.0503	0.0637	0.0552	0.0633	0.0662
Morimotoite	0	0.0492	0.0398	0	0.0364	0	0.0806
Morimotoite-Mg	0.0322	0.0307	0.0312	0.044	0.0406	0.0551	0.0575
Goldmanite	0.0207			0.0108	0.0078	0.0098	0.0101
Spessartine							
Andradite	0.7621	0.7236	0.7575	0.7665	0.7327	0.7741	0.7512
Calderite							0.0076
Skiagite							
Khoharite							
Remainder	0.0566	0.0539	0.043	0.0452	0.0539	0.0296	0.0005
Total	0.9758	0.972	0.9685	0.9746	0.9819	0.9774	1
Recal into:							
And	0.848191	0.788149	0.818476	0.834422	0.79624	0.825267	0.765125
Sch	0.115971	0.124823	0.104808	0.117679	0.120083	0.115991	0.094215
Mor	0.035838	0.087028	0.076715	0.047899	0.083677	0.058742	0.14066
Quality Index	Fair	Fair	Fair	Poor	Poor	Fair	Superior

Sample	Fen 200	Fen 200	Fen 200	Fen 200	Fen 200	Fen 200	Fen 35
Analysis (wt. %)	5	6	7	8	9	10	1
SiO2	32.38	31.91	33.82	32.9	33.1	32.9	35.04
TiO2	6.8	6.65	5.48	5.79	5.94	5.26	3.98
ZrO2							
Al2O3	1.1	1.13	1.12	1.04	1.26	1.24	2.06
V2O3	0.85	0.15	0.32	0.34	0.3	0.41	
FeO / FeOtot	22.17	22.03	23.1	22.71	22.66	22.81	23.45
MnO	0.31	0.31	0.34	0.25	0.3	0.42	0.49
MgO	0.3	0.46	0.43	0.33	0.36	0.36	0.37
CaO	32.64	32.83	33.12	33.03	32.8	32.8	34.51
Na2O	0.29	0.44	0.18	0.19	0.35	0.32	
Total (calc)	96.84	95.91	97.91	96.58	97.07	96.52	99.9
Recalculated (wt. %)							
final FeO	0.82	0	0.99	0.51	0.33	0	0.11
final Fe2O3	23.72	24.48	24.57	24.67	24.81	25.35	25.94
final MnO	0.31	0	0.34	0.25	0.3	0	0.49
final Mn2O3	0	0.34	0	0	0	0.46	0
Total	99.21	98.39	100.37	99.05	99.55	99.1	102.5
End-members							
Kimzeyite							
Schorlomite	0.0709	0.0819	0.0297	0.0511	0.0416	0.0437	0
Schorlomite-Al	0.055	0.0568	0.0552	0.052	0.0626	0.0619	0
Morimotoite	0.0585	0	0.0694	0.0361	0.0234	0	0.0075
Morimotoite-Mg	0.038	0.0585	0.0536	0.0418	0.0453	0.0455	0.045
Goldmanite	0.0289	0.0051	0.0107	0.0116	0.0101	0.0139	
Spessartine							0.0113
Andradite	0.6867	0.704	0.7439	0.7373	0.7458	0.7648	0.7966
Calderite							
Skiagite							
Khoharite							
Remainder	0.0382	0.0572	0.0228	0.0545	0.0426	0.0439	0.0518
Total	0.9762	0.9635	0.9853	0.9844	0.9714	0.9737	0.9122
Recal into:							
An	0.755362	0.781181	0.781572	0.802897	0.811799	0.835026	0.93817
Sc	0.138489	0.153906	0.089199	0.112273	0.113421	0.115296	0
Mo	0.106149	0.064913	0.129229	0.084831	0.07478	0.049678	0.06183
Quality Index	Fair	Poor	Good	Poor	Fair	Poor	Fair

Sample	Fen 43	Fen 43	Fen 43	Fen 43	Fen 43
Analysis (wt. %)	1	2	3	4	5
SiO2	29.74	28.6	28.49	28.4	27.04
TiO2	11.73	14.2	14.79	14.27	16.34
ZrO2					
Al2O3	3.11	2.41	2.34	2.86	2.69
V2O3					
FeO / FeOtot	19.61	19.66	19.12	19.44	19.02
MnO	0.35	0.48	0.52	0.48	
MgO	1	0.96	1.02	1.01	1.03
CaO	32.68	32.38	32.87	32.08	31.93
Na2O					
Total (calc)	98.22	98.69	99.15	98.54	98.05
Recalculated (wt. %)					
final FeO	2.11	3.29	2.91	3.41	4.29
final Fe2O3	19.45	18.19	18.01	17.82	16.37
final MnO	0.35	0.48	0.52	0.48	0
final Mn2O3	0	0	0	0	0
Total	100.17	100.51	100.95	100.33	99.69
End-members					
Kimzeyite					
Schorlomite	0.0998	0.1775	0.1918	0.163	0.2166
Schorlomite-Al	0.1536	0	0.1155	0.1419	0.1347
Morimotoite	0.1477	0.2315	0.2041	0.24	0.3047
Morimotoite-Mg	0.0851	0.0732	0.1131	0.054	0.0372
Goldmanite					
Spessartine					
Andradite	0.4921	0.3712	0.3586	0.3656	0.2757
Calderite	0.0083	0.0114	0.0123	0.0114	
Skiagite					
Khoharite	0.0133	0.0157	0.0047	0.0243	0.0311
Remainder	0	0	0	0	0
Total	0.9999	0.8805	1.0001	1.0002	1
Recal into:					
An	0.503015	0.434966	0.364765	0.379057	0.284549
Sc	0.259021	0.207992	0.312583	0.316122	0.362576
Mo	0.237964	0.357042	0.322653	0.304821	0.352874
Quality Index	Superior	Superior	Superior	Superior	Superior

Sample	ETR2	ETR2	ETR2	ETR3	ETR3	ETR3	ETR7C	ETR7C	ETR7C	MT04 5-2	MT04 5-2	MT04 5-2
Site	CPX-1	CPX-2	CPX-3	CPX-1	CPX-2	CPX-3	CPX-1	CPX-2	CPX-3	CPX-1	CPX-2	CPX-3
Si (cps)	1.12E+06	1.06E+06	1.10E+06	9.97E+05	9.22E+05	9.35E+05	1.16E+06	1.18E+06	1.20E+06	1.68E+06	1.65E+06	1.67E+06
Ca (ppm)	1.53E+05	1.74E+05	1.51E+05	1.78E+05	1.86E+05	1.74E+05	1.70E+05	1.67E+05	1.69E+05	1.79E+05	1.79E+05	1.71E+05
Mn (ppm)	7960	5300	7690	4310	4000	4525	4110	4670	4260	5170	5260	4990
Sr (ppm)	314	594	324	590	562	600	555	548	510	596	408	553
Y (ppm)	11.11	2.86	11.89	4	6.97	3.69	4.54	2.37	5.57	8.28	17.1	6.05
Zr (ppm)	1419	336	1527	488	1106	401	616	220.3	651	440	440	351
Ba (ppm)	b.d.	b.d.	b.d.	b.d.	b.d.	b.d.	1.32	b.d.	1.33	b.d.	b.d.	b.d.
La (ppm)	3.81	5.4	3.89	6.47	8.66	6.81	8.3	6.7	6.93	8.68	9.89	6.99
Ce (ppm)	13.11	15.84	14.5	20.62	24.7	19.43	24.2	20	22.44	27.6	32.4	22.3
Pr (ppm)	2.21	2.41	2.38	2.98	3.73	2.91	3.52	2.89	3.54	4.14	5.58	3.43
Nd (ppm)	10.6	10.6	11	14.2	18.3	13.5	17.1	13.8	14.5	20	29.5	16.5
Sm (ppm)	2.57	2.08	2.65	2.8	3.68	2.67	3.39	2.38	3.25	4.69	7.18	3.51
Eu (ppm)	0.88	0.59	0.88	0.74	0.93	0.77	0.91	0.63	0.89	1.18	2.08	0.91
Gd (ppm)	1.86	1.05	1.78	2.2	3.11	1.86	2.21	1.4	2.79	3.31	5.95	1.93
Tb (ppm)	0.348	0.119	0.305	0.144	0.345	0.181	0.197	0.12	0.258	0.357	0.706	0.267
Dy (ppm)	1.92	0.64	1.56	0.88	1.7	0.78	1.09	0.53	1.08	2.02	3.51	1.24
Ho (ppm)	0.397	0.091	0.285	0.102	0.181	0.165	0.167	0.07	0.142	0.295	0.693	0.192
Er (ppm)	1.48	0.19	1.91	0.21	0.58	0.35	0.52	0.098	0.57	0.91	2	0.79
Tm (ppm)	0.452	0.037	0.45	0.052	0.084	0.039	0.057	0.041	0.07	0.15	0.301	0.126
Yb (ppm)	5.85	0.43	5.16	0.52	1.26	0.52	0.59	0.28	0.62	1.3	3.08	0.92
Lu (ppm)	1.49	0.123	1.4	0.119	0.144	0.125	0.153	0.068	0.157	0.32	0.689	0.185
Ta (ppm)	b.d.	0.31	b.d.	0.352	0.69	0.466	0.55	0.434	0.548	0.643	0.99	0.48
Tot. REE	46.977	39.6	48.15	52.037	67.404	50.11	62.404	49.007	57.237	74.952	103.559	59.29

Sample	PL46	PL46	PL46	PL46	PL46	PL46	PL49	PL49	PL49	PL51	PL51	PL51
Site	CPX-1	CPX-2	CPX-3	CPX-4	CPX-5	CPX-6	CPX-1	CPX-2	CPX-3	CPX-1	CPX-10	CPX-11
Si (cps)	7.20E+07	7.11E+07	6.94E+07	8.00E+07	7.46E+07	7.69E+07	1.26E+06	1.21E+06	1.19E+06	2.12E+07	2.48E+07	2.44E+07
Ca (ppm)							1.63E+05	1.66E+05	1.66E+05			
Mn (ppm)							6100	6130	6500			
Sr (ppm)	1037	857	834	780	805	286.8	627	673	641	379.9	339	599
Y (ppm)	4.26	9.56	9.86	6.93	9.26	22.41	3.08	2.82	3.93	9.99	7.4	7.18
Zr (ppm)	2087	3784	4269	2846	3231	129.3	357	362	602	144.3	587	1446
Ba (ppm)	1.94	b.d.	2.02	0.32	b.d.	574.7	0.51	1.03	2.51	b.d.	1.11	b.d.
La (ppm)	8.39	13.98	14.86	10.26	11	20.5	6.81	6.15	8.21	4.94	5.51	6.11
Ce (ppm)	23.47	41.17	43.82	32.8	33.64	45.21	20.43	20.6	25.1	21.8	20.35	23.84
Pr (ppm)	3.368	5.83	6.38	4.76	4.93	5.19	2.98	3.06	3.85	3.88	3.24	3.74
Nd (ppm)	13.15	25.2	27.01	19.4	20.68	22.69	13.7	12.9	16	18.4	14.91	16.48
Sm (ppm)	2.09	4.33	5.05	3.54	3.83	5.08	2.28	2.09	2.82	5.32	3.29	3.54
Eu (ppm)	0.651	1.354	1.411	1.15	1.153	1.722	0.64	0.7	0.86	1.72	1.03	1.11
Gd (ppm)	1.52	3.6	3.46	2.79	2.62	5.03	1.13	1.41	1.26	4.01	2.42	2.64
Tb (ppm)	0.112	0.355	0.395	0.28	0.284	0.717	0.095	0.168	0.14	0.534	0.261	0.315
Dy (ppm)	0.667	1.67	1.71	1.14	1.4	4.21	0.58	0.67	0.77	2.57	1.71	1.48
Ho (ppm)	0.115	0.288	0.327	0.246	0.278	0.82	0.104	0.087	0.118	0.506	0.273	0.255
Er (ppm)	0.395	0.87	0.907	0.78	0.94	2.43	0.167	0.28	0.39	0.87	0.89	0.94
Tm (ppm)	0.102	0.195	0.172	0.165	0.22	0.33	0.064	b.d.	0.039	0.115	0.23	0.182
Yb (ppm)	1.13	2.26	2.19	1.96	2.3	2.3	0.55	0.5	0.93	0.94	2.27	2.29
Lu (ppm)	0.288	0.502	0.485	0.417	0.629	0.324	0.126	0.118	0.138	0.182	0.476	0.53
Ta (ppm)							0.491	0.451	1.15			
Tot. REE	55.448	101.604	108.177	79.688	83.904	116.553	49.656	48.733	60.625	65.787	56.86	63.452

Sample	PL51	PL51	PL51	PL51	PL51	PL51	PL51	PL51	PL51	PL51	PL51	PL51
Site	CPX-1-1	CPX-1-2	CPX-1-3	CPX-2	CPX-2-1	CPX-2-2	CPX-2-3	CPX-3	CPX-4	CPX-5	CPX-6	CPX-7
Si (cps)	8.33E+05	8.09E+05	8.19E+05	2.17E+07	8.92E+05	8.38E+05	8.57E+05	2.14E+07	2.56E+07	2.48E+07	2.45E+07	2.25E+07
Ca (ppm)	1.72E+05	1.71E+05	1.66E+05		1.42E+05	1.47E+05	1.42E+05					
Mn (ppm)	3410	2832	3160		6550	6850	6470					
Sr (ppm)	372	375	312	338.2	366	446	357	285.2	354.2	371	338.9	326
Y (ppm)	11.04	37.9	60.9	10.02	9.62	9.29	9.2	59.7	3.76	8.19	4.65	77
Zr (ppm)	155.1	663	1530	130.7	863	1207	788	1303	791	631	618	2161
Ba (ppm)	1.11	b.d.	5.7	b.d.	b.d.	1.09	2.8	b.d.	1.21	0.67	1.03	b.d.
La (ppm)	4.47	31.8	37.2	4.79	5.75	6.68	6.25	26.51	9.8	8.34	7.58	20.9
Ce (ppm)	18.8	108	144	21.98	20.5	23.2	22.1	122.9	28.48	27.93	26.06	102.1
Pr (ppm)	3.33	17.6	26.1	3.89	3.38	3.7	3.82	22.16	3.77	4.04	3.58	18.04
Nd (ppm)	18.8	90.2	129.2	19.02	16.3	18	16.5	110	14.25	17.1	14.88	101.7
Sm (ppm)	5.78	21.1	32.9	4.88	3.81	4.31	4.16	28.6	1.99	3.11	2.49	27.9
Eu (ppm)	1.75	6.1	9.01	1.84	1.29	1.3	1.13	9.08	0.546	1.011	0.689	9.34
Gd (ppm)	4.27	15	24.4	3.74	2.49	2.36	2.34	22.8	1.1	2.06	1.39	27.1
Tb (ppm)	0.72	2.05	3.14	0.586	0.399	0.325	0.396	3.29	0.131	0.246	0.141	3.87
Dy (ppm)	3.87	12	17	2.9	2.12	1.77	1.81	16.33	0.63	1.46	0.68	21.4
Ho (ppm)	0.64	1.71	2.92	0.419	0.444	0.416	0.366	2.65	0.102	0.284	0.1	3.81
Er (ppm)	1.48	3.2	6.15	1.03	1.31	1.39	1.09	6.1	0.312	0.95	0.364	8.36
Tm (ppm)	0.156	0.505	0.98	0.107	0.309	0.307	0.285	0.883	0.11	0.194	0.103	1.14
Yb (ppm)	1.51	3.47	7.9	0.99	3.03	2.71	3.08	6.56	1.5	1.58	1.01	8
Lu (ppm)	0.211	0.422	1.37	0.159	0.76	0.66	0.537	1.18	0.294	0.284	0.282	1.14
Ta (ppm)	b.d.	0.82	0.51		0.067	0.173	b.d.					
Tot. REE	65.787	313.157	442.27	66.331	61.892	67.128	63.864	379.043	63.015	68.589	59.349	354.8

Sample	PL51	PL51	PL54	PL54	PL54	PL54	PL55	PL55	PL55	PL55	PL55	PL55
Site	CPX-8	CPX-9	CPX-1	CPX-2	CPX-4	CPX-5	CPX-1	CPX-2	CPX-3	CPX-4	CPX-5	CPX-6
Si (cps)	2.07E+07	2.42E+07	9.78E+07	9.01E+07	9.27E+07	9.16E+07	8.23E+07	8.71E+07	7.79E+07	8.80E+07	8.76E+07	8.68E+07
Ca (ppm)												
Mn (ppm)												
Sr (ppm)	305.4	330.5	433	367.7	436.8	420	367.4	397.7	381	382.7	415	426
Y (ppm)	66.2	8.1	7.6	9.12	8.69	8.66	8.18	8.6	9.13	7.19	7.99	5.92
Zr (ppm)	1601	750	919	2084	1382	1499	327	453	483	931	879	382
Ba (ppm)	b.d.	b.d.	b.d.	0.104	b.d.	b.d.	0.208	0.14	b.d.	0.206	b.d.	b.d.
La (ppm)	48.7	5.16	4.93	5.03	5.34	5.18	4.43	5.24	5.62	4.65	4.78	3.29
Ce (ppm)	214.4	21.1	19.35	19.67	20.71	20.37	20.1	22.93	24.67	18.12	19.61	14.28
Pr (ppm)	34.9	3.43	3.31	3.345	3.503	3.38	3.412	3.89	4.1	2.861	3.09	2.246
Nd (ppm)	165.5	15.42	15.2	15.38	16	15.4	16.33	17.67	18.84	12.51	13.86	9.92
Sm (ppm)	38.4	3.34	3.57	3.71	3.56	3.79	4.14	4.58	4.36	2.65	3.03	2.28
Eu (ppm)	10.97	1.11	1.15	1.237	1.256	1.176	1.475	1.525	1.618	0.896	1.014	0.844
Gd (ppm)	28.2	2.73	2.39	2.8	2.79	2.72	3.26	3.45	3.46	1.87	2.14	1.88
Tb (ppm)	3.78	0.334	0.318	0.415	0.34	0.373	0.456	0.455	0.475	0.243	0.28	0.25
Dy (ppm)	18.91	1.58	1.65	2	1.92	1.83	2.25	2.46	2.32	1.295	1.52	1.407
Ho (ppm)	2.97	0.305	0.273	0.363	0.334	0.323	0.374	0.384	0.389	0.25	0.304	0.239
Er (ppm)	6.95	1.07	0.87	1.12	1.019	0.97	0.778	0.81	0.893	0.84	0.966	0.691
Tm (ppm)	0.916	0.245	0.203	0.248	0.216	0.222	0.135	0.151	0.148	0.198	0.196	0.146
Yb (ppm)	6.78	2.51	2.2	2.86	2.46	2.36	1.215	1.29	1.45	1.93	1.85	1.53
Lu (ppm)	1.37	0.587	0.482	0.747	0.611	0.597	0.288	0.326	0.345	0.394	0.369	0.401
Ta (ppm)												
Tot. REE	582.746	58.921	55.896	58.925	60.059	58.691	58.643	65.161	68.688	48.707	53.009	39.404

Sample	PL59	PL59	PL59	PL59	PL59	PL63	PL63	PL63	PL63	PL63	PL65	PL65
Site	CPX-1	CPX-2	CPX-3	CPX-4	CPX-5	CPX-1	CPX-2	CPX-3	CPX-4	CPX-5	CPX-1	CPX-2
Si (cps)	1.71E+07	2.27E+07	2.29E+07	2.29E+07	2.19E+07	6.05E+07	6.20E+07	6.29E+07	6.68E+07	5.74E+07	2.63E+07	2.47E+07
Ca (ppm)												
Mn (ppm)												
Sr (ppm)	592	525	493	486	462	560	666	555	576	514	432	395
Y (ppm)	b.d.	10.5	18.5	1.59	2.83	4.4	2.15	2.44	4.26	5.72	4.52	7.52
Zr (ppm)	0.32	1812	3110	257	297	524	371	290.2	532	580	746	1255
Ba (ppm)	677	4.1	b.d.	0.68	1.04	b.d.	b.d.	b.d.	0.33	b.d.	0.77	0.89
La (ppm)	b.d.	9.82	8.49	5.61	4.98	6.73	6.03	4.88	6.92	6.61	7.13	8.79
Ce (ppm)	0.048	25.2	22.5	17.95	14.99	21.66	20.27	15.58	23.36	21.38	26.18	34.09
Pr (ppm)	b.d.	3.42	3.02	2.62	2.14	2.951	2.76	2.221	3.17	2.96	4.04	5.44
Nd (ppm)	b.d.	14.6	14.3	10.55	9.18	12.57	10.99	8.39	13.8	15.3	17.68	24.7
Sm (ppm)	b.d.	3.39	4.31	1.69	1.6	2.33	1.72	1.59	2.7	2.76	3.52	6.04
Eu (ppm)	b.d.	1.15	1.78	0.494	0.59	0.895	0.567	0.547	1.01	1.1	1.049	1.78
Gd (ppm)	b.d.	3.21	4.31	0.98	1.29	1.91	1.17	0.95	1.89	2.13	1.97	4.06
Tb (ppm)	b.d.	0.397	0.74	0.056	0.086	0.189	0.108	0.112	0.238	0.239	0.187	0.445
Dy (ppm)	b.d.	2.23	4.19	0.336	0.62	0.98	0.62	0.536	0.92	1.53	1.01	2
Ho (ppm)	b.d.	0.394	0.93	0.04	0.08	0.171	0.055	0.085	0.178	0.172	0.18	0.274
Er (ppm)	b.d.	0.73	2.52	0.09	0.158	0.429	0.223	0.211	0.37	0.43	0.45	0.75
Tm (ppm)	b.d.	0.122	0.197	b.d.	b.d.	0.077	0.03	0.04	0.066	b.d.	0.078	0.126
Yb (ppm)	b.d.	1.17	1.9	0.127	0.28	0.66	0.278	0.49	0.6	0.65	0.79	1.18
Lu (ppm)	b.d.	0.215	0.365	b.d.	0.061	0.139	0.107	0.107	0.146	0.177	0.143	0.205
Ta (ppm)												
Tot. REE	0.048	66.048	69.552	40.543	36.055	51.691	44.928	35.739	55.368	55.438	64.407	89.88

Sample	PL65	PL65	PL65	PL76	PL76	PL76	PL78	PL78	PL78	PL90	PL90	PL90
Site	CPX-3	CPX-4	CPX-5	CPX-1	CPX-2	CPX-3	CPX-1	CPX-2	CPX-3	CPX-1	CPX-2	CPX-3
Si (cps)	3.06E+07	2.91E+07	2.88E+07	9.50E+05	9.23E+05	9.32E+05	9.14E+05	8.93E+05	8.60E+05	1.07E+06	1.11E+06	1.11E+06
Ca (ppm)				1.73E+05	1.72E+05	1.65E+05	1.69E+05	1.64E+05	1.68E+05	1.67E+05	1.68E+05	1.64E+05
Mn (ppm)				5530	4760	5800	5430	5270	5500	6500	6050	5940
Sr (ppm)	333	339	365	566	452	529	515	532	526	579	535	545
Y (ppm)	14.87	6.39	8.4	3.34	8.87	3.81	5.26	5.88	7.21	6.63	4.7	6.39
Zr (ppm)	1758	868	1130	242.3	676	328	407	477	752	710	514	609
Ba (ppm)	3.72	2.26	4.44	b.d.	b.d.	b.d.	b.d.	b.d.	b.d.	b.d.	b.d.	2.35
La (ppm)	6.73	4.68	7.17	6.82	7.78	5.09	6.93	7.39	8.22	7.11	5.52	6.06
Ce (ppm)	28.5	19	28.7	19.37	23.5	16.4	21.87	21.8	24.87	21	17.53	19.56
Pr (ppm)	5	3.26	4.63	3.13	3.81	2.42	3.16	3.11	3.86	2.84	2.77	3.15
Nd (ppm)	24.1	13.3	21	12.4	18	11.5	14.7	14.8	17.4	15.4	12.4	12.6
Sm (ppm)	6.08	2.79	4.43	2.24	4.22	2.1	3.29	3.34	3.18	3.05	2.52	2.86
Eu (ppm)	2.14	1.26	1.59	0.61	1.14	0.69	0.76	0.78	1.07	0.8	0.65	0.82
Gd (ppm)	5.03	2.37	3.06	1.46	3.17	1.17	2	2.41	2.3	1.32	1.72	1.93
Tb (ppm)	0.7	0.315	0.386	0.141	0.352	0.235	0.177	0.228	0.247	0.268	0.226	0.226
Dy (ppm)	3.48	1.3	1.75	0.54	1.88	0.83	1.28	1.17	1.26	1.37	1.01	1.31
Ho (ppm)	0.57	0.27	0.314	0.149	0.276	0.102	0.126	0.16	0.235	0.268	0.152	0.191
Er (ppm)	1.93	0.74	0.86	0.28	0.72	0.5	0.33	0.48	0.46	0.82	0.39	0.59
Tm (ppm)	0.346	0.209	0.213	0.033	0.135	0.083	0.072	0.113	0.17	0.152	0.112	0.157
Yb (ppm)	4.16	1.93	2.41	0.55	1.35	0.76	0.65	0.9	0.87	1.5	1.05	1.93
Lu (ppm)	1.02	0.491	0.531	0.108	0.334	0.217	0.203	0.239	0.329	0.427	0.436	0.53
Ta (ppm)				0.359	0.597	0.251	0.375	0.287	0.336	0.152	0.143	0.153
Tot. REE	89.786	51.915	77.044	47.831	66.667	42.097	55.548	56.92	64.471	56.325	46.486	51.914

Sample	PL91	PL91	PL91	PL91	PL91	PL95	PL95	PL95	PL95	PL95	PL95	PL96B
Site	CPX-1	CPX-2	CPX-3	CPX-4	CPX-5	CPX-1	CPX-2	CPX-3	CPX-1	CPX-2	CPX-3	CPX-1
Si (cps)	8.44E+07	9.25E+07	8.85E+07	8.78E+07	8.87E+07	1.19E+06	1.25E+06	1.15E+06	3.35E+06	3.23E+06	3.32E+06	6.46E+05
Ca (ppm)						1.52E+05	1.46E+05	1.56E+05	1.67E+05	1.66E+05	1.66E+05	b.d.
Mn (ppm)						7670	7410	8660	7800	9010	7750	3.4
Sr (ppm)	587	460.6	538	570	548	400	357	408	459	436	441	26.1
Y (ppm)	6.53	7.97	6.61	6.78	7.62	7.76	19.1	6.14	18.1	6	20.8	b.d.
Zr (ppm)	591	620	547	538	669	1239	1620	850	1990	1031	2690	b.d.
Ba (ppm)	0.262	0.554	0.076	b.d.	0.15	b.d.	1	b.d.	b.d.	2	1.8	b.d.
La (ppm)	8.17	7.84	8.84	7.87	7.51	7.26	7.55	7.55	7.82	9.33	7.32	b.d.
Ce (ppm)	24.67	25.61	29.67	24.7	23.27	31	29.2	30.9	29.3	34.5	29.4	b.d.
Pr (ppm)	3.767	4.11	4.55	3.637	3.611	5.54	5.42	5.41	5.94	6.26	5.79	b.d.
Nd (ppm)	16.9	20.06	20.3	16.16	15.47	27.3	27.9	26.2	30.9	29.5	34.5	b.d.
Sm (ppm)	3.83	4.41	4.36	3.56	3.67	5.2	8.3	4.87	6.9	5.79	8.8	b.d.
Eu (ppm)	1.214	1.44	1.404	1.213	1.337	1.37	2.15	1.09	2.22	1.32	2.89	b.d.
Gd (ppm)	2.46	3.15	2.93	2.6	2.96	3.53	6	2.38	5.39	2.52	7.2	b.d.
Tb (ppm)	0.305	0.324	0.319	0.319	0.358	0.41	0.79	0.255	0.7	0.233	0.92	b.d.
Dy (ppm)	1.32	1.58	1.35	1.453	1.68	1.91	4.18	1.25	4.52	1.29	5.71	b.d.
Ho (ppm)	0.214	0.261	0.211	0.242	0.266	0.302	0.68	0.188	0.73	0.2	0.97	b.d.
Er (ppm)	0.573	0.7	0.562	0.578	0.643	0.72	2.52	0.74	3	0.78	3.55	b.d.
Tm (ppm)	0.092	0.107	0.09	0.098	0.099	0.193	0.47	0.133	0.52	0.189	0.62	b.d.
Yb (ppm)	0.83	0.98	0.785	0.964	1.005	2.45	5.4	1.47	5.81	1.86	6.27	b.d.
Lu (ppm)	0.164	0.219	0.173	0.193	0.191	0.498	0.91	0.488	1.01	0.523	1.32	b.d.
Ta (ppm)						0.121	0.063	0.09	0.054	0.093	0.108	b.d.
Tot. REE	64.509	70.791	75.544	63.587	62.07	87.683	101.47	82.924	104.76	94.295	115.26	0

Sample	PL96B	PL96B	PL96B	PL96B	PL96B	WS01B	WS01B	WS01B	WT4	WT4	WT4
Site	CPX-2	CPX-3	CPX-1	CPX-2	CPX-3	CPX-1	CPX-2	CPX-3	CPX-1	CPX-2	CPX-3
Si (cps)	6.41E+05	7.76E+05	3.05E+06	2.97E+06	3.01E+06	1.03E+06	1.04E+06	1.07E+06	1.18E+06	1.19E+06	1.12E+06
Ca (ppm)	b.d.	1750	1.87E+05	1.82E+05	1.78E+05	1.78E+05	1.76E+05	1.72E+05	1.78E+05	1.68E+05	1.75E+05
Mn (ppm)	3.4	10.5	4020	4320	3850	6290	6020	5890	5590	5430	5680
Sr (ppm)	39.6	16.9	529	622	560	734	658	714	582	521	558
Y (ppm)	b.d.	b.d.	7.05	4.46	5.05	5.32	4.37	3.78	6.18	8.2	9.91
Zr (ppm)	b.d.	0.3	526	469	523	414	471	366	301	314	461
Ba (ppm)	b.d.	1.6	b.d.	b.d.	b.d.	b.d.	b.d.	b.d.	b.d.	b.d.	b.d.
La (ppm)	b.d.	b.d.	7.19	7.36	7.31	8.83	7.51	7.48	8.91	9.05	11.96
Ce (ppm)	b.d.	b.d.	19.7	20	19.6	25.3	22.63	23.01	25.79	29.2	34.5
Pr (ppm)	b.d.	b.d.	3.38	3.26	3.33	3.76	3.27	3.35	3.68	4.44	5.04
Nd (ppm)	0.21	b.d.	14.5	13.6	15.4	19.1	15.6	16.3	16.8	18.8	24.3
Sm (ppm)	b.d.	b.d.	2.92	2.42	2.83	3.6	2.75	2.96	4.14	4.31	5.31
Eu (ppm)	b.d.	b.d.	0.73	0.77	0.89	0.85	0.76	0.8	0.98	1.35	1.25
Gd (ppm)	b.d.	b.d.	1.6	1.94	2.02	2.31	1.45	1.72	2.69	2.9	3.8
Tb (ppm)	b.d.	b.d.	0.278	0.151	0.176	0.223	0.165	0.185	0.288	0.341	0.42
Dy (ppm)	b.d.	b.d.	1.29	0.77	0.94	1.11	0.95	0.9	1.37	1.84	2.33
Ho (ppm)	b.d.	b.d.	0.264	0.133	0.178	0.183	0.133	0.164	0.185	0.314	0.4
Er (ppm)	b.d.	b.d.	0.85	0.46	0.58	0.64	0.33	0.34	0.79	1.08	1.16
Tm (ppm)	0.031	b.d.	0.107	b.d.	b.d.	0.091	0.051	0.056	0.12	0.166	0.174
Yb (ppm)	b.d.	b.d.	1.31	0.44	0.94	0.94	0.57	0.62	0.81	1.69	1.69
Lu (ppm)	b.d.	b.d.	0.252	b.d.	0.118	0.244	0.163	0.114	0.239	0.263	0.387
Ta (ppm)	b.d.	b.d.	0.356	0.306	0.314	0.362	0.497	0.419	0.81	0.7	1.1
Tot. REE	0.241	0	54.371	51.304	54.312	67.181	56.332	57.999	66.792	75.744	92.721

APPENDIX 3 – Trace elements

Clinopyroxene LA-ICP-MS Data

Sample	ETR2	ETR2	ETR2	ETR3	ETR3	ETR3	ETR7C	ETR7C	ETR7C	MT04 5-2	MT04 5-2	MT04 5-2
Site	CPX-1	CPX-2	CPX-3	CPX-1	CPX-2	CPX-3	CPX-1	CPX-2	CPX-3	CPX-1	CPX-2	CPX-3
Si (cps)	1.12E+06	1.06E+06	1.10E+06	9.97E+05	9.22E+05	9.35E+05	1.16E+06	1.18E+06	1.20E+06	1.68E+06	1.65E+06	1.67E+06
Ca (ppm)	1.53E+05	1.74E+05	1.51E+05	1.78E+05	1.86E+05	1.74E+05	1.70E+05	1.67E+05	1.69E+05	1.79E+05	1.79E+05	1.71E+05
Mn (ppm)	7960	5300	7690	4310	4000	4525	4110	4670	4260	5170	5260	4990
Sr (ppm)	314	594	324	590	562	600	555	548	510	596	408	553
Y (ppm)	11.11	2.86	11.89	4	6.97	3.69	4.54	2.37	5.57	8.28	17.1	6.05
Zr (ppm)	1419	336	1527	488	1106	401	616	220.3	651	440	440	351
Ba (ppm)	b.d.	b.d.	b.d.	b.d.	b.d.	b.d.	1.32	b.d.	1.33	b.d.	b.d.	b.d.
La (ppm)	3.81	5.4	3.89	6.47	8.66	6.81	8.3	6.7	6.93	8.68	9.89	6.99
Ce (ppm)	13.11	15.84	14.5	20.62	24.7	19.43	24.2	20	22.44	27.6	32.4	22.3
Pr (ppm)	2.21	2.41	2.38	2.98	3.73	2.91	3.52	2.89	3.54	4.14	5.58	3.43
Nd (ppm)	10.6	10.6	11	14.2	18.3	13.5	17.1	13.8	14.5	20	29.5	16.5
Sm (ppm)	2.57	2.08	2.65	2.8	3.68	2.67	3.39	2.38	3.25	4.69	7.18	3.51
Eu (ppm)	0.88	0.59	0.88	0.74	0.93	0.77	0.91	0.63	0.89	1.18	2.08	0.91
Gd (ppm)	1.86	1.05	1.78	2.2	3.11	1.86	2.21	1.4	2.79	3.31	5.95	1.93
Tb (ppm)	0.348	0.119	0.305	0.144	0.345	0.181	0.197	0.12	0.258	0.357	0.706	0.267
Dy (ppm)	1.92	0.64	1.56	0.88	1.7	0.78	1.09	0.53	1.08	2.02	3.51	1.24
Ho (ppm)	0.397	0.091	0.285	0.102	0.181	0.165	0.167	0.07	0.142	0.295	0.693	0.192
Er (ppm)	1.48	0.19	1.91	0.21	0.58	0.35	0.52	0.098	0.57	0.91	2	0.79
Tm (ppm)	0.452	0.037	0.45	0.052	0.084	0.039	0.057	0.041	0.07	0.15	0.301	0.126
Yb (ppm)	5.85	0.43	5.16	0.52	1.26	0.52	0.59	0.28	0.62	1.3	3.08	0.92
Lu (ppm)	1.49	0.123	1.4	0.119	0.144	0.125	0.153	0.068	0.157	0.32	0.689	0.185
Ta (ppm)	b.d.	0.31	b.d.	0.352	0.69	0.466	0.55	0.434	0.548	0.643	0.99	0.48
Tot. REE	46.977	39.6	48.15	52.037	67.404	50.11	62.404	49.007	57.237	74.952	103.559	59.29

Sample	PL46	PL46	PL46	PL46	PL46	PL46	PL49	PL49	PL49	PL51	PL51	PL51
Site	CPX-1	CPX-2	CPX-3	CPX-4	CPX-5	CPX-6	CPX-1	CPX-2	CPX-3	CPX-1	CPX-10	CPX-11
Si (cps)	7.20E+07	7.11E+07	6.94E+07	8.00E+07	7.46E+07	7.69E+07	1.26E+06	1.21E+06	1.19E+06	2.12E+07	2.48E+07	2.44E+07
Ca (ppm)							1.63E+05	1.66E+05	1.66E+05			
Mn (ppm)							6100	6130	6500			
Sr (ppm)	1037	857	834	780	805	286.8	627	673	641	379.9	339	599
Y (ppm)	4.26	9.56	9.86	6.93	9.26	22.41	3.08	2.82	3.93	9.99	7.4	7.18
Zr (ppm)	2087	3784	4269	2846	3231	129.3	357	362	602	144.3	587	1446
Ba (ppm)	1.94	b.d.	2.02	0.32	b.d.	574.7	0.51	1.03	2.51	b.d.	1.11	b.d.
La (ppm)	8.39	13.98	14.86	10.26	11	20.5	6.81	6.15	8.21	4.94	5.51	6.11
Ce (ppm)	23.47	41.17	43.82	32.8	33.64	45.21	20.43	20.6	25.1	21.8	20.35	23.84
Pr (ppm)	3.368	5.83	6.38	4.76	4.93	5.19	2.98	3.06	3.85	3.88	3.24	3.74
Nd (ppm)	13.15	25.2	27.01	19.4	20.68	22.69	13.7	12.9	16	18.4	14.91	16.48
Sm (ppm)	2.09	4.33	5.05	3.54	3.83	5.08	2.28	2.09	2.82	5.32	3.29	3.54
Eu (ppm)	0.651	1.354	1.411	1.15	1.153	1.722	0.64	0.7	0.86	1.72	1.03	1.11
Gd (ppm)	1.52	3.6	3.46	2.79	2.62	5.03	1.13	1.41	1.26	4.01	2.42	2.64
Tb (ppm)	0.112	0.355	0.395	0.28	0.284	0.717	0.095	0.168	0.14	0.534	0.261	0.315
Dy (ppm)	0.667	1.67	1.71	1.14	1.4	4.21	0.58	0.67	0.77	2.57	1.71	1.48
Ho (ppm)	0.115	0.288	0.327	0.246	0.278	0.82	0.104	0.087	0.118	0.506	0.273	0.255
Er (ppm)	0.395	0.87	0.907	0.78	0.94	2.43	0.167	0.28	0.39	0.87	0.89	0.94
Tm (ppm)	0.102	0.195	0.172	0.165	0.22	0.33	0.064	b.d.	0.039	0.115	0.23	0.182
Yb (ppm)	1.13	2.26	2.19	1.96	2.3	2.3	0.55	0.5	0.93	0.94	2.27	2.29
Lu (ppm)	0.288	0.502	0.485	0.417	0.629	0.324	0.126	0.118	0.138	0.182	0.476	0.53
Ta (ppm)							0.491	0.451	1.15			
Tot. REE	55.448	101.604	108.177	79.688	83.904	116.553	49.656	48.733	60.625	65.787	56.86	63.452

Sample	PL51	PL51	PL51	PL51	PL51	PL51	PL51	PL51	PL51	PL51	PL51	PL51
Site	CPX-1-1	CPX-1-2	CPX-1-3	CPX-2	CPX-2-1	CPX-2-2	CPX-2-3	CPX-3	CPX-4	CPX-5	CPX-6	CPX-7
Si (cps)	8.33E+05	8.09E+05	8.19E+05	2.17E+07	8.92E+05	8.38E+05	8.57E+05	2.14E+07	2.56E+07	2.48E+07	2.45E+07	2.25E+07
Ca (ppm)	1.72E+05	1.71E+05	1.66E+05		1.42E+05	1.47E+05	1.42E+05					
Mn (ppm)	3410	2832	3160		6550	6850	6470					
Sr (ppm)	372	375	312	338.2	366	446	357	285.2	354.2	371	338.9	326
Y (ppm)	11.04	37.9	60.9	10.02	9.62	9.29	9.2	59.7	3.76	8.19	4.65	77
Zr (ppm)	155.1	663	1530	130.7	863	1207	788	1303	791	631	618	2161
Ba (ppm)	1.11	b.d.	5.7	b.d.	b.d.	1.09	2.8	b.d.	1.21	0.67	1.03	b.d.
La (ppm)	4.47	31.8	37.2	4.79	5.75	6.68	6.25	26.51	9.8	8.34	7.58	20.9
Ce (ppm)	18.8	108	144	21.98	20.5	23.2	22.1	122.9	28.48	27.93	26.06	102.1
Pr (ppm)	3.33	17.6	26.1	3.89	3.38	3.7	3.82	22.16	3.77	4.04	3.58	18.04
Nd (ppm)	18.8	90.2	129.2	19.02	16.3	18	16.5	110	14.25	17.1	14.88	101.7
Sm (ppm)	5.78	21.1	32.9	4.88	3.81	4.31	4.16	28.6	1.99	3.11	2.49	27.9
Eu (ppm)	1.75	6.1	9.01	1.84	1.29	1.3	1.13	9.08	0.546	1.011	0.689	9.34
Gd (ppm)	4.27	15	24.4	3.74	2.49	2.36	2.34	22.8	1.1	2.06	1.39	27.1
Tb (ppm)	0.72	2.05	3.14	0.586	0.399	0.325	0.396	3.29	0.131	0.246	0.141	3.87
Dy (ppm)	3.87	12	17	2.9	2.12	1.77	1.81	16.33	0.63	1.46	0.68	21.4
Ho (ppm)	0.64	1.71	2.92	0.419	0.444	0.416	0.366	2.65	0.102	0.284	0.1	3.81
Er (ppm)	1.48	3.2	6.15	1.03	1.31	1.39	1.09	6.1	0.312	0.95	0.364	8.36
Tm (ppm)	0.156	0.505	0.98	0.107	0.309	0.307	0.285	0.883	0.11	0.194	0.103	1.14
Yb (ppm)	1.51	3.47	7.9	0.99	3.03	2.71	3.08	6.56	1.5	1.58	1.01	8
Lu (ppm)	0.211	0.422	1.37	0.159	0.76	0.66	0.537	1.18	0.294	0.284	0.282	1.14
Ta (ppm)	b.d.	0.82	0.51		0.067	0.173	b.d.					
Tot. REE	65.787	313.157	442.27	66.331	61.892	67.128	63.864	379.043	63.015	68.589	59.349	354.8

Sample	PL51	PL51	PL54	PL54	PL54	PL54	PL55	PL55	PL55	PL55	PL55	PL55
Site	CPX-8	CPX-9	CPX-1	CPX-2	CPX-4	CPX-5	CPX-1	CPX-2	CPX-3	CPX-4	CPX-5	CPX-6
Si (cps)	2.07E+07	2.42E+07	9.78E+07	9.01E+07	9.27E+07	9.16E+07	8.23E+07	8.71E+07	7.79E+07	8.80E+07	8.76E+07	8.68E+07
Ca (ppm)												
Mn (ppm)												
Sr (ppm)	305.4	330.5	433	367.7	436.8	420	367.4	397.7	381	382.7	415	426
Y (ppm)	66.2	8.1	7.6	9.12	8.69	8.66	8.18	8.6	9.13	7.19	7.99	5.92
Zr (ppm)	1601	750	919	2084	1382	1499	327	453	483	931	879	382
Ba (ppm)	b.d.	b.d.	b.d.	0.104	b.d.	b.d.	0.208	0.14	b.d.	0.206	b.d.	b.d.
La (ppm)	48.7	5.16	4.93	5.03	5.34	5.18	4.43	5.24	5.62	4.65	4.78	3.29
Ce (ppm)	214.4	21.1	19.35	19.67	20.71	20.37	20.1	22.93	24.67	18.12	19.61	14.28
Pr (ppm)	34.9	3.43	3.31	3.345	3.503	3.38	3.412	3.89	4.1	2.861	3.09	2.246
Nd (ppm)	165.5	15.42	15.2	15.38	16	15.4	16.33	17.67	18.84	12.51	13.86	9.92
Sm (ppm)	38.4	3.34	3.57	3.71	3.56	3.79	4.14	4.58	4.36	2.65	3.03	2.28
Eu (ppm)	10.97	1.11	1.15	1.237	1.256	1.176	1.475	1.525	1.618	0.896	1.014	0.844
Gd (ppm)	28.2	2.73	2.39	2.8	2.79	2.72	3.26	3.45	3.46	1.87	2.14	1.88
Tb (ppm)	3.78	0.334	0.318	0.415	0.34	0.373	0.456	0.455	0.475	0.243	0.28	0.25
Dy (ppm)	18.91	1.58	1.65	2	1.92	1.83	2.25	2.46	2.32	1.295	1.52	1.407
Ho (ppm)	2.97	0.305	0.273	0.363	0.334	0.323	0.374	0.384	0.389	0.25	0.304	0.239
Er (ppm)	6.95	1.07	0.87	1.12	1.019	0.97	0.778	0.81	0.893	0.84	0.966	0.691
Tm (ppm)	0.916	0.245	0.203	0.248	0.216	0.222	0.135	0.151	0.148	0.198	0.196	0.146
Yb (ppm)	6.78	2.51	2.2	2.86	2.46	2.36	1.215	1.29	1.45	1.93	1.85	1.53
Lu (ppm)	1.37	0.587	0.482	0.747	0.611	0.597	0.288	0.326	0.345	0.394	0.369	0.401
Ta (ppm)												
Tot. REE	582.746	58.921	55.896	58.925	60.059	58.691	58.643	65.161	68.688	48.707	53.009	39.404

Sample	PL59	PL59	PL59	PL59	PL59	PL63	PL63	PL63	PL63	PL63	PL65	PL65
Site	CPX-1	CPX-2	CPX-3	CPX-4	CPX-5	CPX-1	CPX-2	CPX-3	CPX-4	CPX-5	CPX-1	CPX-2
Si (cps)	1.71E+07	2.27E+07	2.29E+07	2.29E+07	2.19E+07	6.05E+07	6.20E+07	6.29E+07	6.68E+07	5.74E+07	2.63E+07	2.47E+07
Ca (ppm)												
Mn (ppm)												
Sr (ppm)	592	525	493	486	462	560	666	555	576	514	432	395
Y (ppm)	b.d.	10.5	18.5	1.59	2.83	4.4	2.15	2.44	4.26	5.72	4.52	7.52
Zr (ppm)	0.32	1812	3110	257	297	524	371	290.2	532	580	746	1255
Ba (ppm)	677	4.1	b.d.	0.68	1.04	b.d.	b.d.	b.d.	0.33	b.d.	0.77	0.89
La (ppm)	b.d.	9.82	8.49	5.61	4.98	6.73	6.03	4.88	6.92	6.61	7.13	8.79
Ce (ppm)	0.048	25.2	22.5	17.95	14.99	21.66	20.27	15.58	23.36	21.38	26.18	34.09
Pr (ppm)	b.d.	3.42	3.02	2.62	2.14	2.951	2.76	2.221	3.17	2.96	4.04	5.44
Nd (ppm)	b.d.	14.6	14.3	10.55	9.18	12.57	10.99	8.39	13.8	15.3	17.68	24.7
Sm (ppm)	b.d.	3.39	4.31	1.69	1.6	2.33	1.72	1.59	2.7	2.76	3.52	6.04
Eu (ppm)	b.d.	1.15	1.78	0.494	0.59	0.895	0.567	0.547	1.01	1.1	1.049	1.78
Gd (ppm)	b.d.	3.21	4.31	0.98	1.29	1.91	1.17	0.95	1.89	2.13	1.97	4.06
Tb (ppm)	b.d.	0.397	0.74	0.056	0.086	0.189	0.108	0.112	0.238	0.239	0.187	0.445
Dy (ppm)	b.d.	2.23	4.19	0.336	0.62	0.98	0.62	0.536	0.92	1.53	1.01	2
Ho (ppm)	b.d.	0.394	0.93	0.04	0.08	0.171	0.055	0.085	0.178	0.172	0.18	0.274
Er (ppm)	b.d.	0.73	2.52	0.09	0.158	0.429	0.223	0.211	0.37	0.43	0.45	0.75
Tm (ppm)	b.d.	0.122	0.197	b.d.	b.d.	0.077	0.03	0.04	0.066	b.d.	0.078	0.126
Yb (ppm)	b.d.	1.17	1.9	0.127	0.28	0.66	0.278	0.49	0.6	0.65	0.79	1.18
Lu (ppm)	b.d.	0.215	0.365	b.d.	0.061	0.139	0.107	0.107	0.146	0.177	0.143	0.205
Ta (ppm)												
Tot. REE	0.048	66.048	69.552	40.543	36.055	51.691	44.928	35.739	55.368	55.438	64.407	89.88

Sample	PL65	PL65	PL65	PL76	PL76	PL76	PL78	PL78	PL78	PL90	PL90	PL90
Site	CPX-3	CPX-4	CPX-5	CPX-1	CPX-2	CPX-3	CPX-1	CPX-2	CPX-3	CPX-1	CPX-2	CPX-3
Si (cps)	3.06E+07	2.91E+07	2.88E+07	9.50E+05	9.23E+05	9.32E+05	9.14E+05	8.93E+05	8.60E+05	1.07E+06	1.11E+06	1.11E+06
Ca (ppm)				1.73E+05	1.72E+05	1.65E+05	1.69E+05	1.64E+05	1.68E+05	1.67E+05	1.68E+05	1.64E+05
Mn (ppm)				5530	4760	5800	5430	5270	5500	6500	6050	5940
Sr (ppm)	333	339	365	566	452	529	515	532	526	579	535	545
Y (ppm)	14.87	6.39	8.4	3.34	8.87	3.81	5.26	5.88	7.21	6.63	4.7	6.39
Zr (ppm)	1758	868	1130	242.3	676	328	407	477	752	710	514	609
Ba (ppm)	3.72	2.26	4.44	b.d.	b.d.	b.d.	b.d.	b.d.	b.d.	b.d.	b.d.	2.35
La (ppm)	6.73	4.68	7.17	6.82	7.78	5.09	6.93	7.39	8.22	7.11	5.52	6.06
Ce (ppm)	28.5	19	28.7	19.37	23.5	16.4	21.87	21.8	24.87	21	17.53	19.56
Pr (ppm)	5	3.26	4.63	3.13	3.81	2.42	3.16	3.11	3.86	2.84	2.77	3.15
Nd (ppm)	24.1	13.3	21	12.4	18	11.5	14.7	14.8	17.4	15.4	12.4	12.6
Sm (ppm)	6.08	2.79	4.43	2.24	4.22	2.1	3.29	3.34	3.18	3.05	2.52	2.86
Eu (ppm)	2.14	1.26	1.59	0.61	1.14	0.69	0.76	0.78	1.07	0.8	0.65	0.82
Gd (ppm)	5.03	2.37	3.06	1.46	3.17	1.17	2	2.41	2.3	1.32	1.72	1.93
Tb (ppm)	0.7	0.315	0.386	0.141	0.352	0.235	0.177	0.228	0.247	0.268	0.226	0.226
Dy (ppm)	3.48	1.3	1.75	0.54	1.88	0.83	1.28	1.17	1.26	1.37	1.01	1.31
Ho (ppm)	0.57	0.27	0.314	0.149	0.276	0.102	0.126	0.16	0.235	0.268	0.152	0.191
Er (ppm)	1.93	0.74	0.86	0.28	0.72	0.5	0.33	0.48	0.46	0.82	0.39	0.59
Tm (ppm)	0.346	0.209	0.213	0.033	0.135	0.083	0.072	0.113	0.17	0.152	0.112	0.157
Yb (ppm)	4.16	1.93	2.41	0.55	1.35	0.76	0.65	0.9	0.87	1.5	1.05	1.93
Lu (ppm)	1.02	0.491	0.531	0.108	0.334	0.217	0.203	0.239	0.329	0.427	0.436	0.53
Ta (ppm)				0.359	0.597	0.251	0.375	0.287	0.336	0.152	0.143	0.153
Tot. REE	89.786	51.915	77.044	47.831	66.667	42.097	55.548	56.92	64.471	56.325	46.486	51.914

Sample	PL91	PL91	PL91	PL91	PL91	PL95	PL95	PL95	PL95	PL95	PL95	PL96B
Site	CPX-1	CPX-2	CPX-3	CPX-4	CPX-5	CPX-1	CPX-2	CPX-3	CPX-1	CPX-2	CPX-3	CPX-1
Si (cps)	8.44E+07	9.25E+07	8.85E+07	8.78E+07	8.87E+07	1.19E+06	1.25E+06	1.15E+06	3.35E+06	3.23E+06	3.32E+06	6.46E+05
Ca (ppm)						1.52E+05	1.46E+05	1.56E+05	1.67E+05	1.66E+05	1.66E+05	b.d.
Mn (ppm)						7670	7410	8660	7800	9010	7750	3.4
Sr (ppm)	587	460.6	538	570	548	400	357	408	459	436	441	26.1
Y (ppm)	6.53	7.97	6.61	6.78	7.62	7.76	19.1	6.14	18.1	6	20.8	b.d.
Zr (ppm)	591	620	547	538	669	1239	1620	850	1990	1031	2690	b.d.
Ba (ppm)	0.262	0.554	0.076	b.d.	0.15	b.d.	1	b.d.	b.d.	2	1.8	b.d.
La (ppm)	8.17	7.84	8.84	7.87	7.51	7.26	7.55	7.55	7.82	9.33	7.32	b.d.
Ce (ppm)	24.67	25.61	29.67	24.7	23.27	31	29.2	30.9	29.3	34.5	29.4	b.d.
Pr (ppm)	3.767	4.11	4.55	3.637	3.611	5.54	5.42	5.41	5.94	6.26	5.79	b.d.
Nd (ppm)	16.9	20.06	20.3	16.16	15.47	27.3	27.9	26.2	30.9	29.5	34.5	b.d.
Sm (ppm)	3.83	4.41	4.36	3.56	3.67	5.2	8.3	4.87	6.9	5.79	8.8	b.d.
Eu (ppm)	1.214	1.44	1.404	1.213	1.337	1.37	2.15	1.09	2.22	1.32	2.89	b.d.
Gd (ppm)	2.46	3.15	2.93	2.6	2.96	3.53	6	2.38	5.39	2.52	7.2	b.d.
Tb (ppm)	0.305	0.324	0.319	0.319	0.358	0.41	0.79	0.255	0.7	0.233	0.92	b.d.
Dy (ppm)	1.32	1.58	1.35	1.453	1.68	1.91	4.18	1.25	4.52	1.29	5.71	b.d.
Ho (ppm)	0.214	0.261	0.211	0.242	0.266	0.302	0.68	0.188	0.73	0.2	0.97	b.d.
Er (ppm)	0.573	0.7	0.562	0.578	0.643	0.72	2.52	0.74	3	0.78	3.55	b.d.
Tm (ppm)	0.092	0.107	0.09	0.098	0.099	0.193	0.47	0.133	0.52	0.189	0.62	b.d.
Yb (ppm)	0.83	0.98	0.785	0.964	1.005	2.45	5.4	1.47	5.81	1.86	6.27	b.d.
Lu (ppm)	0.164	0.219	0.173	0.193	0.191	0.498	0.91	0.488	1.01	0.523	1.32	b.d.
Ta (ppm)						0.121	0.063	0.09	0.054	0.093	0.108	b.d.
Tot. REE	64.509	70.791	75.544	63.587	62.07	87.683	101.47	82.924	104.76	94.295	115.26	0

Sample	PL96B	PL96B	PL96B	PL96B	PL96B	WS01B	WS01B	WS01B	WT4	WT4	WT4
Site	CPX-2	CPX-3	CPX-1	CPX-2	CPX-3	CPX-1	CPX-2	CPX-3	CPX-1	CPX-2	CPX-3
Si (cps)	6.41E+05	7.76E+05	3.05E+06	2.97E+06	3.01E+06	1.03E+06	1.04E+06	1.07E+06	1.18E+06	1.19E+06	1.12E+06
Ca (ppm)	b.d.	1750	1.87E+05	1.82E+05	1.78E+05	1.78E+05	1.76E+05	1.72E+05	1.78E+05	1.68E+05	1.75E+05
Mn (ppm)	3.4	10.5	4020	4320	3850	6290	6020	5890	5590	5430	5680
Sr (ppm)	39.6	16.9	529	622	560	734	658	714	582	521	558
Y (ppm)	b.d.	b.d.	7.05	4.46	5.05	5.32	4.37	3.78	6.18	8.2	9.91
Zr (ppm)	b.d.	0.3	526	469	523	414	471	366	301	314	461
Ba (ppm)	b.d.	1.6	b.d.	b.d.	b.d.	b.d.	b.d.	b.d.	b.d.	b.d.	b.d.
La (ppm)	b.d.	b.d.	7.19	7.36	7.31	8.83	7.51	7.48	8.91	9.05	11.96
Ce (ppm)	b.d.	b.d.	19.7	20	19.6	25.3	22.63	23.01	25.79	29.2	34.5
Pr (ppm)	b.d.	b.d.	3.38	3.26	3.33	3.76	3.27	3.35	3.68	4.44	5.04
Nd (ppm)	0.21	b.d.	14.5	13.6	15.4	19.1	15.6	16.3	16.8	18.8	24.3
Sm (ppm)	b.d.	b.d.	2.92	2.42	2.83	3.6	2.75	2.96	4.14	4.31	5.31
Eu (ppm)	b.d.	b.d.	0.73	0.77	0.89	0.85	0.76	0.8	0.98	1.35	1.25
Gd (ppm)	b.d.	b.d.	1.6	1.94	2.02	2.31	1.45	1.72	2.69	2.9	3.8
Tb (ppm)	b.d.	b.d.	0.278	0.151	0.176	0.223	0.165	0.185	0.288	0.341	0.42
Dy (ppm)	b.d.	b.d.	1.29	0.77	0.94	1.11	0.95	0.9	1.37	1.84	2.33
Ho (ppm)	b.d.	b.d.	0.264	0.133	0.178	0.183	0.133	0.164	0.185	0.314	0.4
Er (ppm)	b.d.	b.d.	0.85	0.46	0.58	0.64	0.33	0.34	0.79	1.08	1.16
Tm (ppm)	0.031	b.d.	0.107	b.d.	b.d.	0.091	0.051	0.056	0.12	0.166	0.174
Yb (ppm)	b.d.	b.d.	1.31	0.44	0.94	0.94	0.57	0.62	0.81	1.69	1.69
Lu (ppm)	b.d.	b.d.	0.252	b.d.	0.118	0.244	0.163	0.114	0.239	0.263	0.387
Ta (ppm)	b.d.	b.d.	0.356	0.306	0.314	0.362	0.497	0.419	0.81	0.7	1.1
Tot. REE	0.241	0	54.371	51.304	54.312	67.181	56.332	57.999	66.792	75.744	92.721

Garnet LA-ICP-MS Data

Sample	PL49	PL49	PL49	PL95	PL95	PL95	PL95	PL95	PL95	ETR2	ETR2	ETR2
Site	Gnt-1	Gnt-2	Gnt-3	Gnt-1	Gnt-2	Gnt-3	Gnt-1	Gnt-2	Gnt-3	Gnt-1	Gnt-2	Gnt-3
Si (cps)	7.91E+05	8.04E+05	7.72E+05	2.49E+06	2.50E+06	2.46E+06	7.59E+05	7.41E+05	7.66E+05	6.95E+05	6.55E+05	6.56E+05
Ca (ppm)	2.50E+05	2.66E+05	2.51E+05	580	660	440	b.d.	b.d.	b.d.	2.69E+05	2.82E+05	3.00E+05
Mn (ppm)	4410	4460	4420	5810	5780	5900	6510	6870	5730	4130	4350	4550
As (ppm)				b.d.	b.d.	b.d.						
Sr (ppm)	43.6	48	46.9	b.d.	8.6	6.9	9.4	19.4	26.5	60.1	98.6	81.1
Y (ppm)	957	872	898	0.24	0.65	0.233	b.d.	0.47	0.307	1123	1483	1669
Zr (ppm)	11900	11860	10760	82.7	96.1	70.8	57.5	60.9	77.7	16800	22070	25360
Ba (ppm)	b.d.	b.d.	b.d.	2287	2206	2371	2370	2810	2220	b.d.	3.3	b.d.
La (ppm)	43.1	42.3	33.6	0.173	0.66	0.156	b.d.	0.66	1	46.8	54.6	51.9
Ce (ppm)	347	327	272.9	b.d.	0.64	b.d.	b.d.	0.48	1.39	330	356	330
Pr (ppm)	88.8	85.2	68.5	b.d.	0.256	b.d.	0.012	0.181	0.19	81.1	85.3	79.2
Nd (ppm)	628	614	516	b.d.	0.72	b.d.	b.d.	0.93	0.5	604	632	601
Sm (ppm)	250	249.2	203.4	b.d.	0.095	b.d.	b.d.	0.124	0.08	244	274	274
Eu (ppm)	86.5	82.4	73.1	b.d.	b.d.	b.d.	b.d.	0.068	0.051	86.5	98	105.5
Gd (ppm)	234	229	207.7	b.d.	b.d.	b.d.	b.d.	b.d.	b.d.	267	318	355
Tb (ppm)	35.2	33.7	32.8	b.d.	b.d.	b.d.	b.d.	b.d.	b.d.	38.9	49.5	57.6
Dy (ppm)	201.1	200	191.6	b.d.	0.073	b.d.	b.d.	b.d.	b.d.	229.2	301	366
Ho (ppm)	34.8	32.9	33.5	b.d.	0.021	b.d.	b.d.	0.014	0.0114	39.5	54.1	67.2
Er (ppm)	84.6	82	82.1	0.071	b.d.	b.d.	b.d.	0.018	b.d.	96.5	141.8	174
Tm (ppm)	10.64	10.52	10.88	b.d.	b.d.	b.d.	b.d.	0.0072	b.d.	12.62	17.9	22.88
Yb (ppm)	56.9	56.5	60.7	0.037	b.d.	b.d.	b.d.	0.023	b.d.	66.2	100.1	126.5
Lu (ppm)	7.06	6.7	7.06	b.d.	b.d.	b.d.	b.d.	0.01	0.0028	8.6	12.8	15.59
Ta (ppm)	88.5	86.7	74.1	22.5	24.7	23	8.74	6.98	9.09	108.5	91.7	77.2
Tot. REE	2107.7	2051.42	1793.84	0.281	2.465	0.156	0.012	2.5152	3.2252	2150.92	2495.1	2626.37

Sample	PL91	PL91	PL91	PL91	PL91	PL90	PL90	PL90	PL76	PL76	PL76	PL90
Site	Gnt-1	Gnt-2	Gnt-3	Gnt-4	Gnt-5	Gnt-1	Gnt-2	Gnt-3	Gnt-1	Gnt-2	Gnt-3	Gnt-1
Si (cps)	6.11E+07	6.68E+07	6.57E+07	6.45E+07	6.62E+07	1.94E+06	1.93E+06	1.92E+06	5.86E+05	5.99E+05	5.79E+05	7.30E+05
Ca (ppm)						2.99E+05	2.98E+05	3.04E+05	2.78E+05	2.78E+05	2.84E+05	b.d.
Mn (ppm)	5030	5130	4860	4790	5250	6460	6160	6310	5800	5900	5530	6300
As (ppm)						13.9	12.4	10				
Sr (ppm)						68.8	83.1	82.5	47.8	46	46.6	24.6
Y (ppm)	1117	1111	993	979	1061	1440	1213	1144	1689	1681	1642	0.172
Zr (ppm)	16340	15720	15530	14780	15930	17980	16710	1.95E+04	15830	16820	14850	11.43
Ba (ppm)						b.d.	b.d.	b.d.	b.d.	b.d.	b.d.	1594
La (ppm)	45.6	44.5	44.8	44.7	44.4	54.5	54.3	53.7	44.9	30.5	35.2	0.503
Ce (ppm)	298.6	297.5	314	316	311	401	383	397	315	263.5	283	0.226
Pr (ppm)	73.8	72.3	76.1	75.8	76.4	109.2	102.1	106.4	83	76.3	78.1	0.084
Nd (ppm)	504	510	518	520	544	773	765	773	649	611	631	0.18
Sm (ppm)	230.9	231.5	220.6	223.2	235.3	325	321	314	313.9	310	308	b.d.
Eu (ppm)	99.5	99	93.8	94	100.4	115.1	110.8	102.1	111.9	116.1	115.5	b.d.
Gd (ppm)	268	263.9	244	247.4	259.4	354	326	315	366	373	364	b.d.
Tb (ppm)	45.3	44.1	39.5	39.3	41.9	57.6	48.9	49	57.4	56.3	57.1	b.d.
Dy (ppm)	258.5	250.5	218.6	219.1	236.4	347	300	288	362	360	356	b.d.
Ho (ppm)	48.2	46.7	40.3	39.3	42.5	61.9	52.7	50.6	62.8	63.3	61.2	b.d.
Er (ppm)	115.7	110.2	95.5	96	102.4	154.9	129.6	119.8	160.2	159.7	152.2	0.0000146
Tm (ppm)	14.88	14.46	12.51	12.19	12.95	20.5	16.78	15.08	20.85	20.9	20.61	b.d.
Yb (ppm)	88.7	86.1	74.4	74.4	79.4	122.6	99.7	92.4	116.9	115	114.8	b.d.
Lu (ppm)	10.06	9.77	8.41	8.24	8.86	13.2	11.69	10.49	14.19	14.77	14.14	b.d.
Ta (ppm)	66.6	64.6	52.7	49.8	54	139.2	298	238	105.2	97.9	104.7	6.49
Tot. REE	2101.74	2080.53	2000.52	2009.63	2095.31	2909.5	2721.57	2686.57	2678.04	2570.37	2590.85	0.9930146

Sample	PL90	PL90	WS01B	WS01B	WS01B	ETR3	ETR3	ETR3	PL78	PL78	PL78	PL51
Site	Gnt-2	Gnt-3	Gnt-1	Gnt-2	Gnt-3	Gnt-1	Gnt-2	Gnt-3	Gnt-1	Gnt-2	Gnt-3	Gnt-1
Si (cps)	7.25E+05	7.39E+05	2.50E+03	5.80E+03	5.40E+03	5.27E+05	5.71E+05	5.59E+05	5.62E+05	5.71E+05	5.56E+05	6.50E+05
Ca (ppm)	b.d.	940	b.d.	9.20E+04	b.d.	3.21E+05	2.89E+05	2.92E+05	2.69E+05	2.60E+05	2.70E+05	b.d.
Mn (ppm)	6220	6290	1.13E+06	8.40E+05	9.10E+05	4350	4370	4380	4180	4430	4200	6630
As (ppm)												
Sr (ppm)	20.1	57.8	b.d.	810	b.d.	97.3	74.1	72.2	68.7	59.9	65.1	5.6
Y (ppm)	b.d.	1.05	b.d.	3.6	b.d.	1711	1339	1367	1366	1222	1248	b.d.
Zr (ppm)	14.1	10.48	9.00E+03	7.40E+03	6.50E+03	2.92E+04	20210	17320	19330	16800	14220	4.69
Ba (ppm)	1991	1970	b.d.	110	b.d.	b.d.	b.d.	b.d.	b.d.	1.75	b.d.	1531
La (ppm)	0.048	3.53	b.d.	17.7	b.d.	54.7	53.5	46.6	57.5	48.5	52.8	b.d.
Ce (ppm)	b.d.	5.7	b.d.	46	b.d.	342	366	321	403	334	364.4	0.066
Pr (ppm)	0.022	0.6	b.d.	2.8	b.d.	82.4	85.7	77.1	93.4	82	86	0.0094
Nd (ppm)	b.d.	3.33	b.d.	9	b.d.	620	664	582	672	586	626	0.084
Sm (ppm)	b.d.	0.34	b.d.	3.9	b.d.	290	274	252.3	279.3	250.9	260.3	b.d.
Eu (ppm)	b.d.	0.133	b.d.	b.d.	b.d.	112.2	102	94.3	96.1	92	92.6	b.d.
Gd (ppm)	b.d.	b.d.	b.d.	b.d.	b.d.	379	324	314	311	284.7	294.3	b.d.
Tb (ppm)	b.d.	0.028	b.d.	b.d.	b.d.	61.2	48.2	47.2	46.1	43.3	42.4	b.d.
Dy (ppm)	b.d.	0.112	b.d.	b.d.	b.d.	397	295	297.6	283	254.4	258	b.d.
Ho (ppm)	b.d.	0.031	0.0098	b.d.	b.d.	73.3	51.1	52.1	50.1	45.3	45.1	b.d.
Er (ppm)	b.d.	b.d.	b.d.	b.d.	b.d.	189.7	127.9	132.1	125.6	115	111.2	b.d.
Tm (ppm)	b.d.	0.0025	b.d.	b.d.	b.d.	24.8	17.15	16.78	15.47	14.19	14.59	b.d.
Yb (ppm)	b.d.	b.d.	b.d.	b.d.	b.d.	134.5	97.5	95.1	89.5	80.3	80.1	b.d.
Lu (ppm)	b.d.	b.d.	7.3	b.d.	b.d.	16.36	12.04	11.94	10.86	10.11	9.91	b.d.
Ta (ppm)	6.17	4.19	1330	1070	950	82	99.2	85.5	109.5	67	96.5	3.23
Tot. REE	0.07	13.8065	7.3098	79.4	0	2777.16	2518.09	2340.12	2532.93	2240.7	2337.7	0.1594

Sample	PL51	PL51	ETR7C	ETR7C	ETR7C	WT4	WT4	WT4	PL63	PL63	PL63	PL63
Site	Gnt-2	Gnt-3	Gnt-1	Gnt-2	Gnt-3	Gnt-1	Gnt-2	Gnt-3	Gnt-1	Gnt-2	Gnt-3	Gnt-4
Si (cps)	6.54E+05	6.63E+05	6.91E+05	7.74E+05	7.02E+05	6.85E+05	7.38E+05	7.39E+05	1.61E+07	1.65E+07	1.72E+07	1.68E+07
Ca (ppm)	b.d.	b.d.	3.08E+05	2.88E+05	3.01E+05	2.82E+05	2.85E+05	2.79E+05				
Mn (ppm)	7060	6750	4580	4700	4810	4840	4700	4490	4450	4330	4300	4650
As (ppm)												
Sr (ppm)	16.5	7.8	148	86	98.8	65.8	53.2	57.6				
Y (ppm)	0.44	b.d.	1824	1273	1061	1731	1515	1509	1203	1165	973	1069
Zr (ppm)	29	13.4	2.63E+04	2.25E+04	11470	9330	9160	8370	17980	17100	14100	15720
Ba (ppm)	1461	1544	5.4	b.d.	0.88	b.d.	b.d.	0.68				
La (ppm)	0.65	b.d.	56.2	57.3	66.3	54.2	47.4	47.9	44.5	42.5	44.4	45.4
Ce (ppm)	1.19	b.d.	326	375	439	385	322	330	302.1	285	304	307
Pr (ppm)	0.151	b.d.	71.4	85.9	100.6	94.4	82.3	80.2	73.5	69	71.2	73
Nd (ppm)	0.83	b.d.	556	619	717	702	626	609	530	505	482	523
Sm (ppm)	0.24	b.d.	277	250.3	280	296	281.6	276	237.6	221.9	193.2	219.7
Eu (ppm)	b.d.	b.d.	106.2	95.2	92.9	110.9	105.4	100.9	99.1	93.4	81.7	90.2
Gd (ppm)	b.d.	b.d.	378	311	291	363	340	323	281.2	266.7	226.4	254
Tb (ppm)	0.0079	b.d.	60.3	43.6	40.8	56.9	52.9	53.2	44.9	43.7	36.7	40.1
Dy (ppm)	b.d.	b.d.	400	269	231	348	332	333	263.4	253.9	215.5	229
Ho (ppm)	0.019	b.d.	75.6	49.3	39.1	63.3	58.5	62.7	47	46.3	39	42
Er (ppm)	b.d.	b.d.	198.5	124	95.1	162.8	149.5	156.3	114.1	113.4	93.1	100
Tm (ppm)	b.d.	b.d.	24.8	15.49	12.23	20.8	19.55	19.5	14.97	14.34	12.22	12.54
Yb (ppm)	b.d.	b.d.	138.7	89.2	68.9	119.1	110.5	114.3	88.7	85.3	72.6	77.1
Lu (ppm)	0.019	b.d.	16.46	11.26	8.07	13.96	13.51	13.7	9.6	9.57	8.17	8.48
Ta (ppm)	3.56	3.22	88.7	101.4	115.3	106	93.1	95.6	80.9	75.5	66.1	69.3
Tot. REE	3.1069	0	2685.16	2395.55	2482	2790.36	2541.16	2519.7	2150.67	2050.01	1880.19	2021.52

Sample	PL59	PL59	PL59	PL59	PL59	PL65	PL65	PL96B	PL96B	PL96B	MT04-5-2	MT04-5-2
Site	Gnt-1	Gnt-2	Gnt-3	Gnt-4	Gnt-5	Gnt-1	Gnt-2	Gnt-1	Gnt-2	Gnt-3	Gnt-1	Gnt-2
Si (cps)	1.43E+07	1.41E+07	1.51E+07	1.39E+07	1.44E+07	1.75E+07	1.79E+07	7.23E+05	7.41E+05	7.40E+05	7.73E+05	6.61E+05
Ca (ppm)								2.84E+05	2.87E+05	2.77E+05	3.06E+05	2.82E+05
Mn (ppm)	7190	6810	6700	7120	7080	401	376	3890	3880	3880	6080	5890
As (ppm)												
Sr (ppm)								63	64.2	63.3	68.7	81.7
Y (ppm)	1882	1561	1390	1157	1506	881	291.7	1102	1110	1126	3080	3380
Zr (ppm)	14540	17760	2.61E+04	3.18E+04	16500	19850	19550	16070	14530	17890	16990	17630
Ba (ppm)								b.d.	b.d.	b.d.	b.d.	3.1
La (ppm)	45	54.1	63.7	68.3	51.7	698	619	38.5	39.1	42.5	61.4	58.9
Ce (ppm)	316	361	410	474	360	2696	2283	281	284	304	448	417
Pr (ppm)	81.3	90.5	92.8	108.6	90.7	485	380	71	71.3	74	120.9	120.2
Nd (ppm)	680	682	668	747	684	2562	1914	527	524	540	925	919
Sm (ppm)	372	327	284	294	325	666	402	240.1	224.6	225	484	480
Eu (ppm)	162	142.5	116.2	110.3	136.1	209.4	115.2	87.6	84.2	84.2	179.4	191
Gd (ppm)	453	378	322	293	374	478	239.4	279.4	264	268	611	656
Tb (ppm)	74.5	61	51.6	44.9	57	64.1	25.4	40.9	39.5	39.6	106.6	108.9
Dy (ppm)	412	338	297	257.9	332	303	108.4	256	246.2	247	692	749
Ho (ppm)	71.4	61.4	53.3	45.7	59.2	42.5	13.25	44.9	43.8	45.3	126.8	136.8
Er (ppm)	166.9	139.5	127.8	106.2	133.4	80.7	21.9	114.9	110.6	109.4	339	369
Tm (ppm)	21.25	17.07	16.08	13.64	16.49	8.51	2.16	14.48	13.7	14.63	42	46.6
Yb (ppm)	123.9	100.7	99.6	81.5	100.3	39.7	10.66	79.2	76.2	77.3	242.8	267
Lu (ppm)	14.1	11.25	10.73	8.54	10.81	2.76	0.814	9.43	9.02	9.27	29.5	32.8
Ta (ppm)	128.4	121.2	151	136.5	145	448	332	64.9	73.8	69.1	258	268
Tot. REE	2993.35	2764.02	2612.81	2653.58	2730.7	8335.67	6135.184	2084.41	2030.22	2080.2	4408.4	4552.2

Sample	MT04-5-2	Fen43	Fen43	Fen43	Fen43	Mosonik28	Mosonik28	Mosonik11	Mosonik11	Mosonik11
Site	Gnt-3	Gnt-a1	Gnt-a2	Gnt-b1	Gnt-b2	Gnt-1	Gnt-2	Gnt-1	Gnt-2	Gnt-3
Si (cps)	8.05E+05	1.22E+06	1.21E+06	2.17E+06	2.04E+06	2.18E+06	2.31E+06	1.50E+06	1.49E+06	1.51E+06
Ca (ppm)	3.00E+05	2.87E+05	2.78E+05	2.93E+05	2.92E+05	7770	6360	2.88E+05	2.85E+05	2.89E+05
Mn (ppm)	6030	3400	3630	3260	3550	1221	856	3133	2596	2880
As (ppm)		b.d.	9.6	6.6	b.d.	7.4	4.6	10.8	4.3	7.3
Sr (ppm)	67.7	41.9	53.8	47.7	55.1	804	604	159.2	98.9	50.5
Y (ppm)	2878	497	435	238.8	489	14.73	13.2	150	562	802
Zr (ppm)	16490	3500	2740	2840	6800	93.9	101.7	998	2363	2176
Ba (ppm)	b.d.	b.d.	b.d.	b.d.	b.d.	63.4	47.8	b.d.	b.d.	b.d.
La (ppm)	59.7	57	72.6	64.3	45.6	1.92	1.16	132	49	38.5
Ce (ppm)	467	301	392	361	267	2.28	1.14	672	260.3	212
Pr (ppm)	123.2	66.8	80.3	75	58.3	0.445	0.285	129.9	58.2	48.1
Nd (ppm)	966	437	538	449	397	1.98	1.6	721	393	338
Sm (ppm)	466	148	159.1	123.8	133.5	1	0.89	139.9	136.4	134.1
Eu (ppm)	179.2	45.1	47.7	33.5	45.2	0.42	0.29	33.7	41.2	44.9
Gd (ppm)	628	147.5	144	101.8	136.8	1.26	2.14	94.9	135.3	160
Tb (ppm)	104.5	20.77	19.8	11.12	19.9	0.361	0.245	9.71	21.36	27.5
Dy (ppm)	694	113.5	104.9	59.5	113.6	2.36	2.25	47.9	140.7	190.5
Ho (ppm)	128.7	20.9	18.11	8.84	18.28	0.532	0.43	7.25	25.6	36.3
Er (ppm)	340	48.5	37.7	20.1	46.6	1.29	1.48	16	71.2	101.1
Tm (ppm)	43.2	5.84	4.83	2.09	5.69	0.231	0.181	1.53	8.45	12.52
Yb (ppm)	240.9	33.5	28.1	14.9	35.6	1.16	1.86	7.9	46.2	71.5
Lu (ppm)	28.8	4.35	3.74	2.1	4.81	0.227	0.14	0.75	4.76	7.69
Ta (ppm)	257.5	86.3	141.4	73.7	45.2	5.42	2.98	223.5	76	49.4
Tot. REE	4469.2	1449.76	1650.88	1327.05	1327.88	15.466	14.091	2014.44	1391.67	1422.71

Apatite LA-ICP-MS Data

Sample	PL95	PL95	ETR7C	ETR7C	ETR7C	PL76	PL76	PL76	PL96B	PL96B	PL96B	PL90
Site	Ap-1	Ap-2	Ap-1	Ap-2	Ap-3	Ap-1	Ap-2	Ap-3	Ap-1	Ap-2	Ap-3	Ap-1
Ca (cps)	5.09E+05	5.29E+05	3.94E+05	3.82E+05	3.74E+05	3.08E+05	3.22E+05	3.27E+05	2.56E+05	2.59E+05	2.63E+05	3.01E+05
Si (ppm)	3440	4130	3680	3370	4220	3410	3090	3560	4380	4290	3720	1990
Mn (ppm)	212.4	219.3	167.5	172.5	170.3	150.3	149.4	178.5	175.7	179.7	161	167.6
As (ppm)	59.1	60.1	N/A	N/A	N/A	N/A	N/A	N/A	N/A	N/A	N/A	N/A
Sr (ppm)	6750	6980	6860	7690	7410	7130	7290	8200	7140	7240	7170	6860
Y (ppm)	553	611	351	309	269	361	514	358	336	347	350	487
Zr (ppm)	11.7	13.7	11	14	14.3	13.51	15.3	18.4	6.43	7.9	7.26	3.77
Ba (ppm)	24	25.6	15.1	14.4	17.2	15.3	15.3	17.9	16.2	15.6	13.7	17.4
La (ppm)	2970	3570	1740	1800	2110	2022	2120	2130	2423	2380	2200	1334
Ce (ppm)	7910	8810	4050	4050	4510	4330	4340	4920	5040	4800	4720	2710
Pr (ppm)	1100	1202	506	496	536	563	578	612	645	627	613	342
Nd (ppm)	4910	5280	2110	2070	2080	2328	2430	2470	2550	2510	2380	1469
Sm (ppm)	719	722	331	307	308	366	404	366	383	376	363	257.1
Eu (ppm)	163	167.2	83.2	72.5	71	87.5	106	87.8	94.5	92	91.6	73.8
Gd (ppm)	473	477	220	190	180	234	283	225	240	231.8	234	218
Tb (ppm)	40.2	41.7	20.4	17.4	15.2	21.06	28.3	20.5	20.16	21.11	21.51	24.56
Dy (ppm)	171	182	88	75.7	61	93.8	126.7	86.3	89.6	90.1	91.5	128.9
Ho (ppm)	24.5	24.3	13.2	9.92	8.43	12.51	17.9	12.2	11.89	11.91	12.44	19.88
Er (ppm)	45.3	45.8	25.4	19.2	15.4	24.2	37.7	23	22	22.1	24.5	41.9
Tm (ppm)	4.54	4.83	2.44	2.05	1.41	2.34	3.6	2.44	2.18	2.39	2.36	4.24
Yb (ppm)	18	20.7	12.4	9.01	6.9	10.37	16.6	11.9	9.31	10.3	10.7	18
Lu (ppm)	1.86	2.32	1.35	0.93	0.73	1.2	1.82	1.08	1.1	1.19	1.17	1.41
Ta (ppm)	b.d.	b.d.	b.d.	b.d.	b.d.	b.d.	b.d.	0.032	0.064	0.05	0.03	b.d.
Tot. REE	18550.4	20549.85	9203.39	9119.71	9904.07	10095.98	10493.62	10968.22	11531.74	11175.9	10765.78	6642.79

Sample	PL90	PL90	ETR2	ETR2	ETR2	MT04 5-2	MT04 5-2	MT04 5-2	PL49	PL49	PL49	WS01B
Site	Ap-2	Ap-3	Ap-1	Ap-2	Ap-3	Ap-1	Ap-2	Ap-3	Ap-1	Ap-2	Ap-3	Ap-1
Ca (cps)	3.00E+05	3.06E+05	3.89E+05	3.96E+05	4.01E+05	3.00E+05	3.18E+05	3.11E+05	3.47E+05	3.38E+05	3.58E+05	3.39E+05
Si (ppm)	2400	2480	3760	3410	3770	3820	5210	3480	6000	6290	7270	5730
Mn (ppm)	168.6	196	149.8	84.4	122	144.5	190.9	131.8	199.8	202.1	198.1	164.5
As (ppm)	N/A	N/A	N/A	N/A	N/A	N/A	N/A	N/A	N/A	N/A	N/A	N/A
Sr (ppm)	7350	6660	7550	6650	7220	7380	7050	7480	8090	8520	8120	8680
Y (ppm)	436	474	325	569	400	549	546	538	250.8	303	357	386.2
Zr (ppm)	4.19	5.32	17.78	11.27	15.1	12.25	21.9	9	24.2	25.6	59.1	31.2
Ba (ppm)	19.6	21	19.8	11.1	17.9	18	24.7	17.4	15.4	17.3	16.6	15.2
La (ppm)	1549	1270	2100	2260	2260	2351	2307	2410	2429	2435	2350	2688
Ce (ppm)	3000	2590	4450	5410	4860	4910	5190	5210	5190	5310	5190	5910
Pr (ppm)	376	340	577	694	617	638	653	666	671	630	598	696
Nd (ppm)	1535	1438	2270	2870	2380	2780	2793	2760	2443	2450	2320	2816
Sm (ppm)	256.6	259	343	462	365	448	433	455	324	333	335	388
Eu (ppm)	71.1	70.9	85.8	113.2	89.5	113.7	108.4	110.6	72.9	78.8	81.5	94.4
Gd (ppm)	201.6	214.1	222	314	236	311	308	322	185.6	203.1	214.8	247
Tb (ppm)	22.8	24.41	19.9	29.8	21.9	30.6	29.7	31	15.63	17.39	19.63	22.64
Dy (ppm)	115.4	128.5	77.6	134.4	95	136.5	137.6	135.5	62.9	76.7	91.2	96.5
Ho (ppm)	17.87	20.24	10.87	19.7	13.3	19.61	20.03	19.55	8.19	10.16	12.5	13.39
Er (ppm)	36.9	44.3	21.6	41.9	25.9	38	39.5	38.6	15.7	19.5	24.5	26.3
Tm (ppm)	3.79	4.4	2.02	3.69	2.53	3.71	4.02	3.57	1.63	1.88	2.36	2.58
Yb (ppm)	15.4	17.5	10.6	17.3	12	16.96	19.2	16.35	7.23	8.57	11.41	12.17
Lu (ppm)	1.41	1.59	1.24	1.63	1.2	1.84	2.11	1.83	0.84	0.89	1.27	1.22
Ta (ppm)	b.d.	b.d.	b.d.	b.d.	b.d.	b.d.	0.067	0.02	0.088	0.047	0.042	0.071
Tot. REE	7202.87	6422.94	10191.63	12371.62	10979.33	11798.92	12044.56	12180	11427.62	11574.99	11252.17	13014.2

Sample	WS01B	WS01B	WS01A	WS01A	WS01A	WT4	WT4	ETR3	ETR3	ETR3	PL78	PL78
Site	Ap-2	Ap-3	Ap-1	Ap-2	Ap-3	Ap-2	Ap-3	Ap-1	Ap-2	Ap-3	Ap-1	Ap-2
Ca (cps)	3.37E+05	3.35E+05	2.97E+05	2.98E+05	3.13E+05	4.22E+05	4.14E+05	2.60E+05	2.65E+05	2.48E+05	2.79E+05	2.75E+05
Si (ppm)	4990	6710	5730	6000	5290	7000	7390	3660	4610	4880	4090	4460
Mn (ppm)	96.1	155.4	130.6	170.4	121.6	202	231	125.6	129	128.4	168.1	191.2
As (ppm)	N/A	N/A	N/A	N/A	N/A	N/A	N/A	N/A	N/A	N/A	N/A	N/A
Sr (ppm)	9380	8630	8640	8430	8490	7830	7470	7910	7760	7800	8170	7880
Y (ppm)	408	480	432	430	413	296.2	323	192.9	289	212	282.5	329
Zr (ppm)	24.2	89	64.4	54.3	53.9	21.9	25.6	17.3	28.4	20.7	11.53	18.8
Ba (ppm)	12.6	18.5	17.6	20.1	14.8	17.4	20	16.2	18.3	19.2	18.5	20.3
La (ppm)	2870	2768	2820	2788	2780	2590	2640	2023	1989	2120	2495	2402
Ce (ppm)	6240	5960	5780	5750	6110	5900	5220	3870	3760	3900	5130	5220
Pr (ppm)	720	702	684	690	697	649	614	476	468	489	638	625
Nd (ppm)	2999	2823	2710	2700	2760	2550	2450	1962	1930	2010	2505	2452
Sm (ppm)	422	422	395	382	394	344	332	263	285	272	350	361
Eu (ppm)	100.4	105.4	100.8	97	98.7	79.4	80.8	61.6	69.4	62.5	80.6	84.7
Gd (ppm)	266.2	285	255	250.6	261	192.5	208	159.3	194.4	166.2	199	212
Tb (ppm)	24.81	26.5	24.15	22.34	23.4	17.08	17.3	13.03	19.3	13.69	17.34	18.71
Dy (ppm)	103.4	114.2	101.3	101.7	101.4	72.4	74.3	52.4	80.9	58.6	70.1	80
Ho (ppm)	14.46	16.73	14.29	14.22	14.32	9.72	9.7	6.69	10.97	7.21	8.8	10.16
Er (ppm)	28.1	33	27.5	28.5	29.6	19.1	19.5	12.11	21.6	14	16.4	20.6
Tm (ppm)	2.69	3.48	2.78	2.75	2.54	2.08	2.03	1.16	1.94	1.15	1.66	1.79
Yb (ppm)	11.41	14.67	12.3	13.2	12.14	8.18	9.9	5.1	8.37	5.59	6.64	8.83
Lu (ppm)	1.31	1.84	1.46	1.42	1.38	0.87	1.08	0.56	0.98	0.54	0.82	0.95
Ta (ppm)	0.027	0.04	0.054	0.068	0.03	0.068	0.147	b.d.	b.d.	b.d.	0.033	0.03
Tot. REE	13803.78	13275.82	12928.58	12841.73	13285.48	12434.33	11678.61	8905.95	8839.86	9120.48	11519.36	11497.74

Sample	PL78	PL46	PL46	PL46	PL46	PL46	PL63	PL63	PL63	PL63	PL65	PL65
Site	Ap-3	Ap-1	Ap-2	Ap-3	Ap-4	Ap-5	Ap-1	Ap-2	Ap-3	Ap-4	Ap-1	Ap-2
Ca (cps)	2.69E+05	1.11E+07	1.09E+07	1.07E+07	1.11E+07	1.09E+07	4.76E+06	4.58E+06	4.77E+06	4.48E+06	4.93E+06	4.67E+06
Si (ppm)	7010											
Mn (ppm)	267	218.7	198.5	195	208.4	191.4	149.3	129.9	148.5	155.2	272.8	290.3
As (ppm)	N/A	N/A	N/A	N/A	N/A	N/A	N/A	N/A	N/A	N/A	N/A	N/A
Sr (ppm)	7860	8540	8790	8280	7640	8220	8010	8520	8100	7970	6650	6770
Y (ppm)	376	163.9	145	161.9	163.6	170.8	179.1	166.7	180.7	194.3	484	528
Zr (ppm)	37.6	N/A	N/A	N/A	N/A	N/A	N/A	N/A	N/A	N/A	N/A	N/A
Ba (ppm)	26.8	22.31	22.7	21.2	13.54	17.03	20.6	25.4	21.7	19.6	26.4	30.2
La (ppm)	2116	2028	1937	1881	1870	2020	2105	2300	2086	2198	2715	2615
Ce (ppm)	4470	5120	4670	4710	4490	4980	4650	4910	4670	4730	7500	7220
Pr (ppm)	560	501	499	486	481	510	513	545	502	532	914	848
Nd (ppm)	2310	1794	1708	1674	1640	1772	1818	1929	1737	1876	3670	3530
Sm (ppm)	370	212	195.1	198.8	195.7	211.1	226.1	238.5	226.6	239.2	551	567
Eu (ppm)	89.8	55.6	51.4	52.8	51.9	57.4	61.9	63.2	63	65.5	149.3	151.9
Gd (ppm)	230	167.4	157.8	159.4	155.5	168.5	170.2	172.9	171	180.4	379	387
Tb (ppm)	20.9	10.07	9.2	9.99	9.62	10.5	11.74	11.88	12.81	13.34	34.3	36.2
Dy (ppm)	90.8	38	34.3	37.4	35.3	39.4	44.2	42.2	47.4	50.1	143.5	148.1
Ho (ppm)	12.64	5.28	4.59	5.1	5.12	5.5	5.8	5.65	6.58	6.84	20	21.72
Er (ppm)	23.2	9.63	8.45	9.32	9.49	10.4	10.51	9.72	11.37	11.55	35.9	42.8
Tm (ppm)	2.59	0.964	0.822	0.95	0.968	0.985	0.955	0.839	1.08	1.105	3.59	3.9
Yb (ppm)	12.02	4.52	3.63	4.55	4.48	5.05	3.93	3.61	4.64	4.65	15.74	18.72
Lu (ppm)	1.06	0.469	0.421	0.484	0.468	0.499	0.449	0.362	0.526	0.443	1.46	1.89
Ta (ppm)	0.065	N/A	N/A	N/A	N/A	N/A	N/A	N/A	N/A	N/A	N/A	N/A
Tot. REE	10309.01	9946.933	9279.713	9229.794	8949.546	9791.334	9621.784	10232.861	9540.006	9909.128	16132.79	15592.23

Comments	PL65	PL65	PL65	PL91	PL91	PL91	PL55	PL55	PL55	PL55	PL55
Site	Ap-3	Ap-4	Ap-5	Ap-1	Ap-2	Ap-3	Ap-1	Ap-2	Ap-3	Ap-4	Ap-5
Ca (cps)	4.81E+06	4.71E+06	4.80E+06	2.81E+06	2.86E+06	2.90E+06	1.72E+07	1.52E+07	1.64E+07	1.64E+07	1.55E+07
Si (ppm)											
Mn (ppm)	295	253.9	285	176.7	183.9	184.7	233	199.9	277	231	228.5
As (ppm)	N/A	N/A	N/A	N/A	N/A	N/A	N/A	N/A	N/A	N/A	N/A
Sr (ppm)	7010	7040	7020	7410	7350	7200	6160	6290	7650	6850	5980
Y (ppm)	475	479	484	285	271.8	274	243.5	290	281	270	221.7
Zr (ppm)	N/A	N/A	N/A	N/A	N/A	N/A	N/A	N/A	N/A	N/A	N/A
Ba (ppm)	25.2	28.9	28.5	15.1	14.9	15.53	17.34	17.7	23.2	21.4	16.32
La (ppm)	2517	2350	2523	1779	1775	1808	999	1344	861	1068	1055
Ce (ppm)	7180	6180	6620	4100	3880	4050	2830	3930	2650	3190	3210
Pr (ppm)	866	802	796	526	502	510	304	393	275	324	330
Nd (ppm)	3390	3180	3130	1959	1900	1878	1121	1452	1028	1202	1177
Sm (ppm)	514	508	484	288	270	279	178.1	224.4	177.8	189.8	177.4
Eu (ppm)	143.9	141.4	135	81.5	75.7	76.7	56.5	71.8	61.4	62.7	55.5
Gd (ppm)	350	354	344	209.1	199.2	196.6	144.7	176.3	150.3	154.3	138
Tb (ppm)	32.4	34.7	31.66	17.06	16.56	15.96	14.34	17.36	16.56	15.93	13.3
Dy (ppm)	135.3	148.3	137.5	67.5	62.6	61.3	64.5	76	77.6	73.3	59.2
Ho (ppm)	19.95	21	20.2	9.37	8.75	8.65	9.9	11.82	12.29	11.46	9.01
Er (ppm)	37.2	40.2	37.7	17.39	15.3	15.91	19	22.45	25.6	21.8	16.8
Tm (ppm)	3.52	3.85	3.73	1.62	1.59	1.49	1.884	2.09	2.67	2.27	1.556
Yb (ppm)	15.75	17.6	16.9	7.73	6.7	7.18	7.44	7.58	12.14	9.49	5.59
Lu (ppm)	1.5	1.79	1.602	0.846	0.786	0.75	0.711	0.626	1.281	0.915	0.517
Ta (ppm)	N/A	N/A	N/A	N/A	N/A	N/A	N/A	N/A	N/A	N/A	N/A
Tot. REE	15206.52	13782.84	14281.292	9064.116	8714.186	8909.54	5751.075	7729.426	5351.641	6325.965	6248.873

Sample	204	204	204	204	204	204	418	418	418	43	43
Site	Ap-a1	Ap-a2	Ap-a3	Ap-b1	Ap-b2	Ap-b3	Ap-1	Ap-2	Ap-3	Ap-a1	Ap-a2
Ca (cps)	5.31E+05	5.02E+05	4.80E+05	4.00E+05	3.97E+05	4.00E+05	3.86E+05	3.52E+05	3.57E+05	5.69E+05	6.04E+05
Si (ppm)	1520	1950	1930	1950	1730	1550	b.d.	1010	1540	3400	3800
Mn (ppm)	173.9	170.7	164.8	137.8	135.7	146	212	203	207	109.9	130
As (ppm)	14.6	15.4	16.7	25.4	24.5	24.7	19.8	17.8	18.5	22.1	14.8
Sr (ppm)	6210	6140	6850	7260	7180	7500	5020	5280	4870	5260	4970
Y (ppm)	285	281	323	381	371	380	396	370	422	260	265
Zr (ppm)	7.32	8.18	6.88	4.96	3.9	3.28	0.54	b.d.	0.6	15.09	18.1
Ba (ppm)	38.2	43.1	44.3	34.1	42.6	36.2	40.7	31.2	30.9	27.9	32.3
La (ppm)	1319	1375	1577	1890	2007	1781	2070	1763	1940	1376	1166
Ce (ppm)	2460	2450	2740	3040	3310	2930	3730	3240	3690	2270	1900
Pr (ppm)	284	276	310	344	361	325	435	405	420	265	229
Nd (ppm)	1057	1072	1162	1277	1314	1227	1700	1428	1630	1003	900
Sm (ppm)	154.4	159.3	179.4	192	198	188	251	229	243	158	145
Eu (ppm)	40	40.6	42.8	49.3	49.9	45.9	69.4	60.5	65.6	39.8	38.3
Gd (ppm)	143.8	145	152	166	182.3	173	234	196	227	131.6	137.4
Tb (ppm)	13.45	13.55	15	16.6	16.9	16.7	21.3	19.8	20.3	12.97	12.42
Dy (ppm)	70.9	70.4	78.6	90.9	89.8	84.1	108.3	100.6	111.4	64.4	68.7
Ho (ppm)	12.64	11.56	13.07	14.45	15.41	14.8	17.2	15.8	16.6	10.16	10.63
Er (ppm)	26.4	27.1	30.8	34.4	36.7	36.4	37.4	35.4	39.7	21.9	21.6
Tm (ppm)	2.99	2.79	3.2	3.7	3.99	4.13	4.44	3.86	4	2.27	2.48
Yb (ppm)	15	13.6	16.3	17.4	18.1	18.8	18.6	15.3	17.4	10.5	12.1
Lu (ppm)	1.46	1.55	1.76	1.77	2.14	1.99	2.15	2.06	1.97	1.25	1.46
Ta (ppm)	b.d.	b.d.	b.d.	b.d.	b.d.	b.d.	b.d.	b.d.	b.d.	b.d.	0.018
Tot. REE	5601.04	5658.45	6321.93	7137.52	7605.24	6846.82	8698.79	7514.32	8426.97	5366.85	4645.09

Sample	43	43	43	43	61	61	61	42	42	42	35
Site	Ap-a3	Ap-b1	Ap-b2	Ap-b3	Ap-1	Ap-2	Ap-3	Ap-1	Ap-2	Ap-3	Ap-1
Ca (cps)	5.99E+05	5.57E+05	6.16E+05	5.63E+05	6.07E+05	6.15E+05	6.51E+05	4.82E+05	4.38E+05	4.72E+05	5.30E+05
Si (ppm)	2420	2000	3030	3800	670	1380	1800	2080	1270	1460	1660
Mn (ppm)	96.4	69.8	106.3	139.3	57.4	72	84.4	236	233	238	167.7
As (ppm)	25.6	20.2	14.6	13	37.8	37.5	31.7	16.9	17.8	16.2	15.6
Sr (ppm)	5130	5190	4800	3850	4390	9.30E+03	7.40E+03	3900	4580	4430	6170
Y (ppm)	182.9	245	243	249	255	328	301	287	302	296	225
Zr (ppm)	8.24	11.15	14.9	15.39	0.26	1.02	2.58	2.04	b.d.	0.62	7.09
Ba (ppm)	26.7	11.1	30.7	38.3	11.4	45.1	35.2	35.3	31.1	34.3	34.8
La (ppm)	1610	1355	1195	964	1230	1660	1280	1530	1660	1640	1219
Ce (ppm)	2690	2130	1950	1613	1820	2560	1900	2880	3040	3030	1890
Pr (ppm)	307	255	219	187.1	200	259	213	337	406	363	202
Nd (ppm)	1098	957	799	724	720	900	800	1250	1410	1310	724
Sm (ppm)	142	142.7	124.7	120.7	121	146	130	183	212	189	113.9
Eu (ppm)	38.6	37.6	32.7	33.5	28.5	37.2	33	45.9	51.3	45.9	29.6
Gd (ppm)	124.8	127.3	113.7	115.9	107	145	129	143	152	157	101.7
Tb (ppm)	10.73	11.9	10.12	11.37	10.5	13.5	11.6	13.5	15.2	14	10.53
Dy (ppm)	49.6	58.8	52.7	56.7	51.8	66	59	70	73	66.7	56.4
Ho (ppm)	7.4	9.18	8.07	9.5	8.6	11.4	10.4	11.1	11.6	10.9	10.12
Er (ppm)	14.9	20.1	17.8	21.6	20.5	25.8	24.9	25.7	28.8	26	20.6
Tm (ppm)	1.69	2.06	2.01	2.28	2.32	3.19	2.34	2.72	2.63	2.23	2.15
Yb (ppm)	7.78	10.98	9.7	10.73	9.1	14.5	10.8	12.8	13.4	10.4	11.5
Lu (ppm)	0.91	1.1	1.05	1.21	1.17	1.28	1.33	1.55	1.49	1.37	1.15
Ta (ppm)	b.d.	b.d.	b.d.	b.d.	b.d.	b.d.	b.d.	b.d.	b.d.	b.d.	b.d.
Tot. REE	6103.41	5118.72	4535.55	3871.59	4330.49	5842.87	4605.37	6506.27	7077.42	6866.5	4392.65

Sample	35	35	405	405	405	405	405	405
Site	Ap-2	Ap-3	Ap-a1	Ap-a2	Ap-a3	Ap-b1	Ap-b2	Ap-b3
Ca (cps)	5.17E+05	4.92E+05	5.40E+05	5.03E+05	5.02E+05	4.12E+05	3.84E+05	3.93E+05
Si (ppm)	1860	1600	2400	3190	2800	2980	3040	3300
Mn (ppm)	168.6	148.3	180.4	183.8	190.9	190.9	235	225
As (ppm)	15.3	13.2	38.5	43.9	41.3	40.5	34.7	37.7
Sr (ppm)	5870	6430	4310	4640	4680	4540	4310	4580
Y (ppm)	253	270	551	623	635	525	612	643
Zr (ppm)	7.8	5.06	16.85	18.8	21	17.5	23.2	27.2
Ba (ppm)	32.4	34.9	41.2	37.6	42	43.7	47.2	46.4
La (ppm)	1336	1236	2470	2690	2500	2430	2440	2480
Ce (ppm)	1950	1880	5020	5610	5290	5510	5110	5430
Pr (ppm)	207	205	644	719	654	667	670	659
Nd (ppm)	773	759	2650	2820	2680	2570	2600	2570
Sm (ppm)	115.6	120.3	388	422	397	381	417	381
Eu (ppm)	32.5	30	89.2	97.7	93.3	92.7	94	92.4
Gd (ppm)	123.6	118.1	298	319	300	287	311	306
Tb (ppm)	11.51	12.4	27.6	30.9	31.2	28	31.2	29.5
Dy (ppm)	62.1	64.3	141.3	163	160.3	139.6	157.5	161
Ho (ppm)	11.12	11.1	22.5	24.8	25.7	21.5	26.4	25.9
Er (ppm)	24.6	26.4	52.5	55.3	60.9	50.2	59.9	66.5
Tm (ppm)	2.5	2.52	5.92	6.55	6.6	5.61	7.31	7.22
Yb (ppm)	13.3	12.9	27.4	31.1	33	29.1	34.4	34.5
Lu (ppm)	1.46	1.44	3.18	3.91	3.49	3.46	4.33	4.26
Ta (ppm)	b.d.	b.d.	b.d.	b.d.	b.d.	b.d.	b.d.	0.019
Tot. REE	4664.29	4479.46	11839.6	12993.26	12235.49	12215.17	11963.04	12247.28

Sample	Mosonik28	Mosonik28	Mosonik28	VAL-2	VAL-2	VAL-2	VAL-3	VAL-3	VAL-3
Site	Ap-1	Ap-2	Ap-3	Ap-1	Ap-2	Ap-3	Ap-1	Ap-2	Ap-3
Ca (cps)	4.05E+05	2.20E+05	5.28E+05	4.24E+05	3.81E+05	4.19E+05	4.15E+05	4.17E+05	5.20E+05
Si (ppm)	1460	8.60E+03	1700	270	b.d.	b.d.	b.d.	b.d.	b.d.
Mn (ppm)	118.4	154	90	174	97.8	40.5	137.6	159	118
As (ppm)	19.2	14.5	18	15.9	16.1	12.6	13.5	17.5	13.6
Sr (ppm)	13800	1.04E+04	9.50E+03	9700	8280	7370	8550	8320	8030
Y (ppm)	247	291	175	215	529	529	227	187	200
Zr (ppm)	b.d.	9.6	0.93	b.d.	b.d.	0.63	b.d.	0.44	b.d.
Ba (ppm)	29.3	79	42	18.2	8.7	12.8	10.7	10.3	8.9
La (ppm)	2610	2330	1760	862	525	260	631	780	650
Ce (ppm)	3760	3170	3190	2090	1580	1008	1720	2070	1730
Pr (ppm)	399	371	339	301	244	178	267	299	262
Nd (ppm)	1419	1410	1180	1315	1217	895	1150	1290	1100
Sm (ppm)	184	184	144	224	274	241	217	220	193
Eu (ppm)	39.4	44.5	34.3	54.8	76.1	71.1	54.9	52.8	52
Gd (ppm)	163.8	147	127	168.3	229	213	154	149	140
Tb (ppm)	12.78	14.6	8.9	16.15	26.6	26.6	16.6	15.3	14.2
Dy (ppm)	71	77.4	52.5	73.1	141	136.9	74.6	67.1	59
Ho (ppm)	10.55	13	7.2	10.05	22.7	21.7	10.3	8.8	8.5
Er (ppm)	21.4	28.9	17.9	18.8	52.7	55.3	18	17.1	17
Tm (ppm)	2.05	2.79	1.44	1.88	5.4	7.3	1.67	1.34	1.24
Yb (ppm)	7.28	10.1	6.5	6.93	24.9	39	6.87	6.08	6.2
Lu (ppm)	0.74	1.31	0.56	0.71	2.91	4.8	0.54	0.79	0.48
Ta (ppm)	b.d.	b.d.	b.d.	b.d.	b.d.	b.d.	b.d.	b.d.	b.d.
Tot. REE	8701	7804.6	6869.3	5142.72	4421.31	3157.7	4322.48	4977.31	4233.62